

Aus dem
Comprehensive Pneumology Center (CPC)
Institut für Experimentelle Pneumologie der Ludwig-Maximilians-Universität München
Direktor: Prof. Dr. med. Oliver Eickelberg

Connecting the functions of the proteasome and mitochondria in the lung

Dissertation zum Erwerb des Doktorgrades der Naturwissenschaften
an der Medizinischen Fakultät der Ludwig-Maximilians-Universität München

vorgelegt von
Korbinian Berschneider, geb. Ballweg

aus München

August 2016

**Gedruckt mit Genehmigung der Medizinischen Fakultät der
Ludwig-Maximilians-Universität München**

Betreuerin: PD Dr. rer. nat. Silke Meiners

Zweitgutachter: PD Dr. rer. Nat. Kai Hell

Dekan: Prof. Dr. med. dent. Reinhard HICKEL

Tag der mündlichen Prüfung: 05.08.2016

Table of Contents

Zusammenfassung.....	1
Summary	3
1 Introduction	5
1.1 Protein homeostasis by the proteasome	5
1.1.1 The ubiquitin proteasome system	6
1.1.1.1 Proteasome structure and function	7
1.1.1.2 Regulation of proteasome function	8
1.2 Mitochondrial function and protein homeostasis	11
1.2.1 Mitochondrial protein homeostasis.....	13
1.2.1.1 Mitochondrial unfolded protein response	13
1.2.1.2 Mitochondrial dynamics.....	14
1.2.1.3 Mitochondria-associated degradation	16
1.2.1.4 Mitophagy	17
1.3 Interconnections between mitochondrial and proteasomal function.....	18
1.3.1 Effect of proteasome function on mitochondria	18
1.3.2 Effect of mitochondrial function on the proteasome	20
1.4 Lung aging	24
1.4.1 Molecular mechanisms of aging	24
1.4.2 Proteasome activity in aging.....	24
1.4.3 Mitochondrial function in aging.....	25
1.4.4 Healthy and diseased aging phenotypes of the lung	25
1.4.4.1 Age-related diseases of the lung	26
2 Aims of the study	29
3 Materials and methods	31
3.1 Materials	31
3.1.1 Reagents and chemicals	31

3.1.2	Buffer formulations	34
3.1.3	Cigarette smoke extract preparation	36
3.2	Animal experiments	36
3.2.1	Animals and maintenance	36
3.2.2	Lung function analyses	37
3.2.3	Bronchoalveolar lavage cell analysis	37
3.3	Cell culture	37
3.3.1	Isolation of primary murine alveolar type II cells (pmATII)	37
3.3.2	Cell growth and maintenance	38
3.3.3	Cytotoxicity testing (LDH release)	38
3.3.4	Metabolic activity assay (MTT reduction)	39
3.3.5	Cell proliferation assay (BrdU incorporation)	39
3.3.6	Live/dead assay with Annexin V/PI	39
3.3.7	Measurement of cellular ATP levels.....	39
3.3.8	Analysis of cellular ROS production	40
3.3.9	Measurement of cellular NAD ⁺ and NADH levels.....	40
3.4	Mitochondrial function analysis.....	40
3.4.1	Mitochondrial membrane potential analysis.....	40
3.4.2	Analysis of mitochondrial superoxide production	40
3.4.3	Analysis of mitochondrial morphology	41
3.4.4	Analysis of cellular oxygen consumption	41
3.5	Protein analysis	42
3.5.1	Immunohistochemistry	42
3.5.2	Immunofluorescence staining.....	42
3.5.3	Preparation of protein lysates.....	43
3.5.4	Preparation of mitochondrial fractions.....	43
3.5.5	Western blot analysis.....	44
3.5.6	Detection of oxidatively damaged proteins.....	46

3.5.7	Proteasome activity assay	46
3.5.8	Native-gel proteasome analysis	46
3.5.9	Activity based probe analysis of proteasome activity.....	46
3.5.10	Isolation of 26S proteasomes.....	47
3.5.11	Analysis of nascent protein synthesis	47
3.6	Quantitative real-time RT-PCR analysis.....	48
3.7	Statistical analysis.....	49
4	The effect of mitochondrial dysfunction on proteasome activity and composition	51
4.1	Introduction	51
4.2	Results	52
4.2.1	Proteasome activity is decreased in mtDNA mutator MEFs	55
4.2.2	Assembly of 26S and 30S proteasome complexes is decreased in mtDNA mutator MEFs	56
4.2.3	Mitochondria to proteasome signaling in mtDNA mutator MEFs	59
4.2.4	Increased resistance against proteasome inhibition in mtDNA mutator MEFs.....	63
4.2.5	Protein synthesis is decreased in mtDNA mutator MEFs.....	65
4.2.6	Human dermal fibroblasts harboring mutations in single respiratory chain genes show differentially altered proteasome activity	67
4.3	Discussion.....	70
4.3.1	Dysfunction of the mitochondrial respiratory chain is associated with decreased 26S and 30S proteasome assembly and activity.....	70
4.3.2	Mitochondria to proteasome signaling in mtDNA mutator MEFs	71
4.3.3	Decreased proteasome activity does not induce proteostasis imbalance in mtDNA mutator MEFs.....	74
4.3.4	mtDNA mutator MEFs are less sensitive to bortezomib-induced cell death	75
4.3.5	Reduced proteasome activity in human mitochondrial disorders.....	77
4.3.6	Differential adaptation of proteasomal function to mitochondrial dysfunction	78
5	Mitochondrial function in response to cigarette smoke extract exposure	81
5.1	Introduction	81

5.2	Results	82
5.2.1	Cigarette smoke extract induces mitochondrial hyperfusion in mouse alveolar epithelial cells.....	83
5.2.2	Cigarette smoke extract-induced mitochondrial hyperfusion is associated with increased mitochondrial oxygen consumption and ATP production	89
5.2.3	Low dose cigarette smoke extract treatment does not activate a protein stress response at mitochondria	92
5.3	Discussion.....	96
5.3.1	Nontoxic doses of cigarette smoke extract induce mitochondrial hyperfusion in alveolar epithelial cells.....	96
5.3.2	Mitochondrial hyperfusion is associated with increased mitochondrial function....	98
5.3.3	Nontoxic cigarette smoke exposure does not induce activation of mitochondrial proteostasis pathways	99
5.3.4	A hyperfused mitochondrial network poses a threat to cellular health.....	100
6	Regulation of proteasomal function during healthy aging of the lung	103
6.1	Introduction	103
6.2	Results	103
6.2.1	Immunoproteasome expression is increased in lungs of aged mice	104
6.2.2	26S proteasome-dependent protein degradation is not altered during healthy aging of the lung	108
6.2.3	LMP2 or LMP7 knockout mice have preserved proteasome activity but are not protected from lung aging	110
6.2.4	Absence of a lung aging phenotype in premature aging mtDNA mutator mice.....	114
6.3	Discussion.....	116
6.3.1	Proteasome function is not markedly impaired in aged lungs	116
6.3.2	Immunoproteasome expression is elevated in aged lungs.....	117
6.3.3	Immunoproteasome expression does not causally contribute to the aging phenotype of the lung.....	118
6.3.4	Proteostasis in healthy aging of the lung	119
6.3.5	Mitochondrial function in lung aging.....	120

7	Concluding remarks.....	121
	References.....	125
	Abbreviations	143
	Acknowledgements	149
	Eidesstattliche Versicherung	151

Zusammenfassung

Das Proteom lebender Zellen befindet sich im ständigen Umbau, da zelluläre Proteine beschädigt werden und abgebaut werden müssen oder Zellen sich an veränderte physiologische Bedingungen anpassen. Die zellulären Prozesse, die den Erhalt des funktionalen Proteoms garantieren, werden unter dem Begriff Proteostase zusammengefasst. Das Proteasom stellt dabei eines der bedeutendsten intrazellulären Abbausysteme für beschädigte oder nicht benötigte Proteine dar. Insbesondere fehlgefaltete Proteine müssen zeitnah abgebaut werden um proteotoxische Effekte, wie zum Beispiel die Bildung von Proteinaggregaten zu vermeiden. Der Abbau zellulärer Proteine durch das Proteasom stellt einen sehr energieaufwändigen Prozess in der Zelle dar. Dementsprechend gibt es Hinweise auf eine Verknüpfung und wechselseitige Regulation zwischen den bedeutendsten Energieproduzenten der Zelle, den Mitochondrien, und proteasomaler Aktivität. Darüber hinaus korreliert proteasomale Dysfunktion mit mitochondrialer Fehlfunktion im Rahmen von Alterungsprozessen. Es ist allerdings wenig darüber bekannt, inwieweit mitochondriale Funktion und proteasomale Aktivität direkt miteinander verknüpft sind, vor allem im Kontext chronischer Defekte der mitochondrialen Atmungskette. Darüber hinaus ist weitgehend unbekannt, in welchem Ausmaß diese Prozesse spezifisch zur Lungenalterung oder zur Entwicklung von altersbedingten Lungenerkrankungen wie der chronisch obstruktiven Lungenerkrankung beitragen.

Im ersten Teil dieser Studie wurde die Verknüpfung zwischen mitochondrialer Fehlfunktion und der proteasomalen Aktivität analysiert. Hierfür wurde die proteasomale Funktion in sogenannten „mtDNA mutator Mäusen“, einem Model für chronische Fehlfunktion der mitochondrialen Atmungskette, untersucht. Eine verminderte Proteasomaktivität und eine Reduktion der Anzahl von 26S und 30S Proteasomen in embryonalen Fibroblasten dieser Mäuse bestätigten eine enge Verknüpfung von mitochondrialer und proteasomaler Funktion. Eine verminderte Proteasomfunktion wurde darüber hinaus auch in dermalen Fibroblasten von Patienten gezeigt, die einzelne definierte Mutationen in Genen der mitochondrialen Atmungskette aufweisen. Zusätzlich wurde herausgefunden, dass zu den bereits beschriebenen Signalwegen, weitere regulatorische Mechanismen existieren, die mitochondriale und proteasomale Funktion miteinander verknüpfen.

Um zu untersuchen inwieweit Umwelteinflüsse die mitochondriale Funktion in der Lunge beeinflussen, wurde im zweiten Teil der Studie der Effekt von Zigarettenrauch auf mitochondriale Funktion und Qualitätskontrolle in Lungenepithelzellen bestimmt. Alveoläre Epithelzellen der Maus zeigten eine deutliche Hyperfusion der Mitochondrien und eine begleitende Erhöhung der metabolischen Aktivität nach der Behandlung mit Zigarettenrauchextrakt. Die durch Zigarettenrauchextrakt induzierte mitochondriale Hyperfusion war jedoch nicht mit einer proteostatischen Veränderung der Mitochondrien verknüpft. Darüber hinaus wurde In dieser Studie

Zusammenfassung

keine Beeinflussung der mitochondrialen Proteinqualitätskontrolle durch das Proteasom festgestellt. Mitochondriale Hyperfusion scheint daher eine überlebensfördernde Anpassung von alveolären Epithelzellen an nicht-toxische Konzentrationen von Zigarettenrauchextrakt darzustellen.

Im letzten Teil der Studie wurde die Rolle beider Systeme, Proteasom und Mitochondrien, im Rahmen der Lungenalterung untersucht. Dazu wurden Alterungsprozesse sowie proteasomale Funktion in der Lunge von jungen und alten Wildtyp-Mäusen, Proteasom Reporter-Mäusen und Immunoproteasom Knockout-Mäusen untersucht. Dabei wurde beobachtet, dass die Untereinheiten des Immunoproteasoms in Lungen alter Mäusen hochreguliert waren und dementsprechend die Caspase-ähnliche Aktivität des Proteasoms vermindert war. Knockout-Mäuse für die Immunoproteasom Untereinheiten LMP2 oder LMP7 waren jedoch vor physiologischer Lungenalterung nicht geschützt. Diese Ergebnisse legen nahe, dass die veränderte Funktion des Immunoproteasoms nicht ausschlaggebend für die physiologische Lungenalterung ist. Weiterhin deuten sie darauf hin, dass die Alterungsprozesse in gesunden Lungen keine Veränderung der proteasomalen Funktion einschließen. Darüber hinaus wurde in frühzeitig alternden mtDNA mutator Mäusen keine Verknüpfung zwischen mitochondrialer Fehlfunktion und physiologischer Lungenalterung gefunden.

Zusammenfassend bestätigt diese Studie die Hypothese, dass proteasomale und mitochondriale Funktion eng miteinander verknüpft sind. Darüber hinaus wird gezeigt, dass sowohl das mitochondriale wie auch das proteasomale System Reservekapazitäten haben, die sie dazu befähigen trotz milder Beanspruchungen durch Umwelteinflüsse oder während physiologischer Alterungsprozessen funktionsfähig zu bleiben. Da jedoch beide Systeme eng miteinander verbunden sind könnten bei einer kumulativen Belastung durch altersbedingte Fehlfunktion und Exposition mit schädlichen Umwelteinflüssen, wie z.B. Zigarettenrauch, mitochondriale und proteasomale Fehlfunktion einen Grenzwert überschreiten und somit zu vorzeitigen Alterungsprozessen und der Entwicklung von altersbedingten Krankheiten beitragen.

Summary

In living cells the cellular proteome is under constant remodeling as cells adapt to altered physiological states or as cellular proteins become misfolded and need to be degraded. The cellular processes which grant maintenance of a functional proteome are collectively called proteostasis. The proteasome constitutes one of the major intracellular protein degradation systems and is responsible for the turnover of damaged or unwanted proteins with almost 90% of the intracellular proteins being potential proteasome substrates. Especially for misfolded proteins, a timely degradation is necessary to avoid proteotoxic stress, e.g. by formation of protein aggregates. Degradation of proteins by the proteasome system is a very energy demanding process. Hence it was speculated that proteasomal function is interconnected with the function of mitochondria. Additionally, a correlation between mitochondrial and proteasomal dysfunction exists since a decline in the function of both systems is well recognized as hallmark of aging. However, it is unclear how proteasomal and mitochondrial function are directly linked together, especially in settings of chronic mitochondrial respiratory chain dysfunction. Moreover, limited knowledge is available to which extent proteasomal and mitochondrial functions contribute to aging processes specifically in lung tissue during healthy aging or in the development of age-related lung diseases such as chronic obstructive pulmonary disease.

In the first part of this study, the connection between mitochondrial dysfunction and the proteasome was assessed by analyzing proteasome function in the so-called “mtDNA mutator” mouse model, a model of chronic mitochondrial respiratory chain dysfunction. A strong interconnection between mitochondrial and proteasomal function was confirmed in mouse embryonic fibroblasts of mtDNA mutator mice as in these cells decreased proteasomal activity and reduced levels of assembled 26S and 30S proteasomes was found based on a pronounced mitochondrial respiratory chain dysfunction. Importantly, human dermal fibroblasts from patients with single mutations in mitochondrial genes accordingly showed reduced proteasome activity. Furthermore, it was shown that in addition to acute regulation by reactive oxygen species or ATP levels, further signaling mechanisms exist, which connect mitochondrial and proteasomal function in chronic settings.

Second, to assess mitochondrial alterations in response to environmental challenges in the lung, the effect of cigarette smoke exposure on mitochondrial function and quality control in alveolar epithelial cells was analyzed. Murine alveolar epithelial cells exhibited pronounced mitochondrial hyperfusion after treatment with cigarette smoke extract, which was accompanied by increased metabolic activity. Cigarette smoke extract-induced mitochondrial hyperfusion was not associated with a protein stress response at mitochondria. Furthermore, no alteration in mitochondrial protein quality control by the proteasome was observed. Therefore, mitochondrial hyperfusion seems to be

Summary

an adaptive pro-survival response of alveolar epithelial cell mitochondria to nontoxic concentrations of cigarette smoke extract.

Finally, the specific involvement of both systems, proteasome and mitochondria, in healthy aging of the lung was assessed. Therefore typical features of healthy lung aging and proteasome function were analyzed in young and aged wildtype, proteasome reporter and immunoproteasome knockout mice. Hereby, it was observed that immunoproteasome subunits were upregulated in the lungs of aged mice and the caspase-like proteasome activity was concomitantly decreased. However, aged knockout mice for the immunoproteasome subunits LMP2 or LMP7 showed no alteration in proteasome activities while exhibiting typical lung aging phenotypes. This suggests that immunoproteasome function is dispensable for physiological lung aging in mice. These results indicate that healthy aging of the lung does not involve impairment of proteasome function. Furthermore, no connection between mitochondrial dysfunction and lung aging was found in prematurely aging mtDNA mutator mice.

Altogether, this study confirms the hypothesis that the functions of the proteasome and mitochondria are closely connected. Furthermore, it shows that mitochondria as well as the proteasome system provide some spare capacity, which enables them to remain functional upon mild insults during healthy aging or exposure to mild environmental hazards. However, due to the close interconnection of both systems, the simultaneous burden of an age-related functional decline together with noxious environmental exposures such as cigarette smoke might push proteasomal and mitochondrial dysfunction beyond a damage threshold thereby contributing to the pathogenesis of disease states or to a combined functional decline of both systems as described in aging.

1 Introduction

1.1 Protein homeostasis by the proteasome

Proteins are almost indefinitely versatile macromolecules and are involved in nearly every cellular process. The properties of a protein are by large determined by its amino acid sequence. However, for an appropriate cellular function, proteins need to be in a correctly folded state and integrated in a functional protein interaction network (Hartl et al., 2011; Powers and Balch, 2013; Meiners and Ballweg, 2014). Importantly, proteins must preserve conformational flexibility for correct function and therefore possess only limited thermodynamic stability in their native state (Hartl et al., 2011). Furthermore, altered external conditions, e.g. due to different metabolic conditions or physiological or environmental stressors, additionally challenge the stability of protein conformations (Morimoto and Cuervo, 2014). For these reasons, protein homeostasis, i.e. the maintenance of a functional proteome, is of vital importance for the cell. The term proteostasis covers all cellular processes which grant protein homeostasis throughout the whole life cycle of a protein and involves protein maturation, maintenance of protein folding, and degradation of irreparably misfolded or unwanted proteins (Figure 1-1) (Powers and Balch, 2013; Meiners and Ballweg, 2014; Morimoto and Cuervo, 2014). Protein folding is usually coupled with protein synthesis (Hartl et al., 2011; Meiners and Ballweg, 2014). However, as protein translocation in some organelles, e.g. the endoplasmic reticulum or mitochondria, requires proteins to be unfolded some proteins are ultimately folded only after they reach their target organelle (Zimmermann et al., 2006; Schmidt et al., 2010). Maturation of proteins into their proper folding state and maintenance of a native conformation is mostly assisted by chaperone proteins either in the cytosol or in the target organelles. Newly synthesized or misfolded proteins expose hydrophobic sequences which tend to form protein aggregates. Chaperones transiently bind to these exposed hydrophobic sequences of unfolded or partially folded proteins, thereby preventing aggregate formation. Subsequent ATP-triggered release from the chaperone promotes folding into the functional conformation with several binding and release cycles being possible to ensure correct folding (Hartl et al., 2011). In case folding attempts remain unsuccessful, misfolded proteins are targeted for degradation. Since misfolded proteins are especially prone to form aggregates, a timely degradation is needed (Buchberger et al., 2010; Meiners and Ballweg, 2014). Two major protein degradation systems exist in the cell: the ubiquitin proteasome system and the autophagy-lysosomal pathway (Meiners and Ballweg, 2014). Autophagy refers to “self-eating” and involves sequestration of substrates in double-membraned autophagic vesicles and subsequent degradation in the lysosome. During macroautophagy, which is often simply called autophagy, cytosolic cargo is engulfed by elongation of a double membrane which eventually seals to form the autophagosome. After fusion of the autophagosome with the lysosome, cargo is degraded by

Introduction

lysosomal hydrolases (Levine and Kroemer, 2008). Thereby, a wide range of substrates, such as protein aggregates but also whole organelles, can be degraded by autophagy (Kroemer et al., 2010). Although autophagy was long considered to be a bulk degradation pathway, more selective autophagy pathways such as microautophagy or chaperone mediated autophagy were discovered (Kaushik and Cuervo, 2012). Degradation of specific substrates and soluble proteins is, however, mainly executed by the ubiquitin proteasome system (Meiners and Ballweg, 2014).

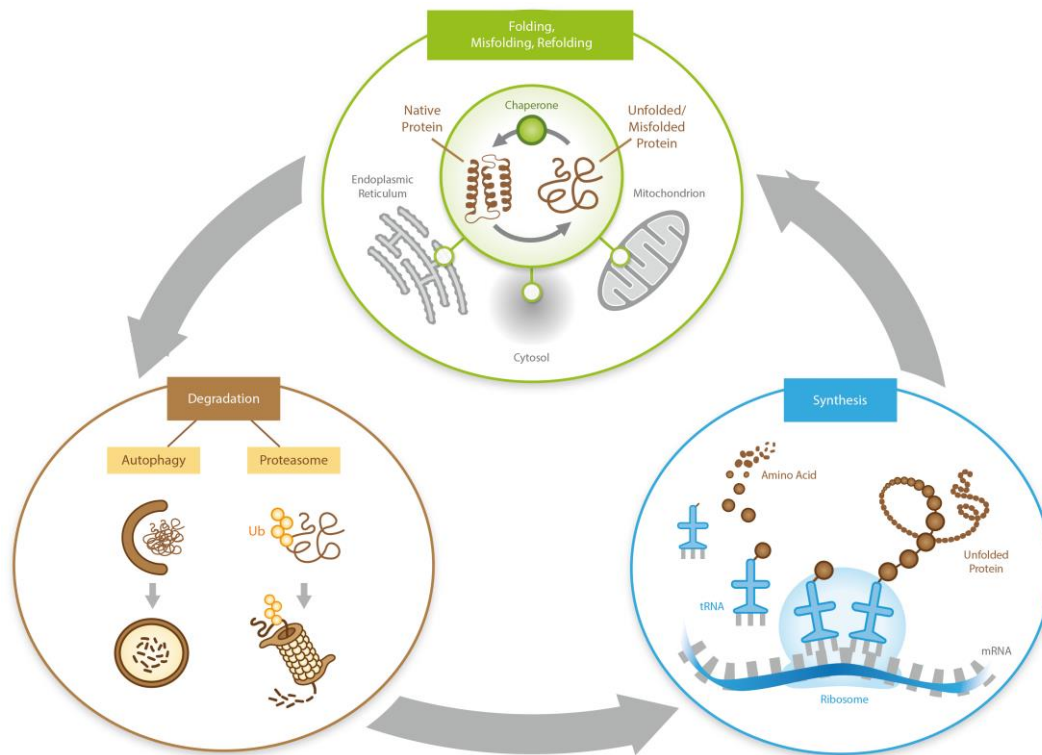


Figure 1-1: Proteostasis during the lifecycle of proteins

Proteostasis takes place throughout the lifecycle of proteins. Proteins are synthesized as a linear polypeptide chain at the ribosomes. Folding into their native structure is assisted by chaperones. Chaperones also maintain the native folding of proteins in the cytosol as well as in other compartments such as endoplasmic reticulum or mitochondria. Sustained protein misfolding induces protein degradation mainly via the proteasomal pathway. For this purpose proteins are tagged with a polyubiquitin chain for recognition by the proteasome and degraded into small peptides. Dysfunctional protein aggregates are mainly removed by engulfment in autophagosomes and degraded after fusion of the autophagosome with lysosomes. Degradation products after autophagic or proteasomal degradation are mostly recycled for the synthesis of new proteins (Meiners and Ballweg, 2014).

1.1.1 The ubiquitin proteasome system

The proteasome is an evolutionary conserved multi-subunit protease and is the major protein degradation pathway in the cell with up to 90 % of the cellular proteome being potential proteasome substrates. The proteasome degrades native as well as misfolded proteins and thus is important for cellular stress responses but also for regulatory and housekeeping purposes (Finley, 2009; Schmidt and Finley, 2013). Generally, attachment of a Lysin-48 (K48)-linked polyubiquitin chain to target

proteins, by a cascade of E1, E2 and E3 ubiquitin ligases, serves as a signal for substrate recognition by the proteasome. However, also ubiquitin-independent degradation pathways and pathways involving ubiquitination on different sites than K48 have been described (Finley, 2009; Komander and Rape, 2012).

1.1.1.1 Proteasome structure and function

The proteasome consists of a core particle, the 20S proteasome, which can associate with several regulatory particles which mediate substrate recognition and proteasome activation (Meiners et al., 2014). The core particle itself consists of four heptameric rings, two α and two β rings in the order “ $\alpha\beta\beta\alpha$ ”, which build up a barrel-like structure (Figure 1-2). Each of the rings consists of seven related but distinct subunits (α 1-7 and β 1-7) with the subunits β 1, β 2 and β 5 harboring the catalytic active sites. Assembly of the proteasome core complex from the 28 individual subunits follows a tightly regulated process and is mediated by proteasome assembly chaperones. The catalytic subunits are assembled as inactive propeptides to avoid premature cleavage of substrates. As a last step of the assembly process the propeptides are autocatalytically cleaved with the active sites facing the inner side of the mature proteasome (Ditzel et al., 1998; Murata et al., 2009).

In the assembled proteasomes the active site of the catalytic subunits lies inside of the central cavity and access to the central channel of the proteasome barrel is restricted by the N-termini of the α subunits. Due to this arrangement the “naked” 20S proteasome core is rather inert and has only low degradation activity (Groll et al., 2000; Finley, 2009; Meiners et al., 2014).

The proteasome contains three distinct catalytic activities. The proteasome subunit β 1 preferentially cleaves substrates after amino acids with acidic residues, β 2 after basic residues and β 5 after hydrophobic residues. The three different active sites are therefore also called caspase-like (C-L), trypsin-like (T-L) and chymotrypsin-like (CT-L) activity, respectively (Finley, 2009; Murata et al., 2009).

The proteasome does not degrade substrates to single amino acids but produces a diverse mix of small oligopeptides (Finley, 2009; Groettrup et al., 2010). While most of these peptides are subsequently degraded to singular amino acids by cytosolic peptidases, some of the generated peptides are further processed and mounted on major histocompatibility complex (MHC) class I molecules and serve as signaling molecules for the immune system (Finley, 2009; Groettrup et al., 2010; Tanaka, 2013). To further assist this process alternative catalytic proteasome subunits are induced in lymphoid tissue and under specific conditions such as virus infection or Interferon (IFN)- γ stimulation and are incorporated into the proteasome core complex. These alternative subunits, LMP2 (β 1i), MECL-1 (β 2i), and LMP7 (β 5i), are preferably incorporated into newly formed proteasomes which assemble into an alternative form of the 20S proteasome known as the immunoproteasome (i20S)(Groettrup et al., 2010; Meiners et al., 2014; Schmidt and Finley, 2013).

Introduction

The immunosubunits are proposed to have altered cleavage specificities and kinetics (Groettrup et al., 2010; Mishto et al., 2014) thereby shifting peptide production towards peptides with hydrophobic C-termini which are preferentially bound by MHC class I molecules (Groettrup et al., 2010). Additionally, immunoproteasomes have been proposed to play a protective role in the cellular response to oxidative stress, which is, however, still a matter of debate (Aiken et al., 2011; Ebstein et al., 2013; Nathan et al., 2013; Seifert et al., 2010). Notably, proteasomes can also exist in mixed forms containing both standard subunits and immunosubunits which further increases the possible variation in cleavage specificity and peptide production by the proteasome (Ferrington and Gregerson, 2012; Meiners et al., 2014; Zanker et al., 2013).

Besides standard- and immunoproteasomes, a third tissue specific proteasome subforms has been described. The alternative subunit $\beta 5t$ was found exclusively expressed in the thymus and incorporates together with LMP2 and MECL-1 in the thymoproteasome (t20S). The $\beta 5t$ subunit exhibits decreased chymotrypsin-like cleavage activity and thymoproteasomes were found to be important for selection of CD8⁺ T-cells in the thymus (Murata et al., 2007; Tanaka, 2013).

1.1.1.2 Regulation of proteasome function

Proteasome activity is mainly regulated by binding of regulatory particles which modulates proteasomal turnover rate and substrate specificity. Four different proteasome activators are known up to date: the 19S regulatory particle, the PA28 $\alpha\beta$ -, the PA28 γ - or the PA200-regulatory particle. Proteasomal activators can bind to one or both ends of the 20S core particle thereby mediating conformational changes in the α subunits leading to an open conformation which enables substrate access. This arrangement leads to pronounced activation of the proteasome upon assembly of regulatory particles and ensures a highly specific turnover as only substrate proteins are gated to the active sites (Gallastegui and Groll, 2010; Li and Rechsteiner, 2001; Meiners et al., 2014; Schmidt and Finley, 2013). In addition to the proteasomal activators another regulatory particle, PI31, exists and was initially described as an inhibitor of proteasomal activity, which is, however, still under debate (Meiners et al., 2014; Schmidt and Finley, 2013).

The 19S regulatory particle is the most abundant and best studied regulator. It consists of two parts: the 10 subunit base complex and the 9 subunit lid complex (Finley, 2009). Binding of the 19S regulator particle can occur either at one end of the 20S core or at both ends, resulting in 26S and 30S proteasome formation, respectively (Figure 1-2). The 19S regulator is required for the degradation of polyubiquitinated proteins as it is responsible for substrate recognition, deubiquitination, unfolding and translocation into the proteasome core (Finley, 2009; Meiners et al., 2014; Unverdorben et al., 2014). 19S-dependent degradation is strictly ATP-dependent and ATP

withdrawal leads to disassembly of 19S particles from the 20S proteasome (Kim et al., 2012; Liu et al., 2006a).

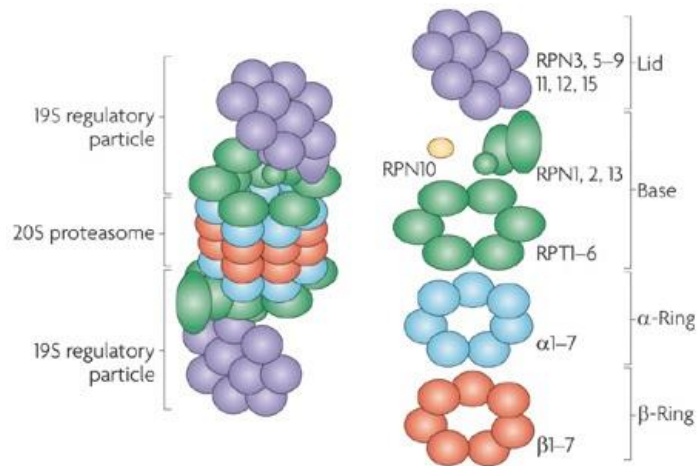


Figure 1-2: Schematic depiction of 30S proteasome particles and subunits

The 30S proteasome consists of two 19S regulatory particles on both sides of the 20S core particle. The 20S core particle consists of two α rings assembled by the subunits α 1-7 and two β rings assembled by the subunits β 1-7. The 19S regulatory particle can be further divided in base and lid and is assembled by several ATPase (Rpt) and non-ATPase (Rpn) subunits (Figure modified from: Murata et al., 2009).

In contrast to the common 19S regulatory particle, the alternative regulators PA28 $\alpha\beta$, PA28 γ and PA200 promote ATP- and ubiquitin-independent degradation. However, further research is still needed to delineate the specific substrates and functions of these alternative regulators. PA28 $\alpha\beta$ is induced in cells treated with INF- γ and highly expressed in professional antigen presenting cells and is therefore believed to play a role in immune defense and antigen presentation (Cascio, 2014). PA28 γ which is present exclusively in the nucleus and PA200 might be involved in degradation of transcription factors and cell cycle regulators or acetylated histones, respectively (Meiners et al., 2014; Schmidt and Finley, 2013). To be degraded in an ubiquitin-independent process substrate proteins need to be at least partially unfolded which can occur in response to aging, protein oxidation or other stress-induced modifications. Additionally, also native proteins which contain large intrinsically disordered sequences can be degraded via ubiquitin-independent mechanisms (Ben-Nissan and Sharon, 2014; Finley, 2009). Of note, different regulatory particles can simultaneously attach to different ends of the proteasome core which opens the possibility of alternative proteasome complexes such as for example 19S-20S-PA28 (Meiners et al., 2014).

An overview about the gene and protein nomenclature of the proteasome subunits and regulatory particles analyzed in this study is given in Table 1-1.

Table 1-1: Gene and protein names of proteasome subunits analyzed in this study

Gene name	Protein name	Localization in the proteasome
PSMA3	$\alpha 7$	20S α ring
PSMB6	$\beta 1$	20S β ring
PSMB7	$\beta 2$	20S β ring
PSMB5	$\beta 5$	20S β ring
PSMB8	LMP7 ($\beta 5i$)	i20S β ring
PSMB9	LMP2 ($\beta 1i$)	i20S β ring
PSMB10	MECL-1 ($\beta 2i$)	i20S β ring
PSMC3	Rpt5	19S ATPase subunit
PSMD7	Rpn8	19S non-ATPase subunit
PSMD11	Rpn6	19S non-ATPase subunit
PSME1	PA28 α	PA28 $\alpha\beta$
PSME3	PA28 γ	PA28 γ

Beyond binding of regulatory particles, proteasome activity can be regulated by posttranslational modifications of proteasomal subunits or by non-covalently binding of signaling molecules. Several posttranslational modifications such as acetylation, phosphorylation, N-acetyl-glucosamylation or oxidation have been detected on proteasomal subunits with most modifications being located at the 20S α subunits or at the 19S regulatory particle. However, it is by now not fully understood how these modifications are introduced and how they affect proteasomal activity. Acetylation of both the 20S proteasome and proteasomal regulators might increase proteasomal activity. One study found activation of the proteasome after 20S acetylation (Wang et al., 2013), while another demonstrated increased degradation of model substrates after PA28 γ acetylation (Liu et al., 2013). Phosphorylation of the proteasome was reported to have activating as well as inactivating effects on the proteasome depending on the positions and the kinases involved (Liu et al., 2006b; Lokireddy et al., 2015; Zhang et al., 2007a). Attachment of O-linked N-acetylglucosamine (O-GlcNAcylation) to 19S subunits decreased 26S complex formation and proteasome activity (Xu et al., 2012; Zhang et al., 2003). Similarly, oxidative modifications were shown to decrease proteasome activity and levels of 26S complexes (Breusing and Grune, 2008; Livnat-Levanon et al., 2014). In addition to posttranslational modifications, non-covalent binding of small signaling molecules can affect proteasomal activity. The most important mediator hereby is the binding of ATP which, as outlined above, is required for 26S complex formation (Kim et al., 2012; Liu et al., 2006a; Peth et al., 2013). Furthermore, NADH was shown to reversibly bind to 19S subunits thereby stabilizing 26S proteasome formation in the absence of ATP. Concordantly, increasing the NADH/NAD⁺ ratio increased proteasome activity (Tsvetkov et al., 2014).

In summary, proteasomal degradation is tightly regulated mainly by the attachment of regulatory particles to the proteasomal core. These regulators thereby mediate quantitative changes in proteasomal degradation but also qualitative differences as they can also modify substrate specificity. It is important to note that many posttranslational modifications also modify proteasomal activity by interfering with complex formation of regulatory particles with the 20S core. This further emphasizes the important role of proteasomal regulators as a fast and adaptive system to regulate proteasomal degradation.

1.2 Mitochondrial function and protein homeostasis

Mitochondria are organelles derived from an endosymbiotic fusion of α -proteobacteria with eukaryotic cells. This unique background leads to some special biological features of these organelles. Mitochondria are double membraned organelles thereby establishing an intraorganellar compartmentalization in matrix, inner mitochondrial membrane (IMM), intermembrane space (IMS) and outer mitochondrial membrane (OMM). Additionally, mitochondria contain their own DNA (mitochondrial DNA: mtDNA) with several hundred copies of mtDNA existing in every cell. While most mitochondrial genes have been transferred to the nucleus during evolution, the mtDNA is still coding for 13 essential proteins of the mitochondrial respiratory chain as well as for 22 tRNAs and 2 ribosomal RNAs (16S and 12S) of the mitochondrial protein biosynthesis machinery (Gaziev et al., 2014; Mishra and Chan, 2014; Nunnari and Suomalainen, 2012). The main cellular task for mitochondria is energy metabolism by generating ATP as a result of oxidative phosphorylation in the respiratory chain (Nicholls and Ferguson, 2002). The respiratory chain consists of four protein supercomplexes (complex I-IV) which build up the electron transport chain (ETC) that utilizes energy, which is gained by the oxidation of nutrients, to generate a proton gradient across the inner mitochondrial membrane. Notably, correct assembly of the supercomplexes of the ETC requires a synchronized expression of nuclear DNA and mtDNA-encoded subunits. The gradient generated by the ETC builds up an electrochemical membrane potential ($\Delta\Psi$) which drives the fifth protein complex in the respiratory chain, the mitochondrial ATP synthase (complex V), to generate ATP by controlled reflux of protons into the mitochondrial matrix (Figure 1-3)(Mishra and Chan, 2014; Nicholls and Ferguson, 2002). Besides ATP production, mitochondria also are important for apoptosis and several cellular biosynthesis pathways such as iron-sulfur-cluster synthesis. Furthermore, they serve as a signaling hub for example by mediating reactive oxygen species (ROS) production or Ca^{2+} signaling (Chandel, 2014; Liesa and Shirihai, 2013; Mishra and Chan, 2014).

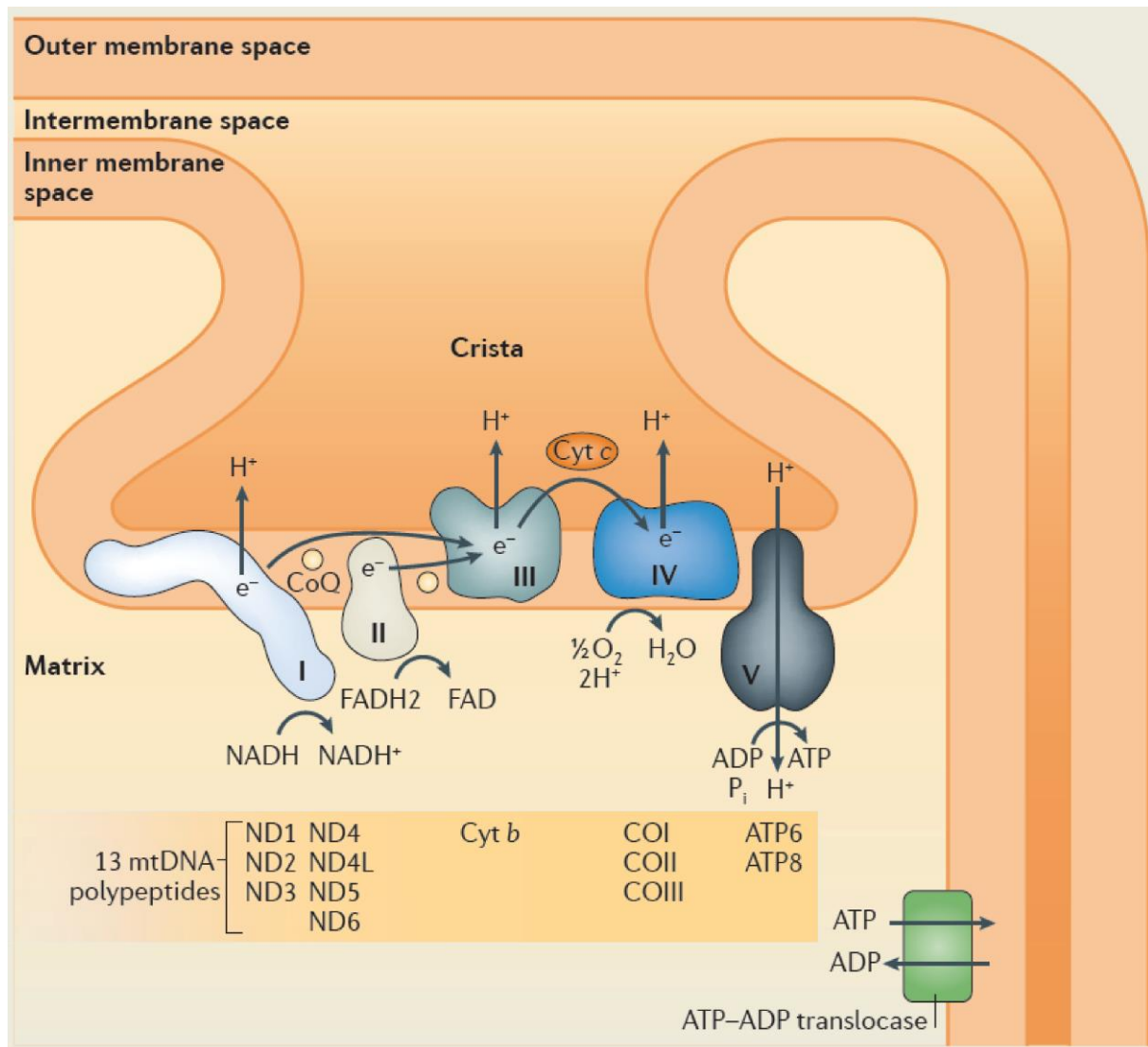


Figure 1-3: Mitochondrial compartmentalization and respiratory chain function

Mitochondria are double membraned organelles consisting of an outer mitochondrial membrane, an intermembranespace, the inner mitochondrial membrane and the matrix. The inner mitochondrial membrane is folded inwards thereby increasing its surface area and generating additional intermembranespace compartments called cristae. The mitochondrial respiratory chain is located in the inner mitochondrial membrane in the cristae regions. Electrons are fed into the respiratory chain by oxidation of NADH or FADH₂ at complex I or complex II, respectively. Electron transport along the respiratory chain is mediated by the soluble shuttle molecules ubiquinone (CoQ) and cytochrome c (Cyt c). ETC activity leads to transport of protons from the matrix to the intermembrane space at complex I, III and IV thereby building up the mitochondrial membrane potential. Proton backflow through complex V powers ATP production in the mitochondrial matrix. ATP and ADP are exchanged with the cytosol via the ATP-ADP translocase in the inner mitochondrial membrane. While most mitochondrial proteins are encoded by nuclear DNA, the 13 depicted subunits of the respiratory chain complexes I, III, IV and V are encoded by mitochondrial DNA and translated in the mitochondrial matrix (Figure modified from Mishra and Chan, 2014).

1.2.1 Mitochondrial protein homeostasis

To maintain these crucial mitochondrial functions, protein homeostasis in the mitochondria needs to be tightly regulated. Therefore, sophisticated quality control systems have evolved to cope with damage of mitochondrial structures. Although mitochondria possess their own genome, most mitochondrial proteins are encoded by nuclear DNA. These mitochondrial proteins are translated in the cytosol, recognized by a mitochondrial target sequence and transported through the mitochondrial protein import machinery into their target compartment where they are folded into their functional conformation (Schmidt et al., 2010). Of note, a first layer of protein quality control comes into action at a very early stage, as damaged or mistargeted proteins can be degraded by the proteasome even before their import (Anand et al., 2013; Bragoszewski et al., 2013; Wrobel et al., 2015). For maintenance of protein homeostasis in the mitochondria, several additional quality control mechanisms exist which involve the mitochondrial unfolded protein response (mtUPR), mitochondrial dynamics, degradation of mitochondrial proteins by the proteasome in a process termed mitochondria-associated degradation (MAD) and degradation of whole mitochondria via the autophagy pathway.

1.2.1.1 Mitochondrial unfolded protein response

Mitochondria possess their own arsenal of molecular chaperones which assist proteins in folding and refolding. Especially as mitochondrial proteins are imported in an unfolded state, a functional folding environment is required to avoid protein aggregation in mitochondria. Matrix chaperones include mitochondrial variants of the cytosolic heat shock proteins (HSPs) such as the mitochondrial mtHSP70 or HSP60. In the intermembrane space the TIM9-TIM10 complex of the mitochondrial import machinery performs chaperone activity and facilitates protein folding (Campello et al., 2013; Pellegrino et al., 2013; Schmidt et al., 2010). In addition to chaperones, mitochondria house several proteases such as the Lon or ClpP proteases in the matrix which perform quality control as well as housekeeping proteolytic tasks (Anand et al., 2013). Additionally, the membrane bound m-AAA (facing the matrix) or i-AAA (facing the IMS) protease complexes or free proteases such as the OMA1 protease in the IMS extend the protease capacities to membrane and IMS compartments (Anand et al., 2013; Campello et al., 2013).

If protein damage in the mitochondria exceeds the folding capacity of the mitochondrial chaperone system, a mitochondrial unfolded protein response (mtUPR) is triggered. The mtUPR signals to the nucleus and induces expression of mitochondrial chaperones and proteases thereby increasing the mitochondrial proteostasis capacity in order to restore mitochondrial homeostasis (Jovaisaite et al., 2013). Most studies assessing the mtUPR were performed in *C. elegans*. In this model organism, accumulating misfolded proteins in the mitochondrial matrix are degraded by the matrix protease

Introduction

ClpP into small peptides. These peptides are transported into the cytosol and lead to activation of the transcription factor ATFS-1. ATFS-1, which contains both a mitochondrial and a nuclear targeting sequence, then translocates to the nucleus where it enhances transcription of mitochondrial quality control proteins such as HSP60 or mtHSP70 chaperones (Pellegrino et al., 2013). In mammals, the mechanism involved in mitochondria to nucleus signaling is far less understood since no mammalian orthologue of ATFS-1 exists. However, it was shown that mammalian mtUPR involves e.g. the transcription factor CHOP (Arnould et al., 2015; Jovaisaite et al., 2013; Pellegrino et al., 2013). Furthermore, in mammals a mechanistically distinct unfolded protein responses for the mitochondrial IMS ($_{IMS}UPR$) exist which leads to increased expression of IMS proteases, induction of proteasome activity and increased mitochondrial biosynthesis (Papa and Germain, 2011; Pellegrino et al., 2013; Radke et al., 2008).

1.2.1.2 Mitochondrial dynamics

Mitochondria are not static but form a dynamic network of tubular organelles with constant fusion and fission activity. The final shape and network connectivity is determined by the balance between fusion and fission events (Youle and van der Bliek, 2012). The mitochondrial network dynamically reacts to cellular stress and constitutes an important mechanism for mitochondrial quality control (Figure 1-4). Mitochondrial fusion allows content mixing in mitochondria, thereby diluting mild damage that might be present in a subset of mitochondria. Fused mitochondria share a common set of proteins and mtDNA molecules. Therefore, fused mitochondria can complement each other and compensate for damaged proteins or mtDNA mutations in one of the fused mitochondria (Mishra and Chan, 2014; Youle and van der Bliek, 2012). Mitochondrial fission, on the other hand, allows for segregation of severely damaged mitochondria. Defective mitochondria can contaminate the mitochondrial network, for example by increased ROS production in the respiratory chain which causes protein oxidation in the mitochondria. Mitochondrial fission acts as a quality control mechanism by sequestering damaged mitochondria from the mitochondrial network. Each fission step produces asymmetrically polarized mitochondria with damaged mitochondria failing to recover and repolarize (Twig et al., 2008; Youle and van der Bliek, 2012). Degradation of fusion mediators on these damaged organelles by the proteasome renders them incapable of reentering the mitochondrial network leaving behind fragmented mitochondria which are subsequently degraded via the autophagy pathway (Jin and Youle, 2012; Tanaka et al., 2010; Twig et al., 2008). Mitochondrial fission together with the removal of severely damaged mitochondria by autophagy thereby increases average mitochondrial health. Mitochondrial health is therefore highly affected by the frequency of fusion and fission events (Patel et al., 2013).

In addition to mitochondrial quality control, mitochondrial fusion and fission affects mitochondrial bioenergetic function. Hence, by dynamically adapting to cellular stress and cellular energy demands,

mitochondrial morphology also represents an important adaptive mechanism for general cellular homeostasis (Liesa and Shirihai, 2013). Mitochondrial elongation was reported in response to a variety of stressors and was therefore termed stress-induced mitochondrial hyperfusion (Blackstone and Chang, 2011; Gomes et al., 2011; Tondera et al., 2009). Mitochondrial hyperfusion provides a stress resolving mechanism for the cell as elongated mitochondria show increased efficiency in ATP synthesis thereby contributing to the cells' ability to repair cellular damage. Additionally, hyperfused mitochondria are protected from degradation by autophagy (Blackstone and Chang, 2011; Gomes et al., 2011). Hence stress-induced mitochondrial hyperfusion is regarded to be a pro-survival response (Blackstone and Chang, 2011; Tondera et al., 2009). Mitochondrial fragmentation, on the other hand, is an early event upon induction of apoptosis. In this sense, mitochondria also contribute to the induction of controlled cell death during overwhelming cellular stress (Elgass et al., 2012; Liesa et al., 2009).

The molecular machinery mediating mitochondrial fusion and fission consists of several large GTPases of the dynamin-related protein family. The key proteins in these processes are dynamin-related protein (DRP) 1 (mitochondrial fission), Mitofusin (MFN) 1 and MFN2 (outer membrane fusion) and optic atrophy (OPA) 1 (inner membrane fusion) (Scorrano, 2013). The mitochondrial fission protein DRP1 resides in the cytosol and needs to be translocated to mitochondria prior mitochondrial fission. DRP1 localization and thereby fission activity is regulated by phosphorylation events. Phosphorylation at Ser⁶¹⁶ induces mitochondrial localization and subsequent fission while phosphorylation at Ser⁶³⁷ inactivates DRP1 (van der Bliek et al., 2013). The fusion mediators MFN1 and MFN2 reside in the outer mitochondrial membrane. MFN1 is described to tether mitochondria together in the fusion process. The exact role of MFN2 still needs to be elucidated but it is suggested to participate in later steps of fusion (Scorrano, 2013). Although usually both mitofusins are expressed in the same cell, MFN1 and MFN2 can maintain fusion without the second mitofusin, showing at least partial redundancy (van der Bliek et al., 2013). Outer membrane fusion is almost always coordinated with inner membrane fusion, which is mainly mediated by OPA1. Several isoforms of OPA1, including at least two long and three short isoforms, are generated by differential cleavage of OPA1 with both long and short isoforms being required for fusion (Quiros et al., 2013; Scorrano, 2013). Upon mitochondrial stress, fusion is inhibited by proteasomal degradation of MFN1 and MFN2 and proteolytic cleavage of long OPA1 isoforms by the IMS protease OMA1 (van der Bliek et al., 2013; Cohen et al., 2008; Quiros et al., 2013).

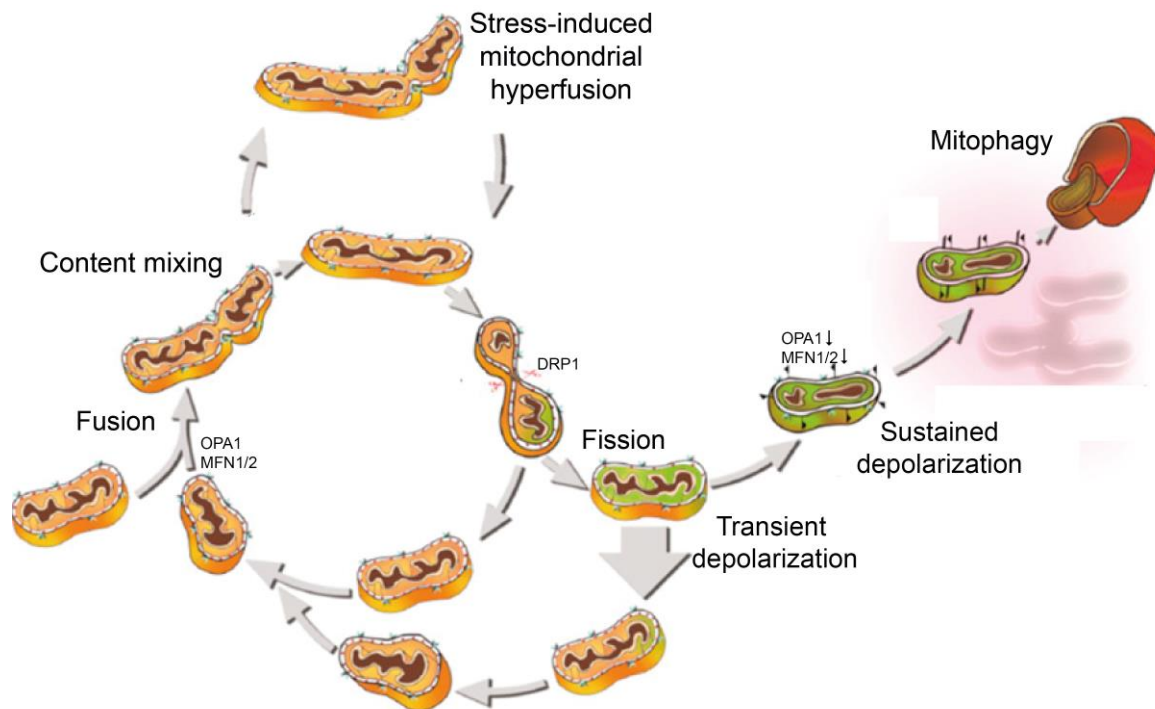


Figure 1-4: Mitochondrial dynamics as part of the mitochondrial quality control system

Mitochondrial dynamics are characterized by a cycle of fusion and fission events. Mitochondrial fusion is mediated by MFN1 and MFN2 responsible for OMM fusion and OPA1 for IMM fusion. Mitochondrial fusion allows content mixing and thereby complementation in damaged mitochondria. Furthermore, under conditions of mild cellular stress the mitochondrial network becomes hyperfused thereby increasing cellular ATP production and sparing mitochondria from autophagy. Mitochondrial fission is mediated by DRP1 and leads to generation of asymmetrically polarized daughter mitochondria. If transient depolarization of daughter mitochondria can be resolved mitochondria reenter the mitochondrial network. Sustained depolarization, however, leads to degradation of MFN1 and MFN2 by the proteasome and to proteolytic cleavage of OPA1 thereby preventing refusion. Fragmented and depolarized mitochondria are subsequently degraded by mitophagy (Figure modified from Liesa and Shirihai, 2013).

1.2.1.3 Mitochondria-associated degradation

In addition to degradation of mitochondrial proteins by mitochondrial proteases, mitochondrial proteins can be degraded by the cytosolic ubiquitin proteasome system. First evidence of degradation of mitochondrial proteins by the ubiquitin proteasome system was given by the finding that several mitochondrial proteins are ubiquitinated in the cell and inhibition of the proteasome leads to accumulation of ubiquitinated mitochondrial proteins (Livnat-Levanon and Glickman, 2011; Margineantu et al., 2007). Indeed, several E3 ubiquitin ligases were found to reside in the OMM and can ubiquitinate mitochondrial proteins (Heo and Rutter, 2011). As the proteasome is excluded from mitochondrial compartments and can only interact at the cytosolic site of the outer mitochondrial membrane a protein retro-translocation mechanism has been proposed to work at the outer mitochondrial membrane (Taylor and Rutter, 2011). In response to mitochondrial damage the cytosolic protein VMS1 localizes to mitochondria and recruits the AAA ATPase p97/VCP and its adaptor protein Npl4. VCP then acts as a translocase and uses ATP to extract proteins from the

mitochondrial membrane and subsequently shuttles them to the proteasome (Heo and Rutter, 2011; Heo et al., 2010; Taylor and Rutter, 2011). Due to its similarity with the endoplasmic reticulum-associated degradation (ERAD) pathway (Claessen et al., 2012), this mitochondrial degradation process was termed mitochondria-associated degradation (MAD) (Chatenay-Lapointe and Shadel, 2010). While the VCP-Npl4 complex is also involved in ERAD where it colocalizes with the adaptor protein Ufd1, VMS1 seems to be exclusive for mitochondrial localization of VCP (Taylor and Rutter, 2011). To date, several proteins which are degraded by this pathway have been recognized such as the mitochondrial fusion mediators MFN1 and MFN2 (Cohen et al., 2008; Karbowski and Youle, 2011; Ross et al., 2015; Xu et al., 2011). Most mitochondrial substrates for the proteasome are proteins of the outer mitochondrial membrane. However, also proteins from inner compartments were described as substrates for proteasomal degradation. The mechanism how these proteins are translocated to the proteasome, however, remains unclear (Azzu and Brand, 2010; Azzu et al., 2010; Heo and Rutter, 2011; Karbowski and Youle, 2011).

Additionally, proteasomes can be recruited to the outer mitochondrial membrane themselves and even adaptor proteins for proteasomes on mitochondria were described. (Launay et al., 2013; Nakagawa et al., 2007; Yoshii et al., 2011) However, whether proteasomal localization to mitochondria is parallel to MAD or interacts with MAD is still unclear (Livnat-Levanon and Glickman, 2011).

1.2.1.4 Mitophagy

If complementation of mitochondrial function by fusion, or refolding or degradation of mitochondrial proteins fails to repair mitochondrial damage, whole organelles can be degraded via the autophagy-lysosomal pathway. This mitochondria-specific autophagy is called mitophagy (Youle and Narendra, 2011). Several distinct mitophagy pathways have been described to date. For example in erythrocytes, removal of mitochondria during differentiation is executed via a pathway dependent on the protein NIX at the OMM (Mishra and Chan, 2014). Mitophagy as a response to mitochondrial damage, however, is mainly regulated by the PINK1/Parkin pathway (Campello et al., 2013; Jin and Youle, 2012; Youle and Narendra, 2011). PINK1 is constantly expressed and imported into mitochondria followed by rapid degradation by mitochondrial proteases. Mitochondrial damage leads to impairment in mitochondrial membrane potential and thereby reduced import of PINK1 in the IMM. Thereby, PINK1 selectively accumulates on damaged mitochondria while it is degraded in healthy mitochondria (Jin and Youle, 2012; Narendra et al., 2010). Upon accumulation of PINK1, the E3 ligase Parkin translocates to mitochondria where it induces ubiquitination of several OMM proteins such as MFN1, MFN2 or VDAC1 (Chan et al., 2011; Geisler et al., 2010; Tanaka et al., 2010; Yoshii et al., 2011). Ubiquitination of OMM proteins subsequently triggers degradation of some proteins by the proteasome system utilizing the MAD pathway. Accordingly, mitophagy also was

found to be decreased in the absence of VCP or after proteasome inhibition (Chan et al., 2011; Tanaka et al., 2010; Yoshii et al., 2011). Additionally, Parkin induces polyubiquitination with lysine 63-linked polyubiquitin chains, which are usually linked to signaling but not proteasomal degradation, and thereby facilitates binding of the ubiquitin receptor protein p62 to mitochondria. p62 can further interact with the autophagy regulator LC3B fostering the engulfment of mitochondria into autophagosomes (Geisler et al., 2010; Youle and Narendra, 2011). However, the exact role of p62 is still unclear as it may or may not be required for PINK1/Parkin mediated mitophagy (Jin and Youle, 2012). Importantly, mitochondrial fission and degradation of mitofusins by the proteasome facilitates mitophagy probably by reducing mitochondrial size and thereby enabling inclusion into the autophagosome (Mishra and Chan, 2014; Youle and Narendra, 2011).

1.3 Interconnections between mitochondrial and proteasomal function

As outlined above, mitochondria possess an extensive arsenal of quality control. The ubiquitin proteasome system, although excluded from mitochondria by the mitochondrial membranes, contributes at several stages to mitochondrial quality control. Proteasomes degrade misfolded mitochondrial proteins in the MAD pathway. Additionally, mitochondrial fusion and fission mediators are degraded by the proteasome and therefore effective segregation of damaged organelles from the mitochondrial network requires proteasomal activity. Lastly, proteasomes might also be involved in the initiation of Parkin-mediated mitophagy.

Furthermore, another possible link between mitochondria and proteasomes is given by the facts that the proteasome and most proteostatic processes are highly dependent on ATP (Buchberger et al., 2010; Kim et al., 2012; Liu et al., 2006a; Zhang et al., 2007b) and the mitochondrial respiratory chain is the main ATP-generating process in the cell (Brand and Nicholls, 2011; Nicholls and Ferguson, 2002).

Consequently, it is tempting to speculate that mitochondrial function and proteasomal function are closely interconnected and play important roles in maintaining cellular and organismal health. However, only few publications directly explored the interconnection between mitochondrial and proteasomal function.

1.3.1 Effect of proteasome function on mitochondria

Some evidence exists for the effect of proteasomal inhibition on mitochondrial function. Treatment with nontoxic doses of proteasome inhibitors decreased activity of mitochondrial respiratory chain complexes I, II, III and V in human fetal fibroblasts (Torres and Perez, 2008). Furthermore, proteasome inhibitor treatment of Chinese hamster ovary cells reduced mitochondrial membrane potential and increased mitochondrial superoxide generation (Maharjan et al., 2014). Additionally,

treatment of neurons with proteasome inhibitors was associated with a decrease in mitochondrial membrane potential as an early step during apoptosis (Goldbaum et al., 2006; Papa et al., 2007). Furthermore, in cells with a chronic, mild decrease in proteasome activity, a reduction of maximal oxygen consumption and decreased viability in the absence of glucose was shown (Sullivan et al., 2004) indicating impaired mitochondrial function. Moreover, increased association of mitochondria with autophagosomes was observed in response to proteasome inhibition (Sullivan et al., 2004). Furthermore, growth of a yeast mutant with a heat sensitive subunit of the 19S proteasome at the restrictive temperature led to reduced mitochondrial numbers by induction of mitophagy (Takeda et al., 2010). Additionally, a siRNA screen in *Drosophila* S2 cells revealed reduced mitochondrial numbers and increased mitophagy in response to the silencing of proteasomal genes (Fukuoh et al., 2014).

In addition to a reduction in mitochondrial function, proteasome inhibition affects mitochondrial morphology and network dynamics. Yeast Rpn11 mutant cells showed decreased growth on glycerol as well as mitochondrial fragmentation (Rinaldi et al., 2007). In contrast, Rpn3 mutants presented large mitochondrial aggregates indicative of increased fusion (Joshi et al., 2011). Furthermore, deletion of the yeast homologue for PA200, Blm10, also induced mitochondrial fragmentation (Tar et al., 2014). Similarly, in human cell lines treated with proteasome inhibitor and in *C. elegans* treated with siRNA against proteasome subunits a fragmented mitochondrial network was observed (Livnat-Levanon et al., 2014). However, it has to be noted that mitochondrial fragmentation and loss of mitochondrial membrane potential usually precedes apoptosis (Liesa et al., 2009) and proteasome inhibition is known to induce apoptosis (Frankland-Searby and Bhaumik, 2012). Therefore, caution has to be taken when assessing the effects of proteasome inhibition on mitochondria, to distinguish between physiological effects due to altered proteasome activity and secondary effects in cell death pathways.

Altogether, proteasome inhibition seems to reduce mitochondrial function thereby increasing mitochondrial ROS production and induction of mitophagy. This is well in accordance with the above described role of the proteasome in mitochondrial quality control. Reduced quality control increases mitochondrial damage which might add to increased mitochondrial ROS production by electron leakage from the respiratory chain (Balaban et al., 2005; Murphy, 2009). Consequently, mitophagy is induced to degrade damaged mitochondria and to compensate for impaired proteasomal quality control. Additionally, as the fusion and fission mediators MFN1 and MFN2 and DRP1 are degraded by the proteasome (Cohen et al., 2008; Wang et al., 2011), an effect of proteasome inhibition on mitochondrial dynamics can well be explained.

1.3.2 Effect of mitochondrial function on the proteasome

In addition to the effect of proteasome dysfunction on mitochondria, some reports demonstrate effects of mitochondrial dysfunction on proteasome function. Mitochondria are the powerhouse of the cell and proteasomes are a huge ATP-consuming machine. Hence, it seems plausible that mitochondrial metabolism can affect proteasome activity. Metabolic sensors such as adenosine monophosphate-activated protein kinase (AMPK) or protein kinase A (PKA) can induce posttranslational modifications of the proteasome and thereby modulate its activity (Ronnebaum et al., 2014; Zhang et al., 2007b). AMPK is the major energy sensor of the cell and is activated upon low ATP availability. AMPK activation subsequently stimulates ATP producing processes and inactivates ATP consuming processes (Hardie et al., 2012). Indeed, AMPK activation was shown to decrease proteasome activity, while in turn AMPK inhibition increased proteasomal activity (Ronnebaum et al., 2014; Viana et al., 2008; Xu et al., 2012). Two potential mechanisms how AMPK influences proteasomal activity have been described. On the one hand, AMPK activation induces O-GlcNAc transferase mediated O-GlcNAcylation of the proteasome promoting 20S-19S disassembly (Xu et al., 2012). On the other hand, AMPK interacts with Rpn6 and was shown to directly phosphorylate this subunit (Moreno et al., 2009). However, how this modification affects proteasome activity is still unknown. In contrast to AMPK-induced inactivation, PKA induces phosphorylation of the 19S proteasome subunits Rpt6 and Rpn6 thereby increasing proteasome activity (Lokireddy et al., 2015; Zhang et al., 2007a). However, although inhibition of mitochondria can for example induce AMPK activation (Distelmaier et al., 2014), a direct connection between mitochondrial and proteasomal function via AMPK or PKA has not yet been described.

In addition to metabolic control of the proteasome, it was reported that an increased need for mitochondrial quality control by the proteasome can lead to proteasomal activation. Induction of the unfolded protein response of the mitochondrial intermembrane space by overexpression of an unstable IMS protein induced an increase in proteasome activity (Papa and Germain, 2011). Likewise, a recent report showed that a defect in the mitochondrial protein import machinery and therefore accumulation of mitochondrial proteins that cannot be correctly imported, induced upregulation of proteasome activity (Wrobel et al., 2015). These results further underline the importance of the proteasome in mitochondrial quality control and suggest an adaptive regulation of proteasomal activity by mitochondrial dysfunction.

The direct effect of mitochondrial dysfunction on proteasome activity was analyzed by some other studies by testing if inhibition of the mitochondrial respiratory chain could induce alterations in proteasome function. Indeed, treatment of HEK cells with rotenone (complex I inhibitor), antimycin A (complex III inhibitor) but not with KCN (complex IV inhibitor) decreased proteasomal degradation of

ubiquitin fused GFP (Chou et al., 2010). Similarly, in NT2 human carcinoma cells, the complex I inhibitors MPP⁺ or rotenone diminished proteasome activity measured by degradation of small peptidic proteasome model substrates (Domingues et al., 2008). These effects were attributed to an increase in mitochondrial ROS production upon respiratory chain inhibitor treatment (Chou et al., 2010; Domingues et al., 2008). Additionally, a recent siRNA screen in *C. elegans* expressing ubiquitinated GFP as a proteasome reporter showed that knockdown of respiratory chain subunits or enzymes involved in mitochondrial metabolic processes decreases proteasome activity. This effect was attenuated by treatment with antioxidants such as N-acetyl cysteine (NAC) (Segref et al., 2014) showing its dependency on cellular ROS. A more detailed description of proteasomal alterations in response to respiratory chain inhibitors was provided by Livnat-Levanon et al. (2014). Treatment of yeast cells or hamster kidney cells with antimycin A led to disassembly of 26S proteasomes thereby decreasing proteasome activity and inducing accumulation of ubiquitinated proteasome substrates. Again, this effect could be partially reverted with DTT showing a dependency of oxidative modifications induced upon respiratory chain inhibition (Livnat-Levanon et al., 2014). This ROS-dependent decrease of proteasomal activity in response to respiratory chain inhibition is well in accordance with the already known influence of ROS on the proteasome system (Aiken et al., 2011; Breusing and Grune, 2008; Wang et al., 2010). However, one caveat remains as it is unclear to which extent this effect is physiologically relevant. It was shown that under unstressed or mildly stressed conditions mitochondrial ROS acts as a signaling molecule in cells and is required for cellular homeostasis (Sena and Chandel, 2012). Pharmacologically inhibiting the respiratory chain, however, strongly and acutely increases mitochondrial ROS production to a level which is probably highly above normal ROS production *in vivo* (Murphy, 2009). Furthermore, much of the effect of mitochondrial ROS *in vivo* might be dependent on the balance between ROS and cellular antioxidant defenses (Sena and Chandel, 2012) and hence might not be well reflected by an acute outburst of ROS production.

As the dependency of 26S proteasomes on ATP is well documented, decreased ATP levels in response to mitochondrial damage were suggested as another mechanism contributing to diminished proteasome activity. Indeed, Huang et al. showed that treatment of primary rat cortical neurons with antimycin A, rotenone or the complex V inhibitor oligomycin induces a decrease in 26S proteasome assembly and subsequent accumulation of ubiquitinated substrates. This correlated with decreased ATP levels in treated cells (Huang et al., 2013). However, as the treatment conditions in this study were associated with induction of necrosis and substantial loss in cell viability (Huang et al., 2013) it is not clear whether loss of proteasome function is causally linked to reduced ATP levels or rather to the induction of cell death or other confounding factors. Another study in primary rat neurons showed that rotenone or MPP⁺-induced decrease in proteasome activity could be reversed by

Introduction

increased glucose supplementation to the cell culture medium which also partially reversed the decrease of ATP in response to inhibitor treatment. Importantly, in contrast to glucose supplementation, the antioxidant NAC was not able to rescue proteasome activity in this study (Höglinger et al., 2003). However, as ATP levels are usually tightly regulated in the cell, treatment with respiratory chain inhibitors induces an acute decrease in ATP production which probably might not reflect the physiological regulation.

In summary, the effect of mitochondrial damage and dysfunction on the proteasome is differentially regulated depending on the nature of mitochondrial damage (Figure 1-5). Mitochondrial protein misfolding in the IMS or defective mitochondrial protein import is associated with increased proteasome activity. On the other hand inhibition of the respiratory chain impairs proteasomal function, which most probably due to highly increased mitochondrial ROS production or decreased ATP availability in the cell. However, the studies are sometimes contradictory, e.g. on whether antioxidants are protective or not. This might be due to differences in cell types or even organisms used in the studies or also due to different concentrations of the applied compounds. Additionally, while these results are strongly dependent on the acute chemical inhibition of the respiratory chain, the effect of more physiological triggers of respiratory chain dysfunction as it might occur in disease or in aging are not well characterized. Therefore, these results give important insights in potential mechanisms which can link mitochondrial dysfunction with proteasome function but they are not sufficient to fully explain the connection between these two systems, e.g. in situations without elevated ROS production.

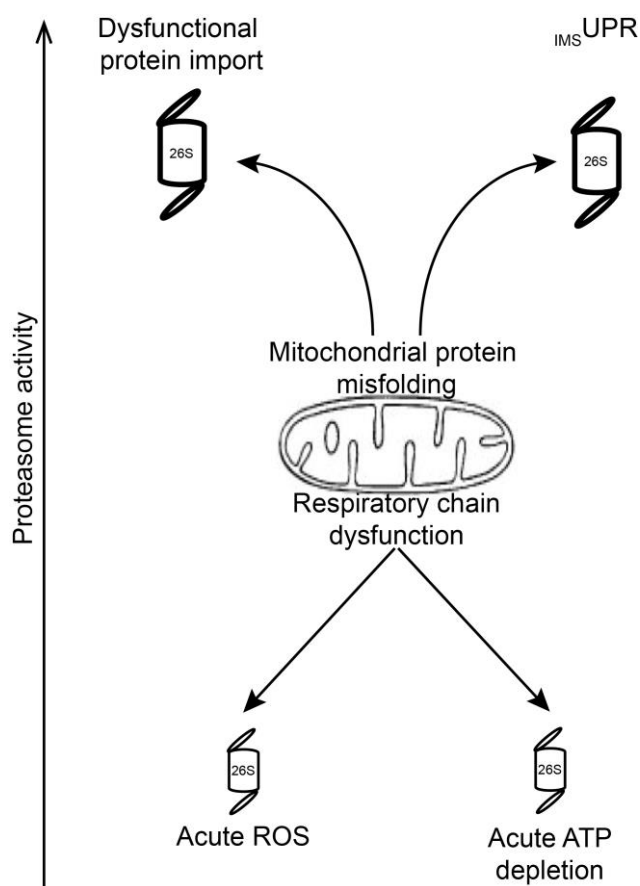


Figure 1-5: Effect of mitochondrial dysfunction on proteasome activity

Mitochondrial dysfunction has diverse effects on proteasome function. Mitochondrial protein misfolding in the mitochondrial intermembrane space or dysfunctional mitochondrial protein import induces an increase in proteasome activity. On the other hand, inhibition of the respiratory chain is associated with decreased proteasome activity and lower levels of assembled 26S and 30S proteasomes. Treatment of cells with respiratory chain inhibitors is signaled to the proteasome by acutely elevated mitochondrial ROS production or diminished ATP availability.

Altogether, proteasomal and mitochondrial function are clearly interconnected as evident by the role of the proteasome system in mitochondrial quality control and also by the observed regulation of proteasomal activity in response to mitochondrial dysfunction. An additional important link is given by a close correlation of mitochondrial and proteasomal function during aging, as both mitochondrial and proteasomal function were described to decline during aging (López-Otín et al., 2013) and in some age-related diseases such as Alzheimer's disease (Ross et al., 2015).

1.4 Lung aging

1.4.1 Molecular mechanisms of aging

Aging is usually defined as a progressive decline of cellular, tissue and organ function that leads to increased vulnerability to disease and eventually death (Kirkwood and Austad, 2000; López-Otín et al., 2013). Several theories have been developed to explain the evolution of aging such as the “mutation accumulation” or the “disposable soma” theory (Kirkwood and Austad, 2000; Ljubuncic and Reznick, 2009). Mechanistically, most theories link the aging process to accumulation of damage during an organism’s life span (Kirkwood and Austad, 2000; López-Otín et al., 2013).

Within this framework, López-Otín et al. recently defined nine “hallmarks of aging” at the cellular level, i.e. genomic instability, telomere attrition, epigenetic alterations, loss of proteostasis, deregulated nutrient sensing, mitochondrial dysfunction, cellular senescence, altered intercellular communication and stem cell exhaustion, that are causally linked with the aging process and together contribute to the loss of function in aged tissues (López-Otín et al., 2013). Intervening with these pathways often extends lifespan in model organisms thereby proving their importance in the aging process (Kennedy and Pennypacker, 2014; López-Otín et al., 2013). Importantly, these interventions can also be used to delay or prevent many age-related diseases (Kennedy et al., 2014) thereby opening the possibility to use these concepts to better describe age-related pathologies (Meiners et al., 2015). Since both proteasomal and mitochondrial function are recognized as hallmarks of aging, this further argues for a close interconnection of mitochondria and the proteasome. However, the effect of aging on proteasomal and mitochondrial function has mostly been studied independently of each other.

1.4.2 Proteasome activity in aging

During aging, a decline in proteasome activity was described in several organisms and tissues such as in brain, liver, muscle, lymphocytes, and heart (Chondrogianni et al., 2014; Keller et al., 2000). Furthermore, overexpression of proteasome subunits in yeast and *C. elegans* was shown to increase lifespan, especially under mild stress conditions (Chen et al., 2006; Vilchez et al., 2012), while flies and mice with genetically decreased proteasome activity exhibited a premature aging phenotype (Tomaru et al., 2012; Tonoki et al., 2009). In addition, a very recent study reported on the particular correlation of immunoproteasome expression with maximum lifespan. Especially, 20S proteasome activity and immunoproteasome expression showed a particular correlation with the maximum lifespan in long-lived primate species and in rodent models with experimentally increased lifespan (Pickering et al., 2015).

1.4.3 Mitochondrial function in aging

For mitochondria, it has long been recognized that mitochondrial function declines during aging (Bratic and Larsson, 2013). Indeed, basal as well as maximal mitochondrial oxygen consumption decreased with aging and electron leakage and ROS production by the respiratory chain is increased in aged organisms. Additionally, mitochondrial number and structure is altered in aging and mutations and deletions in mitochondrial DNA accumulate (Bratic and Larsson, 2013; Edgar and Trifunovic, 2009; López-Otín et al., 2013; Marzetti et al., 2013). The strong correlation of mitochondria and aging also placed mitochondria at the very center of the aging process in the so-called mitochondrial free radical theory of aging. According to this theory, oxidative metabolism in mitochondria induces mitochondrial ROS production which further induces damage to the mtDNA. In turn mtDNA damage results in expression of defective respiratory chain complexes which produce even more ROS leading to a vicious cycle of mitochondrial damage and ROS (Bratic and Larsson, 2013; Marzetti et al., 2013). However, in the last few years the mitochondrial free radical theory of aging has been substantially challenged. First evidence was obtained from transgenic animals which accumulated mitochondrial DNA mutations and showed a premature aging phenotype, however, in the absence of increased ROS production (Trifunovic et al., 2004, 2005). Additionally, increasing antioxidant defense does not prevent aging (Pérez et al., 2009) and also genetic manipulations in mice that increase mitochondrial ROS and oxidative damage do not accelerate aging (Zhang et al., 2009). In contrast, increased levels of ROS were even beneficial for organismal lifespan in some cases (Mesquita et al., 2010; Yun and Finkel, 2014). This new data argues for a more complex role of mitochondria in aging focusing on other signaling pathways of mitochondria.

In summary, a decline of mitochondrial function and alterations of mitochondrial structure and mtDNA integrity are clearly associated with aging. Additionally, interventions that increase lifespan are also associated with improved mitochondrial function (Bratic and Larsson, 2013; López-Otín et al., 2013).

However, despite the clear regulation of mitochondrial and proteasomal function in aging the connection of these two hallmarks of aging seems to be more complex than initially suggested. Furthermore, it remains unclear to which extent the different hallmarks contribute to the aging phenotype of different organs and tissues and to which degree they are affected in healthy or diseased aging.

1.4.4 Healthy and diseased aging phenotypes of the lung

In the lung, characteristic phenotypes of healthy aging and age-related diseases can be described. Lung morphology and physiology significantly changes over the lifetime of an organism and thereby can be used to analyze the effects of molecular mechanisms on the healthy aging process.

Introduction

Lung function increases after birth when the lung matures and peaks at an age of 20-25 years. After this age, lung function progressively declines with aging (Janssens et al., 1999; Sharma and Goodwin, 2006). This loss of function is linked to several structural and functional alterations of the respiratory system such as a decrease in chest wall compliance or loss of respiratory muscle strength (Sharma and Goodwin, 2006). An important structural change during aging is the progressive enlargement of the alveolar space leading to a decrease in the alveolar surface area necessary for gas exchange. In analogy to pathological airspace enlargement, this condition was called “senile emphysema” (Janssens et al., 1999). However, development of senile emphysema was shown to be mechanistically different from disease-related emphysema. Senile emphysema is generally described as “non-destructive” (Janssens et al., 1999; Tuder, 2006). It is thereby in sharp contrast to pathophysiologically altered, emphysematous lungs in which emphysema development is driven by protease/antiprotease imbalance in the extracellular space and hence by protease-induced destruction of connective tissue (Taraseviciene-Stewart and Voelkel, 2008). Emphysema development during healthy aging was not associated with increased extracellular protease activity and tissue destruction (Calvi et al., 2011; Janssens et al., 1999; Sueblinvong et al., 2012; Tuder, 2006) but is rather caused by intracellular factors such as increase in cellular senescence and decreased of extracellular matrix production (Calvi et al., 2011; Taraseviciene-Stewart and Voelkel, 2008). Importantly, these changes are not restricted to humans but can also be found in mice during healthy aging (Calvi et al., 2011) and can therefore be studied in mouse models.

1.4.4.1 Age-related diseases of the lung

Aging is an important risk factor for many chronic lung diseases. A strong increase in incidence with age has been described for chronic lung diseases such as chronic obstructive lung disease (COPD), idiopathic pulmonary fibrosis or lung cancer (Meiners et al., 2015; Thannickal et al., 2015).

Especially COPD was described as a disease of accelerated lung aging (Lee et al., 2011; MacNee, 2009; Mercado et al., 2015). COPD is characterized by progressive airflow limitation which is not fully reversible. Important features of the disease are chronic bronchitis, airway inflammation, increased mucus production and emphysema (Barnes, 2000; Ito, 2009; Tuder and Petrache, 2012). In contrast to senile emphysema in healthy aging, COPD-related emphysema is caused by alveolar wall destruction due to unopposed action of proteases in the alveolar space (Taraseviciene-Stewart and Voelkel, 2008; Tuder and Petrache, 2012). Since exposure to cigarette smoke is closely associated with COPD development it was suggested that exposure to cigarette smoke leads to increased accumulation of damage thereby causing accelerated aging in lung cells which then contributes to disease manifestation (Ito, 2009; Lee et al., 2011). Indeed, cigarette smoke induces alveolar epithelial cell senescence (Tsuji et al., 2004). Senescence of pulmonary cells has been proposed as a pathogenetic mechanisms for the progression of COPD (Müller et al., 2006; Tsuji et al., 2006)

probably due to attenuated tissue repair capacity of senescent cells (Lee et al., 2011; Mercado et al., 2015). Additionally, prematurely aging mouse models with increased amounts of senescent cells are more susceptible to cigarette smoke-induced emphysema generation (Meiners et al., 2015; Sato et al., 2006; Yamada et al., 2015). In further support of the notion of COPD as a disease of accelerated aging, almost all of the molecular mechanisms which have been described as hallmarks of aging have similarly been described in COPD patients (Meiners et al., 2015; Mercado et al., 2015).

Altogether, it is obvious that similar cellular processes that contribute to aging are also involved in the development of chronic lung diseases such as COPD. Environmental factors such as cigarette smoke accelerate the aging process thereby tipping the balance from moderate lung function decline during healthy aging to pathologic dysfunction. Further understanding of how the different hallmarks of aging are interconnected and how they are affected by environmental challenges will therefore deepen our understanding of disease pathogenesis.

2 Aims of the study

Protein quality control in the cytosol and in mitochondria is essential to maintain cellular health and function especially during aging. However, limited knowledge is available on how mitochondrial function and proteasomal function are connected in the context of chronic perturbations of mitochondrial function which are not associated with an increased ROS generation or an acute drop in ATP levels. Furthermore, it is unknown to which extent impairments of mitochondrial or proteasomal functions contribute tissue-specifically to the aging processes in healthy aging of the lung and how they are altered in response to environmental insults to the lung.

The main hypothesis of this work is that mitochondrial and proteasomal functions are interconnected and that chronic mitochondrial perturbations influence the function of the proteasome system. This connection of mitochondrial and proteasome function is signaled by mechanisms beyond acute and excessive ROS production. Furthermore, it is hypothesized, that alterations in mitochondrial and proteasomal function contribute to the aging process in the lung during healthy aging and add to the development of age-related lung disease in response to environmental challenges such as cigarette smoke.

Therefore, this work aims to describe the interconnection between mitochondrial dysfunction and proteasomal activity in model systems related to chronic mitochondrial dysfunction and independent of acute, pharmacological inhibition of mitochondrial function. Furthermore, this study aims to provide insights in the regulation of proteasomal and mitochondrial functions during healthy aging of the lung and in response to cigarette smoke exposure (Figure 2-1).

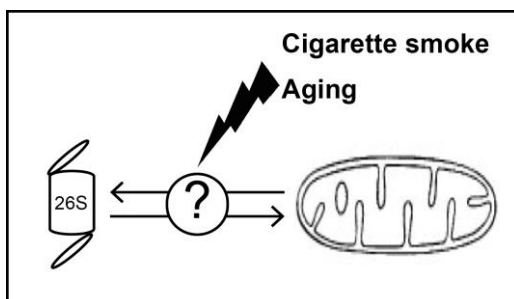


Figure 2-1: Connecting mitochondrial and proteasomal functions in the lung

This study aims to analyze the interconnection between mitochondrial and proteasomal function in settings of chronic mitochondrial dysfunction and to analyze the effect of healthy aging or environmental stress such as cigarette smoke exposure on mitochondrial and proteasomal function in the lung.

To this end, the interplay of mitochondrial and proteasomal function was evaluated in a first step using cells with chronic mitochondrial dysfunction based on mutations in genes of the respiratory chain complexes. Second, to assess mitochondrial alterations in response to environmental challenges in the lung, the effect of cigarette smoke exposure on mitochondrial function and quality

Aims of the study

control was analyzed in lung epithelial cells. Finally, the effect of proteasomal activity and mitochondria function on healthy aging of the lung was analyzed. Therefore, proteasomal function during healthy aging of the lung was comprehensively analyzed in several mouse models. Additionally, it was examined whether mitochondrial dysfunction in a mouse model of premature aging has an effect on the aging phenotype of the lung.

Altogether, these analyses aim to provide insight into how proteasomal and mitochondrial function are interconnected and to describe how proteasomal and mitochondrial function contribute to aging phenotypes in the lung.

3 Materials and methods

3.1 Materials

3.1.1 Reagents and chemicals

The following reagents and chemicals were used during the study:

Table 3-1: Reagents and Chemicals

Reagent	Solvent	Stock concentration	Manufacturer
2,5-diphenyltetrazolium bromide (MTT)	PBS	5 mg/ml	Sigma-Aldrich (St. Louis, MO)
4-(2-hydroxyethyl)-1-piperazineethanesulfonic acid (HEPES)	-	-	AppliChem (Darmstadt, Germany)
4',6-Diamidin-2-phenylindol (DAPI)	PBS	300 nM	Sigma-Aldrich
ABT-488	DMSO	10 mM	Enzo Life Sciences (Farmingdale, NY)
Adenosine triphosphate (ATP)	-	-	Roche (Basel, Switzerland)
Amidoblack staining solution	H ₂ O	2x	Sigma-Aldrich
Antimycin A	DMSO	50 mM	Sigma-Aldrich
Boric acid	-	-	Appllichem
Bortezomib	H ₂ O	2.6 mM	Millennium (Cambridge, MA)
Bovine serum albumin (BSA)	-	-	Sigma-Aldrich
Bromophenol blue	-	-	AppliChem
β -mercaptoethanol	-	-	AppliChem
Carbonyl cyanide 3-chlorophenylhydrazone (CCCP)	DMSO	25 mM	Sigma-Aldrich
Citric acid monohydrate	-	-	AppliChem
Complete [®] protease inhibitor	H ₂ O	25x	Roche
Cycloheximide	DMSO	100 mM	Sigma-Aldrich
DAKO mounting medium	-	-	Dako (Hamburg, Germany)
Dithiothreitol (DTT)	H ₂ O	1 M	AppliChem
Dimethyl sulfoxide (DMSO)	-	-	Roth (Karlsruhe, Germany)
Dodecyltrimethylammonium bromide (DTAB)	H ₂ O	20 %	Sigma-Aldrich

Materials and methods

ECL Plus Detection Reagent	-	-	GE Healthcare (Chalfont St Giles UK)
Ethylenediaminetetraacetate (EDTA)	-	-	AppliChem
Ethyleneglycoletetraacetate (EGTA)	-	-	AppliChem
Eukitt	-	-	Sigma-Aldrich
EX-527	DMSO	10 mM	Sigma-Aldrich
Fetal bovine serum (FBS)	-	-	PAA Laboratories (Pasching, Austria)
Glycerol	H ₂ O	87 %	AppliChem
GSH-magnetic beads	-	-	GE Healthcare
H ₂ O ₂	H ₂ O	30 %	AppliChem
HCl	H ₂ O	37 %	AppliChem
KCl	-	-	AppliChem
Ketamin	-	-	Bela Pharm (Vechta, Germany)
KH ₂ PO ₄	-	-	Sigma-Aldrich
K-lactobionate	-	-	Sigma-Aldrich
KOH	-	-	AppliChem
MACH 2 Rabbit AP-Polymer	-	-	Biocare (Concord, CA)
Mannitol	-	-	Sigma-Aldrich
May-Grünwald staining solution	-	-	Merck (Whitehouse Station, NJ)
MgCl ₂	-	-	AppliChem
MitoSOX Red®	DMSO	5 mM	Life Technologies (Carlsbad, CA)
M-MLV reverse transcriptase	-	-	Sigma-Aldrich
NaCl	-	-	AppliChem
NaN ₃	H ₂ O	1 M	AppliChem
NaOH	-	-	AppliChem
Ni-NTA beads	-	-	Thermo Fisher Scientific (Waltham, MA)
Nonidet P-40	-	-	AppliChem
Oligomycin	DMSO	5 mM	Sigma-Aldrich
Paraformaldehyde (PFA)	PBS	4 %	AppliChem
Penicillin	-	-	Life Technologies

Propidium Iodide Staining Solution	-	-	BD Biosciences (San Jose, CA)
Random hexamers	-	3 µg/µl	Life technologies
Rodent Block M	-	-	Biocare
Rotenone	DMSO	50 mM	Sigma-Aldrich
Rotiblock	H ₂ O	10x	Roth
Roti-Immunoblock	H ₂ O	10x	Roth
Sodiumdeoxycholate	-	-	Roth
Sodiumdodecylsulfate (SDS)	-	-	AppliChem,
Streptomycin	-	-	Life Technologies
Succinyl-leucine-leucine-valine-tyrosine-aminoluciferin (Suc-LLVY-aminoluciferin)	DMSO	2 mM	Promega (Madison, WI)
Succinyl-leucine-leucine-valine-tyrosine-aminomethylcoumarine (Suc-LLVY-AMC)	DMSO	2 mM	Bachem (Bubendorf, Switzerland)
Sucrose	-	-	Sigma-Aldrich
Super Signal West Femto	-	-	Thermo Fisher Scientific
Taurine	-	-	Sigma-Aldrich
Tetramethylrhodamin-methylester perchlorate (TMRM)	DMSO	1 mM	Life Technologies
Tris(hydroxymethyl)-aminomethane (Tris)	-	-	AppliChem
Triton X-100	-	-	Life Technologies
Tween-20	-	-	AppliChem
Uridine	H ₂ O	100 mM	Sigma-Aldrich
Vulcan Fast Red	-	-	Biocare
Xylazine	-	-	Bela Pharm
Z-leucine-arginine-arginine-aminoluciferin (Z-LRR-aminoluciferin)	DMSO	2 mM	Bachem
Z-norleucine-proline-norleucine-aspartate-aminomethylcoumarine (Z-nLPnLD-AMC)	DMSO	2 mM	Bachem
Z-norleucine-proline-norleucine-aspartate-aminoluciferin (Z-nLPnLD-aminoluciferin)	DMSO	2 mM	Bachem

3.1.2 Buffer formulations

The following buffers were used in the study. All buffers were prepared with MiliQ™ water if not stated otherwise.

Table 3-2: Buffer formulations

Buffer	Compounds	Concentration
Annexin V binding buffer (pH 7.4)	HEPES	10 mM
	NaCl	140 mM
	CaCl ₂	2.5 mM
Citrate buffer pH 6	Citric acid monohydrate	1.8 mM
	Sodium citrate tribasic	8.2 mM
FACS Buffer (in PBS)	FBS	2 %
	EDTA	20 μM
Mitochondrial isolation buffer pH 7.4	Mannitol	220 mM
	Sucrose	70 mM
	HEPES	5 mM
	EGTA	1 mM
Native gel running buffer	Tris	89 mM
	Boric acid	89 mM
	EDTA	2 mM
	MgCl ₂	5 mM
	ATP	2 mM
	DTT	1 mM
Phosphate buffered saline (PBS) pH 7.4	NaCl	137 mM
	KCl	2.7 mM
	Na ₂ HPO ₄	10 mM
	KH ₂ PO ₄	2 mM
Proteasome purification buffer	HEPES	25 mM
	Glycerol	10 %
	MgCl ₂	5 mM
	ATP	1 mM
	DTT	1 mM
Respiration buffer pH 7.4	EGTA	0.5 mM
	MgCl ₂	3 mM
	K-lactobionate	60 mM
	Taurine	20 mM
	KH ₂ PO ₄	10 mM
	HEPES	20 mM

Materials and methods

	Mannitol	110 mM
	BSA	1 g/l
RIPA Buffer pH 7.5	Tris	50 mM
	NaCl	150 mM
	Nonidet P-40	1 %
	Sodium deoxycholate	0.5 %
	SDS	0.1 %
SDS PAGE running buffer	Tris	25 mM
	Glycin	192 mM
	SDS	0.1 %
Solubilisation buffer	Na ₂ CO ₃	66 mM
	SDS	2 %
	β-mercaptoethanol	1.5 %
Tris buffered saline and Tween (TBST) pH 7.6	Tris	20 mM
	NaCl	135 mM
	Tween-20	0.02 %
TSDG Buffer pH 7	Tris	10 mM
	KCl	25 mM
	MgCl ₂	1.1 mM
	EDTA	0.1 mM
	DTT	1 mM
	NaN ₃	1 mM
	Glycerol	10 %
Western blot transfer buffer	Tris	25 mM
	Glycine	192 mM
	Methanol	10 %
5x native loading buffer	Tris	250 mM
	Glycerol	50 %
	Bromophenol blue	0.01 %
6x Laemmli buffer	Tris	300 mM
	Glycerol	50 %
	SDS	6 %
	Bromophenol blue	0.01 %
	DTT	600 mM

3.1.3 Cigarette smoke extract preparation

Cigarette smoke extract (CSE) was prepared by bubbling smoke from 6 cigarettes (Research-grade cigarettes (3R4F); Kentucky Tobacco Research and Development Center at the University of Kentucky) through 100 ml of FBS-free cell culture medium at constant airflow. Smoked medium was sterile filtered through a 0.20 µm filter (Minisart; Satorius Stedim Biotech, Göttingen, Germany), divided into aliquots, stored at -20°C and served as the 100 % CSE stock solution. For treatment, CSE was supplemented with 1 % penicillin/streptomycin and diluted with treatment medium to the indicated concentrations directly before use. To assure comparable potency of CSE, each stock solution was tested by MTT assays for having similar cytotoxicity.

3.2 Animal experiments

Animal experiments were conducted in collaboration with Anne Caniard and Ilona Kammerl and with the research groups of Ali Önder Yildirim at the Comprehensive Pneumology Center Munich and the research group of Aleksandra Trifunovic at the University of Cologne.

Lung function analysis, bronchoalveolar lavage and tissue extraction of young and aged Wildtype (WT), ODD-luc reporter and LMP2 or LMP7 knockout mice were performed by Anne Caniard and Ilona Kammerl in collaboration with the research group of Ali Önder Yildirim. Maintenance of mtDNA mutator mice and WT controls was performed by the research group of Aleksandra Trifunovic at the University of Cologne. In all other cases tissue extraction and subsequent analysis was performed by Korbinian Berschneider.

3.2.1 Animals and maintenance

Female C57BL/6J mice at the age of 2 months (young) or 18 months (aged) were obtained from Harlan Laboratories. LMP2^{-/-} (Psmb9^{tm1Stl} (Van Kaer et al., 1994)) or LMP7^{-/-} (Psmb8^{tm1Hjf} (Fehling et al., 1994)) mice with C57BL/6J background were obtained by courtesy of Prof. Dr. Antje Voigt (Charité, Universitätsmedizin Berlin) and ODD-luc reporter mice (129S6-Gt(ROSA)26Sor^{tm1(HIF1A/luc)Kael/J} (Safran et al., 2006)) with FVB background were bought from Jackson Laboratory (Bar Harbor, ME) and housed at the Helmholtz Center Munich in rooms maintained at a constant temperature and humidity with a 12 h light cycle. Animals were allowed food and water *ad libitum*. All animal experiments were conducted under strict governmental and international guidelines and were approved by the local government for the administrative region of Upper Bavaria. MtDNA mutator mice and WT controls were provided by Aleksandra Trifunovic from the University of Cologne and housed according to the standards and rules of the University of Cologne.

For protein and RNA preparation mouse lungs were perfused with PBS before extraction. All organs were shock-frozen in liquid nitrogen directly after extraction and kept at -80°C until processing. For

embedding into paraffin, mouse lungs were fixed by intratracheal instillation of 4 % paraformaldehyde in PBS before extraction.

3.2.2 Lung function analyses

Pulmonary function in mice was measured using the flexiVent system (Scireq, Montréal, Canada). Mice were anesthetized with ketamine-xylazine, tracheostomized and connected to the flexiVent system. Mice were ventilated with a tidal volume of 10 ml/kg at a frequency of 150 breaths/min in order to reach a mean lung volume similar to that of spontaneous breathing. Testing of lung mechanical properties including dynamic lung compliance and resistance was carried out by a software-generated script that took four readings per animal.

3.2.3 Bronchoalveolar lavage cell analysis

Mouse lungs were lavaged by inserting a cannula into the trachea and instilling four times 1 ml of ice-cold sterile PBS into the lungs. Cells in bronchoalveolar lavage fluid were counted and 30,000 cells were used for cytopins. Cytopins were stained according to May-Grünwald and cellular composition was assessed by counting approx. 100 cells per slide.

3.3 Cell culture

3.3.1 Isolation of primary murine alveolar type II cells (pmATII)

PmATII cells were kindly provided by Katrin Mutze after isolation according to the following protocol: pmATII cells were isolated from C57BL/6N mice (Charles River GmbH, Sulzfeld, Germany) at 8-14 weeks of age as describes previously (Corti et al., 1996; Königshoff et al., 2009). Briefly, mouse lungs were lavaged with 500 µl of sterile PBS twice and perfused through the right heart using 0.9 % NaCl solution (B. Braun Melsungen AG, Melsungen, Germany). Lungs were subsequently inflated with 1.5 ml dispase solution (BD Biosciences) and 300 µl of 1 % low melting point agarose (Sigma-Aldrich) and incubated for 45 min at room temperature (RT). Lungs were minced and consecutively filtered through 100 µm, 20 µm, and 10 µm nylon meshes (Sefar, Heiden, Switzerland). The resulting single cell suspension was centrifuged at 200 g for 10 min and the cell pellet was resuspended in DMEM. Incubation of the single cell suspension on petri dishes coated with antibodies against CD45 and CD16/32 (both BD Biosciences) for 30 min at 37°C was performed for depletion of macrophages and lymphocytes. Non-adherent cells were collected and negative selection for fibroblasts was performed by adherence for 25 minutes on cell culture dishes. Again, non-adherent cells were collected and cell viability was determined by trypan blue exclusion. Cell purity was assessed by immunofluorescence staining of cytopsin preparations using antibodies for proSFTPC (Merck Millipore, Darmstadt, Germany), panCK (Dako), CD45 (BD Biosciences), and αSMA (Sigma Aldrich).

Materials and methods

pmATII cells were resuspended in DMEM supplemented with 10 % FBS, 2 mM L-glutamine, 1 % penicillin/streptomycin (both Life Technologies), 3.6 mg/ml glucose (Applichem), and 10 mM HEPES (PAA Laboratories) and cells were cultured for 24 h to allow attachment.

3.3.2 Cell growth and maintenance

Cells were grown at 37°C in a humidified atmosphere containing 5 % CO₂. Growth medium of the cells was changed every two to three days. All cell lines except human dermal fibroblasts were grown until 100 % confluency before passaging into a new cell culture flask. Human dermal fibroblasts were passaged after reaching 70% confluency.

The following growth media were used. All growth media were obtained from Life Technologies.

Table 3-3: Cell culture media

Cell line	Medium	Supplementation
Mouse lung epithelial cell line (MLE12) (growth medium)	RPMI	10 % FBS 1 % Penicillin/Streptomycin (P/S)
MLE12 (treatment medium)	RPMI	1 % Penicillin/Streptomycin (P/S)
pmATII (growth medium)	High Glucose DMEM	10 % FBS 1 % Penicillin/Streptomycin (P/S)
pmATII (treatment medium)	High Glucose DMEM	1 % Penicillin/Streptomycin (P/S)
Mouse embryonic fibroblasts (MEFs)	High Glucose DMEM	10 % FBS 1 % Penicillin/Streptomycin (P/S)
Dermal fibroblasts	High Glucose DMEM	10 % FBS 1 % Penicillin/Streptomycin (P/S) 200 µM Uridine

3.3.3 Cytotoxicity testing (LDH release)

Cytotoxicity was assessed using the cytotoxicity detection kit (Roche) according to the manufacturer's instructions. Cells were seeded into 6-well plates, grown to approx. 80 % confluency and treated for the indicated times. 15 minutes before the end of the treatment, one well was treated with 2 % Triton X-100 to serve as the control for maximal cellular release of Lactate dehydrogenase (LDH). Supernatants were collected, cleared by centrifugation, and LDH content was measured in technical triplicates according to the manufacturer's instructions using a Tristar LB 941 plate reader (Berthold Technologies, Bad Wildbad, Germany). Data were normalized as follows: Untreated cells were set to 0 % cytotoxicity and 2 % Triton X-100-treated cells were set to 100 % cytotoxicity.

3.3.4 Metabolic activity assay (MTT reduction)

Metabolic activity was measured using the 2,5-diphenyltetrazolium bromide (MTT) assay. Cells were seeded into 24-well or 96-well plates with each sample in at least three technical replicates. Cells were grown for 24 h and medium was changed to 500 μ l (24-well plates) or 100 μ l (96-well plates) treatment or control medium as indicated in the figures. After treatment 100 μ l (24-well plates) or 20 μ l (96-well plates) of freshly prepared thiazolyl blue tetrazolium bromide solution (5 mg/ml in PBS) was added to each well and cells were incubated for 30 min at 37°C. The supernatant was aspirated, and blue crystals were dissolved in isopropanol + 0.1 % Triton X-100. Absorbance was measured at 570 nm using a Tristar LB 941 plate reader.

3.3.5 Cell proliferation assay (BrdU incorporation)

Cell proliferation was measured using the cell proliferation BrdU ELISA kit (Roche) according to the manufacturer's instruction. Cells were seeded in 96-well plates and grown for 24 h. 10 μ l of BrdU labeling solution were added to each well and cells were incubated for 2 h. Labeling medium was removed and cells were incubated with 200 μ l fixation solution for 30 min at RT. Afterwards, fixation solution was replaced by anti-BrdU solution and incubated for 90 min at RT. Cells were washed three times with PBS and incubated with 100 μ l substrate solution. After 15 min absorbance was measured at 370 nm and normalized to absorption at 492 nm using a Tristar LB 941 plate reader.

3.3.6 Live/dead assay with Annexin V/PI

Induction of apoptosis or necrosis was analyzed by staining cells with an Annexin V antibody and Propidium iodide (PI). Cells were seeded into 6-well plates and grown for 24 h. Cells were then treated with the indicated compounds. After the treatment, cells were trypsinized, washed twice with PBS and resuspended in 100 μ l Annexin V binding buffer. 5 μ l anti-Annexin V-FITC (BD Biosciences) and 10 μ l PI staining solution were added and cells were incubated for 15 min at room temperature in the dark. After the incubation time, 400 μ l Annexin V binding buffer were added and samples were measured by flow cytometry analysis using the Becton Dickinson LSRII and analyzed using FlowJo software (version 7.6.5).

3.3.7 Measurement of cellular ATP levels

Cellular ATP levels were measured using the CellTiter-Glo assay kit (Promega, Madison, WI). Cells were seeded in 6-well plates and grown for 24 h. If desired, cells were then treated with the indicated compounds. After the treatment cells were trypsinized and 40,000 cells/well were transferred to a white flat bottom 96-well plate. CellTiter-Glo reagent was added and the luminescent signal was measured after shaking the plate thoroughly in a Tristar LB 941 plate reader.

3.3.8 Analysis of cellular ROS production

Cellular ROS generation was analyzed using H₂DCFDA (Life Technologies). Cells were seeded in 6-well plates and grown for 24 h. Cells were then stained for 30 minutes in medium containing 25 μ M H₂DCFDA. Cells were washed with PBS, trypsinized, and resuspended in 500 μ l FACS Buffer. Samples were then analyzed by flow cytometry and ROS production was measured as mean DCF fluorescence intensity.

3.3.9 Measurement of cellular NAD⁺ and NADH levels

Cellular NAD⁺ and NADH levels were measured using the NAD/NADH-Glo assay kit (Promega) according to the manufacturer's introductions. Cells were harvested, washed twice with PBS and 40,000 cells in 50 μ l PBS were transferred to a 96-well plate. Cells were lysed by addition of 50 μ l 0.2 M NaOH with 1 % Dodecyltrimethylammonium bromide (DTAB). The sample was split into two wells and 25 μ l 0.4 M HCl were added to one part constituting the acid-treated part. The plate was incubated for 15 min at 60°C thereby depleting NADH in the acid-treated wells and depleting NAD⁺ in the non-treated wells. After the incubation 25 μ l of 0.5 M Tris solution was added to the acid-treated part. The other part was treated with 50 μ l 0.25 M Tris, 0.2M HCl solution. 20 μ l of each well were transferred to a white flat bottom 96-well plate and 20 μ l of NAD/NADH Glo detection reagent were added. Luminescence was measured in a Tristar LB 941 plate reader. The luminescence signal of the acid-treated wells represents the NAD⁺ levels while the luminescence signal of the non-treated wells represents the NADH levels.

3.4 Mitochondrial function analysis

3.4.1 Mitochondrial membrane potential analysis

Mitochondrial membrane potential was measured by TMRM fluorescence. Cells were seeded in 6-well plates and grown for 24 h. Cells were then treated with the indicated compounds. After the treatment, cells were stained for 30 minutes in medium containing 5 nM TMRM. Cells were washed with PBS, trypsinized, and resuspended in 500 μ l FACS Buffer. Samples were then analyzed by flow cytometry and mitochondrial membrane potential was measured as mean TMRM fluorescence intensity. To ensure total depolarization CCCP was added to the samples to a final concentration of 100 μ M and measurements were repeated after 15, 30 and 60 minutes.

3.4.2 Analysis of mitochondrial superoxide production

Mitochondrial superoxide generation was analyzed using MitoSOX Red[®]. Cells were seeded in 6-well plates and grown for 24 h. Cells were then treated with the indicated compounds. After the treatment, cells were stained for 30 minutes in medium containing 5 μ M MitoSOX Red. Cells were

washed with PBS, trypsinized, and resuspended in 500 μ l FACS Buffer. Samples were then analyzed by flow cytometry and superoxide production was measured as mean MitoSOX fluorescence intensity.

3.4.3 Analysis of mitochondrial morphology

For mitochondrial morphology analysis cells were grown on 15 mm glass coverslips to approx. 50 % confluency and treated for the indicated times. After the treatment, cells were fixed with 4 % PFA for 10 minutes, permeabilized with 0.1 % Triton X-100 in PBS and unspecific binding sites were blocked with Roti-Immunoblock for one hour at RT. After blocking, cells were incubated with anti-cytochrome c antibody (1:1000, BD Bioscience (#556432), San Jose, CA) for 2 h at RT, washed and incubated with an Alexa Fluor® (AF)-488-coupled secondary antibody (1:750, Life Technologies) for one hour at RT. All subsequent steps were performed with minimal light exposure. Cells were washed twice for 10 min with PBS and nuclei were stained with DAPI for 5 min. Finally, cells were mounted on microscopic slides with fluorescence mounting medium and imaged using confocal laser-scanning microscopy (Zeiss LSM710, Oberkochen, Germany).

For quantification, cells were visually categorized into three classes according to their mitochondrial morphology: Cells displaying an intact network of tubular mitochondria were classified as normal. When the network was disrupted and mitochondria appeared predominantly spherical or rod-like, they were classified as fragmented. Cells with considerably elongated mitochondria, which were more interconnected, were classified as hyperfused (Figure 3-1). The mitochondrial morphology of on average 100 cells per condition was determined by a blinded observer.

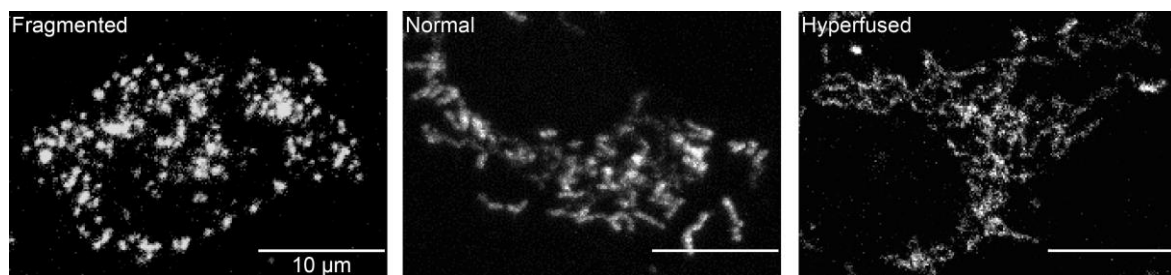


Figure 3-1: Mitochondrial morphology classification

Representative images of mitochondrial staining of cells categorized in the three different groups. Cells with a fragmented mitochondrial network showed small spherical mitochondria. Cells with a normal mitochondrial network had short tubular mitochondria and cells with a hyperfused network displayed elongated and highly connected mitochondria. Scale bars: 10 μ m.

3.4.4 Analysis of cellular oxygen consumption

Oxygen consumption in MLE12 cells was measured in an Oxygraph chamber (Oroboros Instruments, Innsbruck, Austria). Cells were seeded in 10 cm dishes, grown to approx. 80 % confluency and treated with control medium or 25 % CSE-containing medium. After 24 h of treatment, cells were washed

Materials and methods

with PBS, trypsinized, and 5×10^6 cells were transferred in respiration buffer and added into the Oxygraph chamber. Oxygen consumption was measured at basal conditions (basal respiration), after addition of 2.5 μM oligomycin (blocking proton backflow through complex V to measure proton leak), after addition of 1 μM CCCP (uncoupling the respiratory chain to enable unlimited proton flow through the mitochondrial membrane to induce maximum respiration) and after addition of 2.5 μM rotenone/antimycin A (blocking complex I and III to inhibit mitochondrial respiration). These concentrations were also previously shown to be suitable for measuring oxygen consumption rates in MLE12 cells (Das, 2013).

Oxygen consumption in mtDNA mutator MEFs and human dermal fibroblasts was measured using a Seahorse XF analyzer (Seahorse Bioscience) and oxygen consumption values were normalized to cell number as assessed by the CyQuant assay kit (Life technologies). These experiments were performed by Jennifer Wettmarshausen for mtDNA mutator MEFs and by Laura Kremer for human dermal fibroblasts.

3.5 Protein analysis

3.5.1 Immunohistochemistry

For immunohistochemistry analysis of LMP2 in lung tissue, 3 μm thick mouse lung sections were deparaffinized in Xylene and rehydrated. Slides were incubated in solution containing 80 % methanol and 1.8 % H_2O_2 for 20 min to quench endogenous peroxidase activity. Heat-induced antigen retrieval was performed in citrate buffer (pH 6). Slides were washed with TBST buffer, blocked with Rodent Block M for 30 min, washed again and incubated for 60 min with an LMP2 specific antibody (1:500, Abcam, Cambridge, UK). After another washing step, slides were incubated with MACH 2 Rabbit AP-Polymer for 30 min and washed again. Slides were incubated with Vulcan Fast Red for 12 min. Hematoxylin counterstaining was performed, and slides were dehydrated and mounted in Eukitt. Slides were evaluated using a MIRAX scanning system (Zeiss, Oberkochen, Germany).

3.5.2 Immunofluorescence staining

Mouse lung sections (3 μm) were deparaffinized in Xylene, rehydrated and heat-induced antigen retrieval was performed in citrate buffer (pH 6). Slides were washed with PBS and lungs were permeabilized in 0.2 % Triton X-100 in PBS for 15 minutes, blocked in Roti-Immunoblock for 1 h and stained over night with anti-LMP2 antibody (1:500) at 4°C. Slides were then washed again, incubated with an AF-647-coupled secondary antibody (1:750, Life technologies) for 1 h and with DAPI for 30 min. Slides were mounted using DAKO immunofluorescence mounting medium and imaged using

confocal laser-scanning microscopy (Zeiss LSM710, Oberkochen, Germany). Images were analyzed using the Imaris Software (Version 8.0.3, Bitplane, Zürich, Switzerland).

3.5.3 Preparation of protein lysates

Prior to protein extraction, cells were trypsinized, washed with PBS and cell pellets were stored at -20°C until further processing.

For disintegration of frozen mouse tissue, samples were dismembrated using a Mikro-Dismembrator S. Tissue samples were transferred into dismabrating tubes containing a metal grinding ball and shaken two times using frequency of 3000 RPM for 30 seconds.

For preparation of denatured protein lysate, cell pellets or dismembrated tissue were lysed by incubation in RIPA buffer supplemented with Complete® protease inhibitor cocktail for 20 minutes at 4°C. This method was used for Western blots depicted in Figure 5-5A, Figure 5-14A, Figure 5-15A and Figure 5-7A.

For preparation of native protein lysates, cell pellets or dismembrated tissue were lysed in TSDG buffer supplemented with Complete® protease inhibitor cocktail by subjecting them to seven cycles of freezing in liquid nitrogen and subsequent thawing at room temperature. This method was used for all protein lysates if not stated otherwise.

Debris was removed from the protein lysate by centrifugation at 14000 rpm at 4°C for 20 min. The supernatant containing the protein lysate was stored at -20°C until use. Protein content was assessed using the Bio-Rad Quick Start Bradford protein assay (Bio-Rad, Hercules, CA) or the Pierce BCA protein assay kit (Thermo Fisher Scientific).

3.5.4 Preparation of mitochondrial fractions

Mitochondria were isolated by ultracentrifugation after cellular lysis using a cell disruption bomb (Parr Instruments, Moline, IL). In short, cells were seeded in 15 cm dishes, grown to 80 % confluency, and treated. After the treatment, cells were scraped, pelleted, and resuspended in mitochondrial isolation buffer supplemented with Complete® protease inhibitor cocktail. Cells were lysed by stirring for 15 min in a cell disruption bomb at 800 psi nitrogen pressure and subsequent rapid depressurizing. Cell lysates were then centrifuged at 600 g for 10 min to remove nuclei. The supernatant was centrifuged at 8000 g for 10 min to obtain a crude mitochondrial pellet. The supernatant was removed and kept as the cytosolic fraction. Light colored ER membranes were removed from the pellet and the mitochondrial pellet was resuspended in mitochondrial isolation buffer to serve as the mitochondrial fraction. Protein content in the different fractions was determined using the Pierce BCA protein assay kit.

3.5.5 Western blot analysis

For Western blot analysis, 10-20 µg of protein lysates were mixed with 6x Laemmli buffer and incubated at 95°C for 5 minutes. After the incubation, samples were subjected to electrophoresis on 7.5 % - 12 % SDS-PAGE gels and blotted onto polyvinylidenedifluoride (PVDF) membranes. Electrophoretic separation in SDS gels was performed at 90-130 V at room temperature and transfer to PVDF membranes was performed at 250 mA for 90 min at 4°C. Membranes were blocked using Rotiblock (Roth) and treated with antibodies using standard Western blot techniques. The ECL Plus Detection Reagent and Super Signal West Femto were used for chemiluminescent detection and membranes were analyzed using X-Omat LS films (Carestream, Rochester, NY) in a Curix 60 developer (Agfa, Mortsel, Belgium). Densitometry analysis was performed using the ImageLab Software (Biorad, Hercules, CA).

Antibodies used were:

Table 3-4: Antibodies used for western blotting

Antibody	Dilution	Host	Manufacturer	Product No.
Primary Antibodies:				
Anti-AMPKα	1:1000	Rabbit (Rb)	Cell Signaling (Cambridge, UK)	5831
Anti-AMPKβ	1:1000	Rb	Cell Signaling	4150
Anti-ATP5A	1:1000	Mouse (Ms)	Abcam (Cambridge, UK)	Ab14748
Anti-Calreticulin	1:1000	Rb	Cell Signaling	2891
Anti-cleaved Caspase3	1:1000	Rb	Cell Signaling	9661
Anti-DRP1	1:1000	Rb	Cell Signaling	5391
Anti-HSP60	1:1000	Rb	Cell Signaling	4870
Anti-HSP70	1:1000	Rb	Cell Signaling	4872
Anti-HSP90	1:1000	Rb	Cell Signaling	4877
Anti-K48-Ub	1:3000	Rb	Merck Millipore	05-1307
Anti-LMP2	1:500	Rb	Abcam	Ab3328
Anti-LMP7	1:500	Rb	Abcam	Ab3329
Anti-MFN1	1:1000	Ms	Abcam	Ab57602
Anti-MFN2	1:1000	Rb	Abcam	Ab124773
Anti-OPA1	1:5000	Rb	GeneTex (Irvine, CA)	GTX48589
Anti-PA28α	1:1000	Rb	Abcam	Ab155091
Anti-PA28γ	1:1000	Ms	Santa Cruz Biotechnology (Dallas, TX)	Sc-136025
Anti-phospho-4EBP1 (Thr37/46)	1:1000	Rb	Cell Signaling	2855
Anti-phospho-AMPKα (Thr172)	1:1000	Rb	Cell Signaling	2535

Anti-phospho-AMPKβ (Ser108)	1:1000	Rb	Cell Signaling	4181
Anti-phospho-DRP1 (Ser637)	1:1000	Rb	Cell Signaling	6319
Anti-phospho-S6 (Ser235/236)	1:1000	Rb	Cell Signaling	4858
Anti-PINK1	1:500	Rb	Novus Biologicals (Littleton, CO)	NBP1-49678
Anti-PSMA3	1:1000	Rb	Cell Signaling	2456
Anti-PSMD11	1:1000	Rb	Novus Biologicals	NBP1-46191
Anti-PSMD7	1:1000	Rb	Abcam	Ab11436
Anti-S6	1:1000	Rb	Cell Signaling	2317
Anti-Sirt1	1:1000	Rb	Santa Cruz Biotechnology	Sc-15404
Anti-TBP1 (Rpt5)	1:2000	Rb	Bethyl Laboratories (Montgomery, TX)	A303-538A
Anti-VCP	1:1000	Rb	Novus Biologicals	NB100-1558
Anti-VMS1	1:1000	Rb	Cell Signaling	5937
Anti-α1-7	1:1000	Ms	Abcam	Ab22674
Anti-α-Tubulin	1:1000	Ms	GeneTex	GTX628802
Anti-β1	1:1000	Rb	Santa Cruz Biotechnology	Sc-67345
Anti-β5	1:1000	Rb	Santa Cruz Biotechnology	Sc-135011
HRP conjugated anti-GAPDH	1:30000	Rb	Cell Signaling	3683
HRP conjugated anti-β-Actin	1:40000 1:80000	– Ms	Sigma-Aldrich	A5228
Secondary antibodies:				
HRP conjugated anti-mouse IgG	1:40000	Sheep	GE Healthcare	NA931
HRP conjugated anti-mouse IgG	1:30000- 1:50000	Goat (Gt)	Cell Signaling	7076
HRP conjugated anti-rabbit IgG	1:40000	Donkey	GE Healthcare	NA934
HRP conjugated anti-rabbit IgG	1:30000- 1:50000	Gt	Cell Signaling	7074

When total protein levels were used for normalization of protein content, amidoblack staining of membranes was used to determine total protein amount. Therefore, membranes were incubated with Amidoblack staining solution (Sigma-Aldrich) for 5 min and washed with H₂O until blue background staining disappeared. Membranes were then air dried and imaged using the ChemiDoc XRS system (Biorad).

3.5.6 Detection of oxidatively damaged proteins

Oxidatively modified proteins were detected using the OxyBlot Protein Oxidation Detection Kit (Merck Millipore). 5 µl protein lysate were denatured by adding an equal volume of 12 % SDS and derivatized by adding 10 µl 1x 2,4-Dinitrophenylhydrazine (DNPH) solution and incubating for 15 min at room temperature. The derivatization reaction was stopped by adding 7.5 µl neutralization solution and the samples were loaded on a polyacrylamide gel. Separation by electrophoresis and transfer to PVDF membranes was performed using standard Western blot techniques.

3.5.7 Proteasome activity assay

Proteasome activity was measured with the Proteasome-Glo™ Assay System (Promega) according to the manufacturer's instructions. 1-5 µg protein in native lysates were diluted to a total volume of 20 µl and incubated with 20 µl reaction buffer containing luminescent proteasome substrates. Substrates used for determination of proteasome chymotrypsin-like (CT-L), trypsin-like (T-L), and caspase-like (C-L) activities were Succinyl-leucine-leucine-valine-tyrosine-aminoluciferin, Z-leucine-arginine-arginine-aminoluciferin, and Z-norleucine-proline-norleucine-aspartate-aminoluciferin, respectively. Luminescence was measured every 5 min for 1 h in white flat bottom 96-well plates in a Tristar LB 941 plate reader. Blank luminescence values using substrate only were subtracted from each well.

3.5.8 Native-gel proteasome analysis

Individual proteasome complexes were separated using native gel electrophoresis. 10-20 µg protein were mixed with 5x native loading buffer, loaded on precast 3-8 % Tris-acetate gels (Life Technologies) and separated at 150 V for 4 h at 4°C. For overlay activity assay, gels were incubated for 30 min in 50 mM Tris containing 1 mM ATP, 10 mM MgCl₂, 1 mM DTT and 0.05 mM Suc-LLVY-AMC (for CT-L activity) or Z-nLPnLD-AMC (for C-L activity).

For immunoblotting, gels were incubated 15 min in solubilisation buffer and blotted on PVDF membranes using standard Western blot techniques.

3.5.9 Activity based probe analysis of proteasome activity

Analysis of proteasome subunit activity was monitored by using activity based probes (ABP). The fluorescent compound MV151 (Verdoes et al., 2006) was used to specifically label active proteasome subunits in native TSDG cell lysates. Proteasome subunits were labeled by incubating protein lysates with 0.5 µM MV151 in 50 mM HEPES Buffer at 37°C in the dark for 1 h while shaking at 600 rpm. The labeling reaction was stopped by the addition of 6x SDS Laemmli buffer to a final 1x concentration. Samples were then subjected to a SDS gel electrophoresis and active proteasome subunits were

imaged using a Typhoon TRIO+ fluorescent scanner (GE Healthcare). Images were taken at 450 PTM and 50 μm resolution in the Cy3/TAMRA fluorescent channel and analyzed using the ImageJ software. To ensure equal protein loading Gels were stained with Coomassie Blue staining by incubation with PageBlue staining solution (Thermo Fisher Scientific) overnight.

3.5.10 Isolation of 26S proteasomes

26S proteasomes were isolated according to Besche et al. (2009). 300 μl of native protein lysates with $> 2 \mu\text{g}/\mu\text{l}$ protein concentration were incubated with 60 μl magnetic GSH beads and 0.2 mg GST-UBL for 2 h at 4°C. After the incubation time, beads were captured with a magnet and the supernatant was removed and stored as flow through (FT). The beads were then washed four times with proteasome purification buffer. After the washing, 26S proteasomes were eluted from the beads by incubating 15 min at 4°C with 100 μl proteasome purification buffer containing 0.2 mg His₁₀-UIM. The beads were captured and the eluate was kept for further purification. The elution step was repeated and remaining His₁₀-UIM was cleared from the combined eluates by incubation with 80 μl of Ni-NTA beads for 20 min at 4°C. Beads were removed by centrifuging the sample through a 0.22 μm filter (Merck Millipore) and the cleared eluates containing purified 26S proteasomes were used directly or stored at -20°C after supplementing with 40 % glycerol. Protein content in the isolated fractions was assessed using the Bio-Rad Quick Start Bradford protein assay.

Purity of 26S isolations was analyzed by Western blot analysis and silver gel analysis of input, FT and 26S fractions. For silver gel analysis samples were subjected to electrophoresis on 12 % SDS-PAGE gels (90-120 V, 1.5 h). Gels were then fixed by incubation in fixation buffer (50 % Methanol, 12 % Acetic acid, 0.175% Formaldehyde) washed three times for 20 min in 50 % Ethanol, incubated for 1 min in sensitizing buffer (0.02 % Na₂S₂O₃-solution), washed three times for 20 seconds in H₂O and stained by incubation for 20 min in staining solution (0.2 % AgNO₃, 0.028% Formaldehyde). The gel was then washed again three times for 20 seconds in H₂O and bands were developed by incubating the gel in developing buffer (6 % Na₂CO₃, 0.0004% Na₂S₂O₃, 0.0185 % Formaldehyde) for approx. 30 min. Afterwards gels were washed with H₂O and imaged using the ChemiDoc XRS system (Biorad). Appearance of distinct band patterns specific for 26S proteasomes was used as control for purity of the isolations.

3.5.11 Analysis of nascent protein synthesis

Nascent protein synthesis was analyzed using the Click-iT Plus OPP Protein Synthesis Assay Kit (Life Technologies). Cells were seeded in black clear-bottom 96-well plates and left over night to attach to the plate. Cells were then treated with control medium or with medium containing 100 μM cycloheximide for 4 h at 37°C. After the treatment, medium was removed and cells were incubated

Materials and methods

with growth medium containing 20 μ M Click-iT O-propargyl-puromycin (OPP) reagent for 30 min at 37°C. Next, medium was removed, cells were washed with PBS and fixed with 4 % PFA for 15 min at RT. After fixation, cells were permeabilized in 0.5 % TritonX-100 in PBS for 15 min, washed twice with PBS and stained by adding 50 μ l AF-647 picolyl azide containing Click-iT Plus OPP reaction cocktail per well and incubating for 30 min at RT. Afterwards, cells were washed with PBS and nuclei were stained by incubation with HCS NuclearMask Blue Stain in PBS for 30 min. Cells were washed again twice with PBS and fluorescence was measured using the LSM710 fluorescence microscope (Zeiss). Protein synthesis was measured as the mean intensity of the red signal and normalized to cell number assessed by the blue NuclearMask signal.

3.6 Quantitative real-time RT-PCR analysis

Total RNA from tissue was isolated using Roti-Quick-Kit (Roth) and peqGOLD Total RNA Kit (Peqlab, Erlangen, Germany). Total RNA from cells was isolated using Roti-Quick-Kit. 100-1000 ng per sample of total RNA were reverse transcribed using random hexamers and M-MLV reverse transcriptase. Quantitative PCR was performed using the SYBR Green LC480 System (Roche Diagnostics, Mannheim, Germany). The following gene-specific primers were used:

Table 3-5: Mouse primers for qPCR

Gene name	Forward Primer (5'-3')	Reverse Primer (5'-3')
DRP1	AGGAGATGCAGAGGATCATTGAG	ATCAGCAAAGTCGGGGTGTT
MFN1	TGTGTTCCGATTTTCAAGAGGACA	CTCCTGGGCTGCATTATCCG
MFN2	CATGTCCACGATGCCCAAC	GACAAAGTGCTTGAGAGGGG
OPA1	ATGATTGGGCCAGACTGGAA	AGGTAAGCTGGGTGCTCATC
P16	TCGTGAACATGTTGTTGAGGC	CTACGTGAACGTTGCCATC
P21	CGGTGTGAGAGTCTAGGGGA	AGAGACAACGGCACACTTTG
PSMA3	TGAAGAAGGCTCCAATAAACGTCT	AACGAGCATCTGCCAGCAA
PSMB10	GAAGACCGGTTCCAGCCAA	CACTCAGGATCCCTGCTGTGAT
PSMB5	TGCTCGCTAACATGGTGTATCAGTA	GGCCTCTTATCCCAGCCA
PSMB6	AGACGCTGTCACTTACCAACTGG	AAGAGACTGGCGGCTGTGTG
PSMB7	TGCCTTATGTCACCATGGGTTT	TTCCTCTCCATATCTGGCCTAA
PSMB8	TGCTTATGCTACCCACAGAGACAA	TTCACTTTACCCAACCGTC
PSMB9	GTACCGTGAGGACTTGTAGCGC	GGCTGTGCAATTAGCATCCCT
PSMC2	TCCTAAGATCGACCCAACAGTTACC	TTCCTTACAGCCACCAACATCA
PSMC3	AAGCTGAGCAAGATGGCATT	TTCATGGGTGACTCGCAATA
PSMD11	GAATGGGCCAAATCAGAGAA	TGTACTTCCACAAAAGGGC
PSME1	AGGCTTCCACACGCAGATCT	ACCAGCTGCCGATAGTACC

PSME2	CCAGATCCTCCACCCAAGGA	CCGGGAGGTAGCCACACTTA
PSME3	TAGCCACGATGGACTGGATG	CACAAACACCTTGGTTCCTTGAA
PSME4	CATCCTTCAAATAATGGGCG	AAGCTTATGGCTTTCAGGCA

3.7 Statistical analysis

One-way ANOVA with Dunnett's multiple comparison test or student's t-test was used for statistical analysis of mitochondrial membrane potential, mitochondrial superoxide production or ATP levels. Two-way ANOVA with Bonferroni multiple comparison test or one-way ANOVA with Dunnett's multiple comparison test was used for statistical analysis of mRNA expression, protein synthesis or proteasome activity. Differences in lung function were evaluated using student's t-test. Differences in protein expression data were evaluated using t-test or one-way ANOVA with Dunnett's multiple comparison test or two-way ANOVA with Bonferroni multiple comparison test. Alterations in mitochondrial morphology were analyzed using the chi-square test. All statistical analysis was performed using GraphPad Prism software (version 5.00). Significance was indicated in the figures as *: $p < 0.05$, **: $p < 0.01$ or ***: $p < 0.001$.

4 The effect of mitochondrial dysfunction on proteasome activity and composition

Parts of this chapter have been prepared for publication as:

Berschneider K., Kremer L., Meul T., Kukat A., Wettmarshausen J., von Törne C., Hauck S., Geerlof A., Perrochi F., Trifunovic A., Eickelberg O., Prokisch H., Meiners S. (2016). Genetic dysfunction of the mitochondrial respiratory chain impairs proteasome activity.

Berschneider K., Meul T., Kukat A., Eickelberg O., Trifunovic A., Meiners S. (2016). Loss of 26S proteasome activity induces resistance to proteasome inhibition independent of 19S subunit expression.

4.1 Introduction

Mitochondrial and proteasomal functions are important determinants of cellular health. Since both systems readily adapt to environmental stress and cellular alterations, it can be speculated that mitochondrial and proteasomal functions also adapt to changes in the respective other system. However, surprisingly little is known about how mitochondrial and proteasomal functions are connected especially in the context of chronic alterations of their function. As outlined in paragraph 1.3, mitochondrial ROS production is a potential mechanism on how mitochondrial dysfunction affects proteasomal function. However, mitochondrial dysfunction does not necessarily induce an increase in cellular ROS burden. Especially, in the context of aging, cells of the premature aging mtDNA mutator mouse model show a prominent mitochondrial dysfunction without increased cellular or mitochondrial ROS production (Trifunovic et al., 2005). MtDNA mutator mice express a modified version of the mitochondrial DNA polymerase subunit γ (PolG) with an amino acid substitution in the second exonuclease domain of PolG (D257A). This amino acid substitution induces a proofreading deficiency of PolG without affecting its DNA synthesis capacity (Trifunovic et al., 2004). Mice homozygous for the mtDNA mutator allele show a prominent premature aging phenotype with first signs of aging beginning at 25 weeks of age. These mice develop a plethora of aging phenotypes such as kyphosis, alopecia, greying of hairs, weight loss, anemia and die prematurely with a median lifespan of 48 weeks (Trifunovic et al., 2004). The premature aging phenotype was associated with a strongly increased mutation load in mtDNA and decreased respiratory chain activity in mtDNA mutator mice (Trifunovic et al., 2004). Importantly, accumulating mtDNA mutations did not induce increased mitochondrial ROS production despite pronounced respiratory chain dysfunction in mtDNA mutator mice cells and tissue (Trifunovic et al., 2005).

The effect of mitochondrial dysfunction on proteasome activity and composition

Therefore, this model can be used to assess ROS-independent effects of mitochondrial dysfunction on proteasome function.

To understand how mitochondrial respiratory dysfunction affects the proteasome, the function of the proteasome system was assessed in embryonic fibroblasts from mtDNA mutator mice and in human dermal fibroblasts harboring mutations in respiratory chain subunits. Additionally, activation of several possible signaling pathways such as ROS, ATP, or NADH signaling was analyzed and its effect on proteasome activity was assessed.

4.2 Results

To investigate the effect of mitochondrial dysfunction on the proteasome system, first mitochondrial dysfunction was confirmed in mtDNA mutator MEFs (Mut). Mitochondrial oxygen consumption was almost completely abolished in mtDNA mutator MEFs indicating a pronounced respiratory chain dysfunction (Figure 4-1A&B). Indeed, mtDNA mutator MEFs are unable to use mitochondria for ATP production as shown by the strongly impaired mitochondrial ATP production as estimated by the decrease in oligomycin-sensitive respiration (Figure 4-1C). Beside the strong respiratory dysfunction, mitochondrial membrane potential was unchanged between wildtype (WT) and mtDNA mutator MEFs (Figure 4-1D) indicating that other mitochondrial functions such as protein import and export or mitochondrial fusion and fission might still be functional. The function of the mitochondrial membrane potential specific probe TMRM was confirmed by adding CCCP to the samples and measuring residual fluorescence after 15 and 30 min (Figure 4-1E).

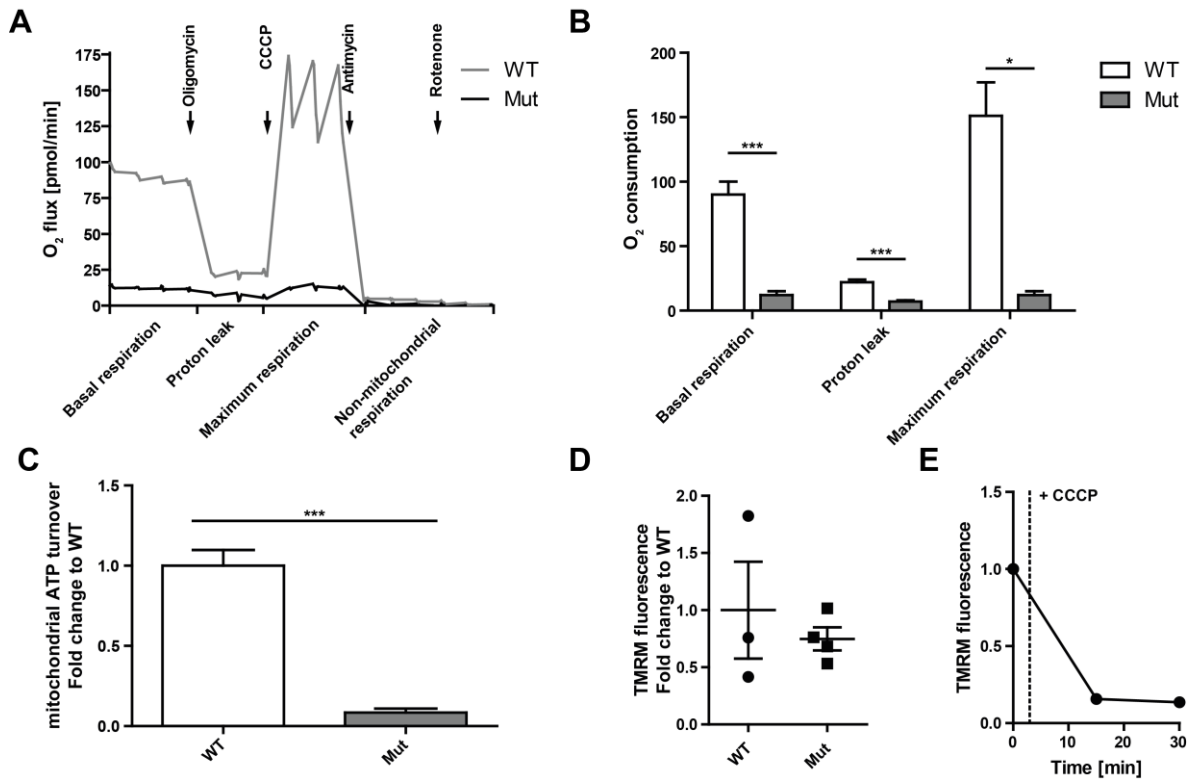


Figure 4-1: Mitochondrial respiration is decreased in mtDNA Mutator MEFs

(A) Cellular oxygen flux under basal conditions, after addition of oligomycin (proton leak), CCCP (maximum respiration), or antimycin A and rotenone (non-mitochondrial respiration) analyzed using the Seahorse XF analyzer. Curves show mean values from three independent wildtype (WT) or four independent mtDNA mutator (Mut) MEF lines. (B) Mean oxygen consumption rate in WT (n=3) and mtDNA mutator (n=4) MEFs. Significance was determined using two-way ANOVA with Bonferroni multiple comparison test. *:p< 0.05, ***:p< 0.001. (C) Mitochondrial ATP production (oligomycin-sensitive respiration) in WT (n=3) and mtDNA mutator (n=4) MEFs. Significance was determined using student's t-test. ***:p< 0.001. (D) Mean fluorescence intensity of WT (n=3) and mtDNA mutator (n=4) MEFs stained with TMRM for assessment of mitochondrial membrane potential measured by flow cytometry analysis. (E) Representative measurement of TMRM fluorescence before and after addition of CCCP to ensure specificity for mitochondrial membrane potential. Values are displayed as mean+SEM. Analysis of mitochondrial oxygen consumption was performed in collaboration with Jennifer Wettmarshausen.

In accordance with unaltered mitochondrial fusion and fission dynamics, as indicated by the stable membrane potential of mtDNA mutator MEFs, no significant differences in mitochondrial morphology were observed between WT and mtDNA mutator MEFs (Figure 4-2).

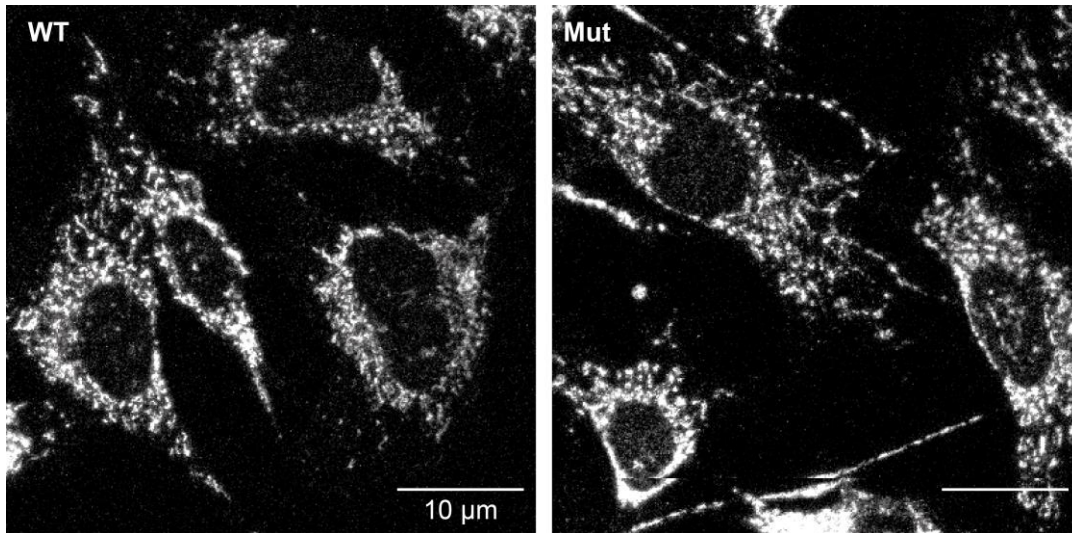


Figure 4-2: Mitochondrial morphology is not altered in mtDNA mutator MEFs

Representative immunofluorescence pictures of WT and mtDNA mutator MEFs stained with anti-cytochrome c antibody.

To further characterize mtDNA mutator MEFs, cellular growth and metabolic activity as well as cellular protein homeostasis were analyzed. Interestingly, mtDNA mutator MEFs showed no reduced growth or overall metabolic activity as analyzed by BrdU incorporation or MTT reduction, respectively (Figure 4-3A&B). Moreover, no broad proteostasis failure was observed in mtDNA mutator MEFs as expression of the chaperones HSP70 and HSP90 was not affected by the mutator phenotype (Figure 4-3C). Similarly, no accumulation of polyubiquitinated proteins was observed in mtDNA mutator MEFs (Figure 4-3D).

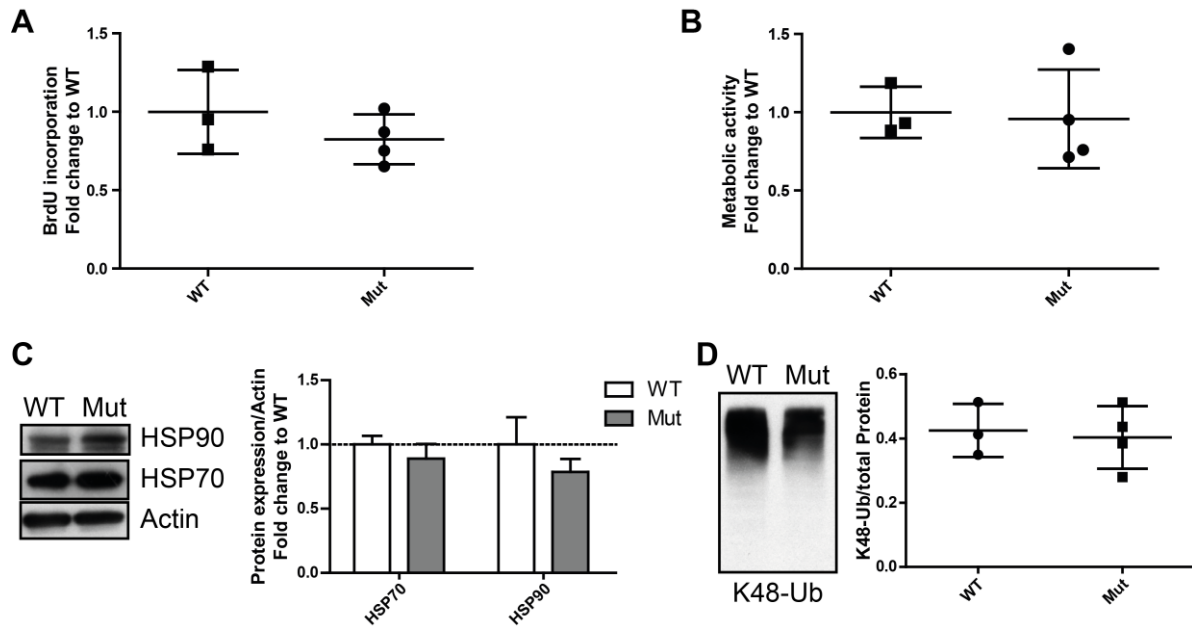


Figure 4-3: Cellular growth and protein homeostasis are not altered in mtDNA mutator MEFs

(A) BrdU incorporation and (B) MTT assay of WT (n=3) and mtDNA mutator (n=4) MEFs. (C) Representative Western blot analysis of HSP70 and HSP90 expression in WT and mtDNA mutator MEFs. Actin was used as a loading control. Densitometric analysis shows mean+SEM of three independent WT and four mutator MEFs lines. Values are displayed as fold changes relative to WT. (D) Representative Western blot analysis of K48-linked ubiquitin levels in WT and mtDNA mutator MEFs. Densitometric analysis shows mean+SEM of three WT and four mutator MEF lines and was normalized to total protein levels as determined by amidoblack staining.

4.2.1 Proteasome activity is decreased in mtDNA mutator MEFs

To analyze the effect of respiratory chain failure on the proteasome, the activity of the catalytic active sites of the proteasome was measured by cleavage of luminogenic model substrates. Activity of all three active sites of the proteasome was significantly attenuated in mtDNA mutator MEFs compared to WT MEFs indicating a pronounced effect of mitochondrial dysfunction on the proteasome in this model (Figure 4-4).

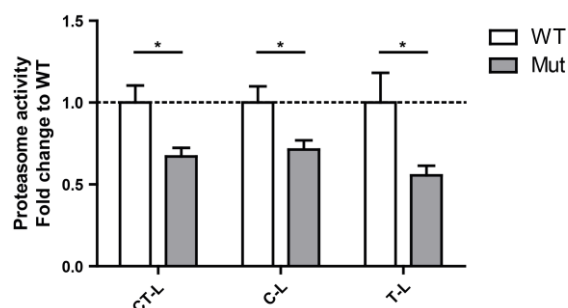


Figure 4-4: Proteasome activity is decreased in mtDNA mutator MEFs

Cleavage of luminogenic model substrates specific for the CT-L, C-L, or T-L active site of the proteasome in WT (n=3) and mtDNA mutator (n=4) MEFs. Bar graphs show mean fold change relative to WT. Significance was determined using two-way ANOVA with Bonferroni multiple comparison test. *:p< 0.05.

The effect of mitochondrial dysfunction on proteasome activity and composition

To assess whether the decreased proteasome activity is associated with decreased proteasome levels, expression of total proteasome subunits was analyzed. In contrast to the changes in proteasome activity, no significant alterations were observed for mRNA or protein expression of subunits of the 20S core particle and the 19S regulatory particle (Figure 4-5).

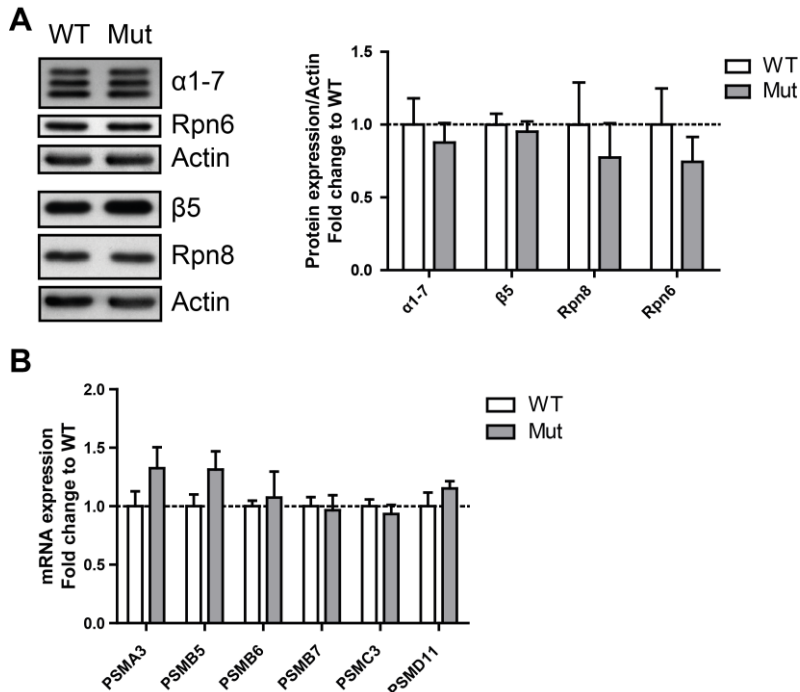


Figure 4-5: Proteasome expression is not altered in mtDNA mutator MEFs

(A) Representative Western blot analysis of 20S (α 1-7, β 5) and 19S (Rpn6, Rpn8) subunit expression in WT and mtDNA mutator MEFs. Actin was used as a loading control. Densitometric analysis shows mean+SEM from three WT or four mtDNA mutator MEF lines. (B) RT-qPCR analysis of proteasome subunit mRNA expression levels in WT (n=3) and mtDNA mutator (n=4) MEFs. Bar graphs show mean+SEM relative to WT.

4.2.2 Assembly of 26S and 30S proteasome complexes is decreased in mtDNA mutator MEFs

Proteasomal activity is mainly regulated by attachment of the 19S regulatory particle to the 20S proteasome core. To test whether 26S or 30S proteasome assembly is impaired in mtDNA mutator MEFs, native gel analysis of proteasome complexes was performed. Interestingly, 20S proteasome activity and complex levels were unaltered in mtDNA mutator MEFs (Figure 4-6A-C). 20S complex levels even tended to be increased in mtDNA mutator MEFs which was, however, not statistically significant. In contrast, attachment of the 19S regulatory particle to one or both ends of the 20S core particle was significantly reduced in mtDNA mutator MEFs, resulting in decreased levels and activity of assembled 26S and 30S proteasome complexes (Figure 4-6A-C).

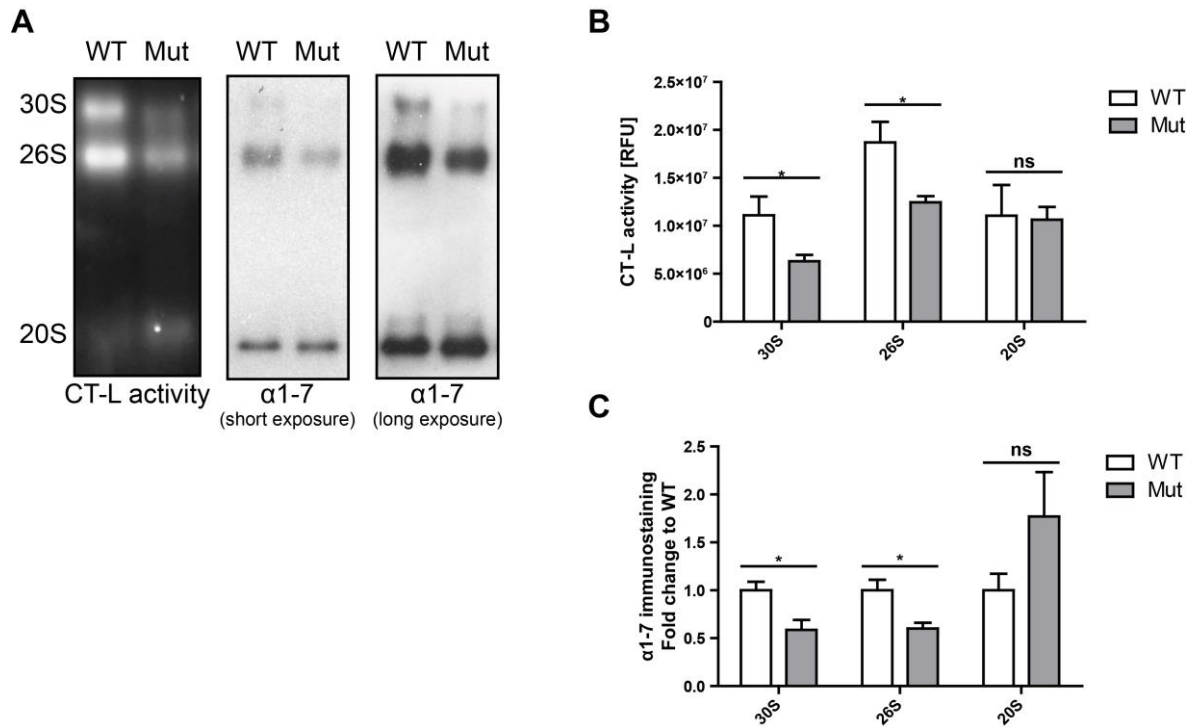


Figure 4-6: 26S and 30S proteasome assembly is impaired in mtDNA mutator MEFs

(A) Representative native gel analysis of proteasome complexes activity in cell lysates from WT and mtDNA mutator MEFs. Panels show CT-L activity overlay of native gels and $\alpha 1-7$ immunostaining after immunoblotting of the native gels. (B) Quantification of CT-L activity and (C) $\alpha 1-7$ immunostaining in native gel assays. Bar graphs show mean+SEM. n=3(WT) - 4(Mut). Significance was determined using student's t-test comparing WT vs. Mut cells. *:p < 0.05, ns: non-significant.

To assess whether association with alternative regulators is altered in mtDNA mutator MEFs, levels of PA28 α and PA28 γ in whole cell lysates and in association with isolated 26S proteasomes were analyzed. Purity of isolated 26S fractions was confirmed by silver gel and western blot analysis. Isolated 26S preparations showed a 26S specific band pattern in the silver gel analysis (Figure 4-7A) and were strongly enriched for both 20S as well as 19S subunits (Figure 4-7B). While no significant expressional changes of PA28 α or PA28 γ were observed in total cell lysate (Figure 4-8A), PA28 γ levels were significantly decreased in fractions of isolated 26S proteasome (Figure 4-8B). Decreased association of PA28 γ with proteasome complexes was further confirmed by immunoblotting of native gels for PA28 γ (Figure 4-8C).

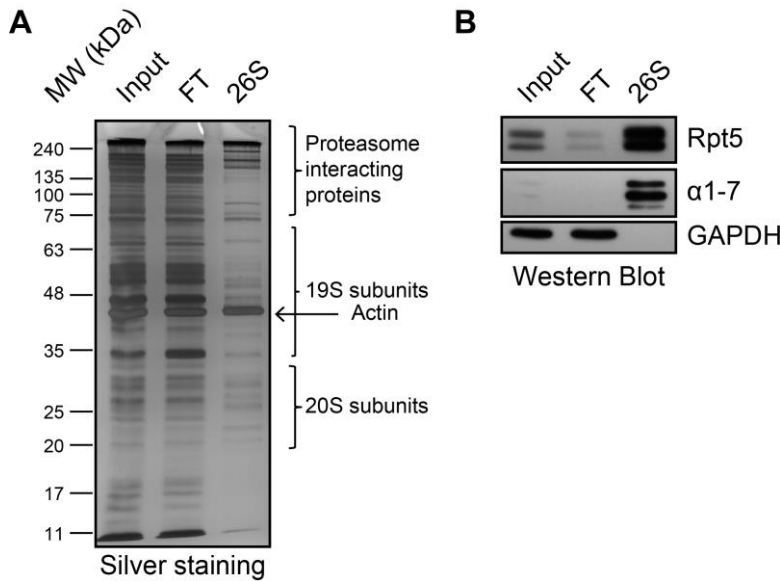


Figure 4-7: Isolation of 26S proteasomes

(A) Representative silver gel analysis of input, flow through (FT) or isolated 26S fractions showing a distinct band pattern for isolated 26S proteasomes. Molecular weight (MW) is given according to a molecular weight standard. (B) Representative western blot analysis for 20S (α 1-7), 19S (Rpt5) or cytosolic (GAPDH) marker proteins in 26S isolations.

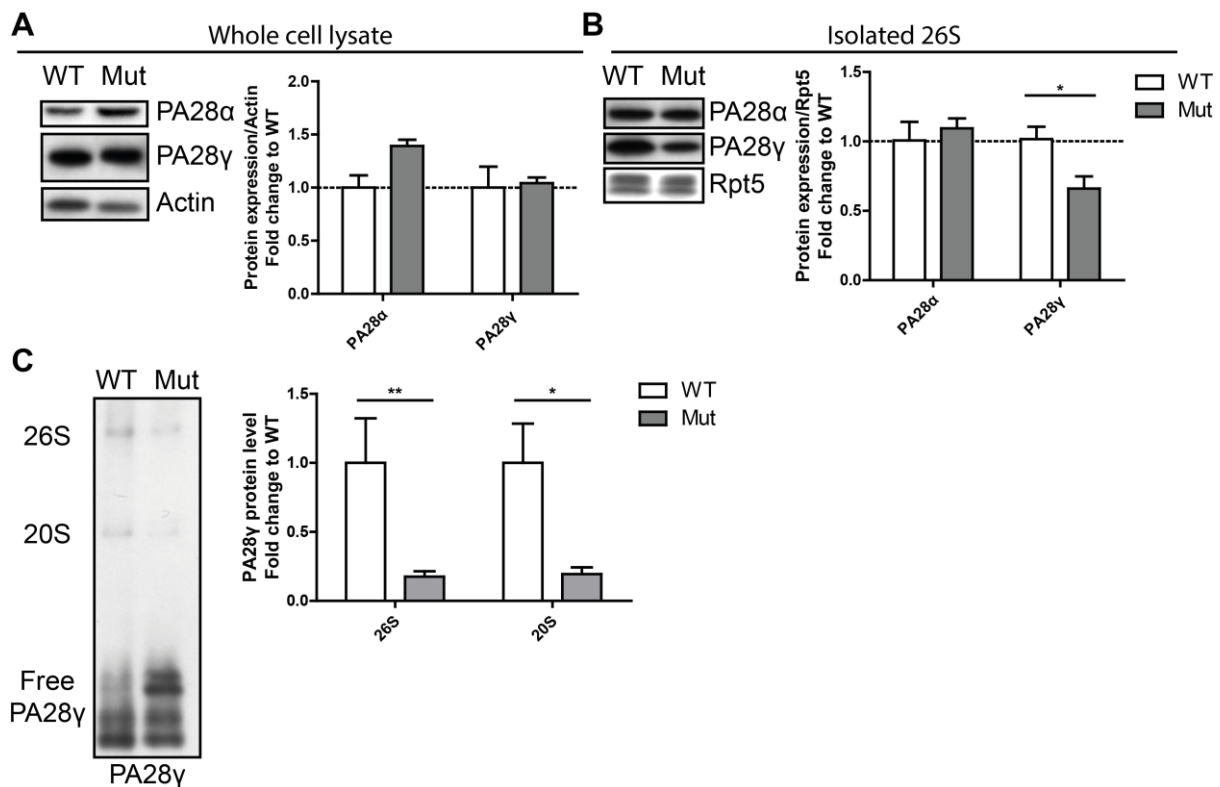


Figure 4-8: Decreased association of proteasome complexes with PA28 γ in mtDNA mutator MEFs

Representative Western blot analysis and quantification of PA28 α and PA28 γ in (A) whole cell lysates and (B) 26S isolations from WT (n=3) and mtDNA mutator (n=4) MEFs. Actin was used as loading control in whole cell lysates and Rpt5 was used in 26S preparations. Significance was determined using two-way ANOVA with Bonferroni multiple comparison test. *:p<0.05 (C) Representative immunoblot and quantification of PA28 γ in native gel assays. Bar graphs show mean+SEM. n=3(WT) - 4(Mut). Significance was determined using student's t-test comparing WT vs. Mut cells. *:p<0.05, **:p<0.01.

In summary, mtDNA mutator MEFs show pronounced dysfunction of the mitochondrial respiratory chain which is associated with reduced assembly and activity of 26S and 30S proteasomes and PA28 γ containing alternative proteasome complexes. Importantly, as the amount of active 20S proteasome complexes is not increased in mtDNA mutator MEFs, diminished 26S and 30S formation is not due to disassembly of these complexes. Moreover, it is not dependent on expressional regulation of 20S or 19S proteasome subunits.

4.2.3 Mitochondria to proteasome signaling in mtDNA mutator MEFs

Attachment of regulatory particles to the proteasome core particle is suggested to be dynamically regulated to allow the cell to adapt proteasome activity to cellular needs (Meiners et al., 2014). To assess the underlying mechanisms of mitochondria to proteasome signaling several signaling pathways were analyzed for being affected by mitochondrial dysfunction and affecting proteasome activity in mtDNA mutator MEFs. As outlined in paragraph 1.3.2, mitochondrial damage can result in elevated leakage of electrons in the respiratory chain and thereby increased generation of ROS. However, as also published previously, mtDNA mutator MEFs do not show increased mitochondrial ROS production (Trifunovic et al., 2005). These data were confirmed in this study: No change was found in the levels of mitochondrial superoxide (Figure 4-9A) or overall cellular ROS (Figure 4-9B) in mtDNA mutator MEFs compared to WT MEFs. Accordingly, the amount of proteins containing oxidative modifications was not significantly changed in mtDNA mutator MEFs as assessed by oxyblot analysis (Figure 4-9C). Furthermore, treatment of mtDNA mutator MEFs with the antioxidant N-acetylcysteine did not have any effect on proteasome activity in these cells (Figure 4-9D&E). These data support the notion that impaired proteasome activity is not due to ROS-mediated signaling in mtDNA mutator MEFs.

The effect of mitochondrial dysfunction on proteasome activity and composition

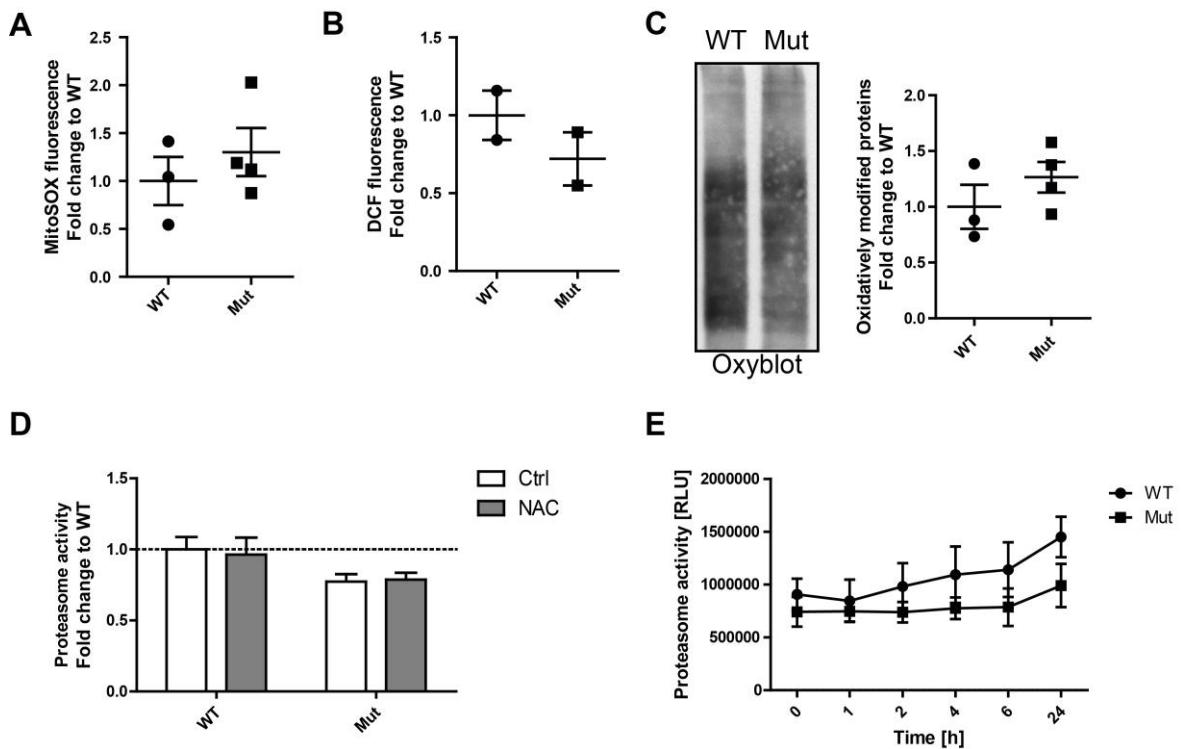


Figure 4-9: No elevated ROS production in mtDNA mutator MEFs

Flow cytometry analysis of WT and mtDNA mutator MEFs stained with (A) MitoSOX Red for detection of mitochondrial superoxide generation, n=3 (WT) - 4(Mut) +SEM, or (B) H₂DCFDA for detection of cellular ROS. n=2+SEM. (C) Representative Oxyblot image and quantification of oxidatively modified proteins from WT (n=3) and mtDNA mutator (n=4) MEFs. (D) CT-L proteasome activity in WT (n=3) and mtDNA mutator (n=4) MEFs after treatment with control or 5 mM NAC-containing medium for 2 h. Bars show mean+SEM. Values were displayed as fold change relative to WT. (E) CT-L proteasome activity in 5 mM NAC treated WT (n=2) and mtDNA mutator MEFs (n=2) over a time-course of 24 h.

26S and 30S proteasome activity is dependent on the availability of ATP and disassembly of 19S and 20S particles was observed in the absence of ATP (Liu et al., 2006a). However when ATP levels were analyzed in WT and mtDNA mutator MEFs no change in total cellular ATP was observed indicating absence of an obvious difference in ATP availability (Figure 4-10A). Since measurement of total ATP levels only reflects the steady state in the cells, additionally activation of the cellular ATP sensor AMPK was analyzed. AMPK is the major energy sensing molecule in the cell and is activated by increased phosphorylation in response to low ATP availability (Hardie et al., 2012). Hence, AMPK activation reflects a low energy status in the cell and low availability of ATP. Thereby it would reflect the physiological situation much more than the measurement of steady state ATP levels. However, no difference in phosphorylation of the AMPK α or β subunits was observed in WT and mtDNA mutator MEFs (Figure 4-10B) indicating absence of AMPK activation.

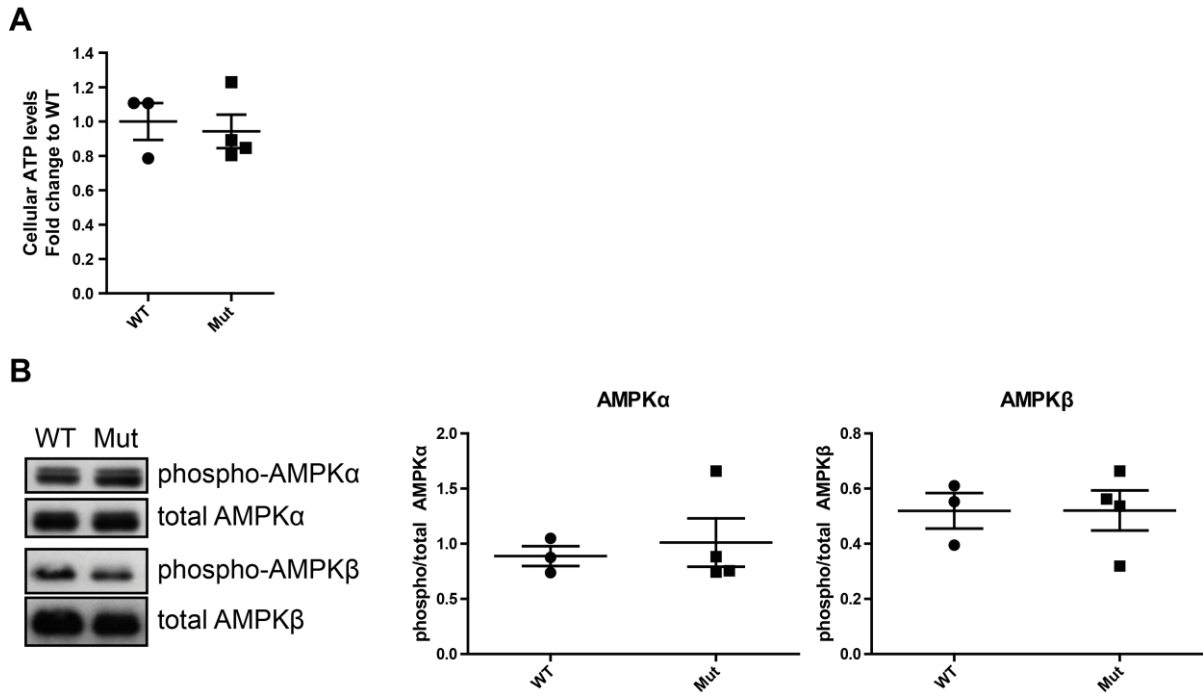


Figure 4-10: No alterations in ATP availability in mtDNA mutator MEFs

(A) Relative ATP levels in WT and mtDNA mutator MEFs. (B) Representative Western blot analysis for phosphorylated and total AMPK α and AMPK β and quantification of phosphorylated/total AMPK α or AMPK β levels in WT (n=3) and mtDNA mutator (n=4) MEFs.

Beside ATP, also the metabolic mediator NADH was shown to affect proteasome function (Tsvetkov et al., 2014). Since NADH is the main substrate for the mitochondrial respiratory chain and mitochondria are the major producer of NADH in the cell (Nunnari and Suomalainen, 2012), it was analyzed if changes in NAD⁺ or NADH occur in mtDNA mutator MEFs and whether these might be responsible for mitochondria to proteasome signaling. While no changes in NAD⁺ levels were observed in mtDNA mutator MEFs, NADH levels were significantly increased compared to WT cells (Figure 4-11). Accordingly, the NAD⁺/NADH ratio was significantly decreased in mtDNA mutator MEFs.

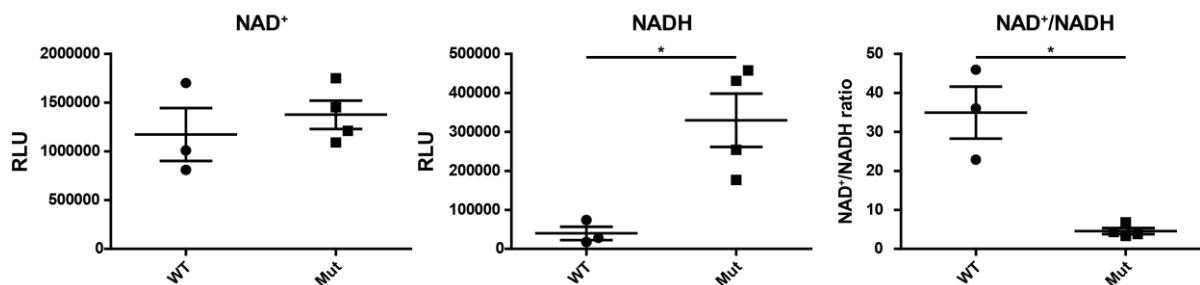


Figure 4-11: NADH levels are increased in mtDNA mutator MEFs

NAD⁺ and NADH levels and the resulting NAD⁺/NADH ratio in WT (n=3) and mtDNA mutator (n=4) MEFs. Significance was determined using student's t-test comparing WT vs. Mut cells. *:p<0.05.

The effect of mitochondrial dysfunction on proteasome activity and composition

To analyze whether the alteration in NADH levels is responsible for the observed change in proteasome activity in mtDNA mutator MEFs, NAD⁺ and NADH levels were modified by treating the cells with the NAD⁺ precursor nicotinamide (NAM) or with the NAD⁺ salvage pathway inhibitor FK866. NAD⁺ can be biosynthetically generated by the cell using NAM as a precursor, while FK866 inhibits this biosynthetic pathway (Stein and Imai, 2014). Hence, treatment with NAM is expected to increase NAD⁺ and NADH levels while FK866 is expected to reduce NAD⁺ and NADH levels. Indeed, treatment of cells with NAM increased NAD⁺ and NADH levels, while FK866 treatment reduced NAD⁺ and NADH levels both in WT and mtDNA mutator MEFs (Figure 4-12A) indicating that NAD⁺ and NADH levels can be experimentally modified in these cells. However, neither treatment with FK866 nor with NAM induced any changes in proteasome activity of WT or mtDNA mutator MEFs (Figure 4-12B) indicating that reduced proteasome activity is independent of NAD⁺ or NADH levels.

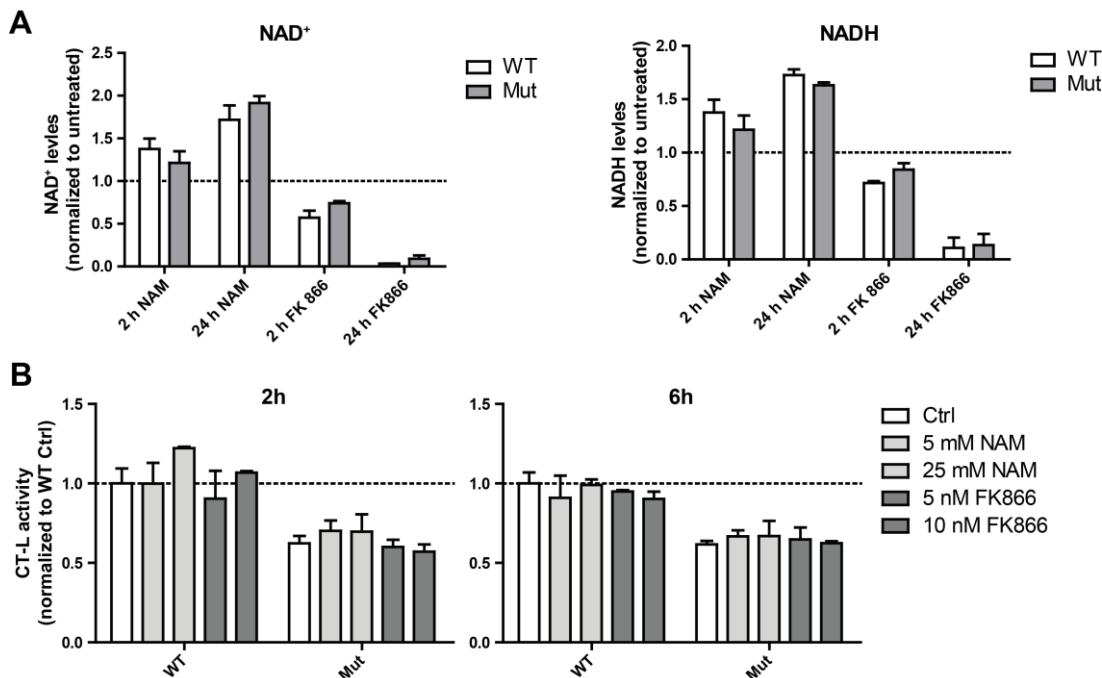


Figure 4-12: Alterations in NAD⁺ or NADH levels do not affect proteasome activity

(A) NAD⁺ and NADH levels in WT (n=2) and mtDNA mutator (n=2) MEFs in response to treatment with 5 mM NAM or 5 nM FK866 for the indicated times. Values are displayed as fold change relative to untreated WT or mtDNA mutator MEFs, respectively. (B) CT-L proteasome activity in WT (n=2) and mtDNA mutator (n=2) MEFs after treatment with NAM or FK866 for the indicated times. Bar graphs show mean+SEM. Values are displayed as fold change relative to WT Ctrl.

NAD⁺ is the main cofactor for enzymes of the Sirtuin deacetylase family and the poly(ADP-ribose)polymerase (PARP) family. Hence, it was additionally investigated whether Sirtuin or PARP activity might be changed by alterations in NAD⁺/NADH ratios, which might thereby indirectly affect proteasome function in mtDNA mutator MEFs. To analyze the effect of altered Sirtuin or PARP activity on proteasome activity, WT and mtDNA mutator MEFs were treated with the PARP inhibitor ABT-488 or the Sirtuin inhibitor EX-527 and proteasome activity was assessed in response to the

treatment. However, proteasome activity did neither change in WT nor in mtDNA mutator MEFs upon treatment with ABT-488 or EX-527 (Figure 4-13) indicating that reduced proteasome activity in mtDNA mutator MEFs is not dependent on PARP or Sirtuin activity.

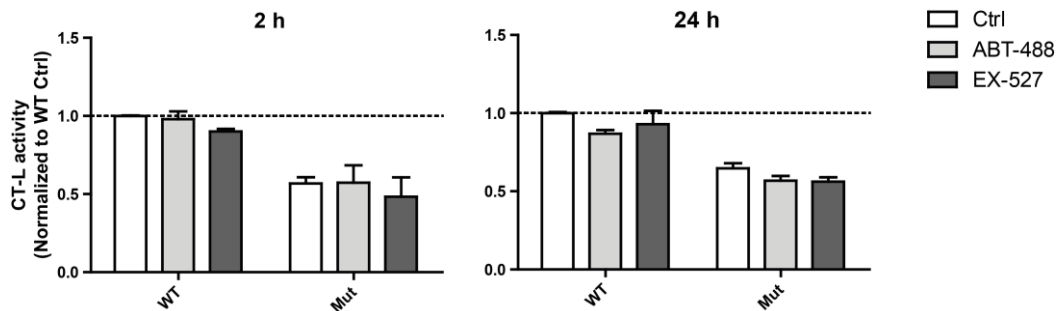


Figure 4-13: Inhibition of Sirtuin or PARP activity does not affect proteasome activity

CT-L proteasome activity in WT (n=2) and mtDNA mutator (n=2) MEFs after treatment with 10 μ M ABT-488 (PARP inhibitor) or 10 μ M EX-527 (Sirtuin inhibitor) for the indicated times. Bar graphs show mean+SEM. Values are displayed as fold change relative to WT Ctrl.

In summary, impaired 26S and 30S proteasome activity in mtDNA mutator MEFs is most probably not mediated by changes in ROS signaling, ATP signaling or NADH signaling since no differential activation of ROS or ATP signaling was found between WT and mtDNA mutator MEFs. Furthermore, experimentally modulation of ROS- or NAD⁺/NADH-dependent signaling pathways did not show any effect on proteasome activity in both WT and mtDNA mutator MEFs.

4.2.4 Increased resistance against proteasome inhibition in mtDNA mutator MEFs

To analyze whether the impairment of proteasome function in mtDNA mutator MEFs decreases the spare proteolytic capacity of the cells and renders the cells more susceptible to further proteotoxic stress, WT and mtDNA mutator MEFs were treated with the proteasome inhibitor bortezomib and the dose-dependent effects on cell viability were analyzed. Unexpectedly, mtDNA mutator MEFs showed an increased resistance to bortezomib, as higher doses of bortezomib were necessary to decrease mtDNA mutator MEF viability to a similar extent as in WT cells (Figure 4-14A). Furthermore, similar doses of bortezomib induced less apoptosis in mtDNA mutator MEFs compared to WT MEFs as revealed by Annexin V/PI staining (Figure 4-14B&C).

The effect of mitochondrial dysfunction on proteasome activity and composition

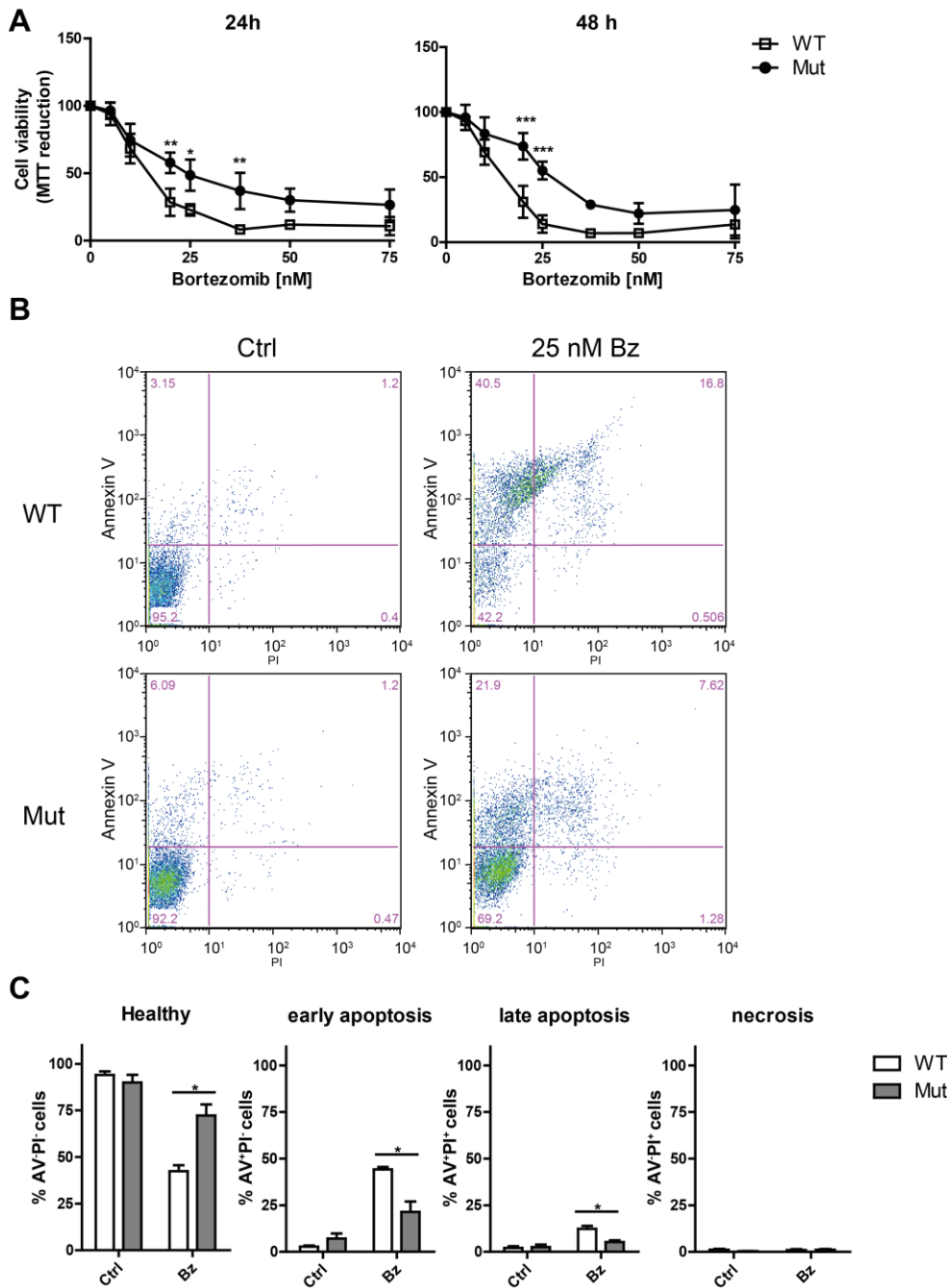


Figure 4-14: Increased resistance to bortezomib in mtDNA mutator MEFs

(A) MTT assay of WT (n=3) and mtDNA mutator (n=4) MEFs treated with the proteasome inhibitor bortezomib for 24 or 48 h. Values were normalized to the control-treated group (0 nM bortezomib) and are displayed as mean+SEM. Significance was determined using two-way ANOVA with Bonferroni multiple comparison test. *:p< 0.05, **:p< 0.01, ***:p< 0.001. (B) Representative flow cytometry analysis of Annexin V and PI staining of 24 h 25 nM bortezomib (Bz) or control-treated WT and mtDNA mutator MEFs. (C) Quantification of healthy (Annexin V⁻/PI⁻), early apoptotic (Annexin V⁺/PI⁻), late apoptotic (Annexin V⁺/PI⁺), or necrotic (Annexin V⁻/PI⁺) cells after 24 h of 25 nM Bz or control treatment in WT (n=3) and mtDNA mutator (n=4) MEFs. Bar graphs show mean+SEM. Significance was determined using student's t-test. *:p< 0.05.

Importantly, the increase in bortezomib resistance was not due to a generally increased resistance to apoptosis as cellular viability in response to H₂O₂ treatment did not differ between WT and mtDNA mutator MEFs (Figure 4-15).

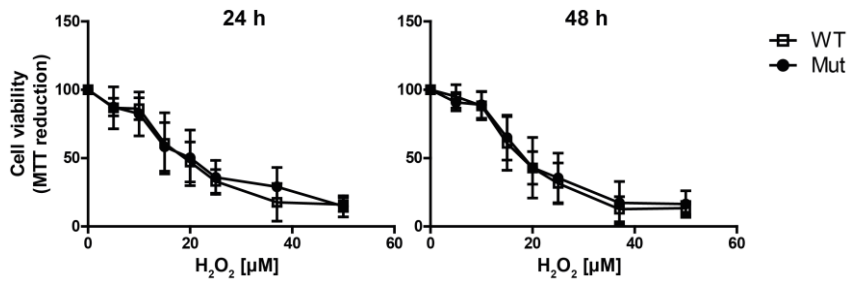


Figure 4-15: No change in cell viability of WT and mtDNA mutator MEFs in response to H₂O₂-induced apoptosis

MTT assay of WT (n=3) and mtDNA mutator (n=4) MEFs treated with H₂O₂ for 24 h or 48 h. Values were normalized to the control-treated group (0 μM H₂O₂) and are displayed as mean+SEM.

Altogether, these data show that despite decreased 26S and 30S proteasome activity, mtDNA mutator MEFs are less sensitive to proteotoxic stress as induced by bortezomib-mediated proteasome inhibition. This effect is specific to proteasome inhibitor-induced apoptosis and does not account for a generally altered susceptibility to apoptosis.

4.2.5 Protein synthesis is decreased in mtDNA mutator MEFs

Proteasomal activity is coupled to cellular protein synthesis (Kalapis et al., 2015; Zhang et al., 2014; Zhao et al., 2015) and a large fraction of newly synthesized polypeptides are directly degraded by the proteasome (Schubert et al., 2000). Furthermore, attenuation of general protein synthesis is a common part of the cellular stress response, e.g. during oxidative stress or ER stress (Grant, 2011; Logue et al., 2013). Therefore, it was analyzed if decreased protein degradation in mtDNA mutator MEFs is also coupled with protein synthesis. Indeed, the overall level of protein synthesis was reduced in mtDNA mutator MEFs while the protein synthesis inhibitor cycloheximide effectively abolished protein synthesis in both WT and mtDNA mutator MEFs (Figure 4-16).

The effect of mitochondrial dysfunction on proteasome activity and composition

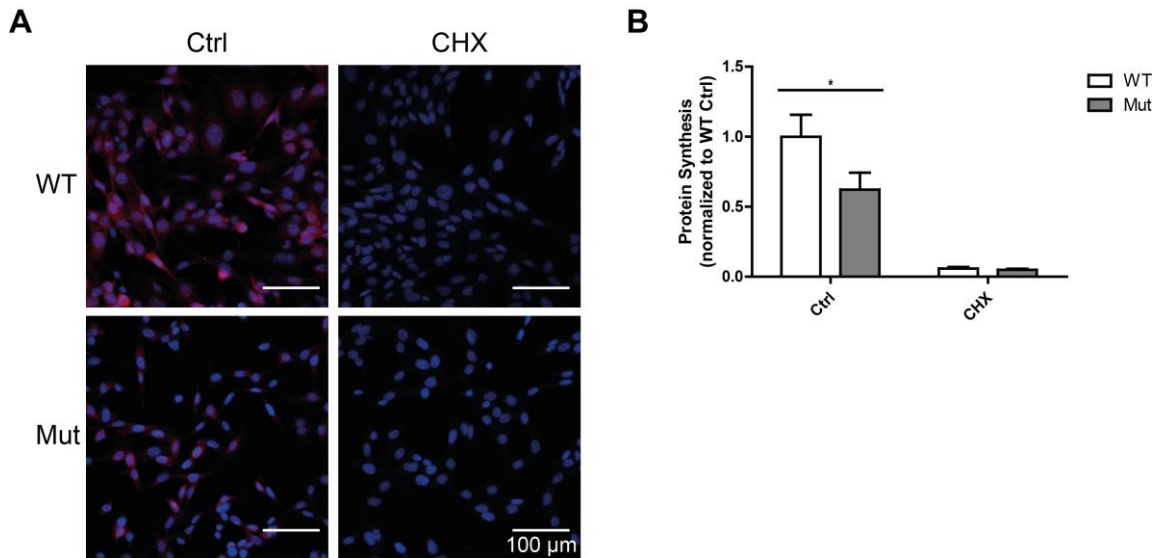


Figure 4-16: Protein synthesis is reduced in mtDNA mutator MEFs

(A) Representative fluorescent images showing nascent protein synthesis (OPP+-AF-647 fluorescence: red) and nuclear staining (blue) of WT and mtDNA mutator MEFs after 4h control (Ctrl) or 100 μ M cycloheximide (CHX) treatment. Scale bars: 100 μ m. (B) Quantification of protein synthesis in WT (n=3) and mtDNA mutator (n=4) MEFs after 4h control or 100 μ M CHX treatment. Bar graphs show mean+SEM. Values are displayed as fold change relative to WT controls. Significance was determined using two-way ANOVA with Bonferroni multiple comparison test. *:p< 0.05.

The mTOR complex is a major metabolic sensor in mammalian cells with the mTOR complex 1 (mTORC1) being a master regulator of protein synthesis (Laplante and Sabatini, 2009). Accordingly, it was analyzed if mTORC1 signaling is changed in mtDNA mutator MEFs by analyzing phosphorylation of the mTORC1 downstream target proteins 4EBP1 or S6 ribosomal protein. However, despite decreased protein synthesis, no significant change was observed in the level of phosphorylated 4EBP1 (Figure 4-17). Additionally, even though total levels of S6 ribosomal protein were decreased in WT cells, changes in the ratio of phosphorylated to total S6 between WT and mutator cells did not reach statistical significance (Figure 4-17).

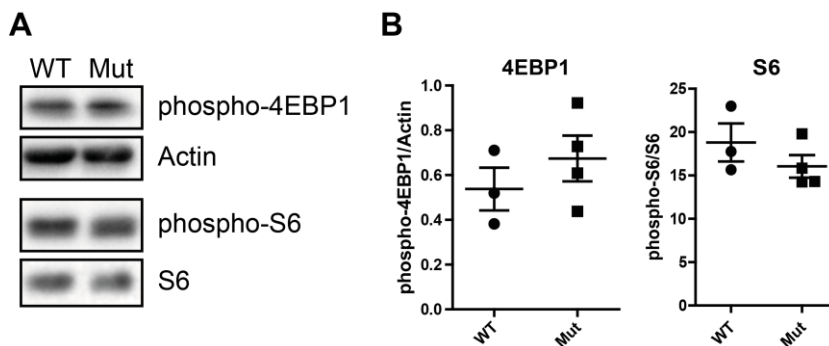


Figure 4-17: mTORC1 signaling is not altered in mtDNA mutator MEFs

(A) Representative Western blot analysis for phosphorylated 4EBP1 and phosphorylated- or total S6 ribosomal protein. (B) Quantification of phospho-4EBP1/Actin and phosphor-S6/S6 levels in WT (n=3) and mtDNA mutator (n=4) MEFs.

4.2.6 Human dermal fibroblasts harboring mutations in single respiratory chain genes show differentially altered proteasome activity

To investigate whether impaired proteasome activity is also observed in patients who suffer from mitochondrial mutations in respiratory chain genes and to analyze if also single mutations in the mitochondrial respiratory chain caused alterations in proteasomal function, human dermal fibroblasts from patients with mitochondrial disorders were analyzed. These human fibroblasts harbor mutations in single mitochondrial genes, which were encoded either in nuclear DNA or in mtDNA. Two independent cell lines without any mutations (Control), one cell line with an uncharacterized mutation (unknown) and one cell line with a mutation in the Tango2 gene which is not involved in the mitochondrial respiratory chain were used as controls. The respective gene mutations of the obtained fibroblast lines are displayed in Table 4-1.

Table 4-1: Mitochondrial gene mutations in human dermal fibroblasts lines used in the study

Gene name	Protein name	Molecular function	Location
NDUFB3	NADH:ubiquinone oxidoreductase subunit B3	Subunit of respiratory chain complex I	Nuclear DNA
ND5	Mitochondrially encoded NADH dehydrogenase 5	Subunit of respiratory chain complex I	mtDNA
unknown	uncharacterized	unknown	unknown
Tango2	Transport and golgi organization 2 homolog	β -oxidation	Nuclear DNA

Mitochondrial oxygen consumption was strongly decreased in fibroblasts with mutations in NDUFB3 and ND5. Fibroblasts with other mutations and also control cells showed no reduction in oxygen consumption (Figure 4-18A). Mitochondrial superoxide generation was significantly increased in fibroblasts with mutations in the NDUFB3 gene but not in any other cell line independent of the respective mitochondrial respiratory chain dysfunction. Treatment of control fibroblast with antimycin A induced a strong increase of superoxide production reaching levels which were additionally elevated compared to NDUFB3 fibroblasts (Figure 4-18B).

The effect of mitochondrial dysfunction on proteasome activity and composition

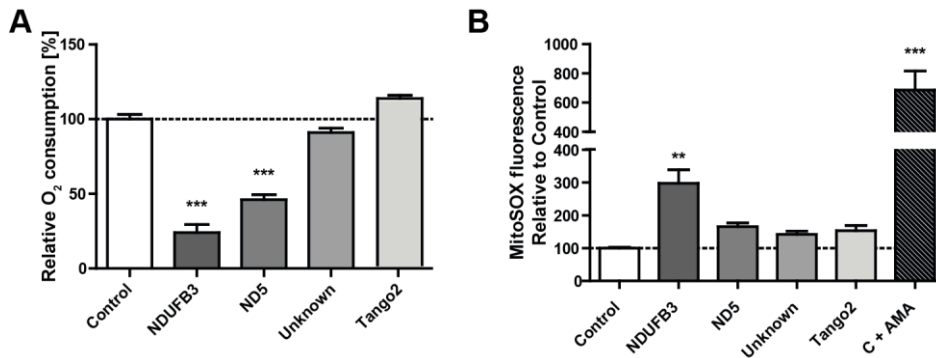


Figure 4-18: Mitochondrial function in human dermal fibroblast lines

(A) Relative rotenone-sensitive oxygen consumption rate in human dermal fibroblast lines. n=8+SEM. (B) Flow cytometry analysis of MitoSOX Red fluorescence for detection of mitochondrial superoxide generation in human dermal fibroblasts. Control cells treated with 50 μ M antimycin A for 30 min (C + AMA) were used as a positive control. n=3-6. Bar graphs show mean+SEM. Values are displayed relative to control cells. Analysis of mitochondrial oxygen consumption was performed by Laura Kremer. Significance was determined using one-way ANOVA with Dunnett's multiple comparison test comparing all groups vs. control group. **:p< 0.01, ***: p< 0.001.

Proteasome activity was slightly but significantly decreased in NDUFB3 and ND5 cells as determined by analysis of the cleavage of CT-L specific luminescent probes (Figure 4-19A). These results were confirmed by activity based profiling of overall proteasome activity which also showed a trend towards decreased activity in NDUFB3 and ND5 cells (Figure 4-19B).

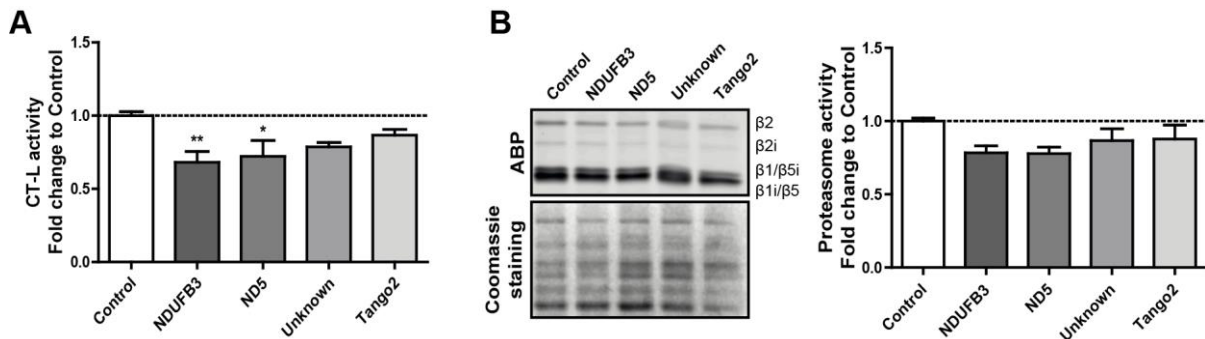


Figure 4-19: Proteasome activity in human dermal fibroblast lines

(A) Cleavage of luminogenic model substrates specific for the chymotrypsin-like active site of the proteasome in human dermal fibroblasts. n=10(Control) - 5(Mutants) +SEM. (B) Representative ABP gel of human dermal fibroblasts resolving individual bands for β 2 and β 2i and overlapping bands for β 1 and β 5i as well as for β 1i and β 5. Coomassie staining was used to ensure equal loading. Quantification shows combined proteasome activity of all active sites. Bar graphs show mean fold change relative to control. n=6(Control) - 3(Mutants) +SEM. Significance was determined using one-way ANOVA with Dunnett's multiple comparison test comparing all groups vs. control group. *:p< 0.05, **: p< 0.01.

Native gel analysis of proteasome activity in human dermal fibroblasts showed a significant decrease in 30S activity of NDUFB3 cells, while no significant change was observed in the other fibroblast lines. Furthermore, for NDUFB3, ND5 and also for Tango2 cells and cells with an uncharacterized mutation activity of the 26S proteasome appeared to be slightly reduced (Figure 4-20).

The effect of mitochondrial dysfunction on proteasome activity and composition

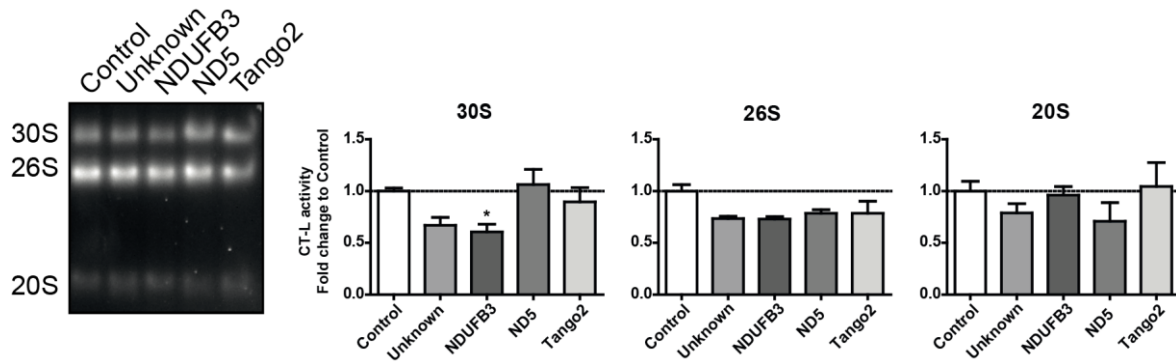


Figure 4-20: Activity of proteasome complexes in human dermal fibroblast lines

Representative native gel analysis of proteasome complex activity in cell lysates from human dermal fibroblasts and quantification of CT-L activity in the overlay assay. Bar graphs show mean fold change relative to control. n=8(Control) - 4(Mutants) +SEM. Significance was determined using one-way ANOVA with Dunnett's multiple comparison test comparing all groups vs. control group. *: p< 0.05.

Furthermore, similar to mtDNA mutator MEFs expression of proteasome subunits was not changed in human dermal fibroblast lines (Figure 4-21).

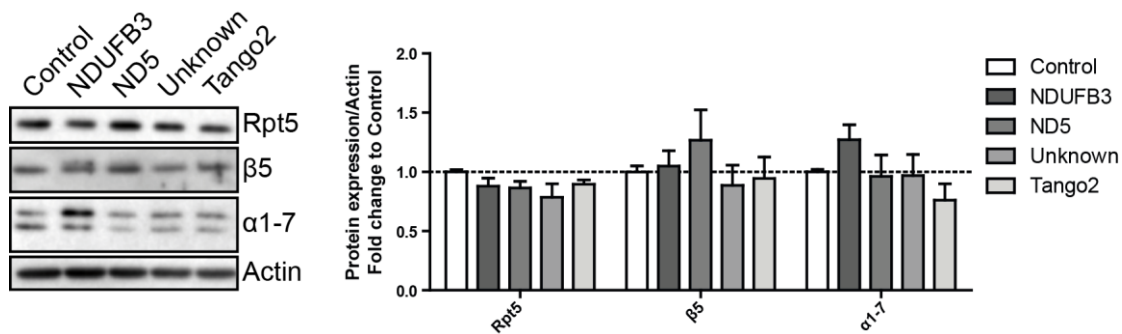


Figure 4-21: Proteasome expression is not changed in human dermal fibroblast lines

Representative Western blot analysis of 20S ($\alpha 7$, $\beta 5$) and 19S (Rpt5) subunit expression in human dermal fibroblast lines. Actin was used as a loading control. Densitometric analysis shows mean+SEM. n=8(Control) - 4(Mutants).

In summary, human dermal fibroblasts with single mutations in the complex I genes NDUFB3 and ND5 show a reduction in basal respiratory chain activity which is accompanied by a slight decrease in proteasome activity. The decrease in proteasome activity appears to be due to a minor reduction in 30S and maybe 26S proteasome complexes. In human dermal fibroblasts with an uncharacterized mutation or a mutation in the β -oxidation gene Tango2 no reduction of respiratory chain activity and no significant reduction in proteasome activity were observed.

4.3 Discussion

Mitochondrial function and protein degradation by the proteasome seem to be closely interconnected. However, little is known on how mitochondrial dysfunction directly affects the proteasome especially in settings of chronic genetic respiratory chain dysfunction. Here, MEFs of the mtDNA mutator mouse were used to analyze the effect of severe and chronic dysfunction of the respiratory chain on proteasomal activity. Proteasomal activity and particularly activity and assembly of the 26S and 30S proteasome complexes were adversely influenced by mitochondrial dysfunction. Importantly, this effect was independent of mitochondrial ROS production, ATP availability or levels of the signaling molecules NAD⁺ and NADH. Furthermore, diminished 26S and 30S proteasome assembly in mtDNA mutator MEFs was associated with increased resistance towards proteasome inhibition and decreased cellular protein synthesis rates. Similar to mtDNA mutator MEFs, human dermal fibroblasts from patients with single mutations in respiratory chain genes also showed a correlation between decreased respiratory chain activity and proteasome activity.

4.3.1 Dysfunction of the mitochondrial respiratory chain is associated with decreased 26S and 30S proteasome assembly and activity

Regulation of proteasomal activity in the cell can mainly be mediated by expressional changes of proteasome subunits or by altered association of proteasomal activators with the proteasome (Paragraph 1.1.1.2) (Meiners et al., 2014; Schmidt and Finley, 2013). In mtDNA mutator MEFs, overall proteasomal activity towards peptidic substrates was decreased in the absence of expressional changes of 19S or 20S proteasome subunits. While activity of 20S proteasome complexes was not changed, activity of 26S and 30S proteasomes was significantly reduced in mtDNA mutator MEFs. This decreased activity was associated with reduced levels of assembled 26S and 30S proteasomes indicating that the observed overall decrease in proteasome activity is mainly caused by diminished assembly of the 19S activator with the 20S core proteasome. Similar to mtDNA mutator MEFs, human dermal fibroblasts from patients with decreased respiratory chain activity also showed decreased proteasome activity which might also be caused by reduced assembly of 26S and 30S proteasomes.

In addition, formation of alternative 20S or 26S proteasome complexes containing PA28 γ was reduced in mtDNA mutator MEFs, while expression levels of the alternative proteasome activators PA28 α and PA28 γ were not altered. Hence, impaired proteasome activity in mtDNA mutator MEFs is based on decreased association of proteasomal activators with the 20S proteasome core particle and independent of proteasome subunit expression. Furthermore, since levels and activity of free 20S proteasomes did not change in mtDNA mutator MEFs, impaired proteasome activity is not due to disassembly of existing 26S or 30S proteasomes but rather due to decreased assembly of newly

formed proteasome complexes. This finding further underlines the importance of association with regulatory particles as a specific way of regulating proteasome activity (Meiners et al., 2014).

Mitochondria have several functions in the cell such as ATP production in the respiratory chain or biosynthesis of several essential molecules. Furthermore, mitochondria are central mediators of cellular signaling, e.g. in apoptosis initiation (Chandel, 2014). Therefore, it is important to delineate which of the diverse functions of mitochondria are associated with alterations of proteasomal function. In mtDNA mutator MEFs, mutations specifically occur in the mtDNA which encodes only few proteins which are all subcomplexes of the respiratory chain while the vast majority of mitochondrial proteins is encoded in the nucleus (Trifunovic et al., 2004). Hence, specifically the respiratory chain complexes are destabilized in mtDNA mutator mice and show increased turnover (Edgar et al., 2009). Accordingly, it is shown here that while respiratory chain function is almost completely abolished in mtDNA mutator MEFs, mitochondrial morphology and mitochondrial membrane potential did not differ between mtDNA mutator MEFs and WT MEFs and also apoptosis is not significantly increased at baseline. Furthermore, cellular growth or overall metabolic activity was not altered in mtDNA mutator MEFs indicating that these cells do not miss any essential biosynthetic products produced in mitochondria. Moreover, other functions of the mitochondria, such as protein import and export which utilizes the mitochondrial membrane potential as a driving force (Schmidt et al., 2010) or mitochondrial apoptosis induction are preserved in mtDNA mutator MEFs. Thereby, the decreased proteasome activity and assembly in mtDNA mutator MEFs is likely to be dependent on the prominent respiratory chain failure in these cells.

4.3.2 Mitochondria to proteasome signaling in mtDNA mutator MEFs

Several pathways are known to regulate the association of proteasomal regulatory particles with the 20S core complex (Paragraph 1.1.1.2). This signaling enables rapid adaptation of proteasomal activity to the cellular state by regulating proteasomal complex formation (Meiners et al., 2014). Furthermore, it is well known that mitochondrial function can communicate to the cell and to the proteasome in several ways (Paragraph 1.3.2).

One prominent example for mitochondrial signaling is mitochondrial ROS, which is a very versatile signaling mediator and often associated with mitochondrial damage (Sena and Chandel, 2012). Mitochondrial ROS production was previously associated with mitochondria to proteasome signaling (Branco, 2010; Chou et al., 2010; Livnat-Levanon et al., 2014; Segref et al., 2014). Importantly, a recent study by Livnat-Levanon et al. observed that decreased proteasome assembly was associated with increased mitochondrial ROS production following acute respiratory chain inhibition, which was partially reversible by addition of antioxidants (Livnat-Levanon et al., 2014). However, in contrast to these findings the mtDNA mutator mouse provides a model of mitochondrial dysfunction which is

The effect of mitochondrial dysfunction on proteasome activity and composition

not associated with increased mitochondrial ROS production (Trifunovic et al., 2005). Indeed, mitochondrial superoxide production, cellular ROS production and the amount of oxidatively modified proteins did not differ between WT and mtDNA mutator MEFs. Furthermore, antioxidant treatment had no effect on the proteasome function in mtDNA mutator MEFs. Hence, the signaling mechanism between mitochondria and the proteasome in mtDNA mutator MEFs is clearly independent of altered mitochondrial ROS production and thereby differs from the mechanisms described previously. One reason for this discrepancy might be that in most studies mitochondrial dysfunction was induced by treatment of cells with mitochondrial inhibitors or by siRNA-mediated knockdown of respiratory chain subunits. This leads to acute mitochondrial stress, which is in contrast to the chronic mitochondrial failure in mtDNA mutator MEFs. Acute ROS generation, however, leaves the cell less time to adapt to altered conditions. Furthermore, acute inhibition of mitochondrial respiratory chain complexes might induce ROS production which is higher than mitochondrial ROS production under physiological conditions (Murphy, 2009). Accordingly, in human dermal fibroblasts harboring mutations in mitochondrial genes, mitochondrial superoxide production did not reach similar high ROS levels as induced in control cells treated with antimycin A.

As mitochondria are best known for producing ATP and 26S and 30S proteasome function is dependent on ATP (Kim et al., 2012; Liu et al., 2006a), it seems plausible that mitochondrial and proteasomal function might be connected by the availability of ATP. Indeed, it was previously shown that a decrease in proteasome activity caused by treatment with mitochondrial respiratory chain inhibitors could be reversed by increased glucose supplementation to cell culture medium (Höglinger et al., 2003). Additionally, acute ATP depletion in response to oligomycin treatment was also associated with 26S proteasome disassembly (Huang et al., 2013). However, in mtDNA mutator MEFs steady state levels of cellular ATP did not differ from WT cells. Additionally, no change was observed in AMPK activation between WT and mtDNA mutator MEFs. Since AMPK is the major energy sensor in the cell and becomes phosphorylated upon low ATP/ADP ratios (Hardie et al., 2012) a decrease in ATP availability should be associated with AMPK activation. These data indicate that mtDNA mutator MEFs are able to maintain their ATP production via mitochondria-independent pathways. Since in this study MEFs were cultured in DMEM containing a high concentration of glucose, mtDNA mutator MEFs are most probably able to meet their energy requirements by performing glycolysis. Accordingly, increased reliance of mtDNA mutator MEFs on glycolysis has been reported previously (Trifunovic et al., 2005). These data therefore indicate that decreased 30S and 26S assembly in mtDNA mutator MEFs is not caused by reduced availability of ATP.

Beside ATP also the metabolic mediator NADH has the ability to affect proteasome function. Mitochondria are the major cellular source for NADH which is used as a substrate in the mitochondrial respiratory chain (Nunnari and Suomalainen, 2012). In mtDNA mutator MEFs NADH

accumulates, which might be based on decreased utilization of NADH due to impaired respiratory chain activity. In line with this finding, it has previously been shown that in rho0 cells, which are devoid of mtDNA, NADH accumulates in the cytosol due to a defective mitochondrial respiratory chain (Olgun and Akman, 2007).

Altered NADH levels and alterations in the NAD⁺/NADH ratio might signal to the proteasome in different ways. On the one hand, altered NADH levels might affect proteasome activity by direct binding of NADH to proteasome subunits. Indeed, NADH was shown to be able to directly bind Rpt2 and stabilize 26S and 30S proteasome complexes (Tsvetkov et al., 2014). On the other hand, alterations in the NAD⁺/NADH ratio might be signaled to the proteasome by an altered activity of NAD⁺ consuming enzymes such as poly(ADP-ribose)polymerases (PARP) or Sirtuin deacetylases. PARP activation and subsequent proteasome polyADP-ribosylation was shown to enhance the activity of 20S proteasomes in response to acute oxidative stress (Ullrich et al., 1999; Luo and Kraus, 2012). Additionally, assembly of 26S proteasomes was decreased after treatment with an inhibitor of the PARP family member TNKS revealing an additional effect of PARylation on 26S activity (Cho-Park and Steller, 2013). Furthermore, although little is known directly about the regulation of proteasomal activity by Sirtuins, decreased Sirtuin activity is associated with decreased protein homeostasis (Tomita et al., 2015) as well as with aging and mitochondrial dysfunction (Imai and Guarente, 2014; Lin, 2004; Mouchiroud et al., 2013; Sack and Finkel, 2012). Hence, altered NAD⁺ or NADH levels as a consequence of mitochondrial dysfunction might signal directly to the proteasome by binding to proteasomal subunits or indirectly by affecting PARP or Sirtuin activities.

However, experimentally manipulation of NADH levels in this study did not change proteasome activity neither in WT MEFs nor in mtDNA mutator MEFs indicating that direct regulation of proteasome activity by NADH levels does not play a prominent role in this setting. Importantly, a direct regulation of the proteasome by NADH due to its binding to Rpt2 was only effective in the absence of ATP (Tsvetkov et al., 2014), indicating that this effect might only be relevant under specific conditions. Furthermore, inhibiting PARP or Sirtuin activity with the specific inhibitors ABT-888 and EX-527, respectively, also did not alter proteasome activity in WT or mtDNA mutator MEFs, thereby suggesting the absence of indirect regulation of proteasome activity via NAD⁺/NADH-dependent pathways. Therefore, while NADH levels are significantly increased in mtDNA mutator MEFs, this does not obviously relate to proteasomal regulation and rather seems to be a parallel effect based on mitochondrial dysfunction. In support of this notion, it was found that tumor cells, which switch from mitochondrial respiration to glycolytic ATP production, i.e. the Warburg effect, also have increased NADH levels (Santidrian et al., 2013) which are, however, associated with increased proteasome activity and a particular sensitivity to proteasome inhibition (Arlt et al., 2009;

Chen and Madura, 2005). Hence, increased NADH levels do not appear to be canonically associated with decreased proteasome activity.

In summary, mitochondrial dysfunction-induced decrease in proteasome activity and 26S assembly in mtDNA mutator MEFs is not dependent on alterations in cellular ROS, ATP, or NADH signaling and is hence signaled by a yet undescribed novel mechanism. Beside the described signaling pathways, regulation of proteasome complex assembly can also take place by introduction of posttranslational modifications to proteasome subunits (Meiners et al., 2014; Schmidt and Finley, 2013) such as recently shown for phosphorylation of Rpn6 (Lokireddy et al., 2015). Hence, future work to identify the mechanistic steps involved in decreased proteasome assembly should involve analysis of posttranslational modifications in 20S or 19S proteasome subunits.

4.3.3 Decreased proteasome activity does not induce proteostasis imbalance in mtDNA mutator MEFs

The proteasome is one of the major protein degradation pathways in the cell and impaired proteasome function has been shown to induce proteostatic imbalance (Goldberg, 2003). Accordingly, inhibition of proteasomal activity induces a manifold cell stress response in order to maintain proteostasis. This cellular response includes induction of cell cycle arrest, attenuation of protein synthesis, initiation of the unfolded protein response, upregulation of heat shock protein expression and proteasome biosynthesis and, in case of prolonged proteasome inhibition, induction of apoptosis (Bush et al., 1997; Frankland-Searby and Bhaumik, 2012; Kawazoe et al., 1998; Kubiczikova et al., 2014; Meiners et al., 2006). Furthermore, reduced activity of the proteasome is associated with accumulation of polyubiquitinated proteins and protein aggregate formation (Heinemeyer et al., 1991; Hipp et al., 2012; Meiners et al., 2006). However, despite decreased proteasome activity in mtDNA mutator MEFs no pronounced proteostasis imbalance was detected as indicated by the fact that expression levels of the heat shock proteins HSP70 and HSP90 as well as cellular growth and viability remained stable. Furthermore, levels of ubiquitinated proteins did not change between WT and mtDNA mutator MEFs. In conclusion, these data show that despite decreased proteasome activity cellular protein homeostasis remains functional in mtDNA mutator MEFs. These findings accord with recently published data which showed the absence of a protein stress response upon mild knockdown of 19S proteasome subunits (Tsvetkov et al., 2015).

4.3.4 mtDNA mutator MEFs are less sensitive to bortezomib-induced cell death

While cellular proteostasis did not appear to be imbalanced in mtDNA mutator MEFs the spare proteolytic capacity of the proteasome might be reduced in these cells. To investigate if mitochondrial dysfunction-induced reduction of 26S and 30S proteasome levels indeed decreases the spare proteolytic capacity in mtDNA mutator MEFs and thereby renders the cells more vulnerable to a second hit, MEFs were treated with the proteasome inhibitor bortezomib. Paradoxically, WT MEFs were significantly more sensitive to proteasome inhibition than mtDNA mutator MEFs. Although it seems counterintuitive that reduced proteasome activity and decreased 26S proteasome assembly protects the cell from further inhibition of the proteasome system, this finding is in line with two recent publications which were utilizing mutational screens or shRNA libraries to assess mechanisms of resistance against proteasome inhibitors. These studies screened for protein mutations or shRNAs which provide survival advantages to cells under conditions of proteasome inhibition. Importantly, mutations in 19S subunits or mild knockdown of 19S subunits, which concordantly reduced 26S and 30S proteasome levels, were protective against proteasome inhibitor treatment. This effect was very specific for proteasome regulator subunits as knockdown of almost any of the 19S subunits mediated protection, while knockdown of 20S core subunits sensitized to proteasome inhibition (Acosta-Alvear et al., 2015; Tsvetkov et al., 2015). Hence, very similar to results obtained with the knockdown of 19S subunits, the observed reduction in assembly of 26S and 30S proteasomes in mtDNA mutator MEFs is associated with increased resistance to proteasome inhibitor treatment.

The present study reveals that decreased assembly of 26S and 30S proteasome is sufficient to induce resistance towards proteasome inhibitors even in the absence of expressional changes of 19S subunits. Hence, loss of 26S proteasome activity is probably mechanistically downstream of the reduced 19S subunit expression applied in the previous studies. Furthermore, this study shows that physiological triggers such as mitochondrial dysfunction can induce proteasomal dysfunction in an extent which contributes to decreased sensitivity to proteasome inhibitors. These results are of especial importance in the light of the therapeutic use of proteasome inhibitors as anti-cancer drugs. Due to increased sensitivity of tumor cells to proteasome inhibition, proteasome inhibitors are used as anti-cancer drugs (Adams, 2004; Kisselev et al., 2012). However, the acquisition of resistance to proteasome inhibitors in tumors is a major problem during therapy (Buac et al., 2013). Importantly, also decreased mitochondrial metabolism and increased aerobic glycolysis – the so-called Warburg effect – is a common feature of tumor cells (Denko, 2008). Furthermore, it was recently shown that in multiple myeloma cells metabolic shifts towards increased glycolysis are also associated with increased resistance to bortezomib (Maiso et al., 2015). Taken together, these data on mitochondrial

dysfunction-mediated proteasome impairment might thus reveal a novel mechanism for resistance to proteasome inhibition in tumor cells.

Several mechanisms may contribute to the increased resistance against proteasome inhibition upon impaired 26S proteasome activity. First, a mild decrease in proteasome activity could induce a hormetic response by upregulation of other stress response pathways thereby providing an already stress-adapted surrounding (Bieler et al., 2009; Meiners et al., 2006). However, in this study as well as in the study of Tsvetkov et al., no induction of the protective heat shock response was observed under baseline conditions (Tsvetkov et al., 2015). Second, redundant proteolytic systems such as the autophagy pathway could take over tasks from an attenuated proteasome system. However, it has previously been described that autophagy is rather suppressed than enhanced in mtDNA mutator MEFs (Li-Harms et al., 2014). Third, it was suggested that decreased protein synthesis and hence a reduced need of protein turnover might be responsible for resistance to proteasome inhibition. Indeed, knockdown of mediators of protein translation also desensitized cells towards proteasome inhibition (Acosta-Alvear et al., 2015). Additionally, increased resistance to proteasome inhibitors was associated with a decreased rate of protein synthesis in cells after knockdown of 19S subunits (Tsvetkov et al., 2015). Accordingly, overall protein synthesis was attenuated in mtDNA mutator MEFs compared to WT MEFs. Since a substantial fraction of proteins is ubiquitinated and targeted for degradation by the proteasome directly after synthesis (Schubert et al., 2000), a reduction of protein synthesis rates would also well accord with the absence of accumulation of polyubiquitinated proteins in mtDNA mutator MEFs. However, while protein synthesis is significantly reduced in mtDNA mutator MEFs and correlates with reduced 26S activity, it is unclear whether decreased protein synthesis is cause or consequence of impaired 26S and 30S assembly in mtDNA mutator MEFs or whether it might be regulated independently.

To analyze regulation of protein synthesis in mtDNA mutator MEFs activity of the mTORC1 pathway, which is a master regulator of protein synthesis (Laplante and Sabatini, 2009), was analyzed in mtDNA mutator MEFs. However, the downstream mediators of mTORC1 signaling 4EBP1 or S6 ribosomal protein did not show significant alteration in mtDNA mutator MEFs.

In summary, these results confirm the paradoxical resistance to proteasome inhibition first described by Acosta-Alvear et al. and Tsvetkov et al. and further extend their relevance in the context of physiologically decreased 26S complex assembly. Additionally, it was shown that changes in 26S proteasome activity are sufficient to induce resistance to proteasome inhibitors and do not require transcriptional alterations of 19S regulatory particle subunits. While decreased protein synthesis might contribute to decreased sensitivity towards proteasome inhibitor-induced cell death a detailed mechanism downstream of reduced 26S and 30S assembly still has to be elucidated. Furthermore,

the possibility that 26S proteasome assembly is impaired upon metabolic switches in tumor cells and might contribute to resistance to proteasome inhibition in tumor cells requires further investigation.

4.3.5 Reduced proteasome activity in human mitochondrial disorders

To analyze whether decreased proteasome activity also manifests in humans with mitochondrial disorders, proteasome activity was analyzed in human dermal fibroblasts that harbor specific mutations in genes of the respiratory chain. Dysfunctions in respiratory chain complexes in humans are associated with heterogeneous disease conditions with a large variety of clinical symptoms (Haack et al., 2012; Munnich and Rustin, 2001). These diseases are associated with a broad spectrum of clinical manifestations for which direct genotype to phenotype correlations are missing (Haack et al., 2012). A mitochondrial disorder is usually suspected in patients presenting neuromuscular disorders in a combination with other non-neuromuscular disorders. These disorders usually have a progressive course and involve seemingly unrelated organs. Furthermore, the number of organs involved frequently increases over the course of the disease (Munnich and Rustin, 2001). However, as the main function of the mitochondrial respiratory chain is production of ATP it is not surprising that mitochondrial disorders are most evident in tissues with high energy demand such as the nervous system, the heart or skeletal muscle (Kanabus et al., 2014).

Here, dermal fibroblasts from control subjects without disease relevant mutations were used as well as patient fibroblasts harboring mutations in NDUF3 (complex I, nuclear DNA encoded) or ND5 (complex I, mtDNA encoded). Furthermore, patient fibroblasts with a mutation in the non-respiratory chain gene Tango2 (β oxidation, nuclear DNA encoded) or with an uncharacterized mutation were analyzed (See also Table 4-1).

Proteasome activity was reduced in cells with NDUF3 and ND5 mutations and thereby correlated well with the decrease in respiratory chain functions. In contrast, cells with an uncharacterized mutation or a mutation in Tango2 which did not show decreased oxygen consumption were able to maintain their proteasome activity on a similar level as control cells. Additionally, while mutations in NDUF3 were associated with increased production of mitochondrial superoxide, generation of mitochondrial superoxide was not different between control cells and cells with ND5 mutations. Hence, dysfunction of the respiratory chain induced loss of proteasome activity in human dermal fibroblasts from patients with mitochondrial disorders independent of an accompanying change in mitochondrial superoxide production.

Reduced proteasomal protein degradation was previously described in cells from patients with a mutation in the human IVD gene which leads to a defect in mitochondrial leucine metabolism and a disease called isovaleric acidemia (IVA) (Segref et al., 2014; Tanaka et al., 1966). In this case proteasomal dysfunction correlated with increased mitochondrial superoxide production in patient

cells (Segref et al., 2014). However, since the *in vitro* activity of respiratory chain complexes was unchanged in an animal model of IVA (Ribeiro et al., 2007) the described effect on the proteasome is probably not caused by altered mitochondrial respiratory chain activity. These data indicate that different regulatory mechanisms are present which signal from mitochondria to the proteasome.

In addition to a different extent of respiratory chain inhibition in the different patient fibroblasts, the specific mutations are located in mtDNA or nuclear DNA encoded genes. Hence, in addition to analyze whether reduced proteasome activity also manifests in patients with mitochondrial disorders it was analyzed if the reduction of proteasome activity is dependent on the localization of the mutated genes.

Proteasome activity was decreased in cells with mutations in the nuclear DNA encoded NDUF3 gene as well as in the mtDNA encoded ND5 gene. Hence, mitochondrial dysfunction-induced attenuation of proteasomal activity appears to be independent of nuclear or mitochondrial location of the mutated gene. NDUF3 and ND5 are both subunits of complex I. A reduction of proteasome activity was only observed in NDUF3 and ND5 mutants but not in other mutants. However, other mutants also showed a milder phenotype without reduction in basal oxygen consumption rates. Hence, it cannot be distinguished whether the observed decrease in proteasome activity is dependent on the location or the extent of the mitochondrial dysfunction. However, as chemical inhibition of different complexes such as complex I, III or V was capable to induce decreased proteasome activity (Chou et al., 2010; Huang et al., 2013; Livnat-Levanon et al., 2014) it seems more likely that the extent but not the molecular basis of the respiratory chain dysfunction is responsible for the loss of proteasome activity.

In summary, reduced proteasome activity also manifests in fibroblasts from patients with mitochondrial disorders. Decreased proteasome activity was clearly associated with reduced respiratory chain activity while it did not correlate with mitochondrial superoxide production. Furthermore, it was not dependent on the localization of the mutation in nuclear or mtDNA encoded genes. These results indicate that indeed the extent of respiratory chain dysfunction is the determinant for decreased proteasome activity in cases of genetic mitochondrial dysfunction.

4.3.6 Differential adaptation of proteasomal function to mitochondrial dysfunction

This study confirms a strong connection between mitochondrial and proteasomal function. This was evident in the context of respiratory chain dysfunction without elevated ROS generation in a model of premature aging and in the context of disease relevant mutations in genes of single respiratory chain subunits. However, the mechanism of signaling between mitochondria and proteasome differs

from previous studies and is probably depending to the acuteness and cause of mitochondrial dysfunction. Reduced proteasome activity in response to acute mitochondrial dysfunction caused by treatment with respiratory chain inhibitors was mediated by an increase in ROS production or decreased ATP availability (Paragraph 1.3.2). In contrast, decreased proteasome assembly based on chronic respiratory chain dysfunction in mtDNA mutator MEFs was independent of cellular ROS or ATP production. Therefore, a model can be proposed in which proteasome activity is differentially regulated by mitochondrial functions depending on the nature of mitochondrial perturbation: Acute respiratory chain inhibition, generating high amounts of mitochondrial ROS, can induce ROS-dependent 26S disassembly (Chou et al., 2010; Livnat-Levanon et al., 2014; Segref et al., 2014). Similarly, acute ATP depletion by mitochondrial inhibition impairs proteasome activity (Höglinger et al., 2003; Huang et al., 2013). In contrast, chronic mitochondrial dysfunction in the mtDNA mutator MEFs leads to decreased levels of assembled 30S and 26S proteasomes by a mechanism independent of increased ROS production or ATP depletion. Furthermore, in human dermal fibroblasts mutations in mitochondrial respiratory genes, which induce decreased oxygen consumption, are associated with decreased proteasome activity which is similarly not dependent on mitochondrial superoxide production.

Furthermore, as outlined in paragraph 1.3.2, mitochondrial perturbations which are not associated with respiratory chain failure such as malfunction of the mitochondrial protein import machinery or excessive accumulation of misfolded proteins in the mitochondrial intermembrane space have opposite effects on proteasomal function as they were shown to increase proteasomal activity (Papa and Germain, 2011; Wrobel et al., 2015). Hence, while respiratory chain deficiency induces a decrease in proteasomal activity via diverse mechanisms, mitochondrial protein misfolding is associated with increased proteasome activity.

In summary, this study confirms the finding that mitochondrial respiratory chain dysfunction is associated with decreased activity of 26 and 30S proteasomes and shows that regulation of proteasome function in response to mitochondrial respiratory chain dysfunction seems to be much more versatile than usually suggested and reaches beyond ROS generation and ATP depletion especially in settings of chronic mitochondrial dysfunction (Figure 4-22).

The effect of mitochondrial dysfunction on proteasome activity and composition

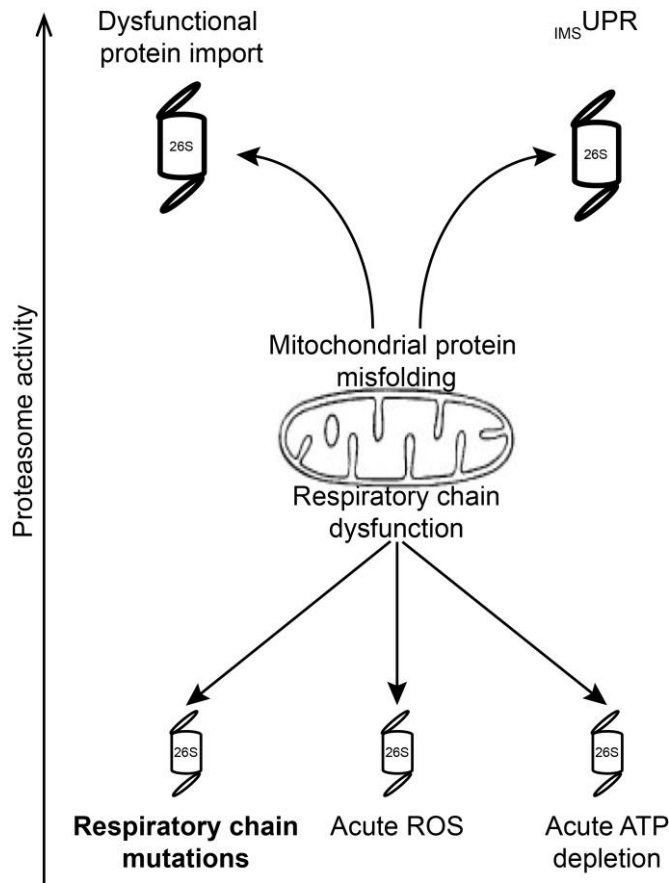


Figure 4-22: Mitochondrial respiratory chain dysfunction is associated with decreased 26S and 30S proteasome activity which is mediated by distinct mechanisms

Mitochondrial protein misfolding in the IMS or dysfunctional protein import increases proteasome activity. In contrast, respiratory chain dysfunction is associated with decreased proteasome activity. Different mechanisms such as mitochondrial ROS signaling or ATP availability can signal between mitochondria and the proteasome. In case of chronic respiratory chain dysfunction due to mutations in respiratory chain genes, impaired 26S and 30S proteasome activity is mediated by yet unknown mechanisms which are independent of ROS or ATP signaling.

5 Mitochondrial function in response to cigarette smoke extract exposure

Parts of this chapter have previously been published as: Ballweg K., Mutze K., Königshoff M., Eickelberg O., and Meiners S. (2014). Cigarette smoke extract affects mitochondrial function in alveolar epithelial cells. *Am. J. Physiol. Lung Cell Mol. Physiol.* 307, L895–L907.

5.1 Introduction

Mitochondrial and proteasomal functions are linked together as dysfunction of mitochondria signals to the proteasome and proteasomal function is required for the maintenance of mitochondrial protein homeostasis (Paragraphs 1.3 and 4). However, it is widely unknown, how mitochondrial function and mitochondrial proteostasis change in response to disease-relevant stimuli in lung cells.

As the lung is directly exposed to air and constantly in contact with the environment, exposure of the lung to noxious environmental agents, such as pollutants or cigarette smoke (CS), is an important determinant for developing chronic lung diseases (Meiners et al., 2015). This is especially evident for chronic obstructive pulmonary disease, for which cigarette smoke is the main risk factor in the western world (Barnes, 2000; Tudor and Petrache, 2012). Cigarette smoke is a complex mixture of different combustion products. It contains thousands of injurious agents and has strong oxidative capacities (Bowler et al., 2004; Nyunoya et al., 2014). Exposure of lung epithelial cells to cigarette smoke initiates an adaptive cellular response which involves proinflammatory and oxidative stress responses (Nyunoya et al., 2014; Bowler et al., 2004). As such, it was recently suggested that cigarette smoke might also induce mitochondrial alterations in lung epithelial cells, which might further contribute to COPD pathogenesis. Additionally, cigarette smoke-induced mitochondrial stress could require the activation of mitochondrial proteostasis systems in order to maintain mitochondrial function. However, a number of studies on the effect of cigarette smoke on mitochondria provide rather conflicting data on mitochondrial function and activation of mitochondrial proteostasis pathways. Mitochondrial fragmentation (Hara et al., 2013) as well increased branching and mitochondria elongation (Hoffmann et al., 2013) have been described in cigarette smoke extract (CSE)-treated cells and in cells isolated from COPD patients. Additionally, decreased mitochondrial membrane potential and induction of mitophagy on the one hand (Mizumura et al., 2014) or increased cellular ATP levels on the other hand (Hoffmann et al., 2013) have been reported. The potentially conflicting results on mitochondrial alterations in response to cigarette smoke in these studies therefore clearly emphasize the need of further studies to fully understand how cigarette smoke affects mitochondrial function.

Importantly, in addition to mitochondrial alterations, cigarette smoke was already shown to affect cellular proteostasis such as autophagy and proteasomal function (Chen et al., 2010; Nyunoya et al., 2014; van Rijt et al., 2012). Hence, both mitochondrial and proteasomal function might be altered in alveolar cells upon exposure to cigarette smoke and thereby might contribute to the development of COPD.

This part aims to identify alterations in mitochondrial morphology, mitochondrial network dynamics and mitochondrial function as well as mitochondrial proteostasis and activation of quality control pathways in a cell culture model of cigarette smoke exposure. To fulfill these aims, lung epithelial cells were treated with low and nontoxic cigarette smoke extract. Nontoxic doses of CSE were considered to more closely resemble a physiologically relevant situation than toxic doses. Cells were thereafter analyzed for mitochondrial morphology, mitochondrial function and for expression and intracellular localization of genes involved in mitochondrial network dynamics or mitochondrial proteostasis.

5.2 Results

In order to analyze the effect of cigarette smoke on mitochondrial function of alveolar epithelial cells, murine lung epithelial (MLE) 12 cells were treated with nontoxic doses of cigarette smoke extract. CSE doses up to 25 % CSE were nontoxic as assessed by the absence of caspase 3 cleavage and LDH release in treated cells (Figure 5-1A&B).

MLE12 cells are a cell line established from pulmonary tumors of a transgenic mouse (Wikenheiser et al., 1993). To also analyze a model which is more closely associated with the physiological situation, additionally primary mouse alveolar epithelial type II cells (pmATII) were analyzed. Importantly, these primary cells were more resistant to CSE and doses up to 50 % CSE did not induce pronounced cytotoxicity (Figure 5-2).

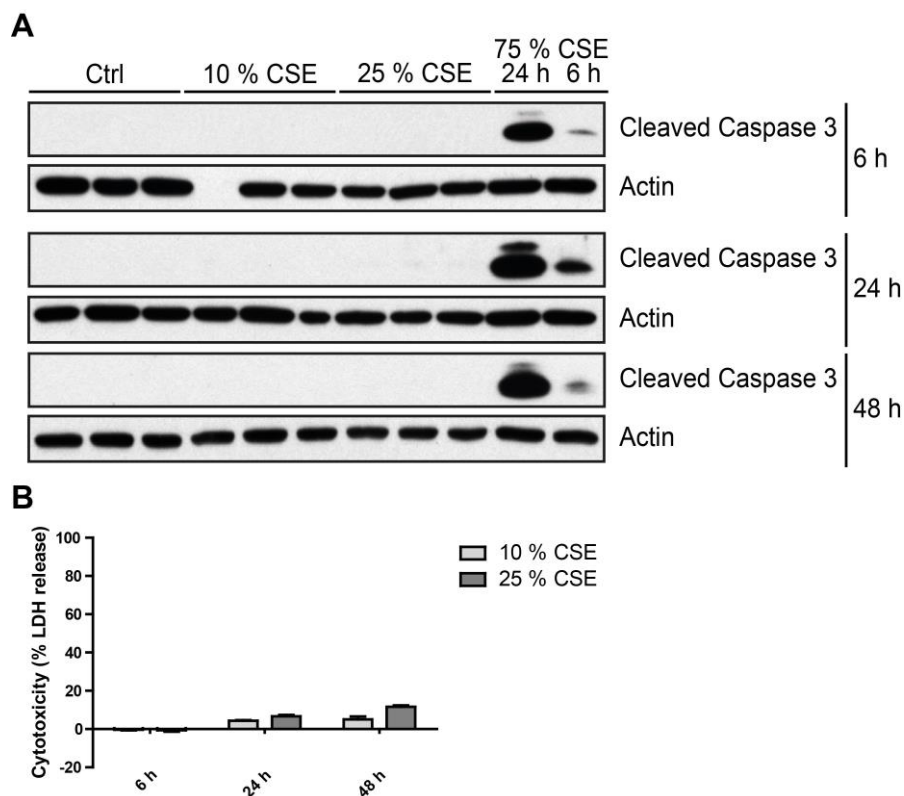


Figure 5-1: Low-doses of CSE are nontoxic in MLE12 cells

(A) Western blot analysis of caspase 3 cleavage in MLE12 cells treated with low dose CSE for 6, 24 or 48 h. Each lane corresponds to lysates from an independent experiment. 24 h 75 % CSE and 6 h 75 % CSE-treated MLE12 cells were used as a positive control for all experimental timepoints. (B) LDH assay of CSE-treated MLE12 cells after 6, 24, and 48 h. n=3. Bar graphs show mean+SEM.

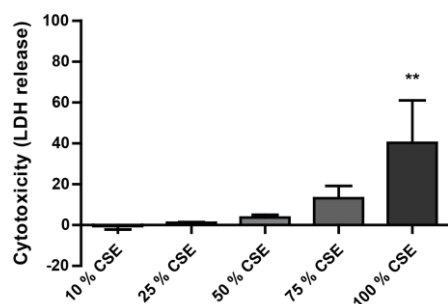


Figure 5-2: CSE doses up to 50 % CSE are nontoxic for pmATII cells

LDH assay of 24 h CSE-treated pmATII cells. n=3. Bar graphs show mean+SEM. Significance was determined using one-way ANOVA with Dunnett's multiple comparison test. **:p< 0.01.

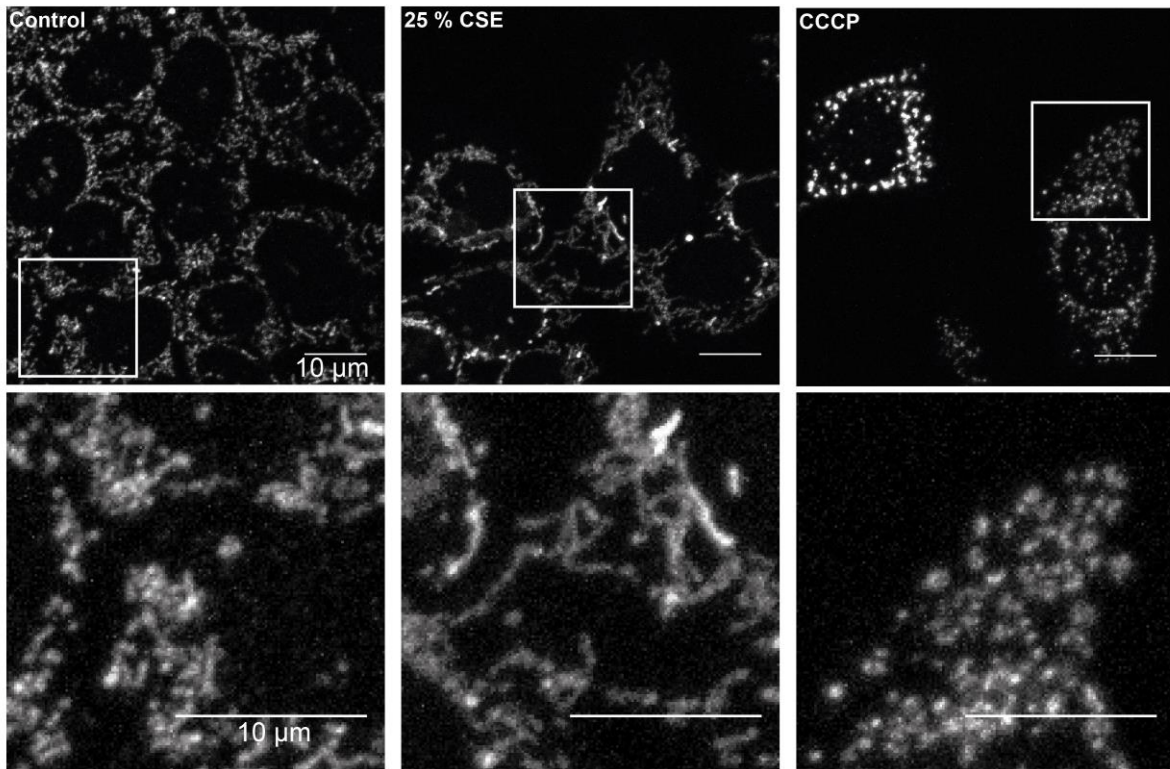
5.2.1 Cigarette smoke extract induces mitochondrial hyperfusion in mouse alveolar epithelial cells

To analyze the effect of nontoxic CSE on mitochondria, mitochondria were stained using a cytochrome c antibody and mitochondrial morphology was analyzed using immunofluorescence microscopy. CSE treatment induced a pronounced elongation of mitochondria and increased mitochondrial network connectivity (Figure 5-3A). In order to quantify CSE-induced changes,

Mitochondrial function in response to cigarette smoke extract exposure

mitochondrial morphology was categorized into three types: “fragmented”, “normal”, or “hyperfused” (see also paragraph 3.4.3). Treatment with CSE significantly increased the proportion of hyperfused mitochondria compared to control treatment after 6, 24 or 48 h (Figure 5-3B). CCCP, which is known to induce mitochondrial fragmentation (Duvezin-Caubet et al., 2006; Tanaka et al., 2010), was used as a positive control. Indeed, CCCP treatment significantly increased the fraction of fragmented cells in a time-dependent manner (Figure 5-3B).

A



B

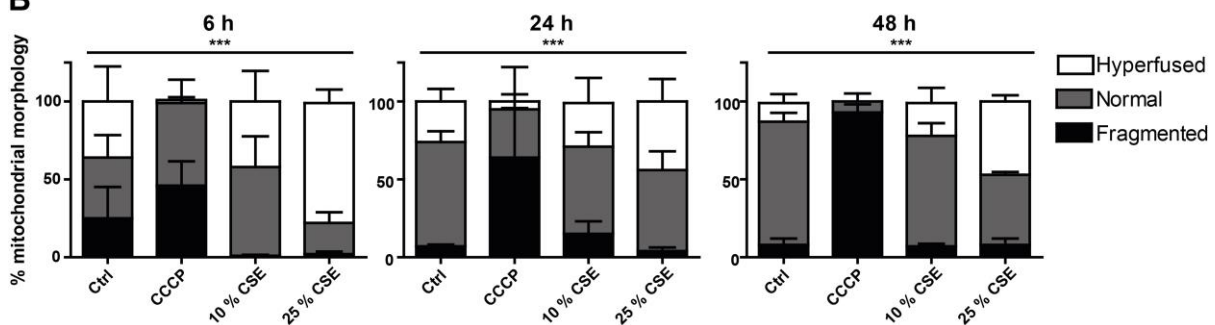


Figure 5-3: CSE treatment leads to mitochondrial hyperfusion in MLE12 cells.

(A) Representative immunofluorescence pictures of MLE12 cells treated with control medium, 25 % CSE, or 10 μM CCCP for 48 h. Scale bars: 10 μm (B) Quantification of mitochondrial morphology in MLE12 cells after 6, 24, and 48 h of treatment. n=3. Bars show mean percentage + SEM. Significance was determined using the chi-square test. ***:p< 0.001.

Similar to MLE12 cells, primary alveolar type II cells treated with 50 % CSE for 24 h showed pronounced mitochondrial hyperfusion with a strong increase in mitochondrial network connectivity (Figure 5-4).

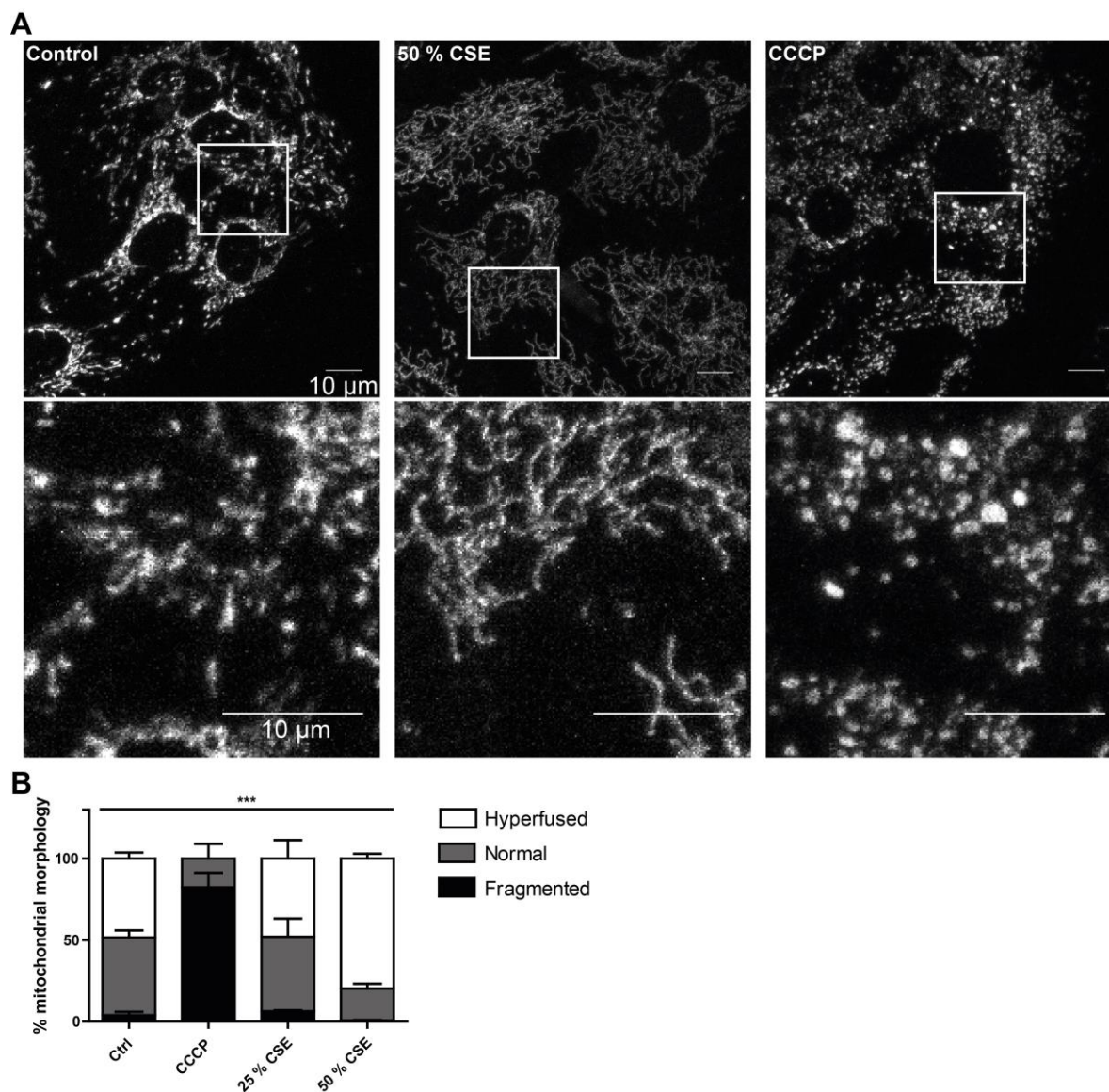


Figure 5-4: CSE induces mitochondrial hyperfusion in pmATII

(A) Representative immunofluorescence pictures of pmATII cells treated with control medium, 50 % CSE, or 10 μ M CCCP for 24 h. Scale bars: 10 μ m (B) Quantification of mitochondrial morphology in 24 h control, CCCP, 25 % or 50 % CSE-treated pmATII cells. n=3. Bars show mean percentage + SEM. Significance was determined using the chi-square test. ***:p< 0.001.

Mitochondrial morphology is regulated by expression, localization and activity of several mitochondrial fusion and fission proteins. Protein and mRNA expression levels of the outer membrane fusion proteins MFN1 and MFN2 as well as the inner membrane fusion protein OPA1 and the mitochondrial fission protein DRP1 were analyzed in total cell lysates of MLE12 cells. MFN2 expression was transiently increased on mRNA and protein level after 24 h of CSE treatment. No significant changes with CSE treatment were observed for expression of MFN1, DRP1 or OPA1 (Figure 5-5 and Figure 5-6). Again, CCCP was used as a positive control and, in accordance with published data (Duvezin-Caubet et al., 2006; Tanaka et al., 2010), induced cleavage of long OPA1 isoforms (a, b) and degradation of MFN2 at early times after treatment (Figure 5-5).

Mitochondrial function in response to cigarette smoke extract exposure

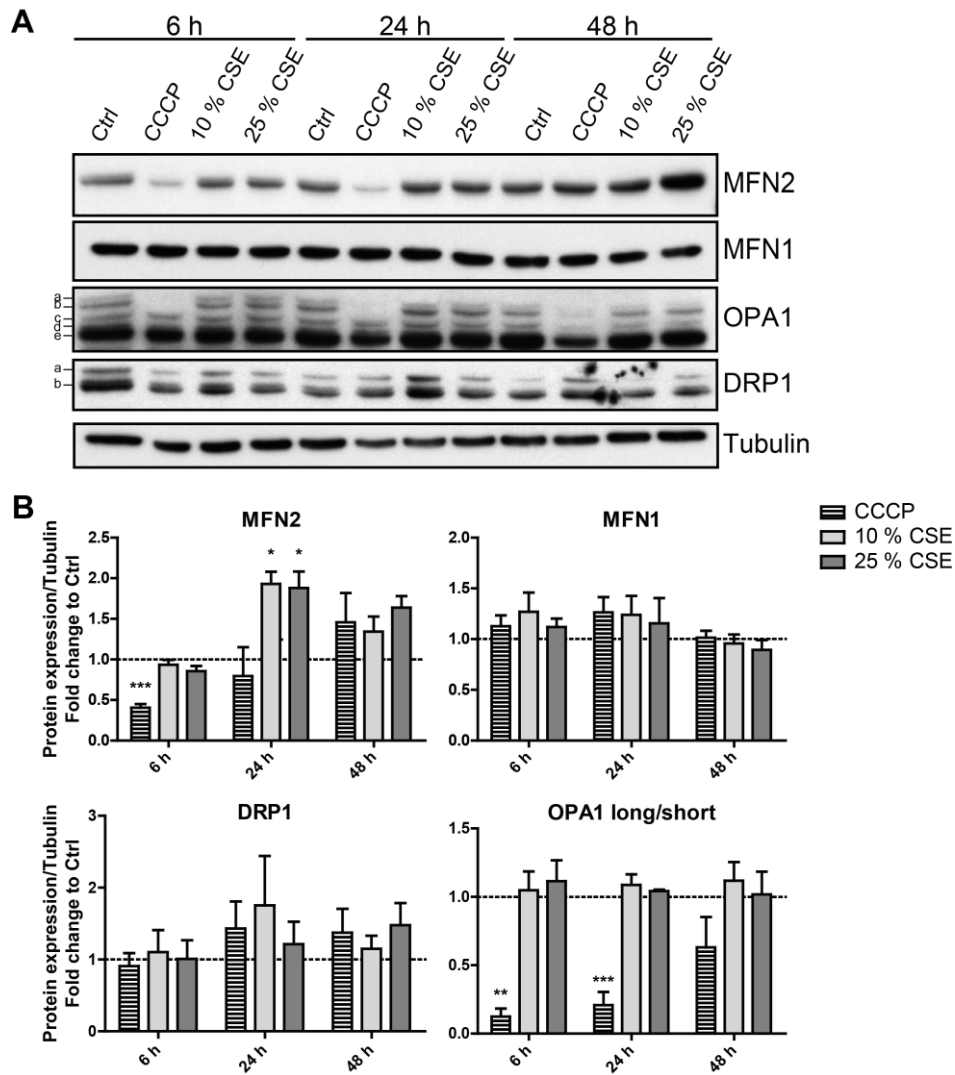


Figure 5-5: MFN2 expression is increased in response to CSE treatment in MLE12 cells

(A) Representative Western blot analysis of mitochondrial fusion (MFN2, MFN1 and OPA1) and fission protein (DRP1) expression in MLE12 cells. Tubulin was used as a loading control. Letters indicate the different isoforms recognized by the respective antibody (OPA1 long: a-b; OPA1 short: c-e; DRP1: a-b). (B) Densitometric analysis of MFN2, MFN1, OPA1 and DRP1 expression in MLE12 cells, n=3-5. Bar graphs show mean±SEM. Values are displayed as fold change relative to time-matched controls. Significance was determined using one-way ANOVA with Dunnett's multiple comparison test comparing treated groups vs. time-matched controls. *:p<0.05, ***p<0.001.

Mitochondrial function in response to cigarette smoke extract exposure

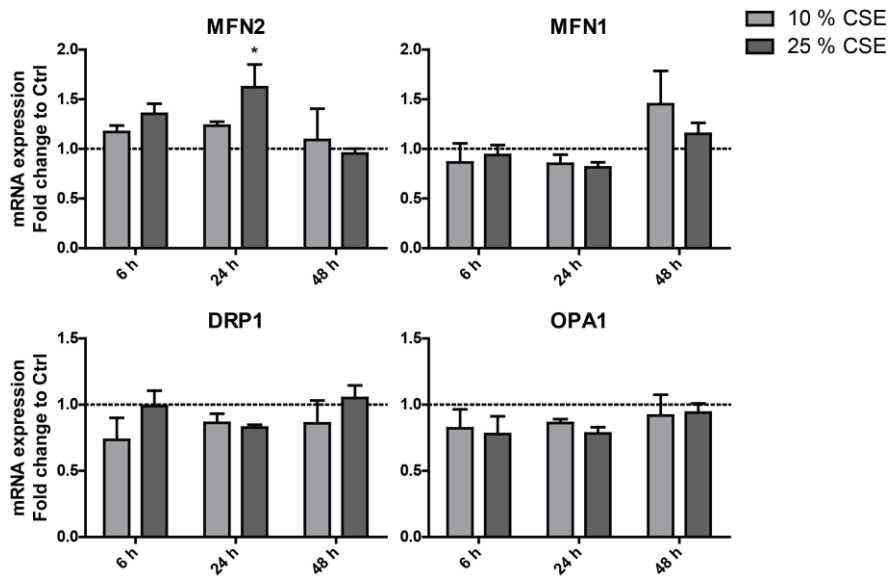


Figure 5-6; mRNA expression of fusion and fission proteins in CSE-treated MLE12 cells

mRNA expression of MFN1, MFN2, DRP1 and OPA1 in MLE12 cells, $n=3+SEM$. Values are displayed as fold change relative to time-matched control cells. Significance was determined using one-way ANOVA with Dunnett's multiple comparison test comparing treated groups vs. time-matched controls. *: $p<0.05$.

In addition to data obtained in MLE12 cells, the fusion protein MFN2 was also upregulated in CSE-treated pmATII cells. The other fusion and fission mediators, MFN1, DRP1, or OPA1 showed no significant changes upon CSE treatment of pmATII cells (Figure 5-7).

Mitochondrial function in response to cigarette smoke extract exposure

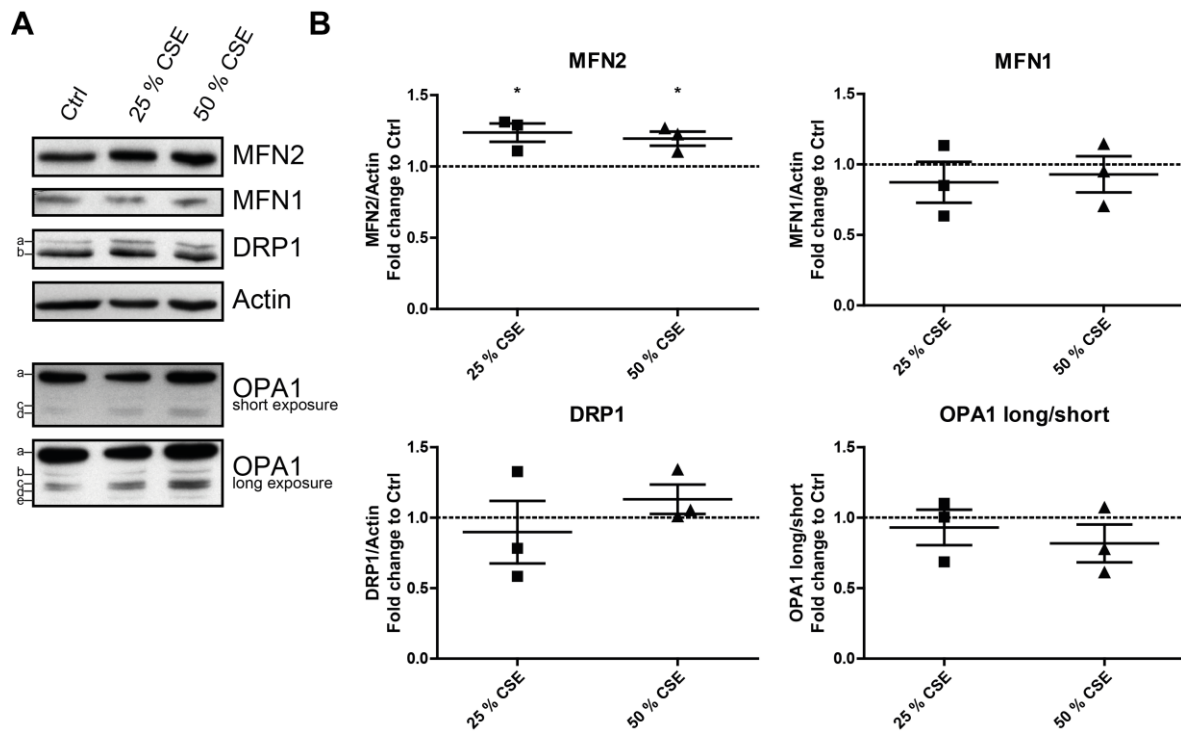


Figure 5-7: MFN2 expression is elevated in 24 h CSE-treated pmATII

(A) Representative western blot analysis of mitochondrial fusion (MFN2, MFN1, and OPA1) and fission protein (DRP1) expression in 24 h CSE-treated pmATII cells. Actin was used as a loading control. Letters indicate the different isoforms recognized by the respective antibody (OPA1 long: a-b; OPA1 short: c-e; DRP1: a-b). (B) Densitometric analysis of MFN2, MFN1, OPA1 and DRP1 expression in pmATII cells, $n=3 \pm$ SEM. Values are displayed as mean fold change relative to untreated cells. Significance was determined using one-way ANOVA with Dunnett's multiple comparison test comparing Ctrl vs. CSE-treated groups. *: $p < 0.05$.

Fission activity of DRP1 requires translocation of DRP1 from the cytosol to mitochondria (Gomes and Scorrano, 2013). Hence, DRP1 levels in response to CSE treatment were analyzed in mitochondrial fractions of MLE12 cells. To this end, a crude mitochondrial isolation was prepared to enrich for mitochondria and associated proteins. Mitochondrial fractions were strongly enriched for mitochondrial proteins such as ATP5A while cytosolic (Actin) or ER-resident proteins (Calreticulin) had decreased abundance (Figure 5-8). No consistent changes in response to CSE treatment were observed for DRP1 levels in the different mitochondrial fractionations indicating absence of DRP1 translocation to mitochondria (Figure 5-9).

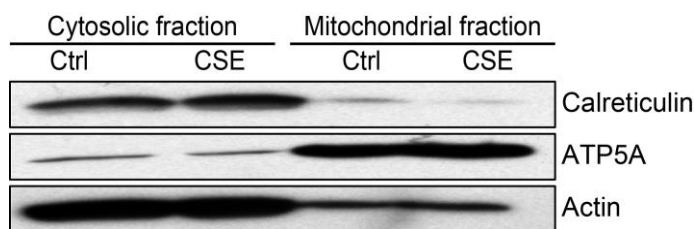


Figure 5-8: Mitochondrial proteins are enriched in mitochondrial fractionations

Representative western blot of mitochondrial fractionation of MLE12 cells treated with 25 % CSE or control (Ctrl) medium for 24 h. Calreticulin was used as marker for ER, ATP5A for mitochondria and Actin as cytosolic marker.

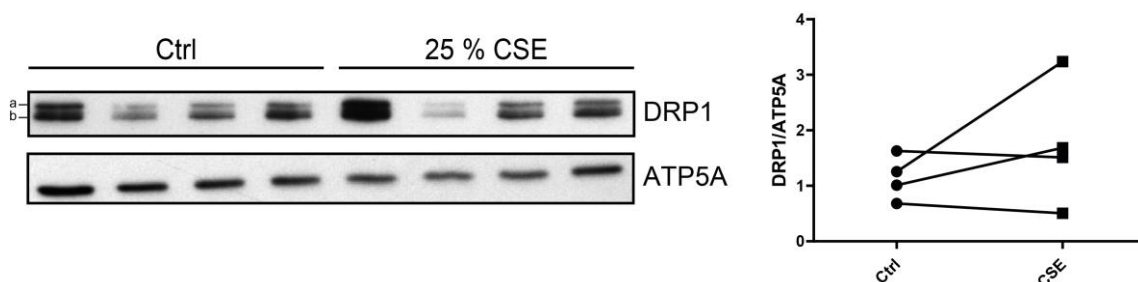


Figure 5-9: No DRP1 translocation to mitochondria in response to CSE treatment

Western blot analysis and densitometric quantification of DRP1 protein levels in four independently prepared mitochondrial fractions of MLE12 cells treated with 25 % CSE or control medium for 24 h. ATP5A was used as loading control. Letters confer to the different isoforms recognized by the respective antibody (DRP1: a-b).

Taken together, these data indicate that nontoxic doses of CSE induce an adaptive response of the mitochondrial network including transient upregulation of MFN2, which results in a pronounced mitochondrial hyperfusion phenotype. Furthermore, these data show that mitochondrial hyperfusion is conserved between MLE12 and pmATII cells as a response to exposure to nontoxic doses of cigarette smoke extract.

5.2.2 Cigarette smoke extract-induced mitochondrial hyperfusion is associated with increased mitochondrial oxygen consumption and ATP production

Mitochondrial hyperfusion has previously been described as a protective stress response which increases mitochondrial ATP production. Several parameters of mitochondrial function were analyzed in response to CSE treatment. Metabolic activity was increased in low dose CSE-treated MLE12 cells as shown in the MTT assay. Importantly, higher doses which are usually associated with cell death significantly decreased metabolic activity (Figure 5-10A). The increase of metabolic activity at low doses was not related to increased cellular proliferation, as CSE treatment rather reduced cellular proliferation even at low doses (Figure 5-10B).

Mitochondrial function in response to cigarette smoke extract exposure

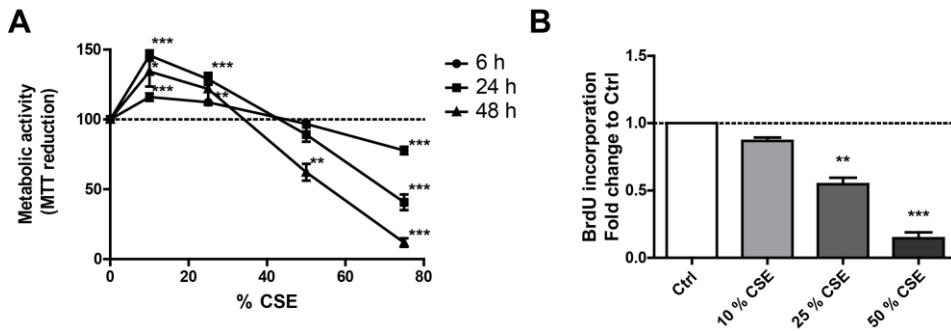


Figure 5-10: Low doses of CSE enhance metabolic activity in MLE12 cells

(A) MTT assay of MLE12 cells after treatment with 10, 25, 50, or 75 % CSE for 6, 24 and 48 h. n=4-6. Data points are presented as mean \pm SEM relative to untreated control cells. Significance was determined using one-way ANOVA with Dunnett's multiple comparison test comparing treated groups vs. time-matched controls. **:p<0.01, ***p<0.001. (B) BrdU incorporation in 24 h CSE-treated MLE12 cells. n=2. Bar graphs show mean+SEM. Values are displayed as fold change relative to untreated cells.

To further assess mitochondrial function, mitochondrial membrane potential was analyzed in response to low dose CSE treatment. Nontoxic doses of CSE significantly increased mitochondrial membrane potential. CCCP treatment was used as a positive control and, as expected, induced a decrease in mitochondrial membrane potential (Figure 5-11).

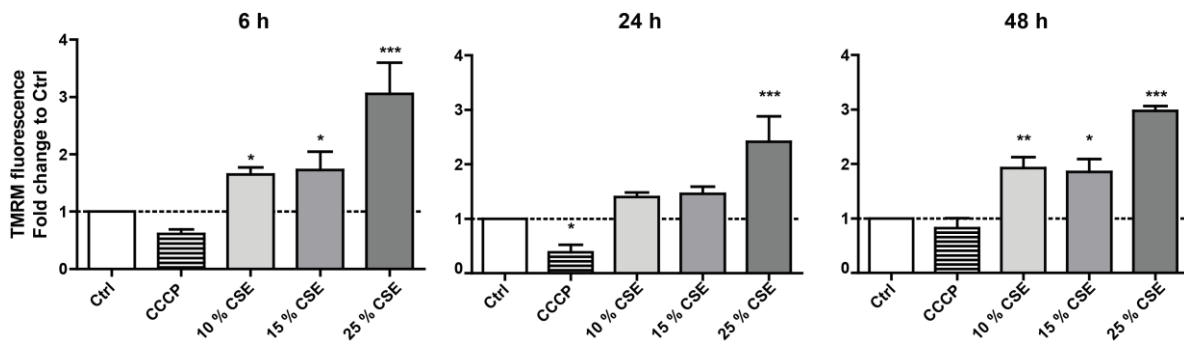


Figure 5-11: CSE treatment increases mitochondrial membrane potential in MLE12 cells

Flow cytometry analysis of MLE12 cells stained with TMRM for assessment of mitochondrial membrane potential after 6, 24, or 48 h of treatment with CCCP, or 10, 15 and 25 % CSE. n=2-5. Bar graphs show mean+SEM. Values are displayed as fold change relative to untreated cells. Significance was determined using one-way ANOVA with Dunnett's multiple comparison test comparing treated groups vs. time-matched controls. *:p<0.05, **:p<0.01, ***p<0.001.

Increased mitochondrial membrane potential is often associated with increased production of mitochondrial superoxide by the respiratory chain (Sena and Chandel, 2012). Therefore, mitochondrial superoxide production after CSE treatment was assessed with the mitochondria-specific probe MitoSOX red. Superoxide production by the mitochondrial respiratory chain was not altered upon CSE treatment (Figure 5-12A). The function of the probe was confirmed by adding antimycin A, a commonly used inducer of mitochondrial superoxide (Mukhopadhyay et al., 2007), which markedly increased MitoSOX-specific fluorescence (Figure 5-12B).

Mitochondrial function in response to cigarette smoke extract exposure

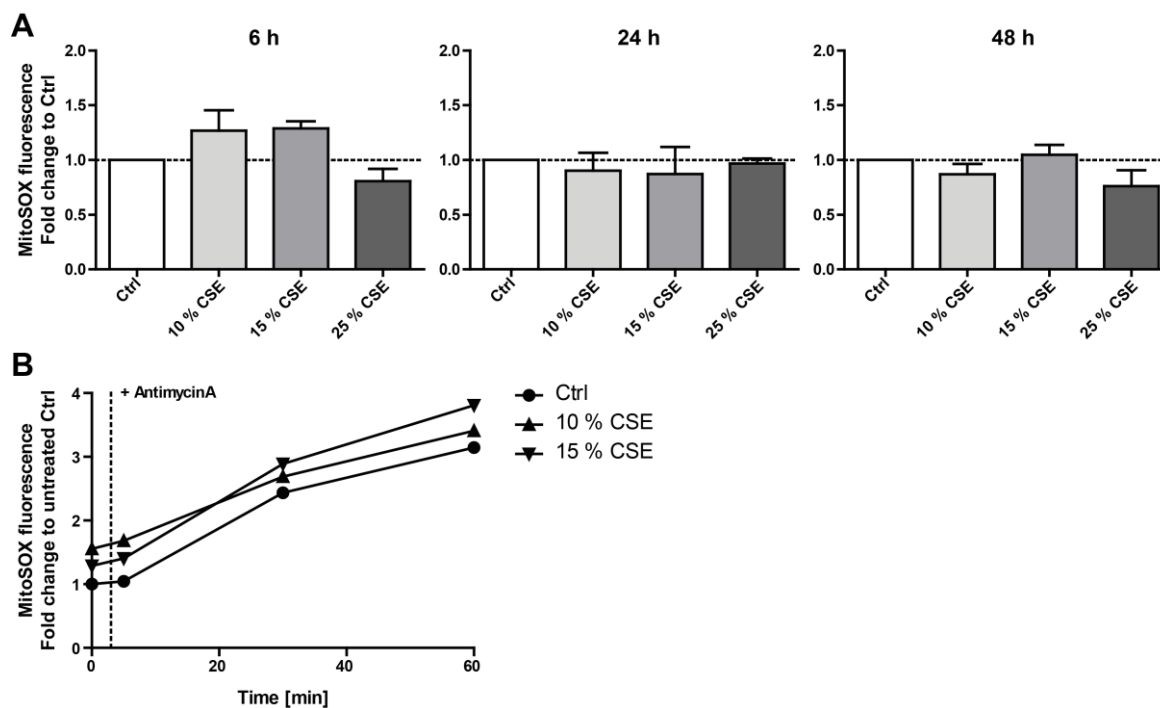


Figure 5-12: Mitochondrial superoxide production is not changed in response to CSE treatment

(A) Flow cytometry analysis of MLE12 cells stained with MitoSOX Red for detection of mitochondrial superoxide generation after 6, 24, or 48 h of treatment with 10, 15, and 25 % CSE. $n=3-6$. Bar graphs show mean+SEM. (B) Representative flow cytometry analysis for MitoSOX fluorescence before and after addition of antimycin A. Values are displayed as fold change relative to untreated control cells.

To directly assess mitochondrial ATP production and function of the respiratory chain cellular oxygen consumption was analyzed. Basal oxygen consumption was slightly increased in CSE-treated cells (Figure 5-13A&B). Reduction of oxygen requires activity of complex I-IV of the respiratory chain which builds up a proton gradient across the inner mitochondrial membrane, which is then used by complex V to generate ATP. These reactions are usually coupled. Therefore, inhibition of proton flow through the mitochondrial inner membrane via complex V also decreases electron flow and oxygen consumption by the respiratory chain complexes I-IV. Residual oxygen consumption after complex V inhibition accounts for proton leak through the mitochondrial membrane and is not contributing to mitochondrial ATP production (Brand and Nicholls, 2011). Proton leak through the mitochondrial membrane was not affected by low dose CSE treatment of MLE12 cells (Figure 5-13A&B). Usually, mitochondria possess a spare respiratory capacity which is not used during baseline respiration. Enabling uncontrolled proton flow across the mitochondrial membrane by using a protonophore such as CCCP leads to uncoupling of respiratory chain activity from ATP production and thereby induces maximal respiratory activity (Brand and Nicholls, 2011). Similar to basal levels, maximal oxygen consumption was significantly increased in CSE-treated cells (Figure 5-13A&B). Finally, after blockade of complex I and III using rotenone and antimycin A only non-mitochondrial respiration remains, which proves dependency of oxygen consumption on mitochondrial activity (Figure 5-13A).

Mitochondrial function in response to cigarette smoke extract exposure

Importantly, these analyses reveal that mitochondrial ATP production, estimated as oligomycin-sensitive respiration, is increased in CSE-treated cells (Figure 5-13C). Accordingly, steady state levels of cellular ATP were slightly increased after CSE treatment (Figure 5-13D).

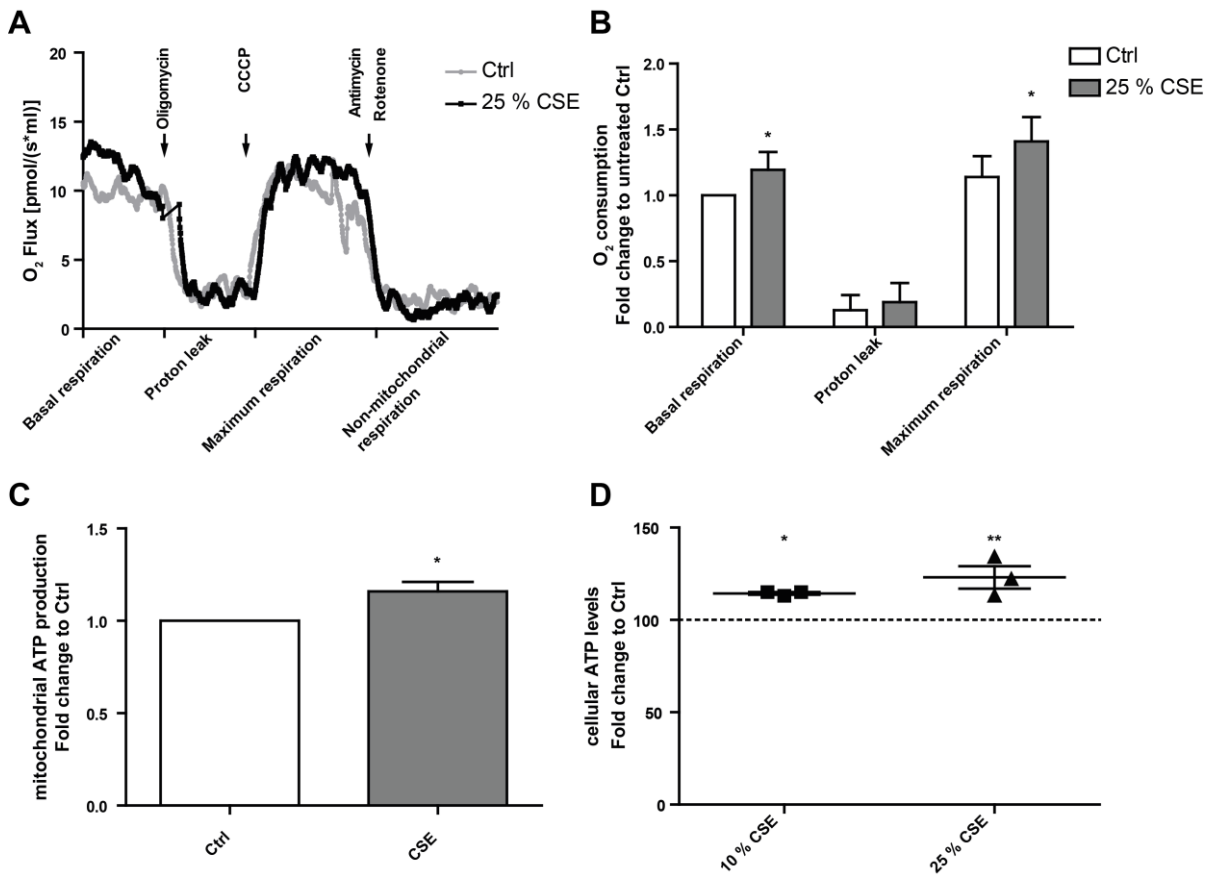


Figure 5-13: Mitochondrial oxygen consumption is increased in CSE-treated cells

(A) Representative curve of one oxygraph experiment depicting the assessment of the various parameters of mitochondrial oxygen consumption rates. Outliers caused by reagent injection were excluded for better visibility. (B) Oxygen consumption rate in MLE12 cells after 24 h of 25 % CSE treatment. $n=5$. Bars show mean+SEM. Non-mitochondrial oxygen consumption was subtracted from all values. Significance was determined using two-way ANOVA with Bonferroni multiple comparison test comparing Ctrl vs. CSE-treated cells. *: $p<0.05$. (C) Mitochondrial ATP production (oligomycin-sensitive respiration) in 24 h CSE-treated MLE12 cells. $n=5$. Bars show mean+SEM. Significance was determined using one-sample t-test. *: $p<0.05$ (D) Cellular ATP levels in MLE12 cells after treatment with 10 or 25 % CSE for 24 h relative to untreated control. Significance was determined using one-way ANOVA with Dunnett's multiple comparison test comparing Ctrl vs. CSE-treated groups. *: $p<0.05$, **: $p<0.01$

In summary, these data demonstrate increased mitochondrial activity and ATP production in response to CSE-induced mitochondrial hyperfusion in MLE12 cells.

5.2.3 Low dose cigarette smoke extract treatment does not activate a protein stress response at mitochondria

Mitochondrial damage induces activation of mitochondrial proteostasis pathways such as the mtUPR, MAD or disposal of damaged mitochondria via mitophagy. To analyze if low dose CSE induces a

protein stress response at mitochondria, expression of the mitochondrial chaperone HSP60 (a marker for mtUPR) and the respiratory chain complex V gene ATP5A (a marker for mitochondrial mass) was analyzed. HSP60 and ATP5A expression was not altered in response to low dose CSE (Figure 5-14A&B) indicating the absence of mtUPR or mitophagy induction. Furthermore, levels of full-length PINK1, which accumulates at the mitochondrial outer membrane as a signal for mitochondrial degradation via the mitophagy pathway, were assessed in mitochondrial fractionations. A double band for full-length PINK1 with a molecular weight of 67 kDa and a single band for cleaved PINK1 at 55 kDa were detected at mitochondria of CSE-treated MLE12 cells. Levels of full-length PINK1 were not altered in response to CSE (Figure 5-14C).

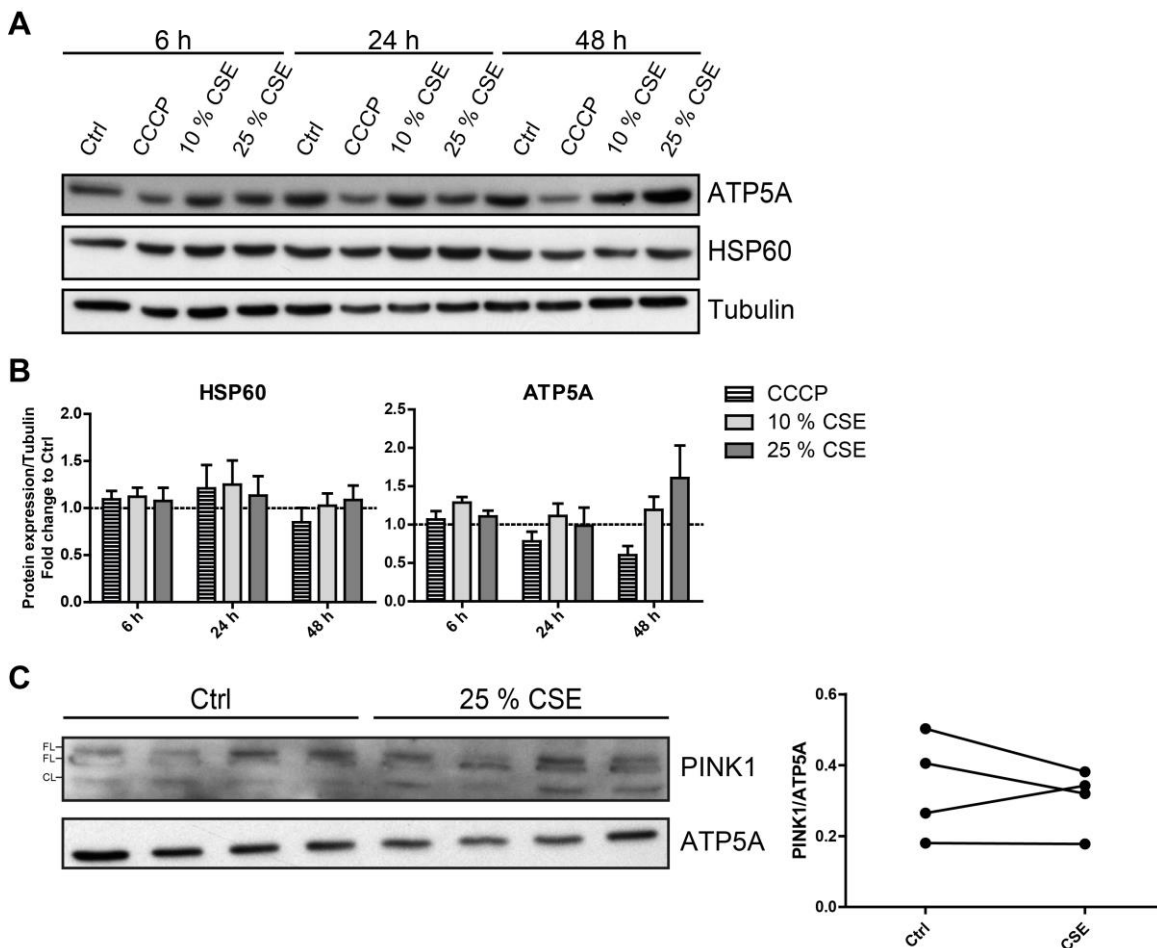


Figure 5-14: CSE does not induce mtUPR or mitophagy activation

(A) Representative Western blot analysis for expression of HSP60 and ATP5A in MLE12 cells treated with CCCP, 10, or 25 % CSE for 6, 24, or 48 h. Tubulin was used as a loading control. (B) Densitometric analysis of HSP60 and ATP5A expression in MLE12 cells. n= 3. Bar graphs show mean+SEM. Values are displayed as fold change relative to untreated cells. (C) Western blot analysis and densitometric quantification of PINK1 protein levels in four independently prepared mitochondrial fractions of MLE12 cells treated with 25 % CSE or control medium for 24 h. ATP5A expression was used as loading control. Two bands were detected for full-length (FL) and one band for cleaved (CL) PINK1.

Mitochondrial function in response to cigarette smoke extract exposure

Taken together, these data indicate that the applied conditions of CSE treatment do not activate a mitochondrial protein stress response. This does not exclude the possibility that retro-translocation of proteins via MAD or proteasomal recruitment to mitochondria are induced to cope with an increased demand for mitochondrial protein turnover upon CSE treatment.

To analyze for the induction of mitochondria-associated degradation, levels of the MAD mediators VCP and VMS1 were analyzed in whole cell lysates. Intriguingly, VMS1 was significantly increased upon 24 h of 10 % CSE treatment, while in other conditions the increase in VMS1 expression did not reach statistical significance (Figure 5-15A&B). Total VCP levels remained unchanged upon CSE or CCCP treatment (Figure 5-15A&B).

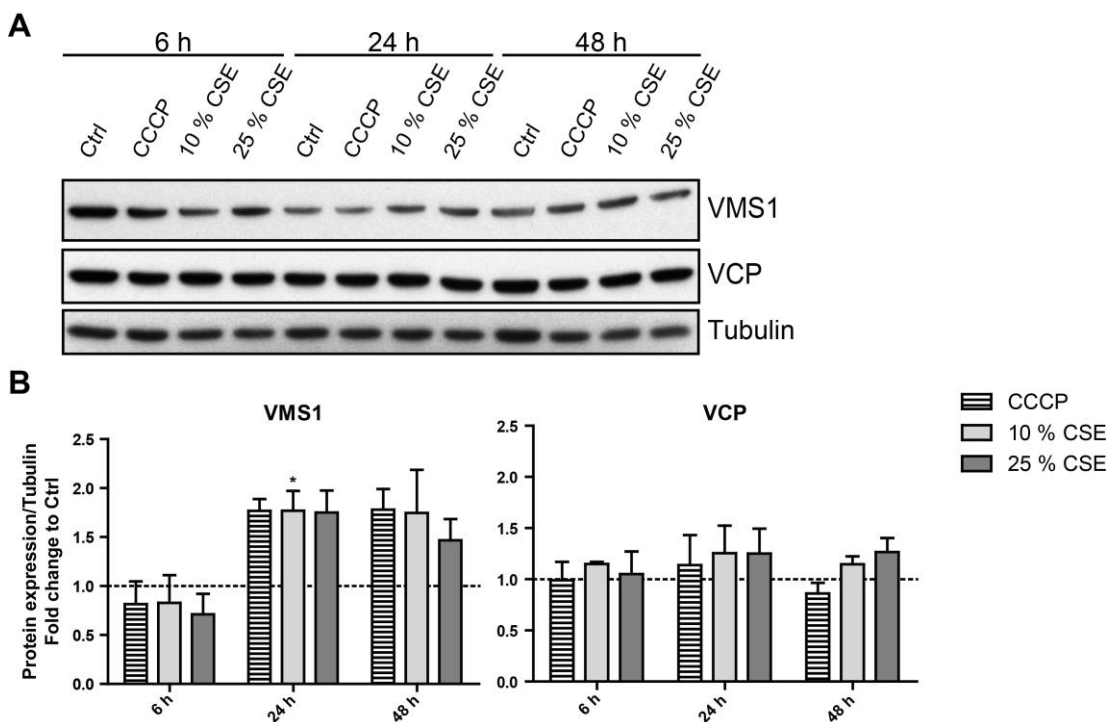


Figure 5-15: Mitochondria-associated degradation is only slightly activated in response to CSE

(A) Representative Western blot analysis of VMS1 and VCP expression in MLE12 cells treated with CCCP, 10 %, or 25 % CSE for 6, 24, or 48 h. Tubulin was used as a loading control. (B) Densitometric analysis of VMS1 and VCP expression in MLE12 cells. n=3. Bar graphs show mean+SEM. Values are displayed as fold change relative to untreated cells. Significance was determined using one-way ANOVA with Dunnett's multiple comparison test comparing treated groups vs. time-matched controls. *:p< 0.05.

To analyze whether the proteasome directly associates with mitochondria, recruitment of proteasomes to mitochondria was analyzed in crude mitochondrial fractions. No significant change in 20S or 19S proteasome subunits at mitochondria was observed in response to CSE treatment (Figure 5-16A). Of note, occurrence of VMS1 in mitochondrial fractions, which would argue in favor of MAD activation, could not be detected in control or CSE-treated cells (data not shown). Additionally, proteasome activity was analyzed in cytosolic and mitochondrial fractions. Proteasome activity was

reduced in response to CSE treatment in the cytosolic fraction but not in the mitochondrial fractions. However, these changes were not statistically significant (Figure 5-16B).

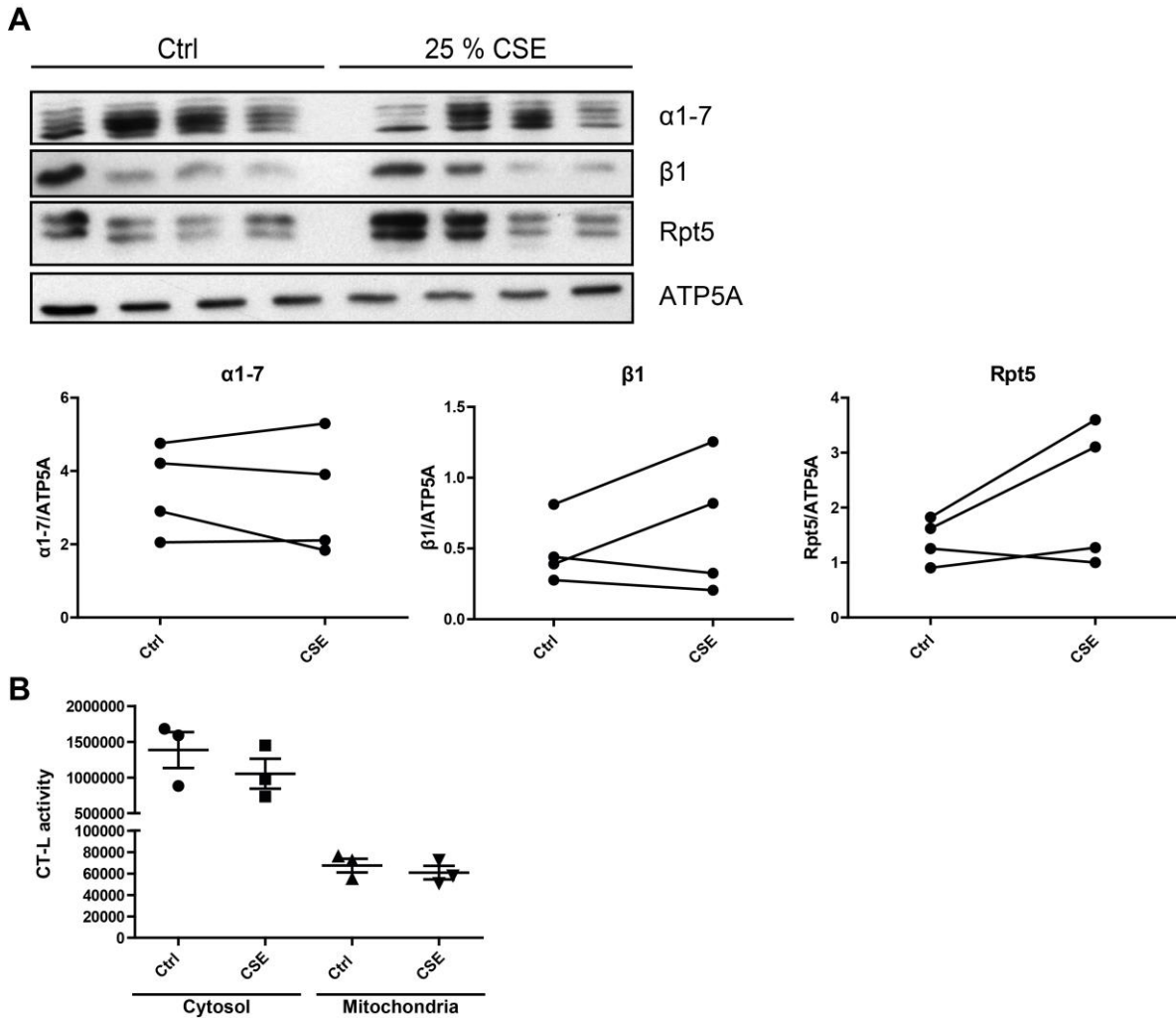


Figure 5-16: No recruitment of proteasomes to mitochondria in response to CSE

(A) Western blot analysis and densitometric quantification of proteasome subunit levels in four independently prepared mitochondrial fractions of MLE12 cells treated with 25 % CSE or control medium for 24 h. ATP5A was used as loading control. (B) CT-L proteasome activity in cytosolic and crude mitochondrial fractions of MLE12 cells treated with 25 % CSE or control medium for 24 h.

In summary, a slight increase in VMS1 expression and, hence, maybe proteasome-mediated mitochondria-associated degradation is seen. However, the absence of induction of the mtUPR, mitophagy, or recruitment of proteasomes to mitochondria indicates that under conditions of low dose CSE treatment, mitochondrial protein homeostasis is not grossly altered and therefore no broad activation of mitochondrial proteostasis pathways is induced.

5.3 Discussion

Exposure of the lung to cigarette smoke is known to be involved in the pathogenesis of chronic lung diseases and contributes to accelerated aging of the lung (Mercado et al., 2015). Exposure of cells to cigarette smoke extract is a commonly used model to study the effect of cigarette smoke in the lung (Nyunoya et al., 2014). Here, low and nontoxic doses of cigarette smoke extract were used. Absence of toxicity was clearly shown by absence of LDH release as an indicator for necrotic cell death and of caspase 3 cleavage as a marker for apoptotic cell death in CSE-treated cells. Moreover, nontoxic doses of CSE did not severely disturb protein homeostasis in mitochondria as induction of mitochondrial quality control pathways was not evident. Nontoxic CSE treatment, however, induced an adaptive response of alveolar epithelial cell mitochondria involving hyperfusion of the mitochondrial network, increased mitochondrial oxygen consumption and a transient increase in MFN2 expression.

5.3.1 Nontoxic doses of cigarette smoke extract induce mitochondrial hyperfusion in alveolar epithelial cells

Exposure of alveolar epithelial cells to low doses of cigarette smoke extract induced mitochondrial hyperfusion as evident by elongated and highly connected mitochondria and increased levels of the mitochondrial fusion protein MFN2. Mitochondrial network dynamics are dependent on a tight balance of the activity of mitochondrial fusion and fission proteins (Youle and van der Bliek, 2012). Mitochondrial hyperfusion can therefore result either from increased fusion activity or from decreased fission activity. Initially, stress-induced mitochondrial hyperfusion was described to be dependent on OPA1 and MFN1, but not on MFN2 (Tondera et al., 2009). In that case, the effect was related to altered activity of the fusion machinery as no expressional changes in fusion proteins occurred (Tondera et al., 2009). Another study described that during oxidative stress mitochondrial hyperfusion is dependent on increased oligomerization and thereby activation of the fusion proteins MFN1 and MFN2. Again, no changes in absolute levels of fusion and fission proteins were observed (Shutt et al., 2012). In contrast to increased fusion in stress-induced mitochondrial hyperfusion, starvation-induced mitochondrial hyperfusion was dependent on phosphorylation of the fission protein DRP1 and its decreased translocation to mitochondria (Gomes et al., 2011).

In this study the fusion protein MFN2 was found to be upregulated in response to low dose CSE exposure, while expression of the mitochondrial mass marker ATP5A, the fusion protein MFN1, the inner membrane fusion protein OPA1, and the mitochondrial fission protein DRP1 were not altered. Importantly, also no change in DRP1 translocation to mitochondria was found in response to CSE. Hence, mitochondrial hyperfusion in this setting is most probably different to starvation-induced hyperfusion and not a result of decreased fission activity.

As expressional changes in fusion or fission proteins were not observed in any of the three aforementioned studies, expressional changes are clearly not necessary to trigger mitochondrial hyperfusion (Gomes et al., 2011; Shutt et al., 2012; Tondera et al., 2009). Rather altered activity of the fusion and fission machinery contributes to mitochondrial hyperfusion. Accordingly, CSE-induced mitochondrial hyperfusion was evident already after 6 h of CSE treatment when no changes in Mitofusin levels are present and hyperfusion lasted up to 48 h when MFN2 levels were already declining to baseline. This argues that changes in activity and not in expression are the decisive factor also for CSE-induced hyperfusion.

Since all mitochondrial fusion proteins are expressed in alveolar epithelial cells, it cannot be delineated whether activity changes in specific fusion or fission proteins are the underlying reason for the observed hyperfusion. However, the observed upregulation of MFN2 speaks in favor of a role of MFN2 in CSE-induced hyperfusion. Several published data indicate that changes in mitochondrial morphology can be associated with endogenous changes of single mitochondrial fusion proteins. Downregulation of MFN2 was associated with mitochondrial fragmentation without changes in MFN1 level (Martorell-Riera et al., 2014). Furthermore, upregulation of MFN1 but not MFN2 was correlated with elongated mitochondria in the brain of ME7-prion-infected mice (Choi et al., 2014). Additionally, a transient endogenous upregulation of MFN2 was found in senescence-induced hyperfusion. This effect was, however, also coupled with decreased activity of the fission machinery (Yoon et al., 2006). Moreover, overexpression of MFN2 in neurons or in pulmonary artery smooth muscle cells also induced mitochondrial elongation (Cagalinec et al., 2013; Ryan et al., 2013). These data show that altered expression levels of single fusion proteins indeed have the capability to functionally influence mitochondrial hyperfusion. Hence, while expressional changes in MFN2 are obviously not the sole reason for the observed mitochondrial hyperfusion, MFN2 upregulation might contribute in addition to changes in fusion protein activity. Thus, changes in fusion protein activity may account for the early induction of hyperfusion with upregulation of MFN2 levels representing an adaptive response which happens in addition to the previously described stress-induced hyperfusion pathways. As levels and activity of mitochondrial fusion and fission proteins need to be tightly balanced, elevated MFN2 levels are probably not maintained over longer periods but decline to baseline.

These results on CSE-induced mitochondrial hyperfusion in alveolar epithelial cells differ from data obtained for bronchial epithelial cells. In one study, mitochondrial fragmentation was observed in primary human bronchial epithelial cells treated with CSE for 48 h. Mitochondrial fragmentation was associated with increased localization of the fission protein DRP1 to mitochondria without any changes for MFN2 or other mitochondrial fusion proteins (Hara et al., 2013). In contrast, another study described elongated and branched mitochondria in bronchial epithelial cells after chronic

exposure to cigarette smoke extract for six months and in primary bronchial epithelial cells isolated from COPD patients (Hoffmann et al., 2013). As these studies were performed in bronchial epithelial cells there is probably a strong cell type dependency for triggering an adaptive mitochondrial hyperfusion response of lung epithelial cells to cigarette smoke extract.

5.3.2 Mitochondrial hyperfusion is associated with increased mitochondrial function

Mitochondrial morphology is closely connected with mitochondrial function. Especially, mitochondrial hyperfusion was reported to be connected with an increased efficiency of ATP production (Gomes et al., 2011; Tondera et al., 2009). Accordingly, CSE-induced mitochondrial hyperfusion was associated with enhanced metabolic activity, increased cellular ATP levels, augmented mitochondrial membrane potential, and elevated oxygen consumption rates in MLE12 cells. These observations are well in agreement with the concept of stress-induced mitochondrial hyperfusion as a protective response to increase the cell's ability to repair damage. Mitochondrial hyperfusion was previously shown to be beneficial in response to a variety of stressors including amino acid starvation, UV exposure, actinomycin, or cycloheximide treatment (Gomes et al., 2011; Tondera et al., 2009). As mitochondrial hyperfusion can also be induced by oxidative stress (Shutt et al., 2012; Yoon et al., 2006), it seems plausible that this survival response is also part of the oxidative stress response to cigarette smoke extract.

While mitochondrial hyperfusion was observed in MLE12 and pmATII cells, the increase in mitochondrial function was only measured in MLE12 cells. This was mainly due to the cumbersome work of culturing sufficient numbers of primary mouse ATII cells for mitochondrial analyses. However, the results obtained for the MLE12 cells might well be extrapolated to pmATII cells as previous studies also observed a clear association between mitochondrial hyperfusion and metabolic activity using different cell types (Gomes et al., 2011; Tondera et al., 2009). In addition, an increase in mitochondrial respiration in response to cigarette smoke exposure was previously shown in pmATII cells. Agarwal et al. showed that in pmATII cells respiring on the mitochondria-dependent substrates pyruvate or palmitate, oxygen consumption rates were significantly increased after CSE or cigarette smoke exposure (Agarwal et al., 2013, 2014). Therefore, although mitochondrial function in pmATII was not directly measured in this study, one can speculate that cigarette smoke-induced mitochondrial hyperfusion, which is shown here to occur in different types of alveolar epithelial cells, also might influence metabolic activity in these cells. Additionally, mitochondrial hyperfusion in CSE-treated bronchial epithelial cells was associated with increased cellular ATP levels (Hoffmann et al., 2013), which further supports the notion of increased mitochondrial respiratory chain activity in response to cigarette smoke.

In summary, cigarette smoke-induced mitochondrial hyperfusion is associated with increased mitochondrial oxygen consumption and ATP production. Therefore, this adaptive mitochondrial response to nontoxic doses of cigarette smoke exposure might be useful for the cell in order to provide ATP for the removal of cigarette smoke-induced damage to cellular functions and structures.

5.3.3 Nontoxic cigarette smoke exposure does not induce activation of mitochondrial proteostasis pathways

Cigarette smoke is well known to induce damage in the cell such as DNA damage or protein oxidation (Bowler et al., 2004; Nyunoya et al., 2014). Additionally, it is known that cigarette smoke induces protein stress responses in the cytosol and in the ER (Kelsen et al., 2008; van Rijt et al., 2012; Wei et al., 2013). We did not, however, observe any alteration in mitochondrial proteostasis in response to CSE treatment of alveolar epithelial cells. Accumulation of misfolded proteins in the mitochondrial matrix, which exceeds the folding capacity of mitochondrial chaperones, triggers the mitochondrial unfolded protein response. Increased expression of HSP60 is one hallmark of mtUPR induction (Jovaisaite et al., 2013; Pellegrino et al., 2013; Zhao, 2002). However, in the case of low dose CSE exposure, no changes in HSP60 expression were observed indicating absence of a pronounced accumulation of damaged mitochondrial proteins.

Irreparable damage to mitochondria induces degradation of whole organelles via mitophagy. The PINK1/Parkin pathway constitutes one major mitophagy pathway in response to mitochondrial damage. Under baseline conditions, PINK1 is rapidly degraded in mitochondria while it is stabilized upon mitochondrial damage (Jin and Youle, 2012; Narendra et al., 2010). No changes in mitochondrial PINK1 levels were observed which indicates absence of PINK1/Parkin-dependent mitophagy. Furthermore, levels of ATP5A as a general marker for mitochondrial mass remained stable upon nontoxic CSE treatment. It can thus be concluded that nontoxic doses of CSE do not broadly activate mitophagy.

Protein damage at mitochondria can also be resolved by degradation of proteins by the cytosolic ubiquitin proteasome system. Degradation of mitochondrial proteins by the proteasome can be mediated by VMS1/VCP-dependent translocation of mitochondrial proteins or by direct association of proteasomes at mitochondria (Heo and Rutter, 2011; Livnat-Levanon and Glickman, 2011). No change in expression was observed for total VCP levels. However, VCP is involved in a plethora of cellular processes including DNA damage responses or ERAD and its function is regulated by several adaptor proteins (Meyer et al., 2012). VMS1 is the adaptor protein of VCP which is specifically involved in MAD (Heo et al., 2010; Meyer et al., 2012). Indeed, VMS1 levels were increased in response to CSE treatment. However, this increase was only found to be significant for 24 h of 10 % CSE treatment. Additionally, recruitment of proteasomes to mitochondria was analyzed by assessing

the presence of proteasome subunits in crude mitochondrial isolations. However, no consistent changes in proteasome levels at mitochondria were observed indicating no increased recruitment of proteasomes to mitochondria.

Altogether, no changes in mitophagy, the mtUPR or in proteasomal recruitment to mitochondria occur upon treatment of MLE12 cells with low doses of CSE. A small increase in VMS1 expression points towards slightly increased MAD which is however not a pronounced effect as it is only significant after 24 h of 10 % CSE treatment. Therefore, nontoxic CSE treatment does not induce a broad mitochondrial protein stress response. Indeed, nontoxic CSE treatment also induced only mild oxidative stress to mitochondria as indicated by the finding that mitochondrial superoxide production was not increased by CSE treatment.

The mild and nontoxic doses of CSE used in this study have different effects on cellular physiology and mitochondrial function than higher, toxic doses. Another study, which reported induction of necrotic cell death by cigarette smoke extract in primary bronchial epithelial cells also observed mitochondrial damage such as decreased membrane potential (van der Toorn et al., 2007). Furthermore, a recent study showed increased PINK1 expression and mitophagy in CSE-treated bronchial epithelial cells and in cigarette smoke-exposed mice. In this study, mitophagy was an upstream event of necrotic cell death which clearly indicates a different outcome of the cigarette smoke treatment (Mizumura et al., 2014). A different mitochondrial response towards toxic CSE doses is plausible since mitochondria are an integral component of apoptosis and necroptosis pathways (Liesa et al., 2009; Vandenabeele et al., 2010). Therefore, the effect of cigarette smoke on pulmonary epithelial cell mitochondria might strongly depend on the dose. Low doses might induce a pro survival response while higher, toxic doses involve mitochondrial damage as well as activation of mitochondrial and non-mitochondrial cell death pathways. In addition to dose and maybe cell type specific effects of smoke on mitochondria, a time-dependent effect has also been observed in wood smoke-treated guinea pigs. Wood smoke exposure led to an initial decrease of mitochondrial function which, however, was fully recovered and even overcompensated at later timepoints (Granados-Castro et al., 2013).

5.3.4 A hyperfused mitochondrial network poses a threat to cellular health

Although nontoxic doses of CSE do not directly harm mitochondria, cigarette smoke-induced mitochondrial hyperfusion might pose a threat to cellular health. While short term mitochondrial hyperfusion is reported as a pro survival response (Blackstone and Chang, 2011; Tondera et al., 2009) a chronically hyperfused mitochondrial network might be detrimental as it slows mitochondrial dynamics and thereby attenuates mitochondrial quality control. This would render the cell more vulnerable to additional stress (Figge et al., 2013). Furthermore, hyperfused mitochondria are spared

from removal via mitophagy (Gomes and Scorrano, 2013). Therefore, sustained mitochondrial hyperfusion, e.g. in response to continuous exposure to nontoxic cigarette smoke, might reduce mitophagy activity and thereby also attenuate its important function for mitochondrial quality control. This mechanism was suggested to account for the occurrence of hyperfused dysfunctional mitochondria in aging muscles (Marzetti et al., 2013). In accordance with this hypothesis, sustained mitochondrial elongation has also been associated with cellular senescence (Lee et al., 2007) and vice versa, induction of cellular senescence is accompanied by mitochondrial elongation (Yoon et al., 2006). Cigarette smoke is known to induce cellular senescence and accelerate aging (Tsuji et al., 2004). Furthermore, induction of senescence in pulmonary cells has been proposed as a pathogenic mechanisms for COPD progression (Mercado et al., 2015; Müller et al., 2006; Tsuji et al., 2006). Therefore, it can be speculated that cigarette smoke extract-induced mitochondrial hyperfusion - although being part of a beneficial adaptive stress response in the first place - contributes to age-related COPD pathogenesis by promoting diminished mitochondrial quality control, impaired cellular stress resistance, and cellular senescence. Importantly, a recent study showed that mitochondrial elongation is found in senescent fibroblasts after 10-15 days of CSE treatment. This study also confirmed impaired mitophagy and increased MFN2 expression in CSE-treated lung fibroblasts (Ahmad et al., 2015). Hence, mitochondrial elongation seems to be an important step in cigarette smoke-induced cellular senescence during COPD development.

6 Regulation of proteasomal function during healthy aging of the lung

Parts of this chapter have previously been published as: Caniard A.*, Ballweg K.*, Lukas C., Yildirim A.Ö., Eickelberg O., and Meiners S. (2015). Proteasome function is not impaired in healthy aging of the lung. *Aging (Albany NY)* 7, 776–792.

6.1 Introduction

In addition to direct exposure to environmental hazards, aging is another major risk factor for the development of chronic lung diseases. Additionally, especially in the lung a prominent phenotype of “healthy”, disease-free aging is described with a decline in lung function and the development of senile emphysema as outlined in paragraph 1.4.4.

Generally, aging is characterized as the progressive loss of cellular, tissue and organ function that leads to increased susceptibility to disease and eventually death. On the cellular level several mechanisms have been identified which contribute to loss of function in aged tissues. López-Otín et al. recently defined nine “hallmarks of aging” that are causally linked with the aging process (López-Otín et al., 2013). Loss of proteostasis has been recognized as one of these hallmarks of aging. As described in paragraph 1.4, proteasome function was shown to decline in several tissues during aging and genetically attenuating or increasing proteasome activity in model organisms was able to shorten or increase lifespan, respectively. However, surprisingly little is known about proteasome function during healthy aging of the lung. So far, only two studies reported a decrease in proteasomal activity in the lungs of aging rats (Breusing et al., 2009; Keller et al., 2000). However, these studies only assessed cleavage of the peptidic probe Suc-LLVY-AMC in whole lung lysates and do not provide further insights in the regulation of proteasomal activity such as changes in proteasome subtypes. To better understand proteasomal regulation during healthy aging of the lung, proteasome expression and activity was comprehensively analyzed in lungs of healthy aged WT mice, proteasome reporter mice and LMP2 or LMP7 knockout mice. Additionally, lung aging and proteasome function in the premature aging mtDNA mutator mouse model was analyzed to assess the effect of mitochondrial dysfunction on the aging phenotype in the lung.

6.2 Results

Lung aging is accompanied by a decrease in lung function and the development of senile emphysema (Janssens et al., 1999). This is also evident in mice lungs (Calvi et al., 2011). As a first step, development of senile emphysema and the concomitant decrease in lung function in the lungs of 18 months old C57Bl/6J mice was confirmed. Indeed, histological sections of aged mice showed a

pronounced increase in alveolar space (Figure 6-1A) when compared to two months old mice. Similarly, decreased lung function parameters were observed in aged mice (Figure 6-1B).

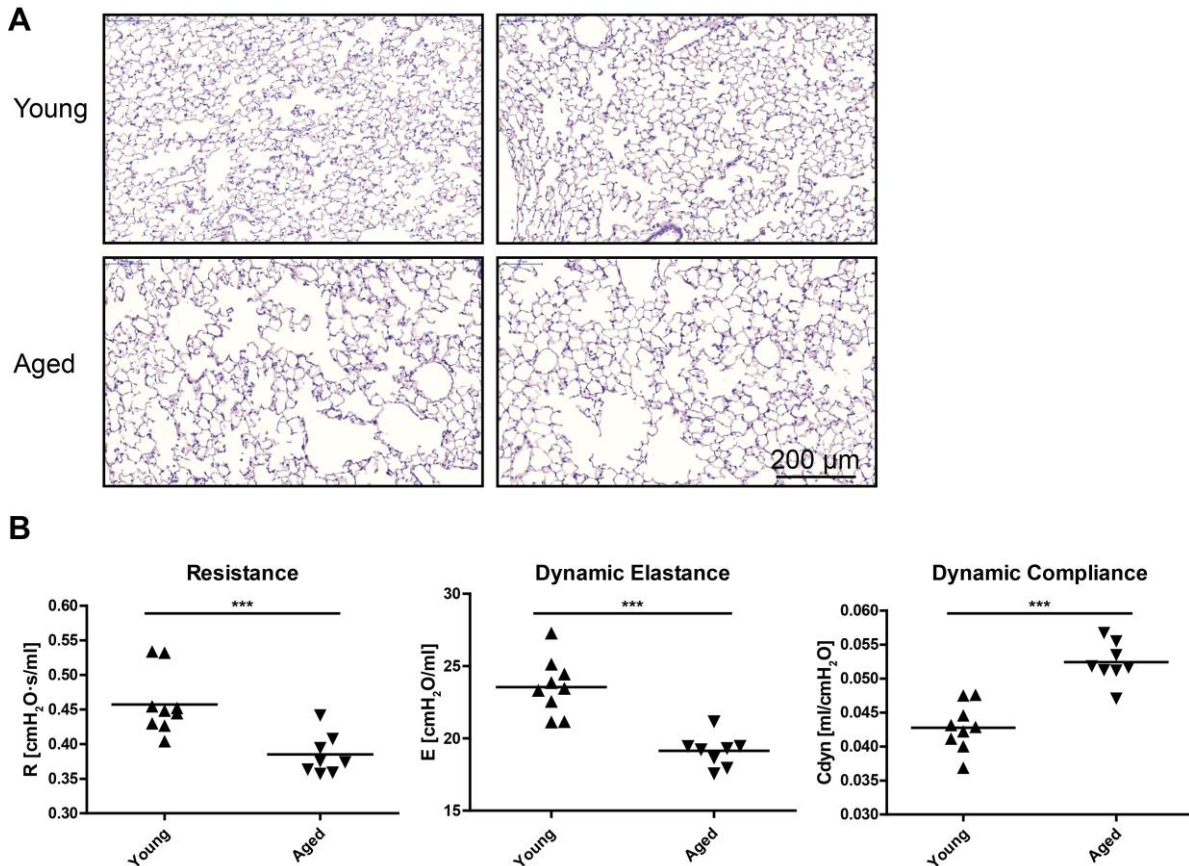


Figure 6-1: Aged mice have senile emphysema and decreased lung function

(A) Representative H&E staining of lung from young (2 months old) and aged (18 months old) wildtype C57Bl/6J mice. Images from two individual animals are depicted per group. H&E stainings were performed by Anne Caniard. (B) Resistance, dynamic elastance and dynamic compliance of lungs of young and aged C57Bl/6J wildtype mice. Significance was determined using student's t-test. ***, $p < 0.001$. Lung function analysis was performed by the lab of Ali Önder Yildirim.

6.2.1 Immunoproteasome expression is increased in lungs of aged mice

To investigate proteasome function in the aged lungs, mRNA and protein expression levels of proteasome subunits were analyzed. Protein expression of the proteasome α -subunits was found to be significantly increased in whole lung lysates of aged mice while the catalytic subunits $\beta 1$ and $\beta 5$ showed a trend towards increased expression which was, however, not statistically significant (Figure 6-2B). The mRNA expression levels of the subunits of the standard proteasome similarly showed a trend towards increased levels, which was only significant for PSMB5 mRNA (Figure 6-2A). Of note, expression of the subunits of the immunoproteasome was significantly upregulated on both mRNA and protein level (Figure 6-2A&B).

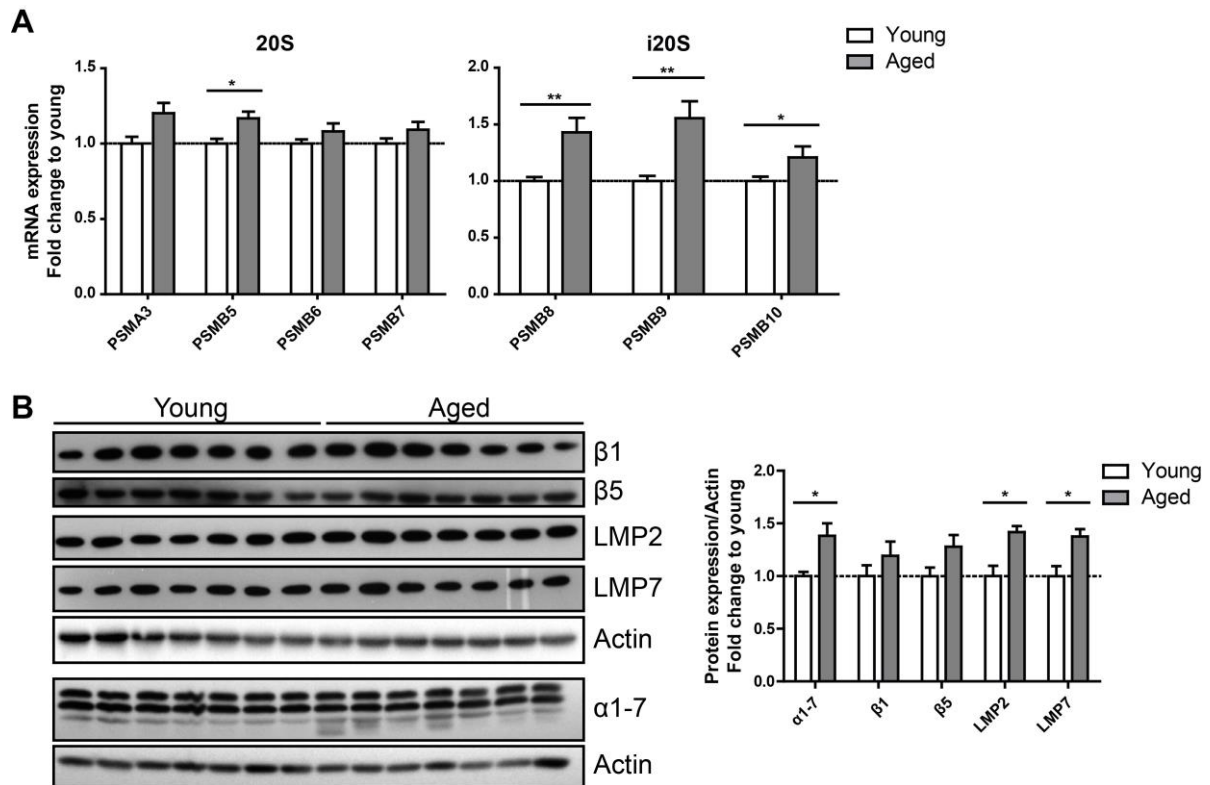


Figure 6-2: Immunoproteasome expression is increased in lungs of aged mice

(A) RT-qPCR analysis of proteasome subunit mRNA expression in young and aged WT mice. n=8. Bar graphs show mean+SEM. (B) Western blot analysis of proteasome subunit expression in young and aged wildtype mice and quantification of protein expression relative to the actin loading control. Bar graphs show mean+SEM. Values are displayed as fold change relative to young mice. Significance was determined using two-way ANOVA with Bonferroni multiple comparison test. *:p< 0.05, **:p< 0.01.

Increased immunoproteasome levels can either result from increased expression of immunoproteasomes in the resident cells of the lung or from increased infiltration of cells expressing high levels of immunoproteasomes such as macrophages. Analysis of the bronchoalveolar lavage (BAL) fluid containing the loosely attached immune cells in the bronchoalveolar space, however, showed no changes in the immune cell composition in young and aged mice (Figure 6-3A&B). Furthermore, immunofluorescence staining of the immunoproteasome subunit LMP2 in lung sections of young and aged mice revealed no change in the relative number of LMP2 positive cells indicating absence of increased immune cell infiltration into aged lungs (Figure 6-3AC&D). To further analyze which cell types are responsible for the observed increase in LMP2 expression, lung slices of young and aged mice were immunohistochemically stained for LMP2 expression. Immunohistochemistry staining for the immunoproteasome subunit LMP2 revealed elevated staining mainly in resident cells of the lung (Figure 6-4) which mostly appear to be alveolar macrophages. Alveolar macrophages have previously been shown to be the most prominent immunoproteasome-expressing cell type in the lung (Keller et al., 2015). In addition, some dispersed staining was apparent in epithelial cells of the lung (Figure 6-4, marked by arrows).

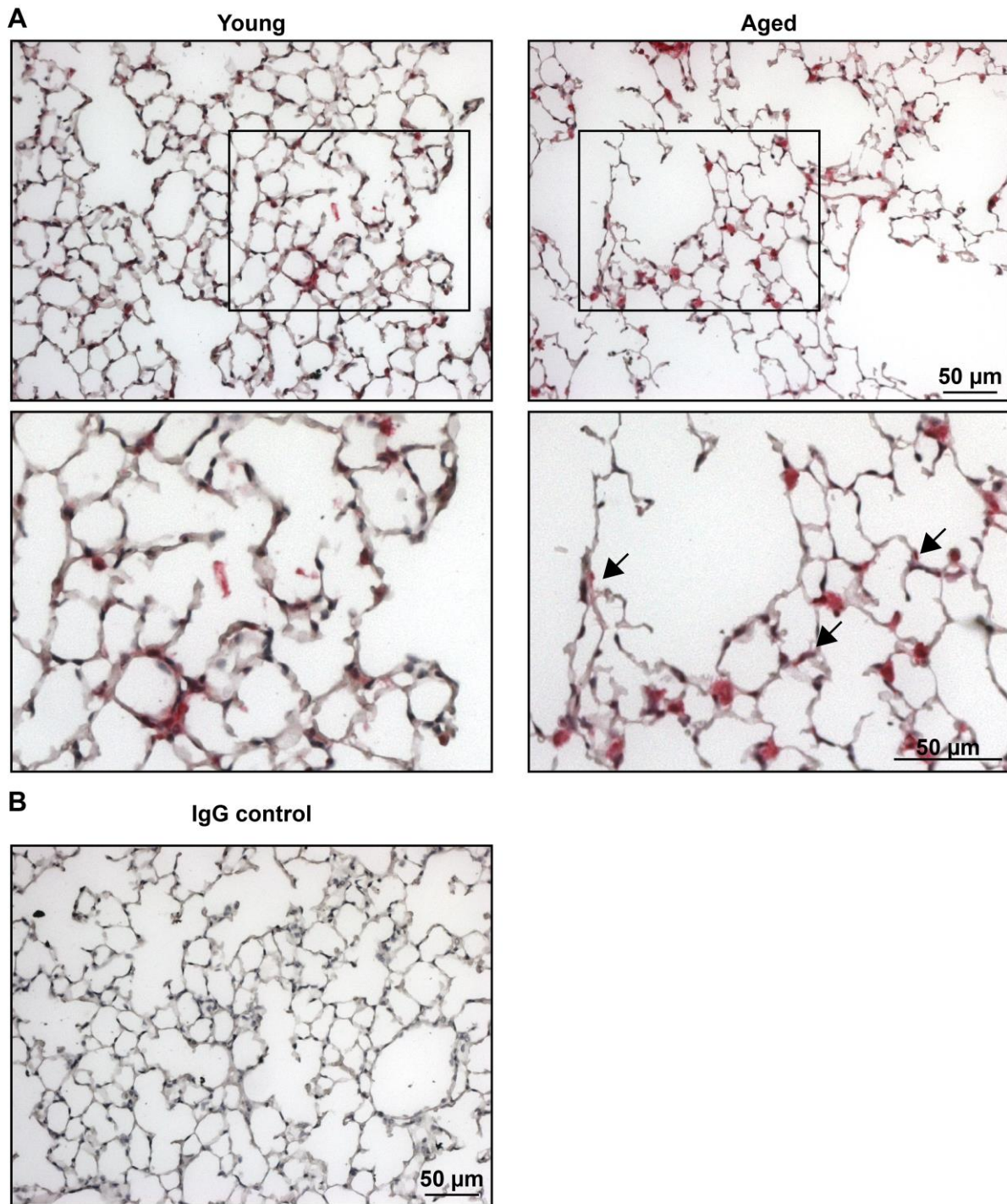


Figure 6-4: LMP2 expression is mainly increased in macrophages in the aged lung

(A) Representative staining of lung sections of young and aged C57Bl/6J wildtype mice. Lung sections were stained with an LMP2 antibody (red) and subsequently counterstained with hematoxylin staining. LMP2 staining was mainly detected in macrophages, with increased intensity in lungs of aged mice. However, in aged mice some positive staining of alveolar epithelial structures was also observed (Arrows). Scale bars: 50 μm (B) Representative immunohistochemistry control staining using an IgG control antibody.

6.2.2 26S proteasome-dependent protein degradation is not altered during healthy aging of the lung

The catalytic activity of the proteasome is not only regulated by the expression of proteasomal subunits but depends on the assembly of standard or immunoproteasome subunits into the 20S catalytic core complex and is further regulated by attachment of regulatory particles (Paragraph 1.1.1). To assess the influence of altered proteasome subunit expression on proteasome activity in aged mice, proteasome activity was measured with small peptidic substrates specific for the different proteasome active sites. Only the caspase-like activity of the proteasome was decreased in aged mice while the chymotrypsin-like and trypsin-like activities did not change during aging (Figure 6-5A). This finding was further confirmed in another mouse strain using lung tissue lysates from FVB mice (Figure 6-5B). Importantly, a decrease in caspase like activity is characteristic for replacement of the standard subunit β 1 by the immunoproteasome subunit LMP2 (Ferrington and Gregerson, 2012; Van Kaer et al., 1994).

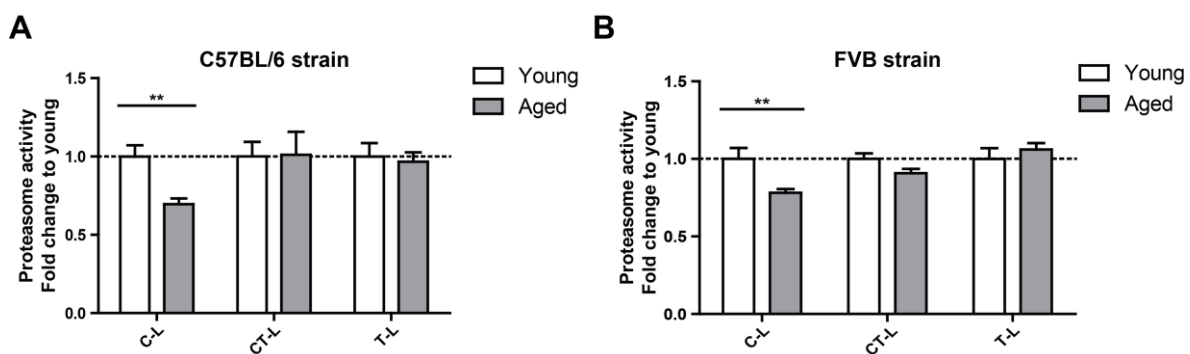


Figure 6-5: Caspase-like proteasome activity is decreased in lung tissue of aged mice

Cleavage of luminogenic model substrates specific for the caspase-like, chymotrypsin-like or trypsin-like active site of the proteasome in lung tissue lysate of (A) C57BL/6J mice (n=8) and in (B) lung tissue lysate of FVB mice (n=6-7). Values are displayed as fold change relative to young mice. Bar graphs show mean+SEM. Significance was determined using two-way ANOVA with Bonferroni multiple comparison test. **:p< 0.01. The proteasome activity assay in FVB mice was conducted by Anne Caniard.

To confirm this specific decrease in proteasome activity and to assign the activity to the distinct proteasome complexes, lung tissue lysates from young and aged mice were subjected to in-gel proteasome activity assays after native electrophoretic separation of proteasome complexes. Intriguingly, the chymotrypsin-like activity of the 26S/30S and 20S proteasome complexes was very similar in young and aged lungs confirming the above results with the peptide substrates (Figure 6-6A&B). The caspase-like activity, however, was again significantly decreased. This decrease was observed predominantly in 20S complexes and not in the assembled 26S or 30S proteasomes of aged lung tissue (Figure 6-6C&D).

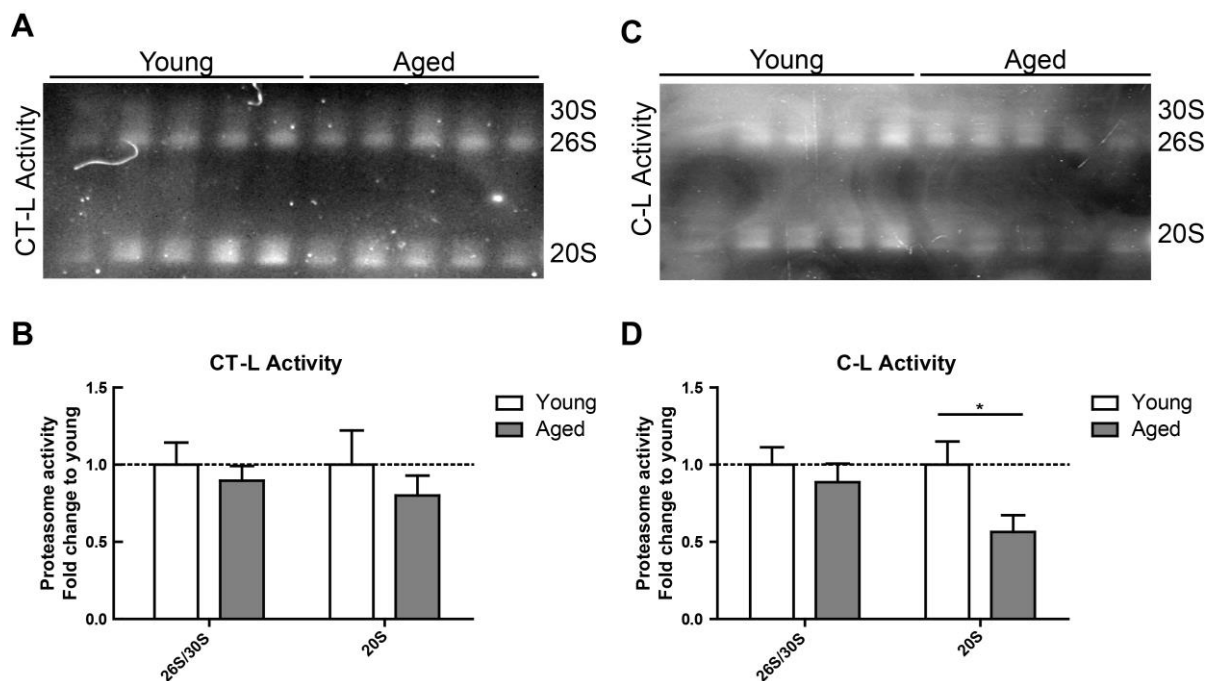


Figure 6-6: Caspase-like activity is decreased in 20S but not in 26S/30S proteasome complexes of aged mice

(A) Native gel analysis of proteasome complexes with activity overlay for the chymotrypsin-like proteasome activity in lung tissue lysates from young and aged C57Bl/6J mice and (B) quantification thereof. (C) Native gel analysis with activity overlay for the caspase-like proteasome activity and (D) quantification thereof. The appearance of 20S double bands is possibly due to the binding of alternative proteasome regulators such as PA28 family members (Hernebring et al., 2013). Bar graphs show mean+SEM. Values are displayed as fold change relative to young mice. Significance was determined using student's t-test. *:p< 0.05. The native gel activity assays shown in this figure were performed by Anne Caniard.

The 26S and 30S proteasomes are responsible for ubiquitin-mediated degradation of proteasome substrates while the 20S proteasome does not degrade ubiquitinated substrates (Finley, 2009). Accordingly, ubiquitin-mediated degradation was not impaired in the lungs of aged mice as indicated by the absence of accumulation of K48-polyubiquitinated proteins (Figure 6-7A). In line with this finding ubiquitin-dependent degradation of the ODD-luc reporter construct was not changed in lungs of aged proteasome reporter mice (Figure 6-7B). These mice express luciferase as a reporter gene fused to the oxygen-dependent degradation domain (ODD). Under normal conditions, luciferase is quickly degraded by the 26S proteasome resulting in a low background luminescent signal. At conditions of proteasome inhibition, however, luciferase accumulates leading to an increased luminescence signal (Goldman et al., 2011; Kimbrel et al., 2009).

In summary, these data indicate that 26S and 30S proteasome activity and thereby ubiquitin-mediated protein degradation is not affected in healthy aging of the lung. However, upregulation of immunoproteasome subunits and changes in the caspase-like activity of 20S proteasomes suggest increased assembly and activity of immunoproteasomes.

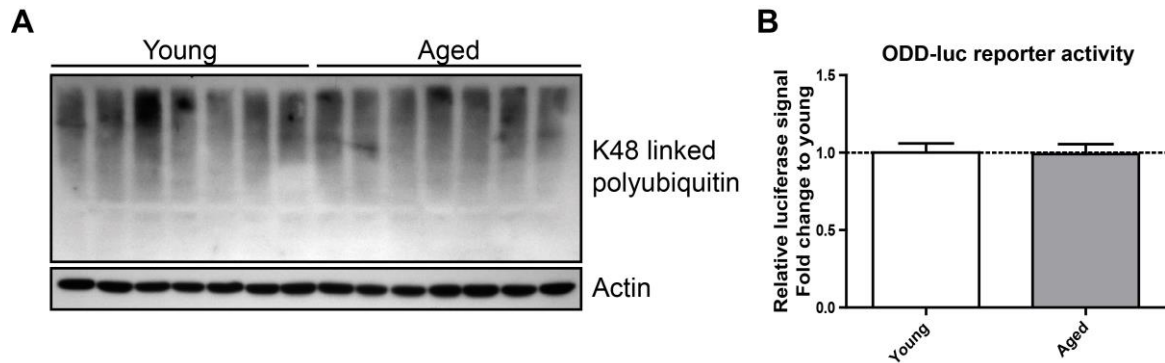


Figure 6-7: Ubiquitin-mediated degradation is not changed in lungs of aged mice

(A) Western blot analysis for lysin-48 (K48)-linked polyubiquitinated proteins in lung tissue lysates from young and aged C57Bl/6J mice. Actin was used as a loading control. (B) Relative luciferase activity in lung tissue of young and aged FVB-luc reporter mice. n=6-7. Bar graphs show mean+SEM. The ODD-luc activity assay was performed by Anne Caniard.

6.2.3 LMP2 or LMP7 knockout mice have preserved proteasome activity but are not protected from lung aging

As immunoproteasome subunits were upregulated in the aging lung, the relevance of the immunoproteasome in the development of senile lung emphysema was assessed by analyzing lung aging in mice deficient for the immunoproteasome subunits LMP2 or LMP7. LMP2 or LMP7 knockout mice exhibit no obvious phenotypic alterations under normal maintenance conditions (Fehling et al., 1994; Van Kaer et al., 1994). Here, no obvious signs of accelerated or decelerated aging were observed in aged LMP2 or LMP7 knockout mice. Importantly, the lungs of aged knockout mice developed a senile emphysema phenotype just as WT mice, indicating that aging of the lung is not affected by deficiency for these immunoproteasome subunits (Figure 6-8A&B). Similar to senile emphysema development, the expressional changes of proteasome subunits in young and aged LMP2 or LMP7 knockout mice showed a very similar pattern as in WT mice. While expression of the standard subunits was unchanged, expression of LMP2 and LMP7 was increased compared to young mice in old LMP7 or LMP2 knockout mice, respectively (Figure 6-9A&B).

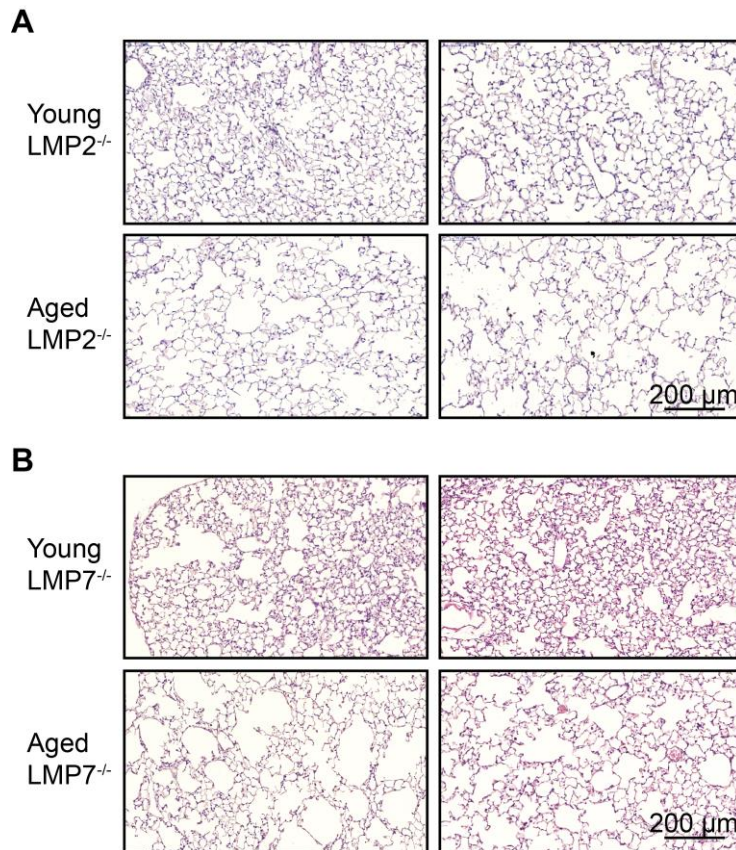


Figure 6-8: Senile emphysema development in the lung of aged LMP2 or LMP7 knockout mice

Representative H&E staining of lungs from young and aged (A) LMP2^{-/-} and (B) LMP7^{-/-} mice. Images from two individual animals are depicted per group. Scale bar: 200 µm. H&E stainings of LMP2^{-/-} mice were performed by Anne Caniard.

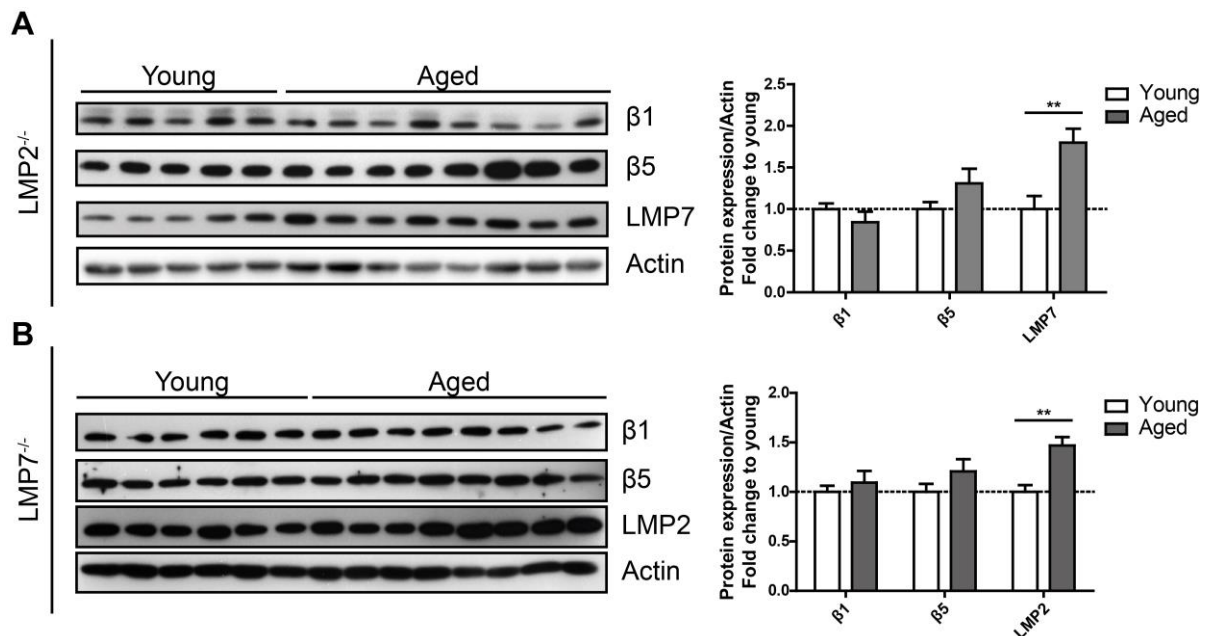


Figure 6-9: Increased expression of remaining immunoproteasome subunits in LMP2 or LMP7 knockout mice

Western blot analysis of proteasome subunit expression and quantification of protein expression relative to the actin loading control in (A) LMP2^{-/-} and (B) LMP7^{-/-} mice. Bar graphs show mean+SEM. Values are displayed as fold change relative to young mice. Significance was determined using two-way ANOVA with Bonferroni multiple comparison test. **:p< 0.01.

Regulation of proteasomal function during healthy aging of the lung

As described above, incorporation of immunoproteasome subunits, especially of LMP2, induces a decrease in the proteasome caspase-like activity (Van Kaer et al., 1994). According to the inability to incorporate LMP2 in proteasome complexes, the caspase-like activity in lungs of young and aged LMP2 knockout mice was significantly increased compared to WT mice. Notably, this effect was even more pronounced in lungs of aged animals (Figure 6-10A&B). Concordantly, and in contrast to WT mice, no changes in proteasome activity were observed between young and aged LMP2 or LMP7 knockout mice using small peptidic substrates on whole lung lysates (Figure 6-11A&B) or in the native gel overlay assay (Figure 6-11C&D). Well in accordance with the lack of changes in proteasomal activity between young and aged animals, the levels of K48 polyubiquitinated proteins were not changed in LMP2 or LMP7 knockout mice during aging (Figure 6-11E&F).

In summary, lungs of aged LMP2 or LMP7 knockout mice have a very similar aging phenotype as aged WT mice including development of senile lung emphysema. However, proteasome function is unchanged in aged LMP2 or LMP7 knockout mice. These results therefore strongly indicate that the immunoproteasome-mediated changes in proteasome activity in WT mice are not related to the development of an aging phenotype in the lung during healthy lung aging.

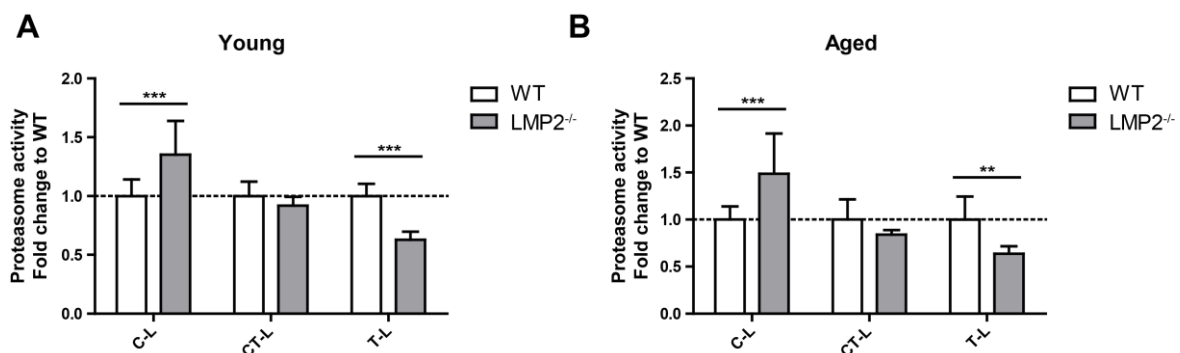


Figure 6-10: Caspase-like proteasome activity is increased in young and aged LMP2 deficient mice

Cleavage of luminogenic model substrates specific for the C-L, CT-L or T-L active site of the proteasome in lung tissue lysate of (A) young and (B) old WT and LMP2 knockout mice. n=5-8. Bar graphs show mean+SEM. Values are displayed as fold change relative to WT mice. Significance was determined using two-way ANOVA with Bonferroni multiple comparison test. **:p< 0.01, ***:p< 0.01.

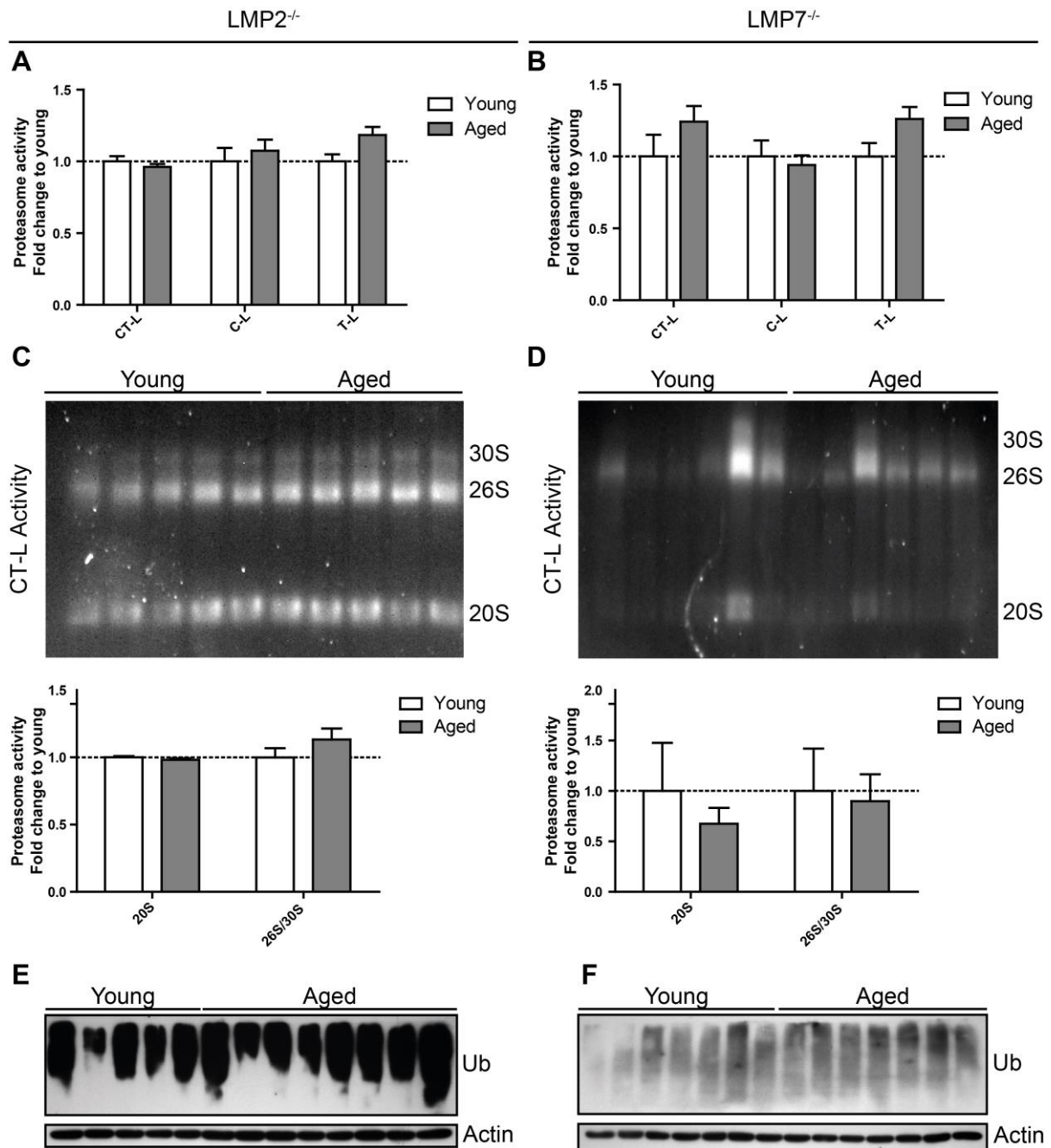


Figure 6-11: No change in proteasome activity in young and aged LMP2 or LMP7 knockout mice

(A) Cleavage of luminogenic model substrates specific for the C-L, CT-L or T-L active site of the proteasome in lung tissue lysate of LMP2^{-/-} (n=5-8) and (B) LMP7^{-/-} (n=6-11) mice. Bar graphs show mean+SEM. (C) Native gel analysis of proteasome complexes with activity overlay for CT-L activity in lung tissue lysate of LMP2^{-/-} or (D) LMP7^{-/-} mice and quantification thereof. Bar graphs show mean+SEM. Values are displayed as fold change relative to young mice. (E) Western blot analysis for K48-linked polyubiquitinated proteins in lung tissue lysates from young and aged LMP2^{-/-} and (F) LMP7^{-/-} mice. Actin was used as a loading control. Native gel analysis of LMP2^{-/-} mice was performed by Anne Caniard.

6.2.4 Absence of a lung aging phenotype in premature aging mtDNA mutator mice

To assess the influence of mitochondrial dysfunction on lung aging and proteasomal function in the aging lung, the premature aging mtDNA mutator mouse model was analyzed for lung aging. Hence, to investigate whether the premature aging phenotype of mtDNA mutator mice also affects the lung, lung histology of prematurely aged mtDNA mutator mice was analyzed. Of note, lungs of ten months old mtDNA mutator mice did not show any obvious signs of histological alterations such as senile emphysema (Figure 6-12).

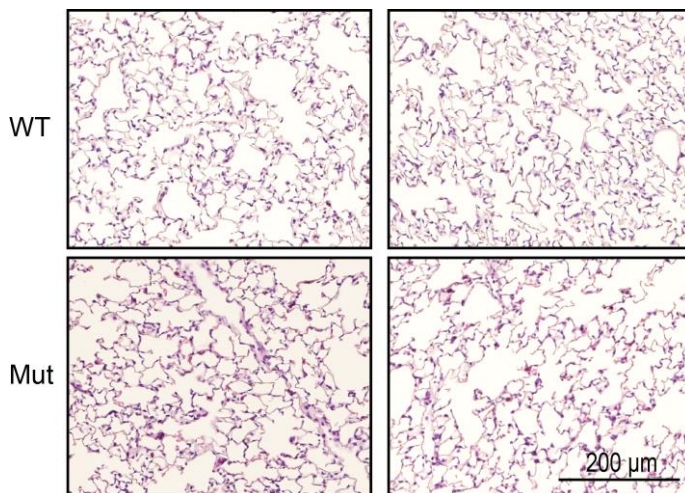


Figure 6-12: Absence of senile emphysema in premature aging mtDNA mutator mice

Representative H&E staining of lungs from ten month old WT and mtDNA mutator (Mut) mice. Images from two individual animals are depicted per group. Scale bar: 200 μm .

Furthermore, molecular markers of aging such as Sirt1 protein and p16 and p21 mRNA expression were analyzed and only a slight decrease in Sirt1 levels but no changes in p16 or p21 expression were observed (Figure 6-13A&B). Similarly, no alterations in proteasome mRNA or protein expression (Figure 6-14A&B) and in proteasome activities were observed in these lungs (Figure 6-14C). Collectively, these data demonstrate that the accelerated aging phenotype of mtDNA mutator mice does not involve premature aging of lung tissue and altered proteasome function.

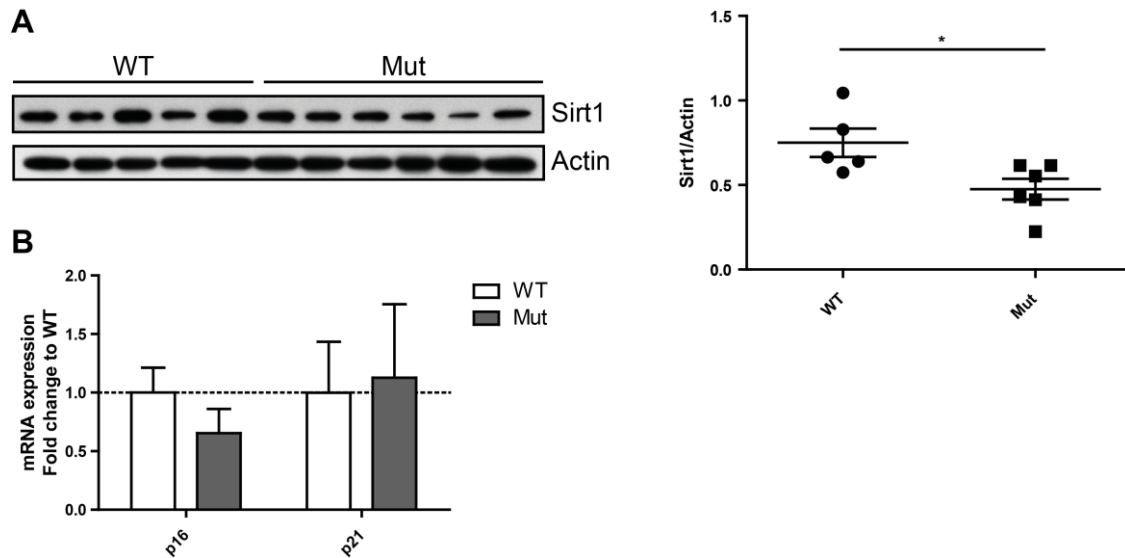


Figure 6-13: No alterations in aging markers in mtDNA mutator mouse lungs

(A) Sirt1 expression in lung tissue lysates of ten month old WT and mtDNA mutator mice and quantification thereof. (B) mRNA expression levels of p16 and p21 in lung tissue of WT and mtDNA mutator mice. n=6-7. Bar graphs show mean+SEM. Significance was determined using student's t-test. *:p< 0.05.

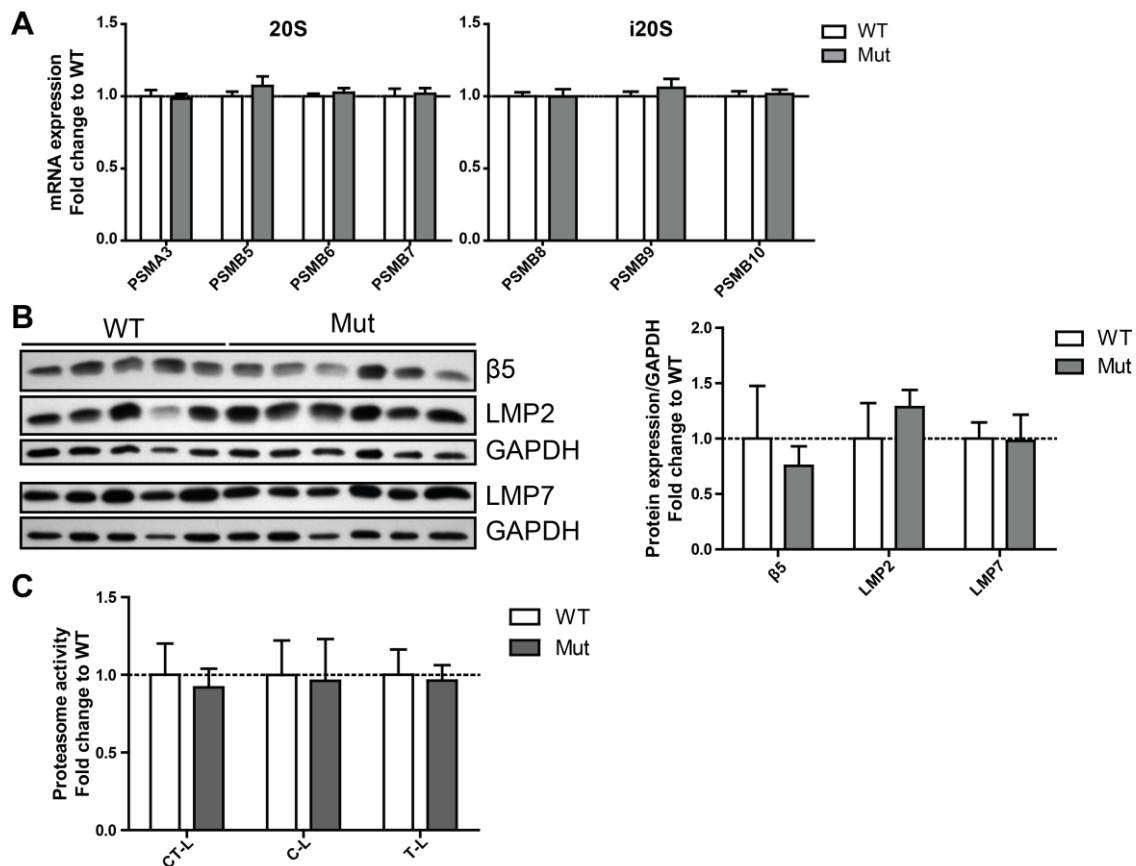


Figure 6-14: No change in proteasome expression and activity in mtDNA mutator mouse lungs

(A) RT-qPCR analysis of proteasome subunit mRNA expression in mtDNA mutator mice. n=6-7. (B) Western Blot analysis of proteasome subunit expression in mtDNA mutator mice and quantification thereof. (C) Cleavage of luminogenic model substrates specific for the CT-L, C-L or T-L active site of the proteasome in lung tissue lysate of mtDNA mutator mice. n=4-9. Bar graphs show mean+SEM. Values are displayed as fold change relative to WT mice.

6.3 Discussion

Proteostasis failure is one of the hallmarks of aging. However, protein homeostasis during healthy aging of the lung still remains to be studied. Here, a comprehensive analysis of proteasome function in lung aging is shown using transgenic proteasome reporter and immunoproteasome knockout mice. Activity of the 26S proteasome and concordantly ubiquitin-mediated degradation of ubiquitinated proteins or a proteasome reporter substrate was not altered in lungs of aged mice. Specifically, only the caspase-like proteasome activity was diminished in lung tissues from aged mice which could be attributed to increased expression of the catalytic immunoproteasome subunits. Mice deficient for the immunoproteasome subunits LMP2 or LMP7 did not show any age-related downregulation of proteasome activity. However, these mice still displayed age-related emphysematous changes in the lung. This argues that single immunoproteasome subunits do not play a protective role for lung aging. Furthermore, no changes in proteasome activity and lung phenotype were observed in lungs of the premature aging mtDNA mutator mice.

6.3.1 Proteasome function is not markedly impaired in aged lungs

Proteasome function was found to decrease during aging in several tissues and species (Chondrogianni et al., 2014; Dahlmann, 2007; Farout and Friguet, 2006; Keller et al., 2000). Proteostasis dysfunction during aging is thought to contribute to tissue damage by decreased degradation of damaged proteins thereby inducing aggregate formation and protein toxicity (Breusing et al., 2009; Chondrogianni et al., 2014; Ding et al., 2006; Farout and Friguet, 2006; Keller et al., 2000). This comprehensive analysis of proteasome activity in the lungs of aged mice, however, revealed that proteasome activity is not substantially impaired during healthy aging. While development of senile emphysema and age-dependent impairment of lung function was observed in lungs of aged mice, the activity of the proteasome was preserved. Only the caspase-like activity of the proteasome was found to decline during aging. However, this specific change of the proteasomal activity in aged lungs did not affect overall ubiquitin-mediated protein degradation. Specifically, the proteasome reporter substrate ODD-luciferase did not accumulate in the lungs of reporter animals during aging. In accordance with this finding, it has been reported that the caspase-like activity has only a minor contribution to overall protein degradation by the proteasome. It rather determines degradation rates of specific substrates and the composition of the degradation products (Kisselev et al., 1999, 2006). Interestingly, a decrease in caspase-like activity was also consistently reported in other tissues during aging while results for the chymotrypsin and trypsin-like activity were not consistent (Dahlmann, 2007).

These results are in contrast to results obtained for the lungs of aged rats in which an impairment of the chymotrypsin-like activity was observed in whole lung tissue of 18-24 months old rats (Breusing

et al., 2009; Keller et al., 2000). This discrepancy might be related to substantial differences in tissue preparation and proteasome activity assays in these studies or to species-related variance. However, the findings are in accordance with several reports that studied proteasome function in aging specifically in the brain: No impairment in ubiquitin-mediated protein degradation was detected by Cook et al using GFP-based proteasome reporter mice (Cook et al., 2009). Similarly, the degradation rate of polyubiquitinated model substrates was not changed in isolated 26S proteasomes from the brains of young and aged rats (Giannini et al., 2013). Additionally, 20S proteasome activity but not 26S proteasome function, which is responsible for ubiquitin-mediated turnover, correlated with species lifespan (Pickering et al., 2015). These data thus suggest that in the course of healthy aging of the lungs not overall ubiquitin-mediated protein degradation is altered but possibly proteasome cleavage specificity.

6.3.2 Immunoproteasome expression is elevated in aged lungs

Immunoproteasome expression is increased in aged mice. Elevated expression of immunoproteasome subunits was found both on mRNA and on proteins levels in whole lung samples. Immunohistochemical analysis showed that increased LMP2 expression occurs in alveolar macrophages and also in alveolar epithelial cells. Increased immunoproteasome content in the lung is well in accordance with the observed decrease in caspase-like activity. Immunoproteasomes have an altered cleavage site specificity which has been attributed to their specific function for the generation of MHC class I epitopes. Immunoproteasomes preferentially generate peptides with hydrophobic C-termini that have a higher affinity for binding into the MHC class I binding groove thereby improving MHC class I epitope generation and subsequent adaptive immune responses (Groettrup et al., 2010). For this reason, immunoproteasomes generally show diminished caspase-like activity (cleavage after acidic residues) compared to standard proteasomes while the other two active sites (cleavage after basic or hydrophobic residues) are not changed (Ferrington and Gregerson, 2012). Accordingly, when immunoproteasome expression was abolished in LMP2 or LMP7 knockout animals the caspase-like proteasome activity was restored to normal. The relative difference in caspase-like activity was already seen by directly comparing young WT and LMP2 knockout mice but it was particularly evident when comparing aged mice. This further argues in favor of the dependence of the caspase-like activity on increased immunoproteasome subunit incorporation in aging. Altogether, these findings imply that, in the lung, the decrease in proteasome activity during aging is not based on a loss of function phenotype of the proteasome but rather on altered proteasome subunit composition.

Induction of immunoproteasomes in aging has also been observed in other tissues such as muscle and brain (Ferrington, 2005; Giannini et al., 2013). Generally, it can be attributed either to enhanced

recruitment of immune cells to the aged tissue or increased formation of immunoproteasomes in resident cells. The immunohistochemical analysis in this study suggests increased LMP2 expression especially in macrophages in the aged lung. Macrophages are the main immunoproteasome-expressing cell type in the lung (Keller et al., 2015) and immunoproteasome expression accounts for approximately 50 % of total proteasome content in macrophages of young mice (I. Kammerl: unpublished data). Although an increase in macrophage content in lungs of aged mice was reported before (Calvi et al., 2011), no changes in the immune cell count in the BAL and no obvious difference in the number of LMP2-positive cells in the lung were found in this study. Hence, elevated LMP2 levels are most probably not due to increased recruitment of immune cells in the aged lung but rather based on increased expression of immunoproteasome subunits in resident cells. Increased expression of immunoproteasome in alveolar macrophages might affect macrophage polarization. Polarization towards anti-inflammatory M2 macrophages was recently described to be enhanced upon immunoproteasome ablation (Chen et al., 2016). Furthermore, altered immunoproteasome expression in non-immune cells might possibly affect immune responses in the lung as it is supposed to alter cleavage site specificity of the proteasome. This might affect epitope processing and thus MHC class I immune surveillance. Therefore, increased immunoproteasome expression might modulate immune responses and possibly add to the risk of autoimmunity (Basler et al., 2013; Eleftheriadis, 2012). Indeed, the prevalence of autoimmune diseases clearly rises with age (Hasler and Zouali, 2005). Alternatively, upregulation of immunoproteasomes might represent a response to increased oxidative stress during aging. Accordingly, oxidative stress increases during aging (López-Otín et al., 2013; Stadtman, 2006) and immunoproteasomes have been suggested to be involved in the degradation of oxidatively modified proteins (Aiken et al., 2011; Ebstein et al., 2013; Nathan et al., 2013; Seifert et al., 2010). Hence, increased expression of immunoproteasomes might also arise from an increased need to degrade oxidatively damaged proteins.

6.3.3 Immunoproteasome expression does not causally contribute to the aging phenotype of the lung

The causal contribution of elevated immunoproteasome expression to aging has not been proven so far. In general, upregulation of immunoproteasome subunits during aging has been proposed as a compensatory mechanism for decreased activity of constitutive proteasomes (Chondrogianni et al., 2014). As immunoproteasomes are not only upregulated during aging but also immunoproteasome expression correlates with species longevity (Pickering et al., 2015), it is most likely that the increase of immunoproteasome expression is a protective and compensatory effect during aging and not part of detrimental age-related changes. Therefore one would expect that LMP2 or LMP7 knockout mice suffer more from age-related alterations of lung structure and function than WT mice. However, no

aggravated changes in lung aging were found in LMP2 or LMP7 knockout mice. This implies that knockdown of singular immunoproteasome subunits does not influence lung aging. Moreover, in lungs of aged LMP2 or LMP7 mice overall proteasome activity was restored indicating that the change in caspase-like proteasome activity in wildtype mice during aging does not causally influence lung aging. Several types of “mixed proteasomes” exist containing partly constitutive subunits and partly immunosubunits (Ferrington and Gregerson, 2012; Meiners et al., 2014). Therefore, it cannot be excluded that double or even triple knockout mice for the immunoproteasome subunits might show altered behavior. However, since the immunoproteasome propeptides generally favor cooperative assembly (De et al., 2003) and the incorporation of MECL-1 requires LMP2 (Groettrup et al., 1997), at least several possibilities of mixed proteasomes are ruled out.

In contrast to these data, another study observed diminished proteasome activity in liver and brain of 12 months old LMP2 knockout mice compared to four months old animals. However, already in this study, strong differences between the two analyzed tissues were observed (Ding et al., 2006). Furthermore, in retinal epithelial cells of aged LMP7 knockout mice, proteasome activity was unchanged and in LMP7 and MECL-1 double knockout mice it was even elevated with age (Hussong et al., 2010). These data therefore argue that in immunoproteasome knockout mice proteasome activity is regulated in a very tissue-specific manner during aging and is not generally related to detrimental age-related changes.

6.3.4 Proteostasis in healthy aging of the lung

Altogether, these findings indicate that healthy aging of the lung and progressive development of senile emphysema does not involve impairment of proteasome function. In support of this notion, a transgenic mouse model with decreased chymotrypsin-like proteasome activity had a preserved lung structure, although these mice developed age-related phenotypes in other organs and tissues and died prematurely (Tomaru et al., 2012; Yamada et al., 2015). As no significant alteration in lung proteasome function was observed here, it is tempting to speculate that protein homeostasis in the lung remains functional upon healthy aging. Damaged proteins tend to aggregate during aging thereby inducing impairment of proteasome function (Andersson et al., 2013; Walther et al., 2015). This leads to disability of the proteasome system to degrade misfolded proteins and thereby increases the load of damaged proteins, which induces a vicious cycle of diminished protein degradation and aggregate formation (Andersson et al., 2013; Bence et al., 2001; Hipp et al., 2012). This model, however, suggests that up to a specific protein damage threshold protein homeostasis may remain functional. In the light of these data it seems plausible to speculate that this threshold is not exceeded during healthy aging of the lung. Therefore, dysregulation of proteostasis as a hallmark of aging is probably of minor importance during lung aging under conditions of healthy aging.

6.3.5 Mitochondrial function in lung aging

In addition to proteasome function, the involvement of mitochondrial dysfunction in lung aging was analyzed. Therefore, the aging phenotype of the lung in the premature aging mtDNA mutator mouse model was assessed. The mtDNA mutator mice accumulate mutations in the mtDNA which leads to mitochondrial dysfunction in aged mice, which was linked to an aging phenotype in several tissues (Trifunovic et al., 2004). However, no signs of senile emphysema were observed in old mtDNA mutator mice. This correlated well with a minor lung aging phenotype in these mice as assessed by molecular markers of aging. Generally, alterations of lung function and lung morphology are not well recapitulated in many premature aging mouse models (Meiners et al., 2015). While some premature aging mouse models, such as the Klotho mice, senescence-accelerated mice or senescence-marker-protein30 deficient mice show airspace enlargement, no lung phenotype was observed e.g. in the telomerase RNA null mice (Alder et al., 2011; Kurozumi et al., 1994; Meiners et al., 2015; Sato et al., 2007). Therefore, formation of senile emphysema is not necessarily associated with some aging factors. Hence, as diminished mitochondrial activity does not result in premature aging of the lung, mitochondrial dysfunction does not appear to be a driving pathway of lung aging.

Together, these data suggest that premature aging based on mitochondrial dysfunction does not primarily affect the aging phenotype in the lung. This finding is parallel to a premature aging mouse model based on decreased proteasome activity. Mice with premature aging based on diminished proteasome activity did not develop a lung aging phenotype and senile emphysema under normal maintenance conditions (Yamada et al., 2015). However, although no signs of lung aging were observed at baseline, these mice were more susceptible for cigarette smoke-induced emphysema development (Yamada et al., 2015).

In summary, these data show that alterations of both proteasomal as well as mitochondrial function are not directly linked to healthy aging of the lung. However, as shown in a premature aging mouse model based on proteasome dysfunction, decreased proteasome activity during aging might well influence the susceptibility to environmental factors during aging. This is well in accordance with the aforementioned concept of a damage threshold which needs to be exceeded. A decrease in the proteolytic capacity or mitochondrial function due to exposition to environmental hazards might exceed the damage threshold thereby tipping the balance towards loss of proteostasis. This process might then further augment age-related tissue damage leading to the development of age-related lung disease by a self-amplifying mechanism. Importantly, impairment of proteasome function has already been reported in response to cigarette smoke and diesel exhaust as well as in smoke- and age-related chronic obstructive diseases of the lung (van Rijjt et al., 2012; Min et al., 2011; Baker et al., 2014; Kipen et al., 2010; Kammerl et al., 2016).

7 Concluding remarks

The aim of this study was to analyze the connection between mitochondria and the proteasome system and to examine how mitochondrial and proteasomal functions are affected during healthy aging of the lung and in the development of age-related lung disease. Therefore, the interconnection of mitochondrial and proteasomal function was analyzed in cellular models of mitochondrial dysfunction. Furthermore, the effect of cigarette smoke exposure on mitochondrial function and proteostasis in lung epithelial cells was analyzed as well as the regulation of proteasomal function during healthy aging of the lung.

The first part of this thesis confirms the hypothesis that mitochondrial function is closely interconnected with proteasomal function. It is shown that strong and persistent dysfunction of the respiratory chain is associated with reduced proteasome activity and lower levels of assembled 26S and 30S complexes. Additionally, mild mitochondrial respiratory chain dysfunction was similarly associated with decreased proteasome activity in cells harboring specific mutations in subunits of the respiratory chain. Furthermore, it is shown that additional regulatory mechanisms exist for signaling of mitochondrial dysfunction to the proteasome in addition to known regulation by acute ROS generation or ATP depletion. Together with the published data which shows that also proteasomal dysfunction is tightly associated with mitochondrial function (see paragraph 1.3.1), this study clearly indicates that mitochondria and the proteasome system are connected in a more complex manner than originally thought.

The second part explores the effect of environmental hazards on mitochondrial function and quality control in the lung and shows that exposure of alveolar epithelial cells to nontoxic doses of cigarette smoke extract induces mitochondrial hyperfusion and elevated mitochondrial respiration in the absence of a protein stress response at mitochondria. Cigarette smoke extract-induced mitochondrial hyperfusion increased cellular metabolic activity and ATP production and thereby can be regarded as part of a protective stress response to acute cigarette smoke stress. However, despite being beneficial in the first place, this response might decrease the adaptation capacity of mitochondrial dynamics and might thereby be detrimental under chronic stress settings.

The third part of this thesis provides novel data on the regulation of proteasomal function during healthy aging and in mitochondrial dysfunction-induced premature aging of the lung. It is shown that immunoproteasome expression is increased in the aging lung which is associated with a concomitant change in the proteasomal cleavage specificities. However, as the aging phenotype is not influenced in immunoproteasome knockout mice, this effect is not a decisive factor for the development of senile emphysema during healthy lung aging. Similarly, as shown in the prematurely aging mtDNA mutator mice, mitochondrial dysfunction does not seem to be the decisive factor during lung aging.

Concluding remarks

However, since the proteasome system shows adaptive changes during healthy aging, these adaptation processes might reduce the additional adaptation capacity of the proteasome system to further insults. Altogether, healthy aging or exposure to nontoxic doses of cigarette smoke alone did not impair proteasomal or mitochondrial function to an extent which is directly inducing pronounced impairment of cellular functions. Hence, this study shows that mitochondria as well as the proteasome system have some spare capacity which enables them to remain functional during mild insults. However, both insults might limit the spare capacity of the proteasome and mitochondria and thereby limit the ability of cells to further adapt to environmental alterations and challenges. Hence, the simultaneous burden of an age-related functional decline together with noxious environmental exposures such as cigarette smoke might push proteasomal and mitochondrial function beyond a damage threshold thereby contributing to the pathogenesis of disease states or to a combined functional decline of both systems as described in aging. Furthermore, as both systems are closely connected it can be speculated that more severe stress which exceeds the damage threshold might tip the balance and induce a vicious cycle of proteasomal dysfunction and mitochondrial dysfunction with each system further attenuating function of the respective other system (Figure 7-1). Hence, this suggests that the different hallmarks of aging should not be considered individually but should also be reflected in context of the interconnections between the different hallmarks.

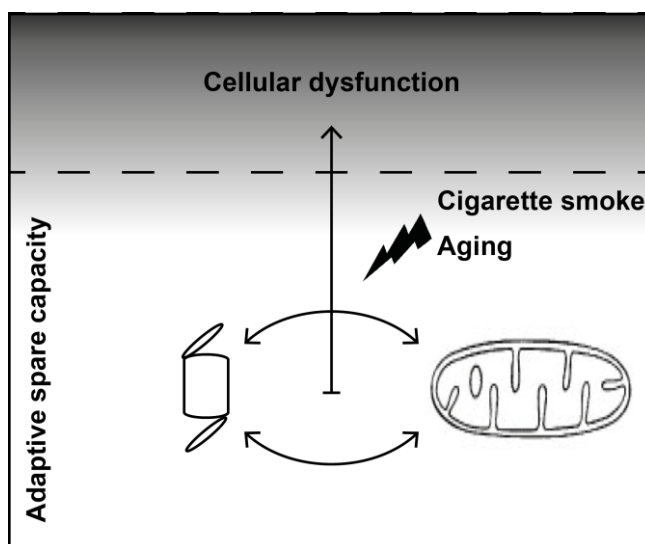


Figure 7-1: Working model: Proteasomal and mitochondrial functions in aging and disease

Proteasome and mitochondria possess a functional spare capacity which enables the cell to adapt to stress and maintain homeostasis during healthy aging or mild environmental insults. However, exposure to stress can reduce the adaptive capacity of both systems. Since proteasomal and mitochondrial functions are closely connected decreasing the spare capacity of one system beyond a damage threshold might attenuate function of the other system and thus drive a vicious cycle leading to cellular dysfunction.

This study describes alterations in mitochondrial and proteasomal function for both aging and cigarette smoke exposure which do not exceed the damage threshold but probably decrease the spare capacity of the cell to respond to additional damage. However, further research is necessary to fully understand the nature of these thresholds and to test the hypothesis that while single impairments of mitochondrial or proteasomal function during healthy aging or upon nontoxic cigarette smoke exposure do not exceed damage thresholds, a combined exposure leads to breakdown of mitochondrial and proteasomal function. Furthermore, this study shows that the interconnection of mitochondrial and proteasomal function is more complex as originally described and further research is needed to elucidate the different mechanistic steps in mitochondria to proteasome signaling. In summary, these experiments contribute to a deeper understanding of how risk factors in individual subjects add together towards a decline in both proteostasis and mitochondrial function during aging and eventually contribute to disease development.

Concluding remarks

References

- Acosta-Alvear, D., Cho, M.Y., Wild, T., Buchholz, T.J., Lerner, A.G., Simakova, O., Hahn, J., Korde, N., Landgren, O., Maric, I., et al. (2015). Paradoxical resistance of multiple myeloma to proteasome inhibitors by decreased levels of 19S proteasomal subunits. *eLife* *4*, e08153.
- Adams, J. (2004). The development of proteasome inhibitors as anticancer drugs. *Cancer Cell* *5*, 417–421.
- Agarwal, A.R., Yin, F., and Cadenas, E. (2013). Metabolic shift in lung alveolar cell mitochondria following acrolein exposure. *AJP Lung Cell. Mol. Physiol.* *305*, L764–L773.
- Agarwal, A.R., Yin, F., and Cadenas, E. (2014). Short-term cigarette smoke exposure leads to metabolic alterations in lung alveolar cells. *Am. J. Respir. Cell Mol. Biol.* *51*, 284–293.
- Ahmad, T., Sundar, I.K., Lerner, C.A., Gerloff, J., Tormos, A.M., Yao, H., and Rahman, I. (2015). Impaired mitophagy leads to cigarette smoke stress-induced cellular senescence: Implications for chronic obstructive pulmonary disease. *FASEB J.* *29*, 2912–2929.
- Aiken, C.T., Kaake, R.M., Wang, X., and Huang, L. (2011). Oxidative stress-mediated regulation of proteasome complexes. *Mol. Cell. Proteomics* *10*, R110.006924.
- Alder, J.K., Guo, N., Kembou, F., Parry, E.M., Anderson, C.J., Gorgy, A.I., Walsh, M.F., Sussan, T., Biswal, S., Mitzner, W., et al. (2011). Telomere length is a determinant of emphysema susceptibility. *Am. J. Respir. Crit. Care Med.* *184*, 904–912.
- Anand, R., Langer, T., and Baker, M.J. (2013). Proteolytic control of mitochondrial function and morphogenesis. *Biochim. Biophys. Acta BBA - Mol. Cell Res.* *1833*, 195–204.
- Andersson, V., Hanzén, S., Liu, B., Molin, M., and Nyström, T. (2013). Enhancing protein disaggregation restores proteasome activity in aged cells. *Aging* *5*, 802–812.
- Arlt, A., Bauer, I., Schafmayer, C., Tepel, J., Muerköster, S.S., Brosch, M., Röder, C., Kalthoff, H., Hampe, J., Moyer, M.P., et al. (2009). Increased proteasome subunit protein expression and proteasome activity in colon cancer relate to an enhanced activation of nuclear factor E2-related factor 2 (Nrf2). *Oncogene* *28*, 3983–3996.
- Arnould, T., Michel, S., and Renard, P. (2015). Mitochondria Retrograde Signaling and the UPRmt: Where Are We in Mammals? *Int. J. Mol. Sci.* *16*, 18224–18251.
- Azzu, V., and Brand, M.D. (2010). Degradation of an intramitochondrial protein by the cytosolic proteasome. *J. Cell Sci.* *123*, 578–585.
- Azzu, V., Jastroch, M., Divakaruni, A.S., and Brand, M.D. (2010). The regulation and turnover of mitochondrial uncoupling proteins. *Biochim. Biophys. Acta BBA - Bioenerg.* *1797*, 785–791.
- Baker, T.A., Bach IV, H.H., Gamelli, R.L., Love, R.B., and Majetschak, M. (2014). Proteasomes in lungs from organ donors and patients with end-stage pulmonary diseases. *Physiol. Res. Acad. Sci. Bohemoslov.* *63*, 311–319.
- Balaban, R.S., Nemoto, S., and Finkel, T. (2005). Mitochondria, Oxidants, and Aging. *Cell* *120*, 483–495.
- Barnes, P.J. (2000). Chronic Obstructive Pulmonary Disease. *N. Engl. J. Med.* *343*, 269–280.

References

- Basler, M., Kirk, C.J., and Groettrup, M. (2013). The immunoproteasome in antigen processing and other immunological functions. *Curr. Opin. Immunol.* *25*, 74–80.
- Bence, N.F., Sampat, R.M., and Kopito, R.R. (2001). Impairment of the ubiquitin-proteasome system by protein aggregation. *Science* *292*, 1552–1555.
- Ben-Nissan, G., and Sharon, M. (2014). Regulating the 20S Proteasome Ubiquitin-Independent Degradation Pathway. *Biomolecules* *4*, 862–884.
- Besche, H.C., Haas, W., Gygi, S.P., and Goldberg, A.L. (2009). Isolation of Mammalian 26S Proteasomes and p97/VCP Complexes Using the Ubiquitin-like Domain from HHR23B Reveals Novel Proteasome-Associated Proteins †. *Biochemistry (Mosc.)* *48*, 2538–2549.
- Bieler, S., Meiners, S., Stangl, V., Pohl, T., and Stangl, K. (2009). Comprehensive proteomic and transcriptomic analysis reveals early induction of a protective anti-oxidative stress response by low-dose proteasome inhibition. *PROTEOMICS* *9*, 3257–3267.
- Blackstone, C., and Chang, C.-R. (2011). Mitochondria unite to survive. *Nat. Cell Biol.* *13*, 521–522.
- van der Blik, A.M., Shen, Q., and Kawajiri, S. (2013). Mechanisms of Mitochondrial Fission and Fusion. *Cold Spring Harb. Perspect. Biol.* *5*, a011072–a011072.
- Bowler, R.P., Barnes, P.J., and Crapo, J.D. (2004). The Role of Oxidative Stress in Chronic Obstructive Pulmonary Disease. *COPD J. Chronic Obstr. Pulm. Dis.* *1*, 255–277.
- Bragoszewski, P., Gornicka, A., Sztolsztener, M.E., and Chacinska, A. (2013). The ubiquitin-proteasome system regulates mitochondrial intermembrane space proteins. *Mol. Cell. Biol.* *33*, 2136–2148.
- Branco, D.M. (2010). Cross-talk between mitochondria and proteasome in Parkinson's disease pathogenesis. *Front. Aging Neurosci.* *2*, 1–10.
- Brand, M.D., and Nicholls, D.G. (2011). Assessing mitochondrial dysfunction in cells. *Biochem. J.* *435*, 297–312.
- Bratic, A., and Larsson, N.-G. (2013). The role of mitochondria in aging. *J. Clin. Invest.* *123*, 951–957.
- Breusing, N., and Grune, T. (2008). Regulation of proteasome-mediated protein degradation during oxidative stress and aging. *Biol. Chem.* *389*, 203–209.
- Breusing, N., Arndt, J., Voss, P., Bresgen, N., Wiswedel, I., Gardemann, A., Siems, W., and Grune, T. (2009). Inverse correlation of protein oxidation and proteasome activity in liver and lung. *Mech. Ageing Dev.* *130*, 748–753.
- Buac, D., Shen, M., Schmitt, S., Kona, F.R., Deshmukh, R., Zhang, Z., Neslund-Dudas, C., Mitra, B., and Dou, Q.P. (2013). From bortezomib to other inhibitors of the proteasome and beyond. *Curr. Pharm. Des.* *19*, 4025–4038.
- Buchberger, A., Bukau, B., and Sommer, T. (2010). Protein Quality Control in the Cytosol and the Endoplasmic Reticulum: Brothers in Arms. *Mol. Cell* *40*, 238–252.
- Bush, K.T., Goldberg, A.L., and Nigam, S.K. (1997). Proteasome Inhibition Leads to a Heat-shock Response, Induction of Endoplasmic Reticulum Chaperones, and Thermotolerance. *J. Biol. Chem.* *272*, 9086–9092.

- Cagalinec, M., Safiulina, D., Liiv, M., Liiv, J., Choubey, V., Wareski, P., Veksler, V., and Kaasik, A. (2013). Principles of the mitochondrial fusion and fission cycle in neurons. *J. Cell Sci.* *126*, 2187–2197.
- Calvi, C.L., Podowski, M., D'Alessio, F.R., Metzger, S.L., Misono, K., Poonyagariyagorn, H., Lopez-Mercado, A., Ku, T., Lauer, T., Cheadle, C., et al. (2011). Critical Transition in Tissue Homeostasis Accompanies Murine Lung Senescence. *PLoS ONE* *6*, e20712.
- Campello, S., Strappazon, F., and Cecconi, F. (2013). Mitochondrial dismissal in mammals, from protein degradation to mitophagy. *Biochim. Biophys. Acta BBA - Bioenerg.* *1837*, 451–460.
- Cascio, P. (2014). PA28 $\alpha\beta$: The Enigmatic Magic Ring of the Proteasome? *Biomolecules* *4*, 566–584.
- Chan, N.C., Salazar, A.M., Pham, A.H., Sweredoski, M.J., Kolawa, N.J., Graham, R.L.J., Hess, S., and Chan, D.C. (2011). Broad activation of the ubiquitin–proteasome system by Parkin is critical for mitophagy. *Hum. Mol. Genet.* *20*, 1726–1737.
- Chandel, N.S. (2014). Mitochondria as signaling organelles. *BMC Biol.* *12*, 34.
- Chatenay-Lapointe, M., and Shadel, G.S. (2010). Stressed-Out Mitochondria Get MAD. *Cell Metab.* *12*, 559–560.
- Chen, L., and Madura, K. (2005). Increased Proteasome Activity, Ubiquitin-Conjugating Enzymes, and eEF1A Translation Factor Detected in Breast Cancer Tissue. *Cancer Res.* *65*, 5599–5606.
- Chen, Q., Thorpe, J., Dohmen, J.R., Li, F., and Keller, J.N. (2006). Ump1 extends yeast lifespan and enhances viability during oxidative stress: central role for the proteasome? *Free Radic. Biol. Med.* *40*, 120–126.
- Chen, S., Kammerl, I.E., Vosyka, O., Baumann, T., Yu, Y., Wu, Y., Irmler, M., Overkleeft, H.S., Beckers, J., Eickelberg, O., et al. (2016). Immunoproteasome dysfunction augments alternative polarization of alveolar macrophages. *Cell Death Differ.* *00*, 1–12.
- Chen, Z.-H., Lam, H.C., Jin, Y., Kim, H.-P., Cao, J., Lee, S.-J., Ifedigbo, E., Parameswaran, H., Ryter, S.W., and Choi, A.M.K. (2010). Autophagy protein microtubule-associated protein 1 light chain-3B (LC3B) activates extrinsic apoptosis during cigarette smoke-induced emphysema. *Proc. Natl. Acad. Sci.* *107*, 18880–18885.
- Choi, H.-S., Choi, Y.-G., Shin, H.-Y., Oh, J.-M., Park, J.-H., Kim, J.-I., Carp, R.I., Choi, E.-K., and Kim, Y.-S. (2014). Dysfunction of mitochondrial dynamics in the brains of scrapie-infected mice. *Biochem. Biophys. Res. Commun.* *448*, 157–162.
- Chondrogianni, N., Sakellari, M., Lefaki, M., Papaevgeniou, N., and Gonos, E.S. (2014). Proteasome activation delays aging in vitro and in vivo. *Free Radic. Biol. Med.* *71*, 303–320.
- Cho-Park, P.F., and Steller, H. (2013). Proteasome Regulation by ADP-Ribosylation. *Cell* *153*, 614–627.
- Chou, A.P., Li, S., Fitzmaurice, A.G., and Bronstein, J.M. (2010). Mechanisms of rotenone-induced proteasome inhibition. *NeuroToxicology* *31*, 367–372.
- Claessen, J.H.L., Kundrat, L., and Ploegh, H.L. (2012). Protein quality control in the ER: balancing the ubiquitin checkbook. *Trends Cell Biol.* *22*, 22–32.

References

- Cohen, M.M.J., Leboucher, G.P., Livnat-Levanon, N., Glickman, M.H., and Weissman, A.M. (2008). Ubiquitin-Proteasome-dependent Degradation of a Mitofusin, a Critical Regulator of Mitochondrial Fusion. *Mol. Biol. Cell* *19*, 2457–2464.
- Cook, C., Gass, J., Dunmore, J., Tong, J., Taylor, J., Eriksen, J., McGowan, E., Lewis, J., Johnston, J., and Petrucelli, L. (2009). Aging Is Not Associated with Proteasome Impairment in UPS Reporter Mice. *PLoS ONE* *4*, e5888.
- Corti, M., Brody, A.R., and Harrison, J.H. (1996). Isolation and primary culture of murine alveolar type II cells. *Am. J. Respir. Cell Mol. Biol.* *14*, 309–315.
- Dahlmann, B. (2007). Role of proteasomes in disease. *BMC Biochem.* *8*, 3–15.
- Das, K.C. (2013). Hyperoxia Decreases Glycolytic Capacity, Glycolytic Reserve and Oxidative Phosphorylation in MLE-12 Cells and Inhibits Complex I and II Function, but Not Complex IV in Isolated Mouse Lung Mitochondria. *PLoS ONE* *8*, e73358.
- De, M., Jayarapu, K., Elenich, L., Monaco, J.J., Colbert, R.A., and Griffin, T.A. (2003). 2 Subunit Propeptides Influence Cooperative Proteasome Assembly. *J. Biol. Chem.* *278*, 6153–6159.
- Denko, N.C. (2008). Hypoxia, HIF1 and glucose metabolism in the solid tumour. *Nat. Rev. Cancer* *8*, 705–713.
- Ding, Q., Martin, S., Dimayuga, E., Bruce-Keller, A.J., and Keller, J.N. (2006). LMP2 knock-out mice have reduced proteasome activities and increased levels of oxidatively damaged proteins. *Antioxid. Redox Signal.* *8*, 130–135.
- Distelmaier, F., Valsecchi, F., Liemburg-Apers, D.C., Lebiezinska, M., Rodenburg, R.J., Heil, S., Keijer, J., Fransen, J., Imamura, H., Danhauser, K., et al. (2014). Mitochondrial dysfunction in primary human fibroblasts triggers an adaptive cell survival program that requires AMPK- α . *Biochim. Biophys. Acta BBA - Mol. Basis Dis.* *1852*, 529–540.
- Ditzel, L., Huber, R., Mann, K., Heinemeyer, W., Wolf, D.H., and Groll, M. (1998). Conformational constraints for protein self-cleavage in the proteasome. *J. Mol. Biol.* *279*, 1187–1191.
- Domingues, A.F., Arduíno, D.M., Esteves, A.R., Swerdlow, R.H., Oliveira, C.R., and Cardoso, S.M. (2008). Mitochondria and ubiquitin-proteasomal system interplay: Relevance to Parkinson's disease. *Free Radic. Biol. Med.* *45*, 820–825.
- Duvezin-Caubet, S., Jagasia, R., Wagener, J., Hofmann, S., Trifunovic, A., Hansson, A., Chomyn, A., Bauer, M.F., Attardi, G., Larsson, N.-G., et al. (2006). Proteolytic Processing of OPA1 Links Mitochondrial Dysfunction to Alterations in Mitochondrial Morphology. *J. Biol. Chem.* *281*, 37972–37979.
- Ebstein, F., Voigt, A., Lange, N., Warnatsch, A., Schröter, F., Prozorovski, T., Kuckelkorn, U., Aktas, O., Seifert, U., Kloetzl, P.-M., et al. (2013). Immunoproteasomes Are Important for Proteostasis in Immune Responses. *Cell* *152*, 935–937.
- Edgar, D., and Trifunovic, A. (2009). The mtDNA mutator mouse: Dissecting mitochondrial involvement in aging. *Aging* *1*, 1028–1032.
- Edgar, D., Shabalina, I., Camara, Y., Wredenberg, A., Calvaruso, M.A., Nijtmans, L., Nedergaard, J., Cannon, B., Larsson, N.-G., and Trifunovic, A. (2009). Random Point Mutations with Major Effects on

- Protein-Coding Genes Are the Driving Force behind Premature Aging in mtDNA Mutator Mice. *Cell Metab.* *10*, 131–138.
- Eleftheriadis, T. (2012). The existence of two types of proteasome, the constitutive proteasome and the immunoproteasome, may serve as another layer of protection against autoimmunity. *Med. Hypotheses* *78*, 138–141.
- Elgass, K., Pakay, J., Ryan, M.T., and Palmer, C.S. (2012). Recent advances into the understanding of mitochondrial fission. *Biochim. Biophys. Acta BBA - Mol. Cell Res.* *1833*, 150–161.
- Farout, L., and Friguet, B. (2006). Proteasome function in aging and oxidative stress: implications in protein maintenance failure. *Antioxid. Redox Signal.* *8*, 205–216.
- Fehling, H.J., Swat, W., Laplace, C., Kühn, R., Rajewsky, K., Müller, U., and von Boehmer, H. (1994). MHC class I expression in mice lacking the proteasome subunit LMP-7. *Science* *265*, 1234–1237.
- Ferrington, D.A. (2005). Altered proteasome structure, function, and oxidation in aged muscle. *FASEB J.* *19*, 644–646.
- Ferrington, D.A., and Gregerson, D.S. (2012). Immunoproteasomes. In *Progress in Molecular Biology and Translational Science*, (Elsevier), pp. 75–112.
- Figge, M.T., Osiewacz, H.D., and Reichert, A.S. (2013). Quality control of mitochondria during aging: Is there a good and a bad side of mitochondrial dynamics? *BioEssays* *35*, 314–322.
- Finley, D. (2009). Recognition and Processing of Ubiquitin-Protein Conjugates by the Proteasome. *Annu. Rev. Biochem.* *78*, 477–513.
- Frankland-Searby, S., and Bhaumik, S.R. (2012). The 26S proteasome complex: An attractive target for cancer therapy. *Biochim. Biophys. Acta BBA - Rev. Cancer* *1825*, 64–76.
- Fukuoh, A., Cannino, G., Gerards, M., Buckley, S., Kazancioglu, S., Scialo, F., Lihavainen, E., Ribeiro, A., Dufour, E., and Jacobs, H.T. (2014). Screen for mitochondrial DNA copy number maintenance genes reveals essential role for ATP synthase. *Mol. Syst. Biol.* *10*, 734–734.
- Gallastegui, N., and Groll, M. (2010). The 26S proteasome: assembly and function of a destructive machine. *Trends Biochem. Sci.* *35*, 634–642.
- Gaziev, A.I., Abdullaev, S., and Podlitsky, A. (2014). Mitochondrial function and mitochondrial DNA maintenance with advancing age. *Biogerontology* *15*, 417–438.
- Geisler, S., Holmström, K.M., Skujat, D., Fiesel, F.C., Rothfuss, O.C., Kahle, P.J., and Springer, W. (2010). PINK1/Parkin-mediated mitophagy is dependent on VDAC1 and p62/SQSTM1. *Nat. Cell Biol.* *12*, 119–131.
- Giannini, C., Kloß, A., Gohlke, S., Mishto, M., Nicholson, T.P., Sheppard, P.W., Kloetzel, P.-M., and Dahlmann, B. (2013). Poly-Ub-Substrate-Degradative Activity of 26S Proteasome Is Not Impaired in the Aging Rat Brain. *PLoS ONE* *8*, e64042.
- Goldbaum, O., Vollmer, G., and Richter-Landsberg, C. (2006). Proteasome inhibition by MG-132 induces apoptotic cell death and mitochondrial dysfunction in cultured rat brain oligodendrocytes but not in astrocytes. *Glia* *53*, 891–901.

References

- Goldberg, A.L. (2003). Protein degradation and protection against misfolded or damaged proteins. *Nature* 426, 895–899.
- Goldman, S.J., Chen, E., Taylor, R., Zhang, S., Petrosky, W., Reiss, M., and Jin, S. (2011). Use of the ODD-Luciferase Transgene for the Non-Invasive Imaging of Spontaneous Tumors in Mice. *PLoS ONE* 6, e18269.
- Gomes, L.C., and Scorrano, L. (2013). Mitochondrial morphology in mitophagy and macroautophagy. *Biochim. Biophys. Acta BBA - Mol. Cell Res.* 1833, 205–212.
- Gomes, L.C., Benedetto, G.D., and Scorrano, L. (2011). During autophagy mitochondria elongate, are spared from degradation and sustain cell viability. *Nat. Cell Biol.* 13, 589–598.
- Granados-Castro, L.F., Rodríguez-Rangel, D.S., Montañaño, M., Ramos, C., and Pedraza-Chaverri, J. (2013). Wood smoke exposure induces a decrease in respiration parameters and in the activity of respiratory complexes I and IV in lung mitochondria from guinea pigs: Wood Smoke Exposure Induces a Decrease in Respiration Parameters. *Environ. Toxicol.* 30, 461–471.
- Grant, C.M. (2011). Regulation of Translation by Hydrogen Peroxide. *Antioxid. Redox Signal.* 15, 191–203.
- Groettrup, M., Standera, S., Stohwasser, R., and Kloetzel, P.M. (1997). The subunits MECL-1 and LMP2 are mutually required for incorporation into the 20S proteasome. *Proc. Natl. Acad. Sci.* 94, 8970–8975.
- Groettrup, M., Kirk, C.J., and Basler, M. (2010). Proteasomes in immune cells: more than peptide producers? *Nat. Rev. Immunol.* 10, 73–78.
- Groll, M., Bajorek, M., Köhler, A., Moroder, L., Rubin, D.M., Huber, R., Glickman, M.H., and Finley, D. (2000). A gated channel into the proteasome core particle. *Nat. Struct. Biol.* 7, 1062–1067.
- Haack, T.B., Haberberger, B., Frisch, E.-M., Wieland, T., Iuso, A., Gorza, M., Strecker, V., Graf, E., Mayr, J.A., Herberg, U., et al. (2012). Molecular diagnosis in mitochondrial complex I deficiency using exome sequencing. *J. Med. Genet.* 49, 277–283.
- Hara, H., Araya, J., Ito, S., Kobayashi, K., Takasaka, N., Yoshii, Y., Wakui, H., Kojima, J., Shimizu, K., Numata, T., et al. (2013). Mitochondrial fragmentation in cigarette smoke induced-bronchial epithelial cell senescence. *AJP Lung Cell. Mol. Physiol.* 305, L737–L746.
- Hardie, D.G., Ross, F.A., and Hawley, S.A. (2012). AMPK: a nutrient and energy sensor that maintains energy homeostasis. *Nat. Rev. Mol. Cell Biol.* 13, 251–262.
- Hartl, F.U., Bracher, A., and Hayer-Hartl, M. (2011). Molecular chaperones in protein folding and proteostasis. *Nature* 475, 324–332.
- Hasler, P., and Zouali, M. (2005). Immune receptor signaling, aging, and autoimmunity. *Cell. Immunol.* 233, 102–108.
- Heinemeyer, W., Kleinschmidt, J.A., Saidowsky, J., Escher, C., and Wolf, D.H. (1991). Proteinase yscE, the yeast proteasome/multicatalytic-multifunctional proteinase: mutants unravel its function in stress induced proteolysis and uncover its necessity for cell survival. *EMBO J.* 10, 555–562.
- Heo, J.-M., and Rutter, J. (2011). Ubiquitin-dependent mitochondrial protein degradation. *Int. J. Biochem. Cell Biol.* 43, 1422–1426.

- Heo, J.-M., Livnat-Levanon, N., Taylor, E.B., Jones, K.T., Dephoure, N., Ring, J., Xie, J., Brodsky, J.L., Madeo, F., Gygi, S.P., et al. (2010). A Stress-Responsive System for Mitochondrial Protein Degradation. *Mol. Cell* *40*, 465–480.
- Hernebring, M., Fredriksson, Å., Liljevald, M., Cvijovic, M., Norrman, K., Wiseman, J., Semb, H., and Nyström, T. (2013). Removal of damaged proteins during ES cell fate specification requires the proteasome activator PA28. *Sci. Rep.* *3*.
- Hipp, M.S., Patel, C.N., Bersuker, K., Riley, B.E., Kaiser, S.E., Shaler, T.A., Brandeis, M., and Kopito, R.R. (2012). Indirect inhibition of 26S proteasome activity in a cellular model of Huntington's disease. *J. Cell Biol.* *196*, 573–587.
- Hoffmann, R.F., Zarrintan, S., Brandenburg, S.M., Kol, A., de Bruin, H.G., Jafari, S., Dijk, F., Kalicharan, D., Kelders, M., Gosker, H.R., et al. (2013). Prolonged cigarette smoke exposure alters mitochondrial structure and function in airway epithelial cells. *Respir. Res.* *14*, 97.
- Höglinger, G.U., Carrard, G., Michel, P.P., Medja, F., Lombès, A., Ruberg, M., Friguet, B., and Hirsch, E.C. (2003). Dysfunction of mitochondrial complex I and the proteasome: interactions between two biochemical deficits in a cellular model of Parkinson's disease: Mitochondrial complex I and the proteasome. *J. Neurochem.* *86*, 1297–1307.
- Huang, Q., Wang, H., Perry, S.W., and Figueiredo-Pereira, M.E. (2013). Negative regulation of 26S proteasome stability via calpain-mediated cleavage of Rpn10 upon mitochondrial dysfunction in neurons. *J. Biol. Chem.* *288*, 12161–12174.
- Hussong, S.A., Kappahn, R.J., Phillips, S.L., Maldonado, M., and Ferrington, D.A. (2010). Immunoproteasome deficiency alters retinal proteasome's response to stress. *J. Neurochem.* *113*, 1481–1490.
- Imai, S., and Guarente, L. (2014). NAD⁺ and sirtuins in aging and disease. *Trends Cell Biol.* *24*, 464–471.
- Ito, K. (2009). COPD as a Disease of Accelerated Lung Aging. *CHEST J.* *135*, 173.
- Janssens, J.P., Pache, J.C., and Nicod, L.P. (1999). Physiological changes in respiratory function associated with ageing. *Eur. Respir. J.* *13*, 197–205.
- Jin, S.M., and Youle, R.J. (2012). PINK1- and Parkin-mediated mitophagy at a glance. *J. Cell Sci.* *125*, 795–799.
- Joshi, K.K., Chen, L., Torres, N., Tournier, V., and Madura, K. (2011). A Proteasome Assembly Defect in rpn3 Mutants Is Associated with Rpn11 Instability and Increased Sensitivity to Stress. *J. Mol. Biol.* *410*, 383–399.
- Jovaisaite, V., Mouchiroud, L., and Auwerx, J. (2013). The mitochondrial unfolded protein response, a conserved stress response pathway with implications in health and disease. *J. Exp. Biol.* *217*, 137–143.
- Kalapis, D., Bezerra, A.R., Farkas, Z., Horvath, P., Bódi, Z., Daraba, A., Szamecz, B., Gut, I., Bayes, M., Santos, M.A.S., et al. (2015). Evolution of Robustness to Protein Mistranslation by Accelerated Protein Turnover. *PLOS Biol.* *13*, e1002291.

References

- Kammerl, I.E., Dann, A., Mossina, A., Brech, D., Lukas, C., Vosyka, O., Nathan, P., Conlon, T.M., Wagner, D.E., Overkleeft, H.S., et al. (2016). Impairment of Immunoproteasome Function by Cigarette Smoke and in COPD. *Am. J. Respir. Crit. Care Med.*
- Kanabus, M., Heales, S.J., and Rahman, S. (2014). Development of pharmacological strategies for mitochondrial disorders. *Br. J. Pharmacol.* *171*, 1798–1817.
- Karbowski, M., and Youle, R.J. (2011). Regulating mitochondrial outer membrane proteins by ubiquitination and proteasomal degradation. *Curr. Opin. Cell Biol.* *23*, 476–482.
- Kaushik, S., and Cuervo, A.M. (2012). Chaperone-mediated autophagy: a unique way to enter the lysosome world. *Trends Cell Biol.* *22*, 407–417.
- Kawazoe, Y., Nakai, A., Tanabe, M., and Nagata, K. (1998). Proteasome inhibition leads to the activation of all members of the heat-shock-factor family. *Eur. J. Biochem.* *255*, 356–362.
- Keller, I.E., Vosyka, O., Takenaka, S., Kloß, A., Dahlmann, B., Willems, L.I., Verdoes, M., Overkleeft, H.S., Marcos, E., Adnot, S., et al. (2015). Regulation of Immunoproteasome Function in the Lung. *Sci. Rep.* *5*, 10230.
- Keller, J.N., Hanni, K.B., and Markesbery, W.R. (2000). Possible involvement of proteasome inhibition in aging: implications for oxidative stress. *Mech. Ageing Dev.* *113*, 61–70.
- Kelsen, S.G., Duan, X., Ji, R., Perez, O., Liu, C., and Merali, S. (2008). Cigarette Smoke Induces an Unfolded Protein Response in the Human Lung: A Proteomic Approach. *Am. J. Respir. Cell Mol. Biol.* *38*, 541–550.
- Kennedy, B.K., and Pennypacker, J.K. (2014). Drugs that modulate aging: the promising yet difficult path ahead. *Transl. Res.* *163*, 456–465.
- Kennedy, B.K., Berger, S.L., Brunet, A., Campisi, J., Cuervo, A.M., Epel, E.S., Franceschi, C., Lithgow, G.J., Morimoto, R.I., Pessin, J.E., et al. (2014). Geroscience: Linking Aging to Chronic Disease. *Cell* *159*, 709–713.
- Kim, Y.-C., Li, X., Thompson, D., and DeMartino, G.N. (2012). ATP Binding by Proteasomal ATPases Regulates Cellular Assembly and Substrate-induced Functions of the 26 S Proteasome. *J. Biol. Chem.* *288*, 3334–3345.
- Kimbrel, E.A., Davis, T.N., Bradner, J.E., and Kung, A.L. (2009). In vivo pharmacodynamic imaging of proteasome inhibition. *Mol. Imaging* *8*, 140–147.
- Kipen, H.M., Gandhi, S., Rich, D.Q., Ohman-Strickland, P., Laumbach, R., Fan, Z.-H., Chen, L., Laskin, D.L., Zhang, J., and Madura, K. (2010). Acute Decreases in Proteasome Pathway Activity after Inhalation of Fresh Diesel Exhaust or Secondary Organic Aerosol. *Environ. Health Perspect.* *119*, 658–663.
- Kirkwood, T.B., and Austad, S.N. (2000). Why do we age? *Nature* *408*, 233–238.
- Kisselev, A.F., Akopian, T.N., Castillo, V., and Goldberg, A.L. (1999). Proteasome Active Sites Allosterically Regulate Each Other, Suggesting a Cyclical Bite-Chew Mechanism for Protein Breakdown. *Mol. Cell* *4*, 395–402.

- Kisselev, A.F., Callard, A., and Goldberg, A.L. (2006). Importance of the Different Proteolytic Sites of the Proteasome and the Efficacy of Inhibitors Varies with the Protein Substrate. *J. Biol. Chem.* *281*, 8582–8590.
- Kisselev, A.F., van der Linden, W.A., and Overkleeft, H.S. (2012). Proteasome Inhibitors: An Expanding Army Attacking a Unique Target. *Chem. Biol.* *19*, 99–115.
- Komander, D., and Rape, M. (2012). The Ubiquitin Code. *Annu. Rev. Biochem.* *81*, 203–229.
- Königshoff, M., Kramer, M., Balsara, N., Wilhelm, J., Amarie, O.V., Jahn, A., Rose, F., Fink, L., Seeger, W., Schaefer, L., et al. (2009). WNT1-inducible signaling protein-1 mediates pulmonary fibrosis in mice and is upregulated in humans with idiopathic pulmonary fibrosis. *J. Clin. Invest.* *119*, 772–787.
- Kroemer, G., Mariño, G., and Levine, B. (2010). Autophagy and the Integrated Stress Response. *Mol. Cell* *40*, 280–293.
- Kubiczkova, L., Pour, L., Sedlarikova, L., Hajek, R., and Sevcikova, S. (2014). Proteasome inhibitors - molecular basis and current perspectives in multiple myeloma. *J. Cell. Mol. Med.* *18*, 947–961.
- Kurozumi, M., Matsushita, T., Hosokawa, M., and Takeda, T. (1994). Age-related changes in lung structure and function in the senescence-accelerated mouse (SAM): SAM-P/1 as a new murine model of senile hyperinflation of lung. *Am. J. Respir. Crit. Care Med.* *149*, 776–782.
- Laplante, M., and Sabatini, D.M. (2009). mTOR signaling at a glance. *J. Cell Sci.* *122*, 3589–3594.
- Launay, N., Ruiz, M., Fourcade, S., Schluter, A., Guilera, C., Ferrer, I., Knecht, E., and Pujol, A. (2013). Oxidative stress regulates the ubiquitin-proteasome system and immunoproteasome functioning in a mouse model of X-adrenoleukodystrophy. *Brain* *136*, 891–904.
- Lee, J., Sandford, A., Man, P., and Sin, D.D. (2011). Is the aging process accelerated in chronic obstructive pulmonary disease?: *Curr. Opin. Pulm. Med.* *17*, 90–97.
- Lee, S., Jeong, S.-Y., Lim, W.-C., Kim, S., Park, Y.-Y., Sun, X., Youle, R.J., and Cho, H. (2007). Mitochondrial Fission and Fusion Mediators, hFis1 and OPA1, Modulate Cellular Senescence. *J. Biol. Chem.* *282*, 22977–22983.
- Levine, B., and Kroemer, G. (2008). Autophagy in the Pathogenesis of Disease. *Cell* *132*, 27–42.
- Li, J., and Rechsteiner, M. (2001). Molecular dissection of the 11S REG (PA28) proteasome activators. *Biochimie* *83*, 373–383.
- Liesa, M., and Shrihari, O.S. (2013). Mitochondrial Dynamics in the Regulation of Nutrient Utilization and Energy Expenditure. *Cell Metab.* *17*, 491–506.
- Liesa, M., Palacin, M., and Zorzano, A. (2009). Mitochondrial Dynamics in Mammalian Health and Disease. *Physiol. Rev.* *89*, 799–845.
- Li-Harms, X., Milasta, S., Lynch, J., Wright, C., Joshi, A., Iyengar, R., Neale, G., Wang, X., Wang, Y.-D., Prolla, T.A., et al. (2014). Mito-protective autophagy is impaired in erythroid cells of aged mtDNA-mutator mice. *Blood* *125*, 162–174.
- Lin, S.-J. (2004). Calorie restriction extends yeast life span by lowering the level of NADH. *Genes Dev.* *18*, 12–16.

References

- Liu, C.-W., Li, X., Thompson, D., Wooding, K., Chang, T., Tang, Z., Yu, H., Thomas, P.J., and DeMartino, G.N. (2006a). ATP Binding and ATP Hydrolysis Play Distinct Roles in the Function of 26S Proteasome. *Mol. Cell* 24, 39–50.
- Liu, J., Wang, Y., Li, L., Zhou, L., Wei, H., Zhou, Q., Liu, J., Wang, W., Ji, L., Shan, P., et al. (2013). Site-specific Acetylation of the Proteasome Activator REG Directs Its Heptameric Structure and Functions. *J. Biol. Chem.* 288, 16567–16578.
- Liu, X., Huang, W., Li, C., Li, P., Yuan, J., Li, X., Qiu, X.-B., Ma, Q., and Cao, C. (2006b). Interaction between c-Abl and Arg tyrosine kinases and proteasome subunit PSMA7 regulates proteasome degradation. *Mol. Cell* 22, 317–327.
- Livnat-Levanon, N., and Glickman, M.H. (2011). Ubiquitin–Proteasome System and mitochondria — Reciprocity. *Biochim. Biophys. Acta BBA - Gene Regul. Mech.* 1809, 80–87.
- Livnat-Levanon, N., Kevei, É., Kleifeld, O., Krutauz, D., Segref, A., Rinaldi, T., Erpapazoglou, Z., Cohen, M., Reis, N., Hoppe, T., et al. (2014). Reversible 26S Proteasome Disassembly upon Mitochondrial Stress. *Cell Rep.* 7, 1371–1380.
- Ljubuncic, P., and Reznick, A.Z. (2009). The Evolutionary Theories of Aging Revisited – A Mini-Review. *Gerontology* 55, 205–216.
- Logue, S.E., Cleary, P., Saveljeva, S., and Samali, A. (2013). New directions in ER stress-induced cell death. *Apoptosis* 18, 537–546.
- Lokireddy, S., Kukushkin, N.V., and Goldberg, A.L. (2015). cAMP-induced phosphorylation of 26S proteasomes on Rpn6/PSMD11 enhances their activity and the degradation of misfolded proteins. *Proc. Natl. Acad. Sci.* 112, E7176–E7185.
- López-Otín, C., Blasco, M.A., Partridge, L., Serrano, M., and Kroemer, G. (2013). The Hallmarks of Aging. *Cell* 153, 1194–1217.
- Luo, X., and Kraus, W.L. (2012). On PAR with PARP: cellular stress signaling through poly(ADP-ribose) and PARP-1. *Genes Dev.* 26, 417–432.
- MacNee, W. (2009). Accelerated lung aging: a novel pathogenic mechanism of chronic obstructive pulmonary disease (COPD). *Biochem. Soc. Trans.* 37, 819–823.
- Maharjan, S., Oku, M., Tsuda, M., Hoseki, J., and Sakai, Y. (2014). Mitochondrial impairment triggers cytosolic oxidative stress and cell death following proteasome inhibition. *Sci. Rep.* 4, 5896–6007.
- Maiso, P., Huynh, D., Moschetta, M., Sacco, A., Aljawai, Y., Mishima, Y., Asara, J.M., Roccaro, A.M., Kimmelman, A.C., and Ghobrial, I.M. (2015). Metabolic Signature Identifies Novel Targets for Drug Resistance in Multiple Myeloma. *Cancer Res.* 75, 2071–2082.
- Margineantu, D.H., Emerson, C.B., Diaz, D., and Hockenbery, D.M. (2007). Hsp90 Inhibition Decreases Mitochondrial Protein Turnover. *PLoS ONE* 2, e1066.
- Martorell-Riera, A., Segarra-Mondejar, M., Munoz, J.P., Ginet, V., Olloquequi, J., Perez-Clausell, J., Palacin, M., Reina, M., Puyal, J., Zorzano, A., et al. (2014). Mfn2 downregulation in excitotoxicity causes mitochondrial dysfunction and delayed neuronal death. *EMBO J.* 33, 2388–2407.

- Marzetti, E., Calvani, R., Cesari, M., Buford, T.W., Lorenzi, M., Behnke, B.J., and Leeuwenburgh, C. (2013). Mitochondrial dysfunction and sarcopenia of aging: From signaling pathways to clinical trials. *Int. J. Biochem. Cell Biol.* *45*, 2288–2301.
- Meiners, S., and Ballweg, K. (2014). Proteostasis in pediatric pulmonary pathology. *Mol. Cell. Pediatr.* *1*, 1–8.
- Meiners, S., Ludwig, A., Lorenz, M., Dreger, H., Baumann, G., Stangl, V., and Stangl, K. (2006). Nontoxic proteasome inhibition activates a protective antioxidant defense response in endothelial cells. *Free Radic. Biol. Med.* *40*, 2232–2241.
- Meiners, S., Keller, I.E., Semren, N., and Caniard, A. (2014). Regulation of the Proteasome: Evaluating the Lung Proteasome as a New Therapeutic Target. *Antioxid. Redox Signal.* *21*, 2364–2382.
- Meiners, S., Eickelberg, O., and Konigshoff, M. (2015). Hallmarks of the ageing lung. *Eur. Respir. J.* *45*, 807–827.
- Mercado, N., Ito, K., and Barnes, P.J. (2015). Accelerated ageing of the lung in COPD: new concepts. *Thorax* *70*, 482–489.
- Mesquita, A., Weinberger, M., Silva, A., Sampaio-Marques, B., Almeida, B., Leao, C., Costa, V., Rodrigues, F., Burhans, W.C., and Ludovico, P. (2010). Caloric restriction or catalase inactivation extends yeast chronological lifespan by inducing H₂O₂ and superoxide dismutase activity. *Proc. Natl. Acad. Sci.* *107*, 15123–15128.
- Meyer, H., Bug, M., and Bremer, S. (2012). Emerging functions of the VCP/p97 AAA-ATPase in the ubiquitin system. *Nat Cell Biol* *14*, 117–123.
- Min, T., Bodas, M., Mazur, S., and Vij, N. (2011). Critical role of proteostasis-imbalance in pathogenesis of COPD and severe emphysema. *J. Mol. Med.* *89*, 577–593.
- Mishra, P., and Chan, D.C. (2014). Mitochondrial dynamics and inheritance during cell division, development and disease. *Nat. Rev. Mol. Cell Biol.* *15*, 634–646.
- Mishto, M., Liepe, J., Textoris-Taube, K., Keller, C., Henklein, P., Weberruß, M., Dahlmann, B., Enekel, C., Voigt, A., Kuckelkorn, U., et al. (2014). Proteasome isoforms exhibit only quantitative differences in cleavage and epitope generation: Antigen processing. *Eur. J. Immunol.* *44*, 3508–3521.
- Mizumura, K., Cloonan, S.M., Nakahira, K., Bhashyam, A.R., Cervo, M., Kitada, T., Glass, K., Owen, C.A., Mahmood, A., Washko, G.R., et al. (2014). Mitophagy-dependent necroptosis contributes to the pathogenesis of COPD. *J. Clin. Invest.* *124*, 3987–4003.
- Moreno, D., Viana, R., and Sanz, P. (2009). Two-hybrid analysis identifies PSMD11, a non-ATPase subunit of the proteasome, as a novel interaction partner of AMP-activated protein kinase. *Int. J. Biochem. Cell Biol.* *41*, 2431–2439.
- Morimoto, R.I., and Cuervo, A.M. (2014). Proteostasis and the Aging Proteome in Health and Disease. *J. Gerontol. A. Biol. Sci. Med. Sci.* *69*, S33–S38.
- Mouchiroud, L., Houtkooper, R.H., Moullan, N., Katsyuba, E., Ryu, D., Cantó, C., Mottis, A., Jo, Y.-S., Viswanathan, M., Schoonjans, K., et al. (2013). The NAD⁺/Sirtuin Pathway Modulates Longevity through Activation of Mitochondrial UPR and FOXO Signaling. *Cell* *154*, 430–441.

References

- Mukhopadhyay, P., Rajesh, M., Haskó, G., Hawkins, B.J., Madesh, M., and Pacher, P. (2007). Simultaneous detection of apoptosis and mitochondrial superoxide production in live cells by flow cytometry and confocal microscopy. *Nat. Protoc.* *2*, 2295–2301.
- Müller, K.-C., Welker, L., Paasch, K., Feindt, B., Erpenbeck, V.J., Hohlfeld, J.M., Krug, N., Nakashima, M., Branscheid, D., Magnussen, H., et al. (2006). Lung fibroblasts from patients with emphysema show markers of senescence in vitro. *Respir. Res.* *7*, 32–42.
- Munnich, A., and Rustin, P. (2001). Clinical spectrum and diagnosis of mitochondrial disorders. *Am. J. Med. Genet.* *106*, 4–17.
- Murata, S., Sasaki, K., Kishimoto, T., Niwa, S.-I., Hayashi, H., Takahama, Y., and Tanaka, K. (2007). Regulation of CD8+ T cell development by thymus-specific proteasomes. *Science* *316*, 1349–1353.
- Murata, S., Yashiroda, H., and Tanaka, K. (2009). Molecular mechanisms of proteasome assembly. *Nat. Rev. Mol. Cell Biol.* *10*, 104–115.
- Murphy, M.P. (2009). How mitochondria produce reactive oxygen species. *Biochem. J.* *417*, 1–13.
- Nakagawa, T., Shirane, M., Iemura, S., Natsume, T., and Nakayama, K.I. (2007). Anchoring of the 26S proteasome to the organellar membrane by FKBP38. *Genes Cells* *12*, 709–719.
- Narendra, D.P., Jin, S.M., Tanaka, A., Suen, D.-F., Gautier, C.A., Shen, J., Cookson, M.R., and Youle, R.J. (2010). PINK1 Is Selectively Stabilized on Impaired Mitochondria to Activate Parkin. *PLoS Biol.* *8*, e1000298.
- Nathan, J.A., Spinnenhirn, V., Schmidtke, G., Basler, M., Groettrup, M., and Goldberg, A.L. (2013). Immuno- and Constitutive Proteasomes Do Not Differ in Their Abilities to Degrade Ubiquitinated Proteins. *Cell* *152*, 1184–1194.
- Nicholls, D.G., and Ferguson, S.J. (2002). *Bioenergetics* (San Diego, Calif: Academic Press).
- Nunnari, J., and Suomalainen, A. (2012). Mitochondria: In Sickness and in Health. *Cell* *148*, 1145–1159.
- Nyunoya, T., Mebratu, Y., Contreras, A., Delgado, M., Chand, H.S., and Tesfaigzi, Y. (2014). Molecular Processes that Drive Cigarette Smoke-Induced Epithelial Cell Fate of the Lung. *Am. J. Respir. Cell Mol. Biol.* *50*, 471–482.
- Olgun, A., and Akman, S. (2007). Mitochondrial DNA-Deficient Models and Aging. *Ann. N. Y. Acad. Sci.* *1100*, 241–245.
- Papa, L., and Germain, D. (2011). Estrogen receptor mediates a distinct mitochondrial unfolded protein response. *J. Cell Sci.* *124*, 1396–1402.
- Papa, L., Gomes, E., and Rockwell, P. (2007). Reactive oxygen species induced by proteasome inhibition in neuronal cells mediate mitochondrial dysfunction and a caspase-independent cell death. *Apoptosis Int. J. Program. Cell Death* *12*, 1389–1405.
- Pellegrino, M.W., Nargund, A.M., and Haynes, C.M. (2013). Signaling the mitochondrial unfolded protein response. *Biochim. Biophys. Acta BBA - Mol. Cell Res.* *1833*, 410–416.

- Pérez, V.I., Van Remmen, H., Bokov, A., Epstein, C.J., Vijg, J., and Richardson, A. (2009). The overexpression of major antioxidant enzymes does not extend the lifespan of mice. *Aging Cell* 8, 73–75.
- Peth, A., Nathan, J.A., and Goldberg, A.L. (2013). The ATP Costs and Time Required to Degrade Ubiquitinated Proteins by the 26 S Proteasome. *J. Biol. Chem.* 288, 29215–29222.
- Pickering, A.M., Lehr, M., and Miller, R.A. (2015). Lifespan of mice and primates correlates with immunoproteasome expression. *J. Clin. Invest.* 125, 2059–2068.
- Powers, E.T., and Balch, W.E. (2013). Diversity in the origins of proteostasis networks — a driver for protein function in evolution. *Nat. Rev. Mol. Cell Biol.* 14, 237–248.
- Quiros, P.M., Ramsay, A.J., and López-Otín, C. (2013). New roles for OMA1 metalloprotease: From mitochondrial proteostasis to metabolic homeostasis. *Adipocyte* 2, 7–11.
- Radke, S., Chander, H., Schäfer, P., Meiss, G., Krüger, R., Schulz, J.B., and Germain, D. (2008). Mitochondrial Protein Quality Control by the Proteasome Involves Ubiquitination and the Protease Omi. *J. Biol. Chem.* 283, 12681–12685.
- Ribeiro, C.A.J., Balestro, F., Grando, V., and Wajner, M. (2007). Isovaleric acid reduces Na⁺, K⁺-ATPase activity in synaptic membranes from cerebral cortex of young rats. *Cell. Mol. Neurobiol.* 27, 529–540.
- van Rijt, S.H., Keller, I.E., John, G., Kohse, K., Yildirim, A.O., Eickelberg, O., and Meiners, S. (2012). Acute cigarette smoke exposure impairs proteasome function in the lung. *Am. J. Physiol. - Lung Cell. Mol. Physiol.* 303, L814–L823.
- Rinaldi, T., Hofmann, L., Gambadoro, A., Cossard, R., Livnat-Levanon, N., Glickman, M.H., Frontali, L., and Delahodde, A. (2007). Dissection of the Carboxyl-Terminal Domain of the Proteasomal Subunit Rpn11 in Maintenance of Mitochondrial Structure and Function. *Mol. Biol. Cell* 19, 1022–1031.
- Ronnebaum, S.M., Patterson, C., and Schisler, J.C. (2014). Minireview: Hey U(PS): Metabolic and Proteolytic Homeostasis Linked via AMPK and the Ubiquitin Proteasome System. *Mol. Endocrinol.* 28, 1602–1615.
- Ross, J., Olson, L., and Coppotelli, G. (2015). Mitochondrial and Ubiquitin Proteasome System Dysfunction in Ageing and Disease: Two Sides of the Same Coin? *Int. J. Mol. Sci.* 16, 19458–19476.
- Ryan, J.J., Marsboom, G., Fang, Y.-H., Toth, P.T., Morrow, E., Luo, N., Piao, L., Hong, Z., Ericson, K., Zhang, H.J., et al. (2013). PGC1^γ-Mediated Mitofusin-2 Deficiency in Female Rats and Humans With Pulmonary Arterial Hypertension. *Am. J. Respir. Crit. Care Med.* 187, 865–878.
- Sack, M.N., and Finkel, T. (2012). Mitochondrial Metabolism, Sirtuins, and Aging. *Cold Spring Harb. Perspect. Biol.* 4, a013102–a013102.
- Safran, M., Kim, W.Y., O’Connell, F., Flippin, L., Gunzler, V., Horner, J.W., DePinho, R.A., and Kaelin, W.G. (2006). Mouse model for noninvasive imaging of HIF prolyl hydroxylase activity: Assessment of an oral agent that stimulates erythropoietin production. *Proc. Natl. Acad. Sci.* 103, 105–110.
- Santidrian, A.F., Matsuno-Yagi, A., Ritland, M., Seo, B.B., LeBoeuf, S.E., Gay, L.J., Yagi, T., and Felding-Habermann, B. (2013). Mitochondrial complex I activity and NAD⁺/NADH balance regulate breast cancer progression. *J. Clin. Invest.* 123, 1068–1081.

References

- Sato, A., Hirai, T., Imura, A., Kita, N., Iwano, A., Muro, S., Nabeshima, Y. -i., Suki, B., and Mishima, M. (2007). Morphological mechanism of the development of pulmonary emphysema in klotho mice. *Proc. Natl. Acad. Sci.* *104*, 2361–2365.
- Sato, T., Seyama, K., Sato, Y., Mori, H., Souma, S., Akiyoshi, T., Kodama, Y., Mori, T., Goto, S., Takahashi, K., et al. (2006). Senescence marker protein-30 protects mice lungs from oxidative stress, aging, and smoking. *Am. J. Respir. Crit. Care Med.* *174*, 530–537.
- Schmidt, M., and Finley, D. (2013). Regulation of proteasome activity in health and disease. *Biochim. Biophys. Acta BBA - Mol. Cell Res.* *1843*, 13–25.
- Schmidt, O., Pfanner, N., and Meisinger, C. (2010). Mitochondrial protein import: from proteomics to functional mechanisms. *Nat. Rev. Mol. Cell Biol.* *11*, 655–667.
- Schubert, U., Antón, L.C., Gibbs, J., Norbury, C.C., Yewdell, J.W., and Bennink, J.R. (2000). Rapid degradation of a large fraction of newly synthesized proteins by proteasomes. *Nature* *404*, 770–774.
- Scorrano, L. (2013). Keeping mitochondria in shape: a matter of life and death. *Eur. J. Clin. Invest.* *43*, 886–893.
- Segref, A., Kevei, É., Pokrzywa, W., Schmeisser, K., Mansfeld, J., Livnat-Levanon, N., Ensenauer, R., Glickman, M.H., Ristow, M., and Hoppe, T. (2014). Pathogenesis of Human Mitochondrial Diseases Is Modulated by Reduced Activity of the Ubiquitin/Proteasome System. *Cell Metab.* *19*, 642–652.
- Seifert, U., Bialy, L.P., Ebstein, F., Bech-Otschir, D., Voigt, A., Schröter, F., Prozorovski, T., Lange, N., Steffen, J., Rieger, M., et al. (2010). Immunoproteasomes Preserve Protein Homeostasis upon Interferon-Induced Oxidative Stress. *Cell* *142*, 613–624.
- Sena, L.A., and Chandel, N.S. (2012). Physiological Roles of Mitochondrial Reactive Oxygen Species. *Mol. Cell* *48*, 158–167.
- Sharma, G., and Goodwin, J. (2006). Effect of aging on respiratory system physiology and immunology. *Clin. Interv. Aging* *1*, 253–260.
- Shutt, T., Geoffrion, M., Milne, R., and McBride, H.M. (2012). The intracellular redox state is a core determinant of mitochondrial fusion. *EMBO Rep.* *13*, 909–915.
- Stadtman, E.R. (2006). Protein oxidation and aging. *Free Radic. Res.* *40*, 1250–1258.
- Stein, L.R., and Imai, S. (2014). Specific ablation of Nampt in adult neural stem cells recapitulates their functional defects during aging. *EMBO J.* *33*, 1321–1340.
- Sueblinvong, V., Neujahr, D.C., Todd Mills, S., Roser-Page, S., Ritzenthaler, J.D., Guidot, D., Rojas, M., and Roman, J. (2012). Predisposition for Disrepair in the Aged Lung: *Am. J. Med. Sci.* *344*, 41–51.
- Sullivan, P.G., Natasa B. Dragicevic, Jian-Hong Deng, Yidong Bai, Edgardo Dimayuga, Qunxing Ding, Qinghua Chen, Annadora J. Bruce-Keller, and Jeffrey N. Keller (2004). Proteasome Inhibition Alters Neural Mitochondrial Homeostasis and Mitochondria Turnover. *J. Biol. Chem.* *279*, 20699–20707.
- Takeda, K., Yoshida, T., Kikuchi, S., Nagao, K., Kokubu, A., Pluskal, T., Villar-Briones, A., Nakamura, T., and Yanagida, M. (2010). Synergistic roles of the proteasome and autophagy for mitochondrial maintenance and chronological lifespan in fission yeast. *Proc. Natl. Acad. Sci.* *107*, 3540–3545.

- Tanaka, K. (2013). The Proteasome: From Basic Mechanisms to Emerging Roles. *Keio J. Med.* 62, 1–12.
- Tanaka, A., Cleland, M.M., Xu, S., Narendra, D.P., Suen, D.-F., Karbowski, M., and Youle, R.J. (2010). Proteasome and p97 mediate mitophagy and degradation of mitofusins induced by Parkin. *J. Cell Biol.* 191, 1367–1380.
- Tanaka, K., Budd, M.A., Efron, M.L., and Isselbacher, K.J. (1966). Isovaleric acidemia: a new genetic defect of leucine metabolism. *Proc. Natl. Acad. Sci. U. S. A.* 56, 236–242.
- Tar, K., Dange, T., Yang, C., Yao, Y., Bulteau, A.-L., Fernandez Salcedo, E., Braigen, S., Bouillaud, F., Finley, D., and Schmidt, M. (2014). Proteasomes associated with the Blm10 Activator Protein Antagonize Mitochondrial Fission Through Degradation of the Fission Protein Dnm1. *J. Biol. Chem.* 289, 12145–12156.
- Taraseviciene-Stewart, L., and Voelkel, N.F. (2008). Molecular pathogenesis of emphysema. *J. Clin. Invest.* 118, 394–402.
- Taylor, E.B., and Rutter, J. (2011). Mitochondrial quality control by the ubiquitin–proteasome system. *Biochem. Soc. Trans.* 39, 1509–1513.
- Thannickal, V.J., Murthy, M., Balch, W.E., Chandel, N.S., Meiners, S., Eickelberg, O., Selman, M., Pardo, A., White, E.S., Levy, B.D., et al. (2015). Blue Journal Conference. Aging and Susceptibility to Lung Disease. *Am. J. Respir. Crit. Care Med.* 191, 261–269.
- Tomaru, U., Takahashi, S., Ishizu, A., Miyatake, Y., Gohda, A., Suzuki, S., Ono, A., Ohara, J., Baba, T., Murata, S., et al. (2012). Decreased Proteasomal Activity Causes Age-Related Phenotypes and Promotes the Development of Metabolic Abnormalities. *Am. J. Pathol.* 180, 963–972.
- Tomita, T., Hamazaki, J., Hirayama, S., McBurney, M.W., Yashiroda, H., and Murata, S. (2015). Sirt1-deficiency causes defective protein quality control. *Sci. Rep.* 5, 12613.
- Tondera, D., Grandemange, S., Jourdain, A., Karbowski, M., Mattenberger, Y., Herzig, S., Da Cruz, S., Clerc, P., Raschke, I., Merkwirth, C., et al. (2009). SLP-2 is required for stress-induced mitochondrial hyperfusion. *EMBO J.* 28, 1589–1600.
- Tonoki, A., Kuranaga, E., Tomioka, T., Hamazaki, J., Murata, S., Tanaka, K., and Miura, M. (2009). Genetic Evidence Linking Age-Dependent Attenuation of the 26S Proteasome with the Aging Process. *Mol. Cell. Biol.* 29, 1095–1106.
- van der Toorn, M., Slebos, D.-J., de Bruin, H.G., Leuvenink, H.G., Bakker, S.J.L., Gans, R.O.B., Koeter, G.H., van Oosterhout, A.J.M., and Kauffman, H.F. (2007). Cigarette smoke-induced blockade of the mitochondrial respiratory chain switches lung epithelial cell apoptosis into necrosis. *AJP Lung Cell. Mol. Physiol.* 292, L1211–L1218.
- Torres, C.A., and Perez, V.I. (2008). Proteasome modulates mitochondrial function during cellular senescence. *Free Radic. Biol. Med.* 44, 403–414.
- Trifunovic, A., Wredenberg, A., Falkenberg, M., Spelbrink, J.N., Rovio, A.T., Bruder, C.E., Bohlooly-Y, M., Gidlöf, S., Oldfors, A., Wibom, R., et al. (2004). Premature ageing in mice expressing defective mitochondrial DNA polymerase. *Nature* 429, 417–423.
- Trifunovic, A., Hansson, A., Anna Wredenberg, Anja Rovio, Eric Dufour, Ivan Khvorostov, Johannes Spelbrink, Rolf Wibom, Howard Jacobs, and Larsson, N.-G. (2005). From the Cover: Somatic mtDNA

References

- mutations cause aging phenotypes without affecting reactive oxygen species production. *Proc. Natl. Acad. Sci.* *102*, 17993–17998.
- Tsuji, T., Aoshiba, K., and Nagai, A. (2004). Cigarette Smoke Induces Senescence in Alveolar Epithelial Cells. *Am. J. Respir. Cell Mol. Biol.* *31*, 643–649.
- Tsuji, T., Aoshiba, K., and Nagai, A. (2006). Alveolar Cell Senescence in Patients with Pulmonary Emphysema. *Am. J. Respir. Crit. Care Med.* *174*, 886–893.
- Tsvetkov, P., Myers, N., Eliav, R., Adamovich, Y., Hagai, T., Adler, J., Navon, A., and Shaul, Y. (2014). NADH Binds and Stabilizes the 26S Proteasomes Independent of ATP. *J. Biol. Chem.* *289*, 11272–11281.
- Tsvetkov, P., Mendillo, M.L., Zhao, J., Carette, J.E., Merrill, P.H., Cikes, D., Varadarajan, M., van Diemen, F.R., Penninger, J.M., Goldberg, A.L., et al. (2015). Compromising the 19S proteasome complex protects cells from reduced flux through the proteasome. *eLife* *4*, e08467.
- Tuder, R.M. (2006). Aging and Cigarette Smoke: Fueling the Fire. *Am. J. Respir. Crit. Care Med.* *174*, 490–491.
- Tuder, R.M., and Petrache, I. (2012). Pathogenesis of chronic obstructive pulmonary disease. *J. Clin. Invest.* *122*, 2749–2755.
- Twig, G., Elorza, A., Molina, A.J.A., Mohamed, H., Wikstrom, J.D., Walzer, G., Stiles, L., Haigh, S.E., Katz, S., Las, G., et al. (2008). Fission and selective fusion govern mitochondrial segregation and elimination by autophagy. *EMBO J.* *27*, 433–446.
- Ullrich, O., Reinheckel, T., Sitte, N., Hass, R., Grune, T., and Davies, K.J. (1999). Poly-ADP ribose polymerase activates nuclear proteasome to degrade oxidatively damaged histones. *Proc. Natl. Acad. Sci. U. S. A.* *96*, 6223–6228.
- Unverdorben, P., Beck, F., Śledź, P., Schweitzer, A., Pfeifer, G., Plitzko, J.M., Baumeister, W., and Förster, F. (2014). Deep classification of a large cryo-EM dataset defines the conformational landscape of the 26S proteasome. *Proc. Natl. Acad. Sci. U. S. A.* *111*, 5544–5549.
- Vandenabeele, P., Galluzzi, L., Vanden Berghe, T., and Kroemer, G. (2010). Molecular mechanisms of necroptosis: an ordered cellular explosion. *Nat. Rev. Mol. Cell Biol.* *11*, 700–714.
- Van Kaer, L., Ashton-Rickardt, P.G., Eichelberger, M., Gaczynska, M., Nagashima, K., Rock, K.L., Goldberg, A.L., Doherty, P.C., and Tonegawa, S. (1994). Altered peptidase and viral-specific T cell response in LMP2 mutant mice. *Immunity* *1*, 533–541.
- Verdoes, M., Florea, B.I., Menendez-Benito, V., Maynard, C.J., Witte, M.D., van der Linden, W.A., van den Nieuwendijk, A.M.C.H., Hofmann, T., Berkens, C.R., van Leeuwen, F.W.B., et al. (2006). A fluorescent broad-spectrum proteasome inhibitor for labeling proteasomes in vitro and in vivo. *Chem. Biol.* *13*, 1217–1226.
- Viana, R., Aguado, C., Esteban, I., Moreno, D., Viollet, B., Knecht, E., and Sanz, P. (2008). Role of AMP-activated protein kinase in autophagy and proteasome function. *Biochem. Biophys. Res. Commun.* *369*, 964–968.
- Vilchez, D., Morantte, I., Liu, Z., Douglas, P.M., Merkwirth, C., Rodrigues, A.P.C., Manning, G., and Dillin, A. (2012). RPN-6 determines *C. elegans* longevity under proteotoxic stress conditions. *Nature* *489*, 263–268.

- Walther, D.M., Kasturi, P., Zheng, M., Pinkert, S., Vecchi, G., Ciryam, P., Morimoto, R.I., Dobson, C.M., Vendruscolo, M., Mann, M., et al. (2015). Widespread Proteome Remodeling and Aggregation in Aging *C. elegans*. *Cell* *161*, 919–932.
- Wang, D., Fang, C., Zong, N.C., Liem, D.A., Cadeiras, M., Scruggs, S.B., Yu, H., Kim, A.K., Yang, P., Deng, M., et al. (2013). Regulation of Acetylation Restores Proteolytic Function of Diseased Myocardium in Mouse and Human. *Mol. Cell. Proteomics* *12*, 3793–3802.
- Wang, H., Song, P., Du, L., Tian, W., Yue, W., Liu, M., Li, D., Wang, B., Zhu, Y., Cao, C., et al. (2011). Parkin ubiquitinates Drp1 for proteasome-dependent degradation: implication of dysregulated mitochondrial dynamics in Parkinson's disease. *J. Biol. Chem.* *286*, 11649–11658.
- Wang, X., Yen, J., Kaiser, P., and Huang, L. (2010). Regulation of the 26S Proteasome Complex During Oxidative Stress. *Sci. Signal.* *3*, ra88–ra98.
- Wei, J., Rahman, S., Ayaub, E.A., Dickhout, J.G., and Ask, K. (2013). Protein Misfolding and Endoplasmic Reticulum Stress in Chronic Lung Disease. *CHEST J.* *143*, 1098–1105.
- Wikenheiser, K.A., Vorbroker, D.K., Rice, W.R., Clark, J.C., Bachurski, C.J., Oie, H.K., and Whitsett, J.A. (1993). Production of immortalized distal respiratory epithelial cell lines from surfactant protein C/simian virus 40 large tumor antigen transgenic mice. *Proc. Natl. Acad. Sci. U. S. A.* *90*, 11029–11033.
- Wrobel, L., Topf, U., Bragoszewski, P., Wiese, S., Sztolsztener, M.E., Oeljeklaus, S., Varabyova, A., Lirski, M., Chroscicki, P., Mroczek, S., et al. (2015). Mistargeted mitochondrial proteins activate a proteostatic response in the cytosol. *Nature* *524*, 485–488.
- Xu, J., Wang, S., Viollet, B., and Zou, M.-H. (2012). Regulation of the Proteasome by AMPK in Endothelial Cells: The Role of O-GlcNAc Transferase (OGT). *PLoS ONE* *7*, e36717.
- Xu, S., Peng, G., Wang, Y., Fang, S., and Karbowski, M. (2011). The AAA-ATPase p97 is essential for outer mitochondrial membrane protein turnover. *Mol. Biol. Cell* *22*, 291–300.
- Yamada, Y., Tomaru, U., Ishizu, A., Ito, T., Kiuchi, T., Ono, A., Miyajima, S., Nagai, K., Higashi, T., Matsuno, Y., et al. (2015). Decreased proteasomal function accelerates cigarette smoke-induced pulmonary emphysema in mice. *Lab. Invest.* *95*, 625–634.
- Yoon, Y.-S., Yoon, D.-S., Lim, I.K., Yoon, S.-H., Chung, H.-Y., Rojo, M., Malka, F., Jou, M.-J., Martinou, J.-C., and Yoon, G. (2006). Formation of elongated giant mitochondria in DFO-induced cellular senescence: Involvement of enhanced fusion process through modulation of Fis1. *J. Cell. Physiol.* *209*, 468–480.
- Yoshii, S.R., Kishi, C., Ishihara, N., and Mizushima, N. (2011). Parkin Mediates Proteasome-dependent Protein Degradation and Rupture of the Outer Mitochondrial Membrane. *J. Biol. Chem.* *286*, 19630–19640.
- Youle, R.J., and van der Bliek, A.M. (2012). Mitochondrial Fission, Fusion, and Stress. *Science* *337*, 1062–1065.
- Youle, R.J., and Narendra, D.P. (2011). Mechanisms of mitophagy. *Nat. Rev. Mol. Cell Biol.* *12*, 9–14.
- Yun, J., and Finkel, T. (2014). Mitohormesis. *Cell Metab.* *19*, 757–766.

References

- Zanker, D., Waithman, J., Yewdell, J.W., and Chen, W. (2013). Mixed Proteasomes Function To Increase Viral Peptide Diversity and Broaden Antiviral CD8+ T Cell Responses. *J. Immunol.* *191*, 52–59.
- Zhang, F., Su, K., Yang, X., Bowe, D.B., Paterson, A.J., and Kudlow, J.E. (2003). O-GlcNAc modification is an endogenous inhibitor of the proteasome. *Cell* *115*, 715–725.
- Zhang, F., Hu, Y., Huang, P., Toleman, C.A., Paterson, A.J., and Kudlow, J.E. (2007a). Proteasome function is regulated by cyclic AMP-dependent protein kinase through phosphorylation of Rpt6. *J. Biol. Chem.* *282*, 22460–22471.
- Zhang, F., Paterson, A.J., Huang, P., Wang, K., and Kudlow, J.E. (2007b). Metabolic Control of Proteasome Function. *Physiology* *22*, 373–379.
- Zhang, Y., Ikeno, Y., Qi, W., Chaudhuri, A., Li, Y., Bokov, A., Thorpe, S.R., Baynes, J.W., Epstein, C., Richardson, A., et al. (2009). Mice deficient in both Mn superoxide dismutase and glutathione peroxidase-1 have increased oxidative damage and a greater incidence of pathology but no reduction in longevity. *J. Gerontol. A Biol. Sci. Med. Sci.* *64*, 1212–1220.
- Zhang, Y., Nicholatos, J., Dreier, J.R., Ricoult, S.J.H., Widenmaier, S.B., Hotamisligil, G.S., Kwiatkowski, D.J., and Manning, B.D. (2014). Coordinated regulation of protein synthesis and degradation by mTORC1. *Nature* *513*, 440–443.
- Zhao, Q. (2002). A mitochondrial specific stress response in mammalian cells. *EMBO J.* *21*, 4411–4419.
- Zhao, J., Zhai, B., Gygi, S.P., and Goldberg, A.L. (2015). mTOR inhibition activates overall protein degradation by the ubiquitin proteasome system as well as by autophagy. *Proc. Natl. Acad. Sci. U. S. A.* *112*, 15790–15797.
- Zimmermann, R., Müller, L., and Wullich, B. (2006). Protein transport into the endoplasmic reticulum: mechanisms and pathologies. *Trends Mol. Med.* *12*, 567–573.

Abbreviations

A

AAA	ATPase associated with various cellular activities
ABP	Activity based probe
ADP	Adenosine diphosphate
AF	Alexa Fluor®
AMA	Antimycin A
AMC	7-amino-4-methylcoumarine
AMP	Adenosine monophosphate
AMPK	Adenosine monophosphate-activated protein kinase
ANOVA	Analysis of variance
ATFS-1	Activating transcription factor associated with stress-1
ATP	Adenosine triphosphate
ATP5A	ATP synthase subunit alpha

B

BAL	Bronchoalveolar lavage
BrdU	Bromodeoxyuridine
BSA	Bovine serum albumin
Bz	Bortezomib

C

<i>C. elegans</i>	<i>Caenorhabditis elegans</i>
cAMP	Cyclic AMP
CCCP	Carbonyl cyanide 3-chlorophenylhydrazone
C-L	Caspase-like
COPD	Chronic obstructive pulmonary disease
CS	Cigarette smoke
CSE	Cigarette smoke extract
CT-L	Chymotrypsin-like
Ctrl	Control

D

Da	Dalton
DAPI	4',6-diamidin-2-phenylindol
DCF	2',7'-dichlorofluorescein
DMEM	Dulbecco's modified Eagle's medium
DMSO	Dimethyl sulfoxide

Abbreviations

DNA	Deoxyribonucleic acid
DNPH	2,4-Dinitrophenylhydrazine
DRP1	Dynamin-related protein 1
DTAB	Dodecyltrimethylammonium bromide
DTT	Dithiothreitol
E	
EDTA	Ethylenediaminetetraacetate
EGTA	Ethyleneglycoltetraacetate
ER	Endoplasmic reticulum
ERAD	ER-associated degradation
ETC	Electron transport chain
F	
FACS	Fluorescence activated cell sorting
FBS	Fetal bovine serum
FIS1	Mitochondrial fission 1 protein
FITC	Fluorescein isothiocyanate
G	
GAPDH	Glyceraldehyde 3-phosphate dehydrogenase
GFP	Green fluorescent protein
GSH	Glutathione
H	
H ₂ DCFDA	2',7'-dichlorodihydrofluorescein diacetate
HEK	Human embryonic kidney cells
HEPES	4-(2-hydroxyethyl)-1-piperazineethanesulfonic acid
HRP	Horseradish peroxidase
HSP	Heat shock protein
I	
IFN	Interferon
IMM	Inner mitochondrial membrane
IMS	Intermembrane space
J	
K	
K48	Lysine 48
L	
LC3B	Light chain 3 B
LDH	Lactate dehydrogenase
LMP	Low molecular mass polypeptide

Luc	Luciferase
M	
MAD	Mitochondria-associated degradation
MECL-1	Multicatalytic endopeptidase complex-like-1
MEF	Mouse embryonic fibroblasts
MFN	Mitofusin
MHC	major histocompatibility complex
MiD	Mitochondrial dynamics protein
MLE	Murine lung epithelial cells
mRNA	Messenger RNA
mtDNA	Mitochondrial DNA
mTOR	Mammalian target of rapamycin
MTT	2,5-diphenyltetrazolium bromide
mtUPR	Mitochondrial unfolded protein response
N	
NAC	N-acetyl cysteine
NAD ⁺	Nicotinamide adenine dinucleotide
NAM	Nicotinamide
ND5	NADH dehydrogenase 5
NDUFB3	NADH dehydrogenase (ubiquinone) 1 beta subcomplex 3, 12kDa
NIX	Nineteen kDa interacting protein-3 (NIP-3)-like X protein
Npl4	Nuclear protein localization protein 4
O	
ODD	Oxygen-dependent degradation domain
O-GlcNAc	O-linked N-acetylglucosamine
OMM	Outer mitochondrial membrane
OPA1	Optic atrophy 1
OPP	O-propargyl-puromycin
P	
p16	Cyclin-dependent kinase inhibitor 2A, multiple tumor suppressor 1
p21	Cyclin-dependent kinase inhibitor 1
PA	Proteasome activator
PAGE	Polyacrylamide gel electrophoresis
PARP	Poly(ADP-ribose)polymerases
PBS	Phosphate buffered saline
PFA	Paraformaldehyde

Abbreviations

PI	Propidium iodide
PI	Proteasome inhibitor
PINK1	PTEN-induced putative kinase 1
PKA	Protein kinase A
pmATII	Primary murine alveolar type II cells
PolG	DNA polymerase subunit gamma
PSMA	Proteasome subunit alpha type
PSMB	Proteasome subunit beta type
PSMC	26S proteasome ATPase regulatory subunit
PSMD	26S proteasome non-ATPase regulatory subunit
PVDF	Polyvinylidenedifluoride
Q	
qPCR	Quantitative polymerase chain reaction
R	
RNA	Ribonucleic acid
ROS	Reactive oxygen species
Rpm	Rounds per minute
Rpn	Regulatory particle non-ATPase
Rpt	Regulatory particle AAA-ATPase
RT	Reverse transcriptase
RT	Room temperature
S	
SDS	Sodium dodecyl sulphate
SEM	Standard error of the mean
Ser	Serine
shRNA	Small hairpin RNA
siRNA	Small interfering RNA
Sirt1	NAD-dependent deacetylase sirtuin-1
T	
Tango2	transport and Golgi organization 2
TIM	Translocase of inner mitochondrial membrane
T-L	Trypsin-like
TMRM	Tetramethylrhodamin-methylester perchlorate
TOM	Translocase of outer mitochondrial membrane
Tris	Tris(hydroxymethyl)-aminomethane
tRNA	Transfer RNA

U

UPR Unfolded protein response
UPS Ubiquitin proteasome system

V

VCP Valosin-containing protein
VDAC1 Voltage-dependent anion channel 1
VMS1 VCP/Cdc48-associated Mitochondrial Stress responsive 1

W

WT Wild type

X

Y

Z

Abbreviations

Acknowledgements

Many people accompanied me in the time of the generation of this thesis and I'm extraordinary grateful for all the inspiration and the help and support I was given during this time.

First of all, I want to thank my supervisor Silke Meiners for the great scientific guidance. I've learned a lot about science in general and the proteasome in particular. Thank you especially for the discussions, for always openly sharing your thoughts and for the countless ideas we developed. Thank you also for your constant support and for encouraging me to develop further.

I also want to thank Oliver Eickelberg, Director of the CPC, for enabling me to pursue my PhD at his Institute and in particular for contributing to my thesis committee and for his critical judgment and advice throughout this time. Thank you for your open critics and for persisting on constant improvement.

I further want to thank Fabiana Perrochi for her contribution to my thesis committee and for all her advises for the analysis and the understanding of mitochondrial biology. I also want to thank Fabiana for letting me work in her lab and sharing her methods with me. In this regard I want to thank all members of her lab for their kindness and support and especially Jennifer Wettmarshausen for helping me with all the methods and always being open for me.

I thank Aleksandra Trifunovic and Alexandra Kukat for sharing their mtDNA mutator mice with me and for the helpful input on our project ideas. I especially thank Alexandra Kukat for her kindness and her support with all my project-related and other questions and for providing an open atmosphere for me in Cologne.

I am, furthermore, grateful to all other people I was able to collaborate with, for sharing their ideas, providing material and for the time they invested in helping me. Here, I want to especially name Kathrin Mutze, Tom Conlon and Ali Önder Yildirim within the CPC and Laura Kremer and Holger Prokisch at the institute of human genetics of the Helmholtz center Munich.

A special thanks goes to the people of the CPC research school "Lung biology and disease". Thank you all for the great time during the research school meetings. Especially I want to thank the head of the research school Melanie Königshoff and also Camille Beunèche and Doreen Franke for the organization and for all the support in and around the graduate school.

Of outstanding importance for me during the time of my PhD were the fellow people of the "Meiners Lab". Ilona Kammerl, Vanessa Welk, Christina Lukas, Alessandra Mossina, Nora Semren, Anne Caniard, Sabine van Rijt, Angela Dann, Deniz Bölükbas, Oliver Vosyka, Tobias Baumann and Thomas Meul. I want to thank you for all your input, the help with the experiments, the feedback on my ideas

Acknowledgements

and most of all for sharing all the happy and not-so-happy times. Especially, I want to thank Thomas for the good teamwork and all the work we did together. Thank you all for making the time of my PhD such a great time and also for making it great fun - on Tuesdays and also on every other day.

Last but not least, I also want to thank everyone else who contributed to my thesis and especially the reviewers of this document for the time and motivation they dedicate to make this thesis successful.

Eidesstattliche Versicherung

Hiermit erkläre ich, Korbinian Berschneider, an Eides statt, dass ich die vorliegende Dissertation mit dem Thema

„ Connecting the functions of the proteasome and mitochondria in the lung “

selbstständig verfasst, mich außer der angegebenen keiner weiteren Hilfsmittel bedient und alle Erkenntnisse, die aus dem Schrifttum ganz oder annähernd übernommen sind, als solche kenntlich gemacht und nach ihrer Herkunft unter Bezeichnung der Fundstelle einzeln nachgewiesen habe.

Ich erkläre des Weiteren, dass die hier vorgelegte Dissertation nicht in gleicher oder in ähnlicher Form bei einer anderen Stelle zur Erlangung eines akademischen Grades eingereicht wurde.

Ort/Datum

Unterschrift